Surgical lighting

Knulst, Arjan

DOI
10.4233/uuid:19182ec3-bffe-4b2c-a366-ef58c11d2e4f

Publication date
2017

Document Version
Final published version

Citation (APA)
Knulst, A. (2017). *Surgical lighting*. [Dissertation (TU Delft), Delft University of Technology].
https://doi.org/10.4233/uuid:19182ec3-bffe-4b2c-a366-ef58c11d2e4f

Surgical Lighting

Proefschrift

Ter verkrijging van de graad van doctor

aan de Technische Universiteit Delft,

op gezag van de Rector Magnificus prof. Ir. K.C.A.M Luyben

voorzitter van het College voor Promoties,

in het openbaar te verdedigen op

maandag, 15 mei, 2017 om 15:00 uur

door

Andries Jacob KNULST

Master of Science,

geboren te Bergen op Zoom, Nederland

Dit proefschrift is goedgekeurd door de

Promotor: Prof. dr. J. Dankelman

De promotiecommissie bestaat uit:

Rector Magnificus,	voorzitter
Prof. dr. J. Dankelman	promotor

onafhankelijke leden:

Prof. dr. F.W. Jansen	Leiden Un. Med. Center
Prof. dr. J.F. Lange	EU Rotterdam
Prof. dr. ir. R.H.M. Goossens	IO, TU Delft
Prof. dr. ir. C.A. Grimbergen	3mE, TU Delft, U-Amsterdam
Dr. E. Laporte	Instituto de Cirugia Hospital Quir
Dr. ir. F.P. Wieringa	Maastricht UMC / IMEC

Cover design: Arjo Loeve, www.ArjoLoeve.nl
Printing: Ipskamp drukkers
ISBN/EAN: 978-94-028-0594-9

The studies described in this thesis were carried out within the MISIT group at the department of BioMechanical Engineering, Faculty of 3mE, Delft University of Technology, the Netherlands
This research is supported by the Dutch Technology Foundation STW, applied science division of NWO and the Technology Program of the Ministry of Economic Affairs.

Table of Contents

x

Summary

The surgical light is an important tool for surgeons to create and maintain good visibility on the surgical task. Chapter 1 gives background to the field of (surgical) lighting and related terminology. Although the surgical light has been developed strongly since its introduction a long time ago, the last decades only minor developments have been made. This lack of significant development suggests that the current state of surgical lighting is perfectly developed and functions without any flaws. However, literature might give a different perspective. Apparently, despite the lack of significant developments in surgical illumination, the current surgical lighting systems are not good enough yet. This thesis aims to identify problems associated with the use of surgical lights and to improve surgical illumination.

Ergonomic problems of surgical lighting systems have been indicated by surgeons according to literature; however, the underlying causes are not clear. The aim of this study (Chapter 2) is to assess the problems in detail. Luminaire use during 46 hours of surgery was observed and quantified. Furthermore, a questionnaire on perceived illumination of and usability problems with surgical luminaires was issued among OR-staff in 13 hospitals. The results showed that every 7.5 minute a luminaire action (LA) takes place, intended to reposition the luminaire. Of these LAs, 74% was performed by surgeons and residents. For 64% of these LAs the surgical tasks of OR-staff were interrupted. The amount of LAs to obtain a well-lit wound, the illumination level, shadows, and the illumination of deep wounds were most frequently indicated lighting aspects needing improvement. Different kinematic aspects of the pendant system of the lights that influence usability were also mentioned: high forces for repositioning, ease of focusing and aiming, ease of moving, collisions of the luminaire, entangling of pendant arms, and manoeuvrability. Based on these results conclusions regarding to improvement of surgical lighting systems are formulated. Focus for improvements should be on minimizing the need for repositioning the luminaire by studying and improving illumination characteristics (Chapters 3-8), and on minimizing the effort for repositioning by studying and improving the system mechanics (Chapters 9-13).

The illumination performance of surgical luminaires is quantified by performance indicators defined in an international standard. The remaining maximum illuminance in relevant situations, the light field size, and the spectral characteristics are performance indicators used by hospitals as input for luminaire opting processes. However, industry focuses on illuminance when communicating with health care professionals. The aim of this study (Chapter 3) is to evaluate whether these standards are sufficient to describe luminaire performance, especially for modern LED lighting technology. Illuminance distribution and spectrum measurements were performed on 5 different state-of-the-art (LED) surgical luminaires. The results showed that changing situations not only changed the maximum illuminance but also changed the light field sizes and shapes, introducing substantial differences between luminaires. Moreover, coloured cast

shadows and light colour variations across the light field were observed for 3 luminaires using differently coloured LEDs. Both the changing light field sizes and shapes, and the cast shadows and light colour variations for LED luminaires are not covered by the current standard. The standard should therefore be extended to incorporate these aspects, especially for such a high-end application as surgical lighting.

Hospitals may have difficulties in selecting proper surgical lights based on information provided by industry. The aim of this study (Chapter 4) is to evaluate the illumination characteristics of LED lights objectively to ease the selection of surgical lighting. The illuminance distribution of five main and four auxiliary lights was measured in eight clinically relevant scenarios. For each light and scenario, the maximum illuminance Ec [kilolux] and the size of the light field d10 [millimetres] were computed. The results showed: that large variations for both Ec (25-160 klx) and d10 (109-300mm) existed; that using auxiliary lights reduced both Ec and d10 with up to 80% and 30%; that with segmented lights uneven light distributions occurred; and that with coloured-LED lights shadow edges on the surgical field became coloured. Objective illuminance measurements showed a wide variation between lights and a superiority of main over auxiliary lights. Uneven light distributions and coloured shadows indicate that LED lights still need to converge to an optimal design.

For undisturbed vision the design of surgical overhead and head-mounted lights is focused on providing shadow free light. However, shadow is reported as an important cue for depth perception in mono-visual as well as in stereo-visual situations. As surgeons repeatedly touch delicate tissue with their instruments, their depth-perception should not be hampered. This study (Chapter 5) evaluated the influence of shadow on human performance when executing stereo-visual pointing tasks. Two experiments were performed; Experiment 1 studied the effect of the existence of shadows, Experiment 2 studied the effect of the direction of shadows. Subjects were instructed to point random sequences of virtual targets accurately under different shadow situations. The subject's performance was described by the spatial error E (distance to target [mm]). Experiment 1 showed that both large and small high-contrast shadows gave a significantly smaller spatial error E (4.8, 4.6 mm, respectively) than either low-contrast shadows (5.6 mm) or no shadows (6.3 mm). Experiment 2 showed that the Error varied (2.1 to 3.2 mm) for different illumination directions. The Error decreased with an increasing angle between the line-of-sight and line-of-light. Illuminating from the centre or from the left side of the observer gave better results than from the right side. Surgical lights should provide a clear shadow from a light source that illuminates from within the vertical plane through the line-of-sight, and with a 90° angle with respect to the line-of-sight to maximize the depth-perception of a surgeon.

Visual performance and visual comfort are a combined effect of the lumination characteristics and the illuminated objects. This study (Chapter 6) aims to assess the effect of the luminance ratio of the wound and its direct surroundings on the visual performance and comfort of humans. Visual performance (Score and Threshold) and

perceived Comfort were tested on 40 subjects during 7 Luminance ratios (0.1 to 7.0) using a contrast discrimination task at the Centre and Edge of the wound. Highest scores, lowest thresholds, and highest comfort were obtained for Luminance ratios around 1. The colour difference between wound and surroundings seemed to have a dominant effect as the Edge Score was reduced by a factor 0.8, and the Edge Threshold was increased by a factor 2.2 compared to the Centre. For good surgical illumination both luminance and colour need to be balanced to obtain maximum visual performance and comfort, invariant to the task location within the wound.

A new lighting device for open surgery of difficult access wounds was designed: the Extender add-on. The performance of the Extender is evaluated and compared with the conventional solutions used in the operating room (OR) on illumination quality (Chapter 7). A cylindrical setup was built to measure the distribution of light in a simulated pelvic wound. The light was provided by a head-mounted light, an OR light, and a pair of Extender prototypes. The results showed that the Extender prototypes provided 12.2 lumens inside the wound, whereas the head-mounted light gave 5.7 lumens. The Extenders provided smoothly angular distributed light from 0° to 180°, whereas the head-mounted light and OR light only provided light from 115° to 180°. The Extender prototypes had a promising performance in terms of light distribution. It is expected that a more accurately produced Extender will increase performance in terms of illumination quantity and illumination distribution smoothness even further.

Current surgical lighting systems have a fixed shape lumination pattern whereas the wound and surroundings have a variable shape and characteristics. A lighting system that is able to adapt its shape and light distribution to the characteristics of the wound might improve visual performance. Chapter 8 describes the development of a new concept for lighting using bendable stripes with LEDs. The basic idea of placing LEDs on a bendable surface is very simple and elegant. To achieve a functional system it is important to investigate the effects of the different design choices, such as shape of the stripes, number of LEDs, number of stripes, and LED power. The influence of these choices will be evaluated by simulation using a computational model to identify the optimal parameters for the design. The final design is evaluated using the computational model and a physical prototype consisting of one luminaire segment. The system is able to produce light fields that can have fairly complex shapes at a good range of different sizes. It was possible to give recommendations about aspects like spot size and strip number. The physical test model indicates that the calculated system seems to function in a way that is close to how it would in a real-life situation. Given the results it can be concluded that a system, which is able to modify the light field in real time and that requires minimal control effort, can be a good addition to the operating room.

High handling forces of surgical lighting systems limit their usability. To make improvements to the mechanical design of the system the behaviour of the system should be understood. Therefore, this study (Chapter 9) presents a model that predicts handling forces of the system. Geometry and joint friction torques of a real lighting system were measured and implemented in a validated force model. Mean, standard

deviation within the spatial region, minimum and maximum forces were computed for 3 different regions of the working area. The mean (and standard deviation within the spatial region) forces were 129 (106) N in the centre region, and 61 (14) N and 60 (17) N in more off-centre regions. The simulation results showed high handling forces in the central region, explaining the observed repositioning patterns of the surgical light during surgery. The model can also be used to compare different lighting systems, or to evaluate the effect of design changes.

Chapter 10 investigates whether a three- or four-arm pendant design could improve the performance of a pendant system in terms of mean, maximum and variation of handling forces for different parts of the working area. A validated simulation model was used to compare two-, three-, and four-arm designs on the mean, maximum and variation of handling forces across different parts of the working area. In the most frequently used area, the three-arm design reduced the mean force by 3.8x and the variation of force 19.4x. The locations of the maximum forces were shifted to less frequently used areas. The four-arm design did not outperform the three-arm design. The three-arm design improved the performance and usability of the pendant system as handling forces were reduced in the most intensively used part of the working area. However, the singularities were not completely annihilated, so a more fundamentally different mechanism is required.

The goal of this study (Chapter 11) is to design a surgical luminaire suspension system that improves luminaire repositioning by a more fundamental approach. A computer aided method was devised to optimise the mechanism kinematics to the required movement space in the operating room. This resulted in 13900 serial combinations of revolute joints, prismatic joints and links. Based on a scoring routine, a selection of concepts was made and further assessed. The resulting concept is an adaptation of the translational subsystem of the conventional suspension mechanism and is considered most feasible. The adaptations consist of a rail system from which the mechanism is suspended and a wrapping pair that couples the two vertical rotations of the pendant-type mechanism. As a result, the horizontal movement space is improved and described without singularity.

The redesign of the translational subsystem - without the possibility of singularity - is compared to the conventional translational subsystem in a user experiment with 14 participants. Chapter 12 described this study. The experiment is performed outside the operating room, with one setup that can be altered between two designs; an uncoupled state with the kinematics of the conventional subsystem, and a coupled state with the redesigned kinematics. The work cost of a movement in the conventional uncoupled state is confirmed to depend on the spatial orientation of the mechanism, which is not the case in the new coupled state. Due to these different kinetics the movement patterns with the coupled mechanism are more consistent between participants, the duration of movements is shorter, less problems occur and participants are able to better control the movements. This result validates the redesign and confirms the hypothesis that a translational subsystem without the

possibility of singularity within its movement space will improve luminaire repositioning.

Position adaptions of surgical lights occur frequently and interrupt the surgical procedure. A semi-automatically adaptable lighting system controlled by a wireless pointer could minimize the need for and impact of adaptations. A low-cost pointer and tracking system based on four Wii-remotes™ could be sufficient for such a task. Chapter 13 studies such system. The accuracy and precision of the system were determined using single markers at a known position. The pointer was also evaluated on orientation estimation and wound shape reconstruction. For single markers the absolute accuracy was 2.8mm, and the precision was 0.72mm. The pointer centre location could be estimated with 9.8mm accuracy and 0.27mm precision, and the pointer angle with 2.2° accuracy and 0.7° precision. The location and radius of a 100mm and 220mm diameter wound could be reconstructed with a maximum error of 8mm and 36mm respectively. The tracking system is therefore suitable for low-accuracy tracking tasks underneath the surgical light.

Although research on surgical illumination has not been a topic of much research in the last decades, this thesis shows that there is much to gain in terms of ergonomics, optimal illumination and improved interaction with surgical lights. Chapter 14 is the closing chapter of this thesis, discussing and concluding to which extend the thesis goals were achieved. It was concluded that the frequency of luminaire adjustments and the high adjustment forces of the current system are the main issues encountered during use of surgical lights. The approach of this project was to improve surgical illumination by reducing the frequency of luminaire adjustments through improved illumination techniques and conditions, and by reducing the adverse effects of adjustments for the surgeon through improved mechanics and through an alternative method of illumination control. Although clinical user evaluations have not been done, the functional evaluations have shown that in-wound lights sources and adaptive surgical lights can improve the illumination distribution across the surgical task. Also, functional evaluations have shown that alternative and more intuitive suspension systems for surgical lights reduce the required handling forces for luminaire adjustments. The feasibility of a Wii-based tracking system for control of adaptive, actuated surgical lights was demonstrated. Finally, integration of the knowledge and concepts presented in this thesis is expected to lead to improved surgical illumination.

Chapter 1

Introduction to surgical lighting

The surgical light is an important tool for surgeons to create and maintain good visibility on the surgical task. Although the surgical light has been developed strongly since its introduction a long time ago, the last decades only minor developments have been made. This lack of significant development suggests that the current state of surgical lighting is perfectly developed and functions without any flaws. However, literature might give a different perspective. Apparently, despite the lack of significant developments in surgical illumination, the current surgical lighting systems are not good enough yet. This thesis aims to identify problems associated with the use of surgical lights and to improve surgical illumination.

1.1 Motivation

The surgical light is an important tool for surgeons to create and maintain good visibility on the surgical task. Although the surgical light has been developed strongly since its introduction a long time ago, the last decades only minor developments have been made. Besides the adoption of new light source technologies, not much has changed in surgical illumination. This lack of significant development suggests that the current state of surgical lighting is perfectly developed and functions without any flaws. However, literature might give a different perspective. According to three studies (Patkin 2003; Matern and Koneczny 2006; Matern and Koneczny 2007) surgical lights were experienced as a major source of irritation and problems during use of the lights. 71% of German surgeons experienced problems with the use of their lights. The problems ranged from colliding suspension arms to problematic positioning of the lights, and from hard to focus to insufficient illumination of the wound. 41% already had experienced a potential hazard for the patient or surgical personnel that were evoked by the surgical light. Apparently, despite the lack of significant developments in surgical illumination, the current surgical lighting systems are not good enough yet. This thesis aims to identify problems associated with the use of surgical lights and to improve surgical illumination.

1.2 History and developments

During the Middle Ages surgery was mainly done at public places, using daylight for good illumination of the surgical workplace. Later on, facilities dedicated for surgery were developed, allowing spectators to watch the procedure. These facilities had the appearance of a theatre, with seats around the operating table and were, therefore, called operating theatres. Operating theatres were mainly build on the top floor of buildings, with many windows in the ceiling to achieve a well-lit workplace. An example of one of the oldest existing operating theatres can be found in the Old Operating Theatre Museum, located in the garret of St-Thomas' Church in Southwark (Fig. 1.1). Some operating theatres had some mirrors in the corners of the operating theatre to reduce blockage of the natural light by the surgeons themselves.

Figure 1.1 Old operating theatre in the Old Operating Theatre Museum, Southwark (Reeve 2004).

In the 1880s electric lighting was introduced in the operating theatre. Initially, this technology provided very diffuse, poorly controlled light that emitted large amounts of heat towards the surgeon and the wound. Since then, technological improvements have led to very stable, well controlled, and focused overhead surgical luminaires that use one or more halogen or gas discharge light sources (Fig. 1.2a) to provide large amounts of light to the surgical task whilst minimizing the radiant heat toward the surgeon and the wound. Nowadays, modern surgical lights are increasingly equipped with multiple Light Emitting Diode (LED) light sources (Fig. 1.2b) that allow even more control over the illumination and radiant heat, although halogen and gas discharge based lights are still available as an established alternative. All those surgical luminaires have to comply to the requirements of the standard for surgical lights (IEC 2009).

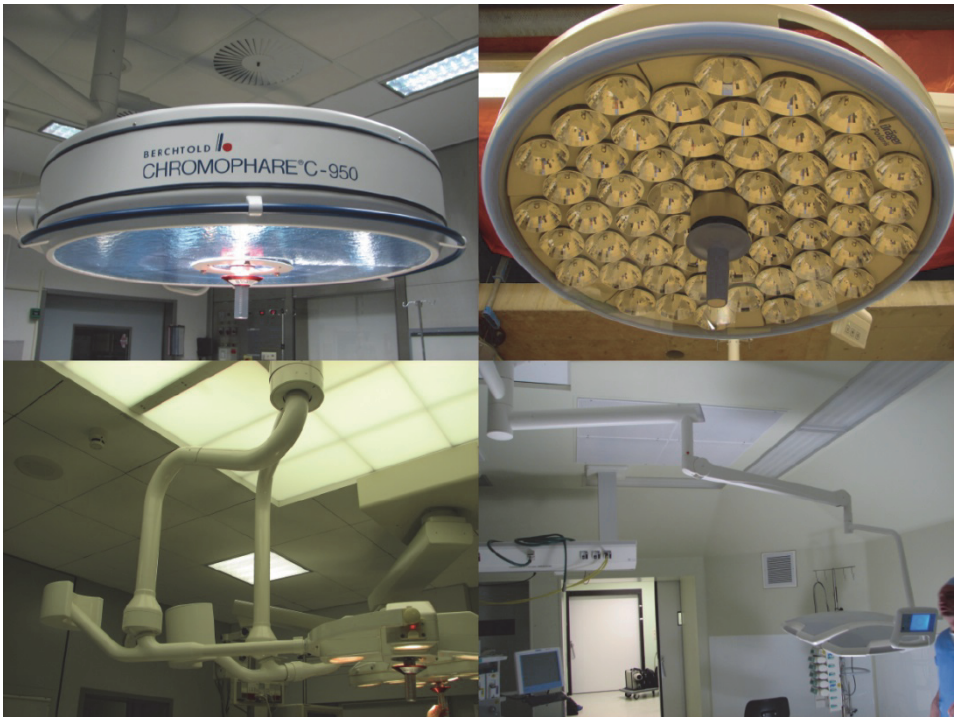

Figure 1.2 a. An older, halogen based surgical light (upper left) and b. a modern LED based surgical light (upper right). C. An older suspension system with a counterweight (lower left) and d. a modern suspension system with a spring-arm (lower right).

The first electric surgical lights were mount at a fixed position somewhere above the operating table. However, as lights became more powerful and more focused, soon the need arose for lights that could be positioned and directed. This need has led to the development of pendant arm suspension systems, inspired by the suspension systems of hair dryers. In the 1950s, the suspension systems typically consisted of an arm that was mount to the wall or the ceiling of the operating room, connected to a second arm that carried the surgical light at one end, and a counterweight for balancing at the other end (Fig. 1.2c). The connecting rotational joints allowed for 3D positioning of the light, and the light itself was attached to a yoke that enabled aiming of the light. The light could be operated by the surgeon using a sterile handle attached to the light. During further developments the counterweight was replaced by a spring-arm system that used a spring to statically balance the weight of the surgical light (Fig. 1.2d). This pendant system is the standard in today's operating rooms.

1.3 Background

1.3.1 Background on light and vision

Some understanding of basic concepts and terminology on light and vision is required before reading this thesis. Therefore, some basic concepts and terminology is condensed in this section. For a more extensive reading and thorough understanding of the concepts of light and colour vision the work of Boyce on Human Factors in Lighting (Boyce 2003) might be a good start.

Light

Light is a specific part of the electromagnetic spectrum that creates a response in the human visual system, and is characterized by electromagnetic wavelengths (λ) ranging from 380 to 780 nm. The sensitivity of the human eye is not identical for each wavelength, and therefore, the response of the human eye to electromagnetic radiation is characterized by a relative spectral sensitivity curve. This relative spectral sensitivity curve is dependent on both the visual conditions and individual differences. Therefore, during the last hundred years the 'Commision Internationale de l'Eclairage' (CIE) has agreed on a set of Standard Observers V(λ) for different visual conditions. These relative spectral sensitivity curves are the basis for the conversion between radiometric data and photometric data by weighing the measured electromagnetic spectrum with a spectral sensitivity curve. Whereas radiometric data is characterized by radiant flux [W], irradiance [W/m^2], radiance [$W/m^2/sr$], and radiant intensity [W/sr]; photometric data is characterized by luminous flux [lm], illuminance [lux or lm/m^2], luminance [cd/m^2], and luminous intensity [cd] (Table 1.1).

Table 1.1 Photometric quantities

Measure	Definition	Units
Luminous flux	The part of the radiant flux that produces a visual sensation.	Lumens (lm)
Luminous intensity	The luminous flux emitted into a small cone into a certain direction, expressed as lumens per unit solid angle.	Candela (cd or lm/sr)
Illuminance	The luminous flux per unit area incident at a point of a surface.	lm/m^2 (lux)
Luminance	The luminous flux emitted from a surface in a given direction divided by the projected area of the emitting surface.	cd/m^2

When light reaches the surface of an object the light is partly reflected, partly transmitted and partly absorbed by the object, depending on the optical properties of

the object. The object does not interact the same way with different wavelengths of the incident light. The reflection, transmission and absorption are wavelength dependent. When light falls on an object and is reflected then the spectrum of the reflected light is the product of the spectrum of the incident light and of the spectral reflection of the object.

Colour

The human visual system contains basically four different sensors that are sensitive to light: rods (for vision during dark conditions) and three types of cones (for colour vision). To represent the colour of light, three mathematical colour matching functions $x(\lambda)$, $y(\lambda)$, $z(\lambda)$ have been defined that convert a certain electromagnetic spectrum into three imaginary primary colours X, Y and Z. Again, different colour matching functions exist, and CIE has agreed on a number of Standard Observers. The obtained primary colours can be converted to colour coordinates or CIE 1931 chromaticity coordinates: x, y and z. By definition, $x+y+z=1$, so only two coordinates are required to define the chromaticity of light, and commonly, only x and y are defined. Besides the CIE 1931 (x,y) chromaticity system other colour systems exist. These alternative colour systems are mathematical conversions that attempt to make the colour systems more perceptually uniform.

Although the CIE colorimetric system is the most complete and most widely accepted way to quantify colour, it is rather complex. Therefore, two single-number metrics have been derived to characterize the colour properties of a light source: correlated colour temperature (CCT) and CIE General Colour Rendering Index (CRI). The CCT is a metric that compares the colour appearance of the light emitted by the light source under consideration to some standard blackbody light source. CRI is a metric that compares the appearance of a set of surface colours illuminated by the light source under consideration to the appearance when illuminated by some standard blackbody light source.

The human visual system

The human visual system consists of the eyes and the brain. The eyes are purely the sensory system of the visual system, visually connecting the brain to the outside world. The eye consists of an optical part and a neural part. The optical part has a pupil, a variable opening that regulates the amount of light that enters the eye, and an adjustable lens to focus the incoming image onto the neural part. The neural part consists of a large amount of four different types of photosensitive cells that together form the neural retina. These cells form the earlier mentioned rods and cones. The photosensitive cells convert incoming visual stimuli into electrical signals that will be processed by the neural retina and the visual cortex in the brain. This signal processing is highly complex and still not completely understood.

The human visual system can process information in an enormous range of luminances, but not all at once. The visual system adapts itself to the actual visual conditions, finding a trade-off between sensitivity and discrimination. These adaptations involve three mechanisms: change in pupil size, neural adaptation, and

photochemical adaptation. Neural adaptation is the fastest mechanism (200ms), operating at moderate luminance levels, and can correct 2-3 log units. Change in pupil size is slower (0.3 to 1.5s) and has a limited effect. Photochemical adaptation is the slowest process, it takes the cones 10-12 minutes, and the rods 60 minutes to achieve their maximum sensitivity. It is required for the large changes in luminance levels. The visual system approximately adapts to luminances present within 20° of visual angle.

The colour of light and objects under certain illumination conditions can easily be measured and represented by chromaticity coordinates. However, the way colours are seen and perceived by humans is a more complicated matter. For colour perception factors like the illumination level, the context of the surrounding luminances, the colour of the light, etc. play an important role. Colour appearance models have been developed to estimate the perception of colours. Most of these models can only be used in very simple and controlled laboratory conditions.

1.3.2 Background on suspending surgical lights in the operating room

Pendants

In a typical Operating Room (OR) the operating table is placed in the centre of the OR, with all kinds of equipment placed on pendant systems that suspend the equipment from the ceiling. The pendant systems allow relocation of the equipment within a certain area defined by the size and construction of the pendant. Also the surgical lights are connected to a pendant system. In most ORs, the pendant system of the lights is mounted at the centre of the ceiling, above the operating table. Fig 1.3 displays a surgical light and its suspension system. The suspension system consists of a horizontal arm, a spring arm, a spindle, and a yoke. The spindle forms the connection between the ceiling and the suspension system. The arms are connected by rotational joints that provide two degrees of freedom in the horizontal plane. The spring arm offers a degree of freedom in the vertical plane and statically balances the weight of the light. The yoke offers two or three rotational degrees of freedom to the light, depending on the design. In total, the surgical light can be adjusted over five or six degrees of freedom over a large working range, constrained by the dimensions of the pendant arms.

Laminar Air Flow

Nowadays, many operating rooms are equipped with a Laminar Air Flow (LAF) system that provides a sterile, laminar air flow to the surgical table to reduce the risk of contamination of the wound. Objects between the LAF exit and the surgical table can distort the laminar flow, introducing turbulence and therefore increase the risk of contamination of the wound. Also surgical lights and their suspension can distort the air flow. This has been shown by both experiments and simulations (Memarzadeh and Manning 2002; Zoon, van der Heijden et al. 2010), where an increased particle count was monitored at the location of the wound. However, clinical evidence for an increased wound infection rate is lacking. The distortion of the LAF by surgical lights was outside the scope of this thesis, as the focus was on improved illumination and usability.

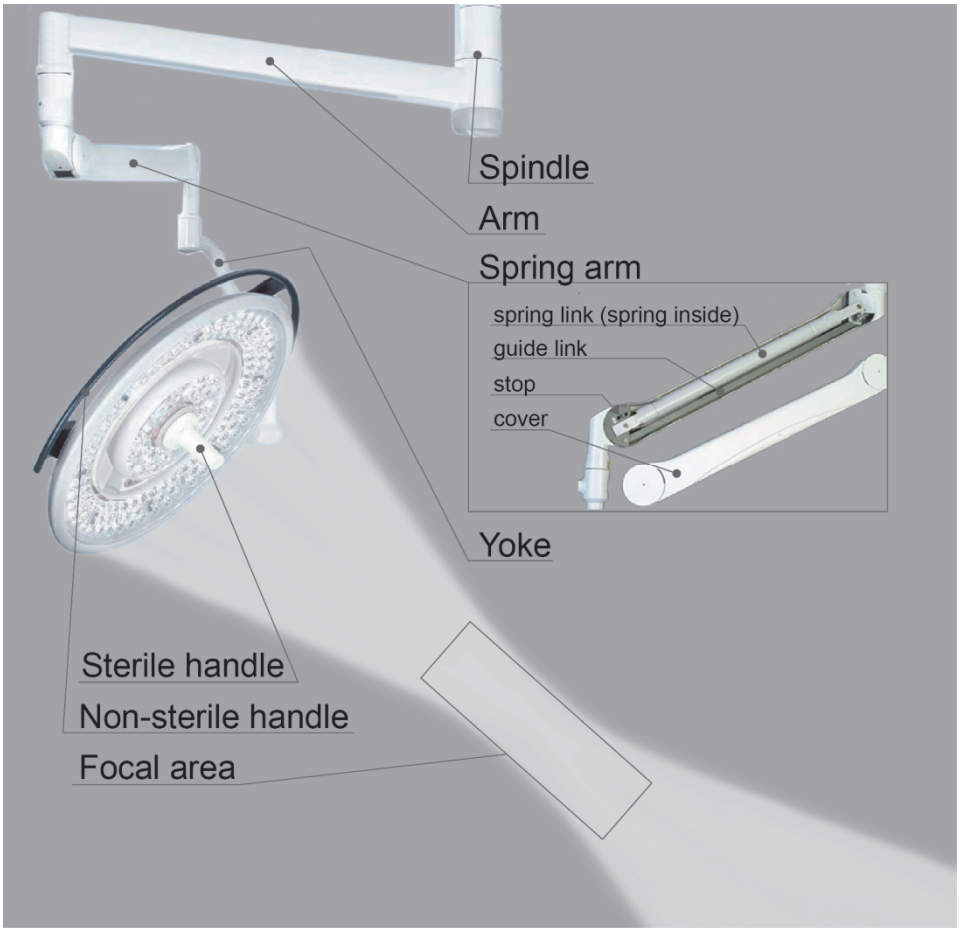

Figure 1.3 Picture of a typical suspension system of a surgical light.

1.4 Scope and goal

Although literature reports problems with surgical lighting as perceived by surgeons, an objective analysis of these problems has not been given. The use and flaws of surgical lighting systems needs to be studied and analysed to come with directions for improvements of surgical lighting and to develop an improved surgical lighting system that allows surgeons to work on an optimally illuminated task. This thesis aims to gain and implement knowledge that can be used to improve surgical illumination. Therefore, the current situation will be analysed to define what problems can be observed in the current situation and to isolate the causes for these problems. This approach will pinpoint issues around illumination systems and around suspension systems that need attention, improvements or even new knowledge in order to come up with ideas that may lead to better surgical illumination. These ideas will be

implemented into functional prototypes and evaluated on feasibility and functionality, both for illumination related and suspension related ideas.

Three main goals were specified that together will lead to improved surgical illumination:

1. Identify and analyse the problems associated with the use of surgical lights.
2. Improve illumination characteristics of surgical lights by:
   - gaining knowledge required to improve surgical illumination,
   - implementing the obtained knowledge in new ideas and solutions,
   - evaluating these solutions on their functionality and feasibility.
3. Improve suspension of surgical lights by:
   - gaining knowledge required to improve surgical suspensions,
   - implementing the obtained knowledge in new ideas and solutions,
   - evaluating these solutions on their functionality and feasibility.

1.5 Structure and the contents of this work

This thesis consists of three parts (Fig. 1.4). **Part 1** is an introduction on the use of and problems with the surgical light, investigated using an observation study and a questionnaire. Chapter 2 will describe the methodology and results of the observation study and the questionnaire.

Part 2, spanning Chapters 3 to 8, focuses on the reduction of the need for adjustments of the luminaire. Chapter 3 will investigate whether the current standard for surgical lights enforces sufficient descriptive parameters for the state-of-the-art surgical lights. Chapter 4 will study the illumination performance of state-of-the-art surgical lights under varying conditions according to an extended set of descriptive parameters. Chapter 5 will investigate the relevance of shadows for depth perception during open surgery, including the effect of complete elimination of shadows. Chapter 6 will study the importance and the effects of the balance in luminance ratios across the surgical field on the visual performance and comfort of surgeons. Chapter 7 will study the concept of an illumination method using small light sources inside a small, deep wound. Chapter 8 will investigate the design and evaluation of an adaptable surgical light that offers the functionality to tune the light beam to the geometry of a wound for good distribution of the illumination. All chapters in this part of the thesis will contribute to improved surgical illumination with less need for adjustments during surgery.

Part 3, spanning Chapters 9 to 13, focuses on the reduction of the negative effects of adjustments of the luminaire, e.g., on improving the interaction between the surgeon and the light. In Chapter 9 a model will be developed that describes the mechanical behaviour of a typical surgical suspension system. Chapter 10 will evaluate the effect of adding more joints to the suspension system on the mechanical behaviour of the system. Chapter 11 will explore a more fundamental, extensive approach to optimizing the suspension system layout. Chapter 12 will evaluate an improved suspension system that is free of singularities and easy to actuate. Chapter 13 will evaluate the

suitability of an affordable sensor system for easy control of the position, orientation and illuminance distribution of the luminaire.

Chapter 14 forms the closing chapter of this thesis, discussing how the findings of this thesis have contributed to improved surgical illumination. Also, the integration of some of the different proposed solutions will be discussed. And finally, it will be discussed to what extend the goals of this thesis have been met.

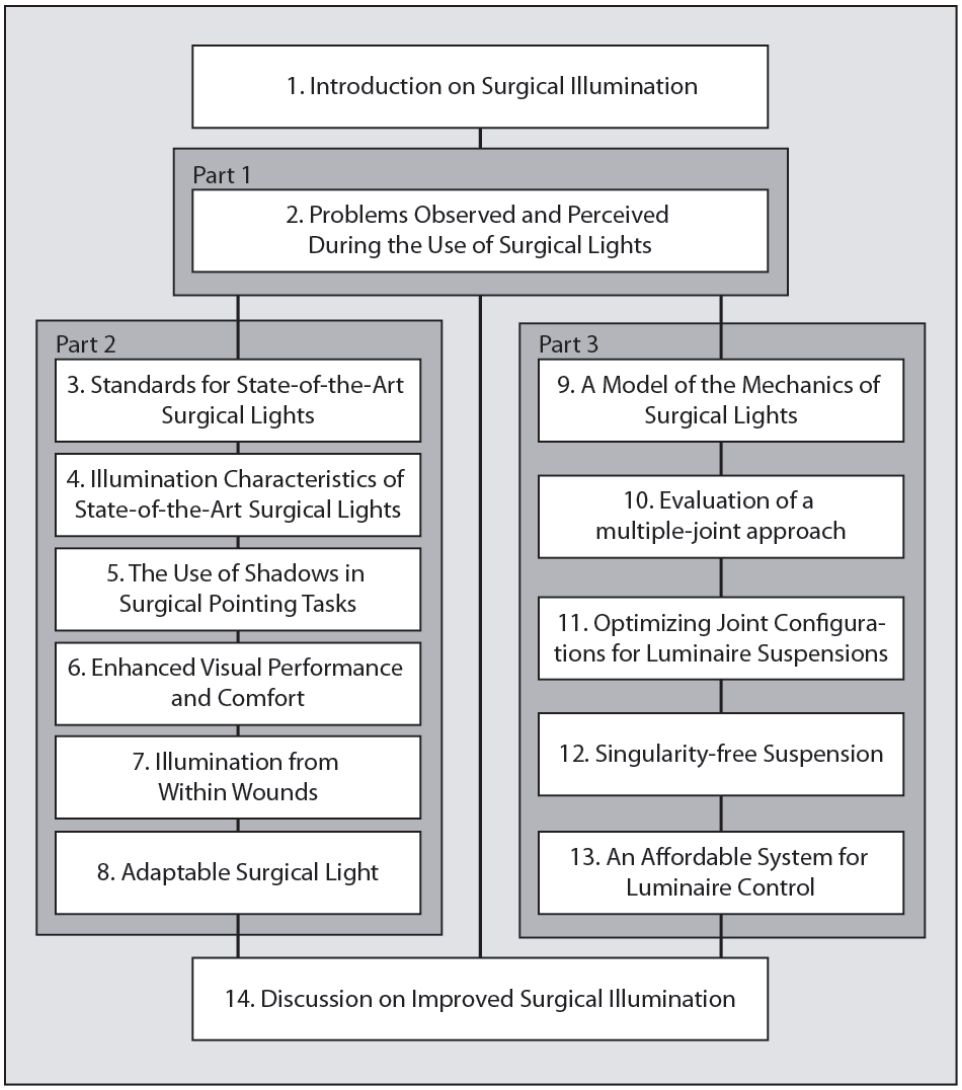

Figure 1.4 Thesis structure and layout

1.6 References

Boyce, P. R. (2003). Human factors in Lighting, Taylor & Francis Ltd.

IEC (2009). International Standard - Medical electrical equipment - Part 2-41 Particular requirements for the safety of surgical luminaires and luminaires for diagnosis. Geneva, International Electrotechnical Commission**:** 38.

Matern, U. and S. Koneczny (2006). "Working conditions in the operating room: Surgeons surveyed during the Annual Meeting of the German Society of Surgery 2004." Ergebnisse der umfrage zu den arbeitsbedingungen im OP auf dem Deutschen Chirurgenkongress 2004 **131**(5): 393-400.

Matern, U. and S. Koneczny (2007). "Safety, hazards and ergonomics in the operating room." Surgical Endoscopy **21**(11): 1965-1969.

Memarzadeh, F. and A. P. Manning (2002). Comparison of operating room ventilation systems in the protection of the surgical site. ASHRAE Transactions, Honolulu, HI.

Patkin, M. (2003). "What surgeons want in operating rooms." Minimally Invasive Therapy and Allied Technologies **12**(6): 256-262.

Reeve, M. (2004). Interior of The Old Operating Theatre. Creative Commons Attribution-ShareAlike license. Wikipedia**:** Old Operating Theatre Interior, London. Photograph by Michael Reeve, 31 May 2004.

Zoon, W. A. C., M. G. M. van der Heijden, et al. (2010). "On the applicability of the laminar flow index when selecting surgical lighting." Building and Environment **45**(9): 1976-1983.

Chapter 2

Indicating Shortcomings in Surgical Lighting Systems

Arjan J. Knulst, Rik Mooijweer, Frank W. Jansen, Laurents P.S. Stassen,
Jenny Dankelman

Minimally Invasive Therapy & Allied Technologies 20(5): 267-275, 2011

Ergonomic problems of surgical lighting systems have been indicated by surgeons; however, the underlying causes are not clear. The aim of this study is to assess the problems in detail. Luminaire use during 46 hours of surgery was observed and quantified. Furthermore, a questionnaire on perceived illumination of and usability problems with surgical luminaires was issued among OR-staff in 13 hospitals. The results showed that every 7.5 minute a luminaire action (LA) takes place, intended to reposition the luminaire. Of these LAs, 74% was performed by surgeons and residents. For 64% of these LAs the surgical tasks of OR-staff were interrupted. The amount of LAs to obtain a well-lit wound, the illumination level, shadows, and the illumination of deep wounds were most frequently indicated lighting aspects needing improvement. Different kinematic aspects of the pendant system of the lights that influence usability were also mentioned: high forces for repositioning, ease of focusing and aiming, ease of moving, collisions of the luminaire, entangling of pendant arms, and manoeuvrability. Based on these results conclusions regarding to improvement of surgical lighting systems are formulated. Focus for improvements should be on minimizing the need for repositioning the luminaire, and on minimizing the effort for repositioning.

2.1 Introduction

For many years, illumination of wounds during surgery has been done by surgical luminaires. Such a surgical lighting system (SLS) basically consists of a large, heavy luminaire suspended from the wall or ceiling by a two-arm pendant system. The luminaire has been designed such that high-intensity light is supplied to the wound while minimizing shadows of heads and hands of the surgical team. The pendant system has been designed to allow great flexibility in positioning of the luminaire and to stabilize the position of the luminaire in a certain position.

Although the fundamental design of the SLS has not been changed for years, surgeons still complain about their SLSs. Ergonomic shortcomings of several aspects in operating rooms, including surgical lighting have been indicated by different authors (Quebbeman 1993; Geisse 1994; Berguer 1996; Berguer 1997; Berguer 1999; Rohrich 2001; Patkin 2003; Matern and Koneczny 2007). A German and an Australian study both have indicated a need for ergonomic improvements of the lighting system (Patkin 2003; Matern and Koneczny 2007). Complaints varied from colliding pendant arms to lights banging against heads and from insufficient illumination to one-handed adjustments of the lights being impossible. The underlying causes of these problems and how often and in what situations these problems occur were not studied. For improvement of SLSs, more detailed information on shortcomings and problems of SLSs is needed.

The aim of this study was to assess the shortcomings of SLSs in more detail and indicate areas of interest for improvements in the design of SLSs. An observational study in the Operating Room (OR) during various types of surgery was used to detect and quantify problems of perioperative luminaire usage. An online questionnaire was used to extend the observed findings by the user experience of both surgeons and assistants to different SLSs and to different Dutch hospitals. The outcome of the study pinpoints areas of interest for improving SLSs.

2.2 Materials and Methods

2.2.1 Observational study

The study was carried out in the Reinier de Graaf Hospital in Delft, a large non-university teaching hospital. Observations were done in two ORs having the same SLS consisting of a large main luminaire (Berchtold Chromophare C950) and a small auxiliary luminaire (Berchtold Chromophare D530 plus). Both luminaires have an adjustable focus and illumination level, and 6 degrees of freedom (3 translations of the luminaire, 2 rotations of the luminaire and 1 rotation of the complete SLS around its central ceiling mount).

In the study the use of the OR luminaires during 46 hours of surgery (14 procedures) was observed. The surgical procedures were selected with the surgeons for both their routine nature and likeliness for luminaire actions (LAs). Some procedures included multiple wound locations at different locations of the body, some had large wound areas and others had narrow and deep wounds. The selected procedures were: 6 gastrointestinal, 2 vascular, 3 breast, and 2 thyroid gland surgical procedures.

During surgery all SLS-related actions of any OR staff were recorded, initially only on a predefined fill-out spreadsheet, and during the last 10 procedures also by a video camera. The video camera captured only the SLS and OR staff interacting with the SLS, the patient remained out of the camera's sight. OR staff was asked to explain the reason for the LA, but only if the clinical situation allowed this communication to the observer.

Afterwards, the video recordings were analysed manually and the results were added to the spreadsheet. The complete spreadsheet listed:

- the function of the luminaire operator (LO) performing the LA: either being surgeon, resident, assisting nurse, or circulating nurse;
- whether the LO was actually performing surgical tasks at the moment of LA;
- the type of the LA: either translating or rotating the luminaire, adapting the illumination level, or adapting the focus of the light;
- the duration of the LA, defined from the moment that the operator starts looking for the luminaire to begin interaction until the LO ends his interaction by continuing his original task;
- whether relocations of the luminaire did take place along the shortest route in 3D space;
- whether the relocation was one- or two handed;
- the phase of surgery: four phases were determined:

1. initializing: the team is ready to start, but no incision is made yet,
2. surgery:
    - Opening: from first incision to the placement of retractors,
    - Surgical tasks: from placement of retractors until removal of the retractors,
    - Closing: from removal of the retractors until the last stitch,
3. finalizing: the wound is closed, but still some actions to the patient are being performed;

- any additional comments on the LA.

2.2.2 Questionnaire

To extend our findings from the observational study to other hospitals an online questionnaire was formulated. Thirteen hospitals were included, being university and non-university teaching hospitals. Each questionnaire was tailored to the SLSs installed in those hospitals. The questionnaires were spread in each hospital among surgeons, residents, and OR nurses by surgeons that supported the study.

The questionnaire consisted of two parts:

1. a series of questions to profile the participant, and to let them indicate procedures where lighting is perceived as cumbersome;
2. items in which the participant had to indicate their most used SLS from a listing of pictures and whether or not different aspects for lighting and usability of this SLS had to be improved.

The results of the questionnaire were exported to MS Excel for analysis.

2.3 Results

2.3.1 Observational study

During the observed 46 hours of surgery, in total 364 LAs were noticed, resulting in an average of one LA every 7.5 minutes. All those LAs were identified as repositioning actions of the luminaire. The light beam's focus or the illumination levels were never adapted during the observation period. The dominant reason (97%) for the LAs was a change of the surgeon's area of interest where optimal vision was needed.

Figure 2.1 shows which OR staff member performed the LAs during surgery as percentage of the total number of LAs. The surgeons performed 45% of all observed LAs, and in 97% of those LAs these were interrupting their surgical tasks to do the LA. Residents took 25% of the LAs, during which they were interrupting their surgical tasks in 73% of the cases. Assisting nurses took 22% of the LAs (0% interrupting surgical tasks) and circulating nurses took 7% of the LAs (0% interrupting surgical tasks). In total, 64% of all LAs surgical tasks were interrupted for repositioning the light.

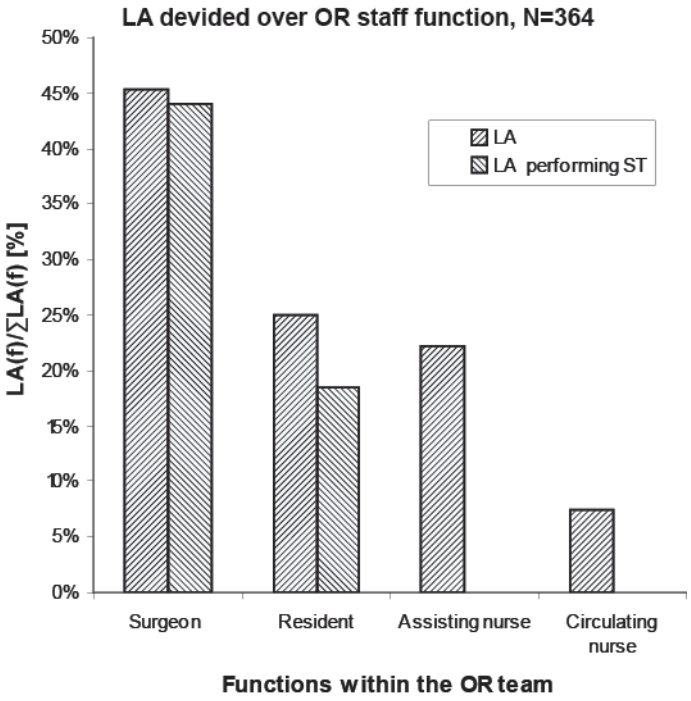

Figure 2.1 Luminaire actions (LA) performed by OR-staff members. In many LA the staff member was simultaneously performing surgical tasks (ST) that were interrupted for the LA.

Figure 2.2 displays in what phases of surgery the LAs occurred. Most LAs (67%) took place during phase 2b, where actual surgery in the wound was being performed. During the opening and closing of the wound 30% of the LAs were done, mainly

because the knife or the needle driver were followed with the light pattern when progressing along the line of incision.

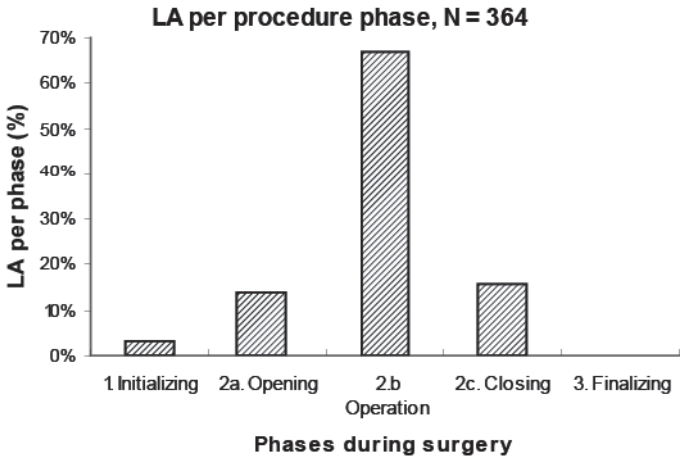

Figure 2.2 Luminaire actions (LA) performed in different phases of the surgical procedure.

The LAs that were recorded on video (249 LAs) could be more extensively analysed afterwards. Figure 2.3 shows a histogram of the duration of the LAs, stacked by surgical phase. Most LAs (78%) took less than 8 seconds to complete the action. The remaining 22% LAs took longer to complete because of complications during the LA.

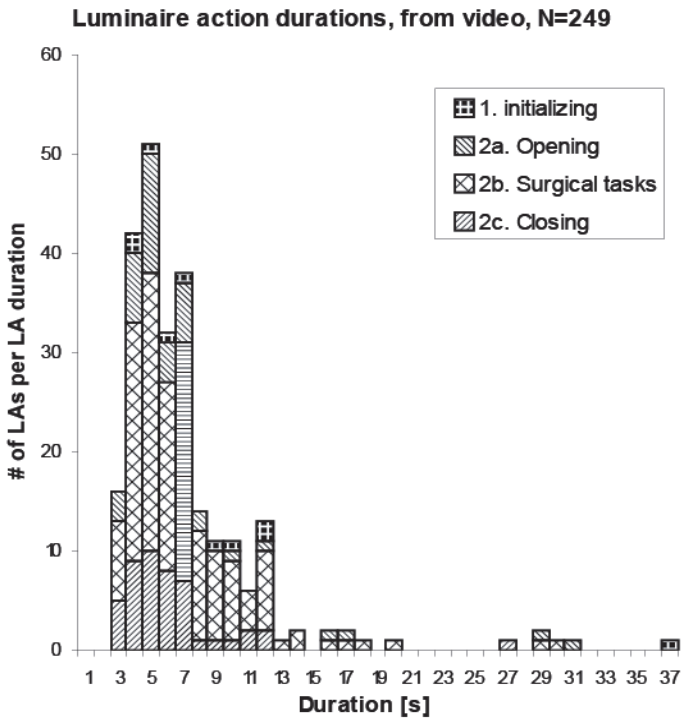

Figure 2.3 Stacked Histogram in which the duration of every single luminaire action (LA) that was recorded on video is distributed over 1-second intervals.

The median LA durations - overall and per phase of surgery - are given in Fig. 2.4. The outliers indicate the most problematic adaptations of the SLS. Clearly, most complications occurred during surgery phases 2a-2c, where they have the highest impact on distraction of the surgical team.

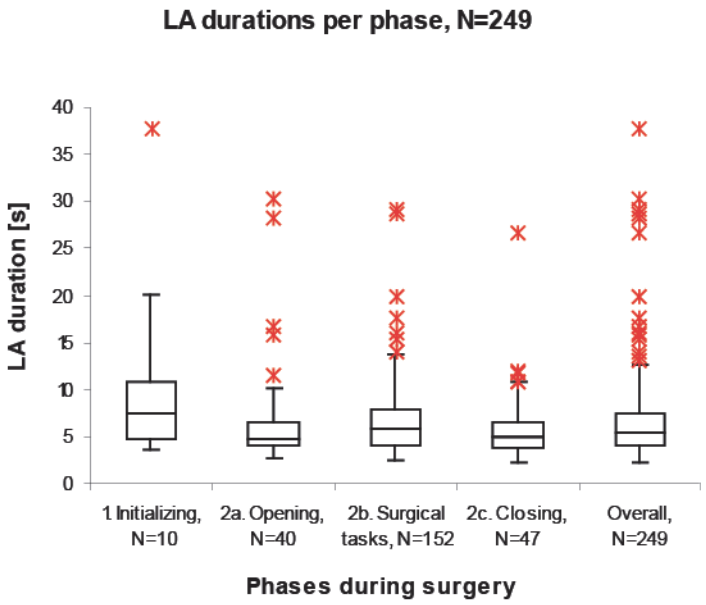

Figure 2.4 Boxplot displaying Luminaire action (LA) durations during surgery, analysed for the complete dataset (Overall) and per phase of surgery (phase 1 to 2c).

Figure 2.5 depicts the observed complications:

1. Mechanical problems (24 events): These problems included high forces, requiring two-handed adaptations; locking of the pendant system, in which moving it by operating the sterile handle is completely impossible, in some cases the circulating nurse had to help on the repositioning.
2. Collisions of the luminaire against any object (17 events): when moving the luminaire around, it bumps into other lights, to heads of OR-staff, to its own ceiling mount, and to IV-poles.
3. Out of reach: Surgeon had to stand up (4 events): from a sitting posture the lights were hard to reach or control.

If such complications occurred, they caused the median duration of the LAs to double, as is shown in Fig. 2.6.

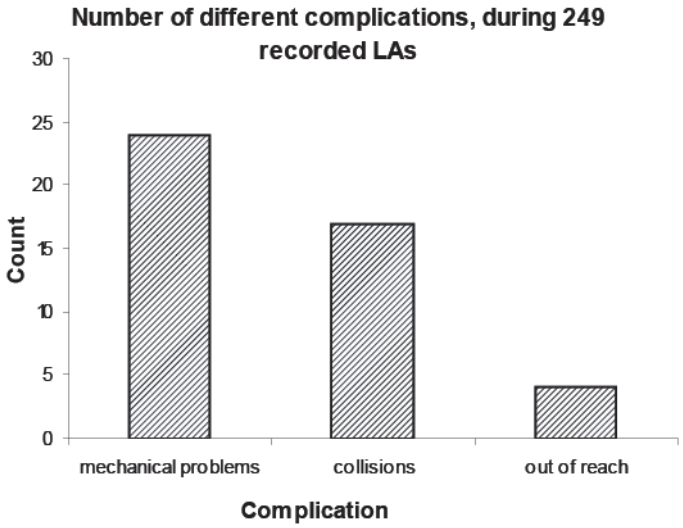

Figure 2.5 Different types of complications in luminaire use that were observed during performing luminaire actions.

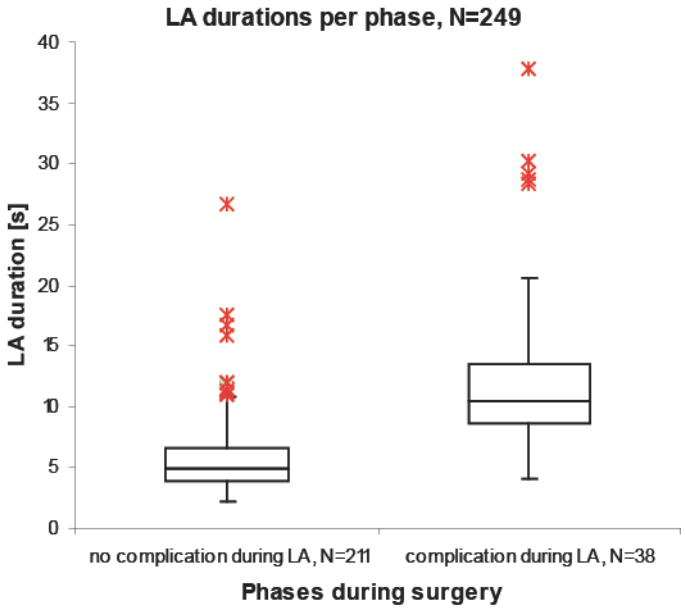

Figure 2.6 The effect of complications (Fig. 5) during LA on LA duration.

Figure 2.7 shows whether the LA was a pure translational movement of the luminaire, or a pure rotational movement, or a combination of these. Almost 30% were pure rotations of the luminaire, consisting of slight adjustments of the location of the light pattern on the wound. Most LAs (66%) were combinations of translations and

rotations, either because of larger changes of the light pattern location, or because of change of the angle of the light beam.

The video analysis showed that in 56% of all LAs the luminaire was not repositioned from any point A to B along the shortest possible path, but along an alternative trajectory. LAs where the shortest path was followed took about 66% the median duration of a non-shortest path LA (4.5 vs. 6.8 s).

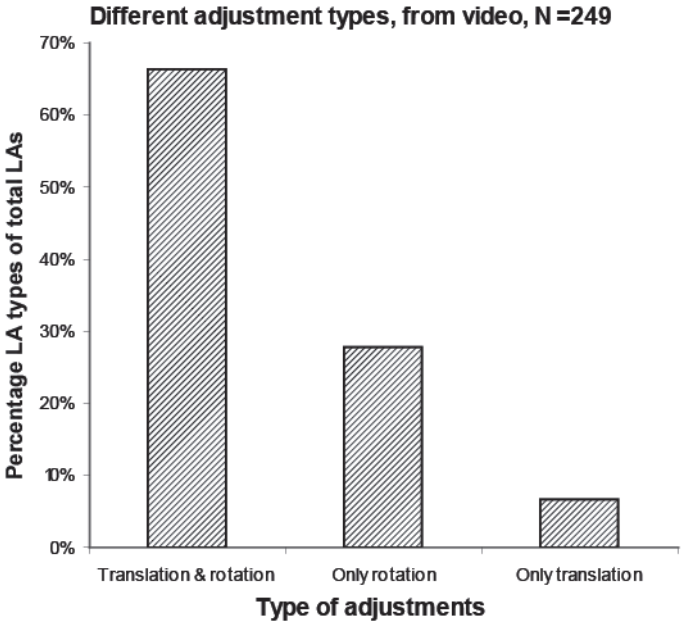

Figure 2.7 An overview of the different types of luminaire positioning actions.

2.3.2 Questionnaire

Part 1. The questionnaire was completed by 98 OR staff members from 12 hospitals, of whom 43 (43%) were surgeons, 16 (16%) were residents, and 40 (40%) were OR nurses. Most participants were female (57%) and 43% were male. Of the surgeons, 51% were general surgeons, 16% vascular surgeons, and the remaining 33% were either orthopaedic, trauma, thoracic, or gynaecological surgeons. Most participants (91%) were working in ORs equipped with 2 luminaires, and two groups of each 4% were working with 1 or 3 luminaires. Many of the surgeons (88%) indicated that they experienced problematic lighting during surgery. The top 4 examples of procedures that have problematic lighting that were mentioned are: transthoracic surgery (23%), (deep) pelvic surgery (21%), rectal surgery (15%), and deep abdominal surgery (15%). In general, the problematic types of surgery seem to have a deep wound with a narrow entrance to the cavity.

Part 2. Figure 2.8 shows where OR staff saw needs for improvement on 9 light-related aspects of SLSs. The results for each aspect of lighting are split for suggestions of surgeons, residents, and OR-nurses. The mostly indicated areas of attention for

improvements –and thus the most perceived problems- were: the illumination of deep wounds, the frequency of repositioning the light to keep proper illumination, reduction of shadows, and the illumination level of the light beam.

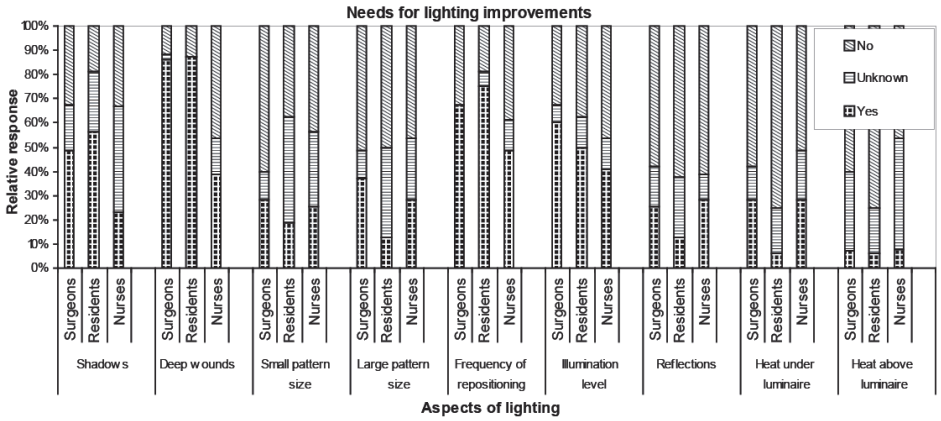

Figure 2.8 Responses of surgeons (N=43), residents (N=16), and OR-nurses (N=39) on the question if improvement was needed for 9 different aspects of lighting.

Figure 2.9 displays where OR staff indicated room for improvement on 8 usability-related aspects of SLSs. The results for each aspect of usability were subdivided in suggestions of surgeons, residents, and OR-nurses. Compared to Fig. 2.8, the general need for improvements on usability seem to be higher than for lighting. Moreover, the indicated aspects for improvement were not limited to a few items, but covered almost all questioned aspects. These results confirm the observed problems in the OR.

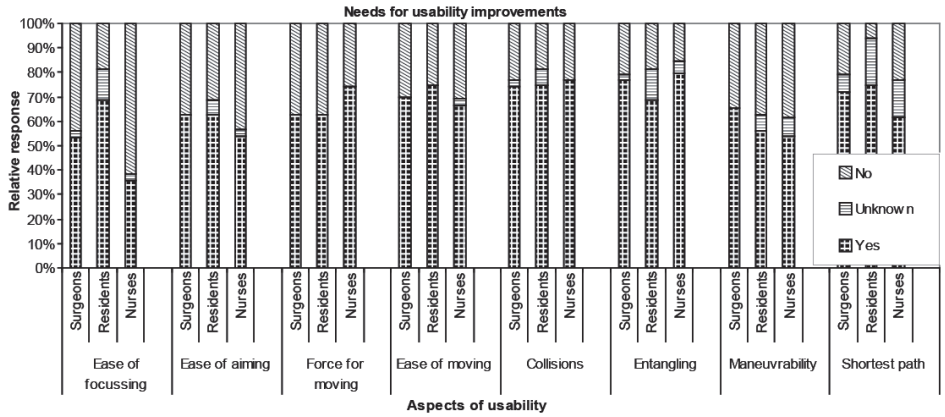

Figure 2.9 Responses of surgeons (N=43), residents (N=16), and OR-nurses (N=39) on the question if improvement was needed for 8 different aspects of usability.

2.4 Discussion

This study shows that the need for repositioning the luminaire during surgery is high, and that repositioning is cumbersome. The focus of improving surgical lighting systems should be on minimizing the need for repositioning the luminaire, and on minimizing the forces required for such actions.

The aim of this study was to assess shortcomings of surgical lighting systems (SLSs) and indicate areas of interest for design improvements of SLSs, by observing SLS usage during 46 hours of surgery and by a questionnaire filled out by 98 OR-staff members. It was shown that luminaire actions (LAs) occur frequently, every 7.5 minutes. Furthermore, it was shown that those LAs were dominantly done by the surgeon, interrupting the surgical tasks. The reason for these LAs was to re-establish good lighting at changing working areas within wounds, especially in large wounds, in small deep wounds, and in case of multiple wounds. Different mechanical shortcomings of the SLSs caused more than one fifth of the LAs to be cumbersome to perform and to take more time to complete. High operating forces and immobility of the luminaire in certain positions seemed to cause most of the LA problems, together with the expected risk of collision. These observations were also perceived as problematic by OR staff, as shown by the questionnaire.

The validity of our observational findings was extended by using a questionnaire in different university and non-university teaching hospitals to check the observed problems of SLSs. The numbers of hospitals, staff members and different surgical disciplines that were included in this questionnaire were limited. Due to this limitation some problems that are specific for certain surgical disciplines might be overlooked. However, the general problems with SLS use - like lighting deep wounds, shadows, and mechanical issues - are likely to be valid in any surgery as the basic task and setup of the SLS is identical, although the frequency of problem occurrence might be different because of differences in the surgical situation.

Most LAs were performed by surgeons and residents, while they were performing surgical tasks. This is logic, as only they can judge when lighting is insufficiently directed or what improvement in illumination can be expected when the luminaire is repositioned. Therefore, it is wise that they are in command of the lighting system. However, it is undesirable that their attention is drawn away from surgery frequently, for an unnecessary long period of time or too intensively. Especially in crucial situations inadequate lighting or a cumbersome repositioning process to obtain a well-lit situation was reported to create potential hazards (Matern and Koneczny 2007).

A sound surgical lighting solution will provide always good illumination at a wide range of locations simultaneously, thus minimizing the need for and effect of luminaire repositioning. As small-entrance deep wounds were reported to be difficult to illuminate, the development of tailored lighting solutions might be advisable for these cases. Surgical headlights might improve lighting in these cases, but they have drawbacks in terms of comfort, mobility, and user-friendliness. In such way, the need for frequent luminaire repositioning will be reduced. A further experimental study with wound models – especially the hard-to-illuminate wounds - and different illumination

concepts, including the use of surgical headlights, will give better insights on this matter.

Meanwhile, when the need for luminaire repositioning arises, the surgeon should be able to perform this task with minimal effort and by paying minimal attention to this secondary task. An important issue is the high forces that are required to reposition the luminaire, and that are to be exerted in -ergonomically- a challenging posture: above the head. These forces seem to vary with the position of the luminaire relative to its ceiling mount. Close to this ceiling mount the required operating forces will increase enormously, and cause even an immovable luminaire, presumably because of a severe reduction of the moment arm whilst friction moments in the pendant system still need to be overcome. Also the large number of repositioning via non-shortest paths can be explained by the large forces in some areas of the workspace. A model is currently being developed to estimate the contribution of different mechanical parameters to the required operating force in different luminaire positions. With the help of such a model an improved low-operating force pendant system can be developed.

Attention should also be paid to the risk of collisions and entanglement of the luminaire or pendant with heads, other luminaires, or pendant arms. Especially in ORs with many pendant arms for various pieces of equipment these collisions and entanglements are problematic. Solving this problem is not straightforward. A lighting system without pendants would tackle this aspect, but would induce reduced mobility and flexibility of the system, causing many situations hard to illuminate. A robotic, intelligent pendant system on the other hand, could avoid collisions when repositioning the luminaire; however, this increases complexity and costs. Further analysis on collision prevention is required.

2.5 Conclusion

In conclusion, this study pinpointed illumination and usability shortcomings of present surgical lighting systems. The quintessence of improving surgical luminaires is minimizing the need for repositioning the luminaire by the surgical team and minimizing the forces required for these actions. In that way, surgeons will be able to concentrate on their main task, and perform surgery in a well-illuminated wound and by a user-friendly lighting system.

2.6 References

Berguer, R. (1996). "Ergonomics in the operating room." American Journal of Surgery **171**(4): 385-386.

Berguer, R. (1997). "The application of ergonomics in the work environment of general surgeons." Reviews on Environmental Health **12**(2): 99-106.

Berguer, R. (1999). "Surgery and ergonomics." Archives of Surgery **134**(9): 1011-1016.

Geisse, J. K. (1994). "The dermatologic surgical suite." Seminars in Dermatology **13**(1): 2-9.

Matern, U. and S. Koneczny (2007). "Safety, hazards and ergonomics in the operating room." Surgical Endoscopy **21**(11): 1965-1969.

Patkin, M. (2003). "What surgeons want in operating rooms." Minimally Invasive Therapy and Allied Technologies **12**(6): 256-262.

Quebbeman, E. J. (1993). "Preparing the operating room. Care of the surgical patient: A publication of the committee on pre and postoperative care." Scientific American **5**: 1-13.

Rohrich, R. J. (2001). "Why I hate the headlight ... and other ways to protect your cervical spine." Plastic and Reconstructive Surgery **107**(4): 1037-1038.

Chapter 3

Standards and performance indicators for surgical luminaires

Arjan J. Knulst, Laurents P.S. Stassen, Cornelis A. Grimbergen, Jenny Dankelman

Standards and performance indicators for surgical luminaires.
LEUKOS 6(1): 37-49, 2009.

The illumination performance of surgical luminaires is quantified by performance indicators defined in an international standard (IEC 2000).The remaining maximum illuminance in relevant situations, the light field size, and the spectral characteristics are performance indicators used by hospitals as input for luminaire opting processes. Industry however focuses on illuminance when communicating with health care professionals. The aim of this study is to evaluate whether these standards are sufficient to describe luminaire performance, especially for modern LED lighting technology. Illuminance distribution and spectrum measurements were performed on 5 different state-of-the-art (LED) surgical luminaires. The results showed that changing situations not only changed the maximum illuminance but also changed the light field sizes and shapes, introducing substantial differences between luminaires. Moreover, coloured cast shadows and light colour variations across the light field were observed for 3 luminaires using differently coloured LEDs. Both the changing light field sizes and shapes, and the cast shadows and light colour variations for LED luminaires are not covered by the current standard. The standard should therefore be extended to incorporate these aspects, especially for such a high-end application as surgical lighting.

3.1 Introduction

Surgical luminaires are supposed to provide high quality, bright, comfortable and true colour illumination of a wound, even in difficult situations like deep cavities, and with the surgeons' heads and hands situated between the light source and the surgical site (Beck 1978, 1981; Dain, Hood et al. 1998; Gregory 1987; Hadrot 1999; Loonam and Millis 2003; Quebbeman 1993). Traditionally, these luminaires are most commonly designed as a large hemispherical reflector that contains a halogen or high intensity discharge light source. The reflector focuses the light to the desired focal point at the surgical field, provides sufficient deep cavity penetration, and minimizes the effect of shadows cast by objects between the luminaire and the surgical field. A relative new lighting technology is the white Light Emitting Diode (LED). Since white light LED technology has made major improvements, many manufacturers implement state-of-the-art LED technology in surgical luminaires. Although white LED technology is fairly new, many fundamentally different luminaire designs have been developed. However, the concept of these designs has not yet been fundamentally tested.

Performance measures for the illumination characteristics of surgical luminaires are defined by the international standard for surgical luminaires (IEC 2000). This standard describes a series of worldwide accepted measures that define the illumination characteristics at the position of the surgical site, in different well-defined scenarios. The different scenarios are simulated and simplified representations of situations like deep wounds or surgeon's heads obstructing the light beam between the luminaire and the wound. Typical illumination characteristics that are defined in the standard are the maximum illuminance at the centre of the light field and the light field size. The light field size needs to be measured in the unobstructed scenario only (IEC 2000), with the luminaire set to the smallest and largest illuminated field possible. The remaining maximum illuminance in these different scenarios as percentage of the unobstructed scenario is defined as a measure for luminaire performance (IEC 2000). The standard further describes colorimetric tests to be performed at maximum illuminance, in the centre of the light field. The light beam's correlated colour temperature, colour rendering index R_a, and chromaticity co-ordinates should lie within defined boundaries (IEC 2000). Ideally, all parameters mentioned above are presented in the product files by the manufacturers, to be used by hospitals as input for luminaire opting processes. Remarkably, in communication with health care professionals, manufacturers and their representatives often only mention maximal illuminance.

The primary aim of this study is to evaluate whether the change in maximum illuminance in different scenarios plus the smallest and largest available light field diameter in the unobstructed situation are sufficient parameters to describe the illuminance performance of the luminaire. For example, it might be that the whole illuminance distribution changes during varying scenarios, thereby changing the size and even the shape of the light field. Therefore, we measured the whole illuminance distribution during different scenarios to obtain the changes in light field size and shape.

The secondary aim of this study is to evaluate whether measuring the spectral characteristics at the light field centre is sufficient to describe the spectral characteristics for LED luminaires. As LED luminaires contain multiple light sources, the spectral properties might vary across the illuminated field. Therefore, spectral properties were measured at different locations in the illuminated field.

3.2 Materials and methods

3.2.1 Setup

The IEC standard defines illumination measurements that should be performed in the measurement plane, a horizontal plane 1 meter below the luminaire, centred on the point of maximum illuminance, the Light Field Centre "LFC". The illuminance at the LFC is called the central illuminance "E_c". The illuminance distribution on the measurement plane should be measured along four lines through the LFC lying 45° apart. On each of these lines, the points where the illuminance reaches 10% of the central illuminance should be determined. The distance between those points is by definition the light field diameter. Ideally, the illumination distribution should be radially decreasing, from the LFC outward.

A setup has been developed (Figure 3.1) to measure the illuminance distribution according to the IEC standard. A flat plate (60x60 cm) was used as illumination measurement plane. Four lines (numbered 1 to 4) were drawn through the centre of the plate, 45° apart. Along each of the four lines an aluminium ruler could be fixated. A calibrated photometer with a 13 mm sensor surface was secured to a slider that could be moved along the ruler to measure the illuminance. The illuminance was measured along each line, from the centre outward with a radial sample distance of 10 mm. A deep wound was simulated by placing a black PVC tube over the photometer as specified in the standard (IEC 2000). The heads of two surgeons were simulated by two circular masks, dimensions as specified in the standard (IEC 2000), placed 60 cm above the photometer head, and above line 3. The lowest light emitting surface of the luminaire was placed 1 m above the photometer head, and the vertical axis of the luminaire was centred above the measurement plane centre such that the luminaire's LFC coincides with the measurement plane centre, and the axis of the boom-luminaire connection was placed in parallel to line 1.

A calibrated spectroradiometer was standing by for spectral measurements in case unexpected colorimetric observations would happen. The luminaire was positioned 1 m above the sensor head during the spectral measurements. Both measured data from the spectroradiometer and the photometer were stored in a computer.

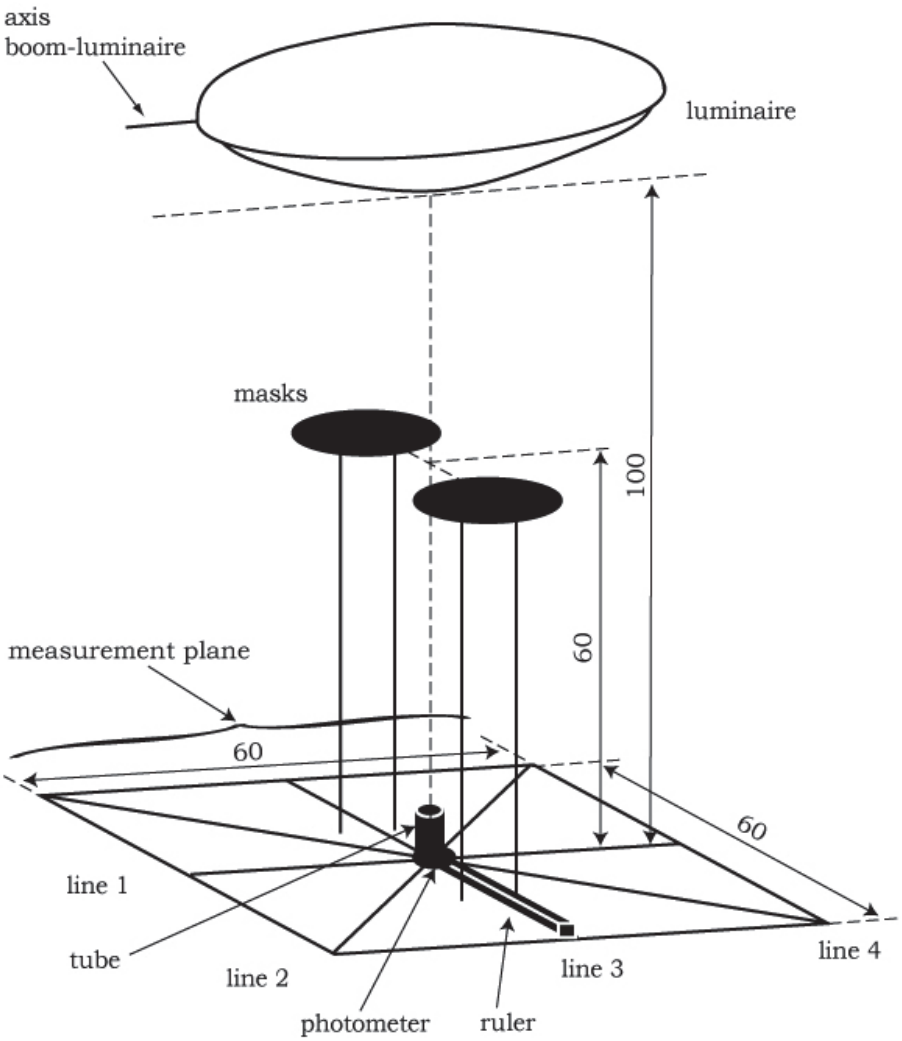

Figure 3.1 The setup designed for illuminance measurements. Dimensions are in cm. The Light Field Centre (LFC) is located in the measurement plane at the intersection point of the lines 1 to 4.

3.2.2 Scenarios and luminaires

To evaluate the illuminance distribution, eight scenarios were defined as different configurations of the measurement setup (Figure 3.1). Scenarios S1 to S4 had the luminaire set to the smallest light field, and scenarios L1 to L4 had the luminaire set to the largest light field. The scenarios and their definition are listed in Table 3.1. The illuminance distribution is measured over each line for each scenario. The standard (IEC 2000) requires reporting of the absolute maximum illuminance for S1, the maximum illuminances relative to E_c in Scenario S1 for S1 to S4, and the absolute light field diameters for S1 and L1.

Table 3.1 Definition of the eight scenarios. (a) a tube was placed, (b) two masks were placed, (c) the luminaire's light field diameter was set to the smallest or the largest possible.

Scenario	Tube (a)	Two masks (b)	Light field diameter (c)
Small 1 (S1)	No	No	Smallest
Small 2 (S2)	Yes	No	Smallest
Small 3 (S3)	No	Yes	Smallest
Small 4 (S4)	Yes	Yes	Smallest
Large 1 (L1)	No	No	Largest
Large 2 (L2)	Yes	No	Largest
Large 3 (L3)	No	Yes	Largest
Large 4 (L4)	Yes	Yes	Largest

Five different luminaire types were measured in operating rooms of two hospitals. One luminaire had a halogen light source, one had single colour LEDs, one had multiple colour chips in one LED unit, and two luminaires had a mixture of coloured LEDs. During the measurements the surgical luminaire was the only activated light source. The measured luminaires are shown in Figure 3.2, and are listed in Table 3.2.

Table 3.2 Overview of the measured luminaires and four relevant properties.

Type	Label	Light source technology	Adjustable colour temperature	Focusable	Rotational symmetric
Berchtold C950	A_1	Halogen	No	Yes	Yes
Maquet PowerLED 700	B_1	Cool white LEDs	No	No	Yes
KLS-Martin MarLED V16	C_1	Multicolour chip LEDs	Yes: min. 3800K max. 4800K	Yes, and option to create oval shaped light field	No
Trumpf iLED 5	D_1	Mixture of white and coloured LEDs	Yes: min. 3500K max. 5000K	Yes	No
Trilux Aurinio L160	E_1	Mixture of white and coloured LEDs	No	Yes	No

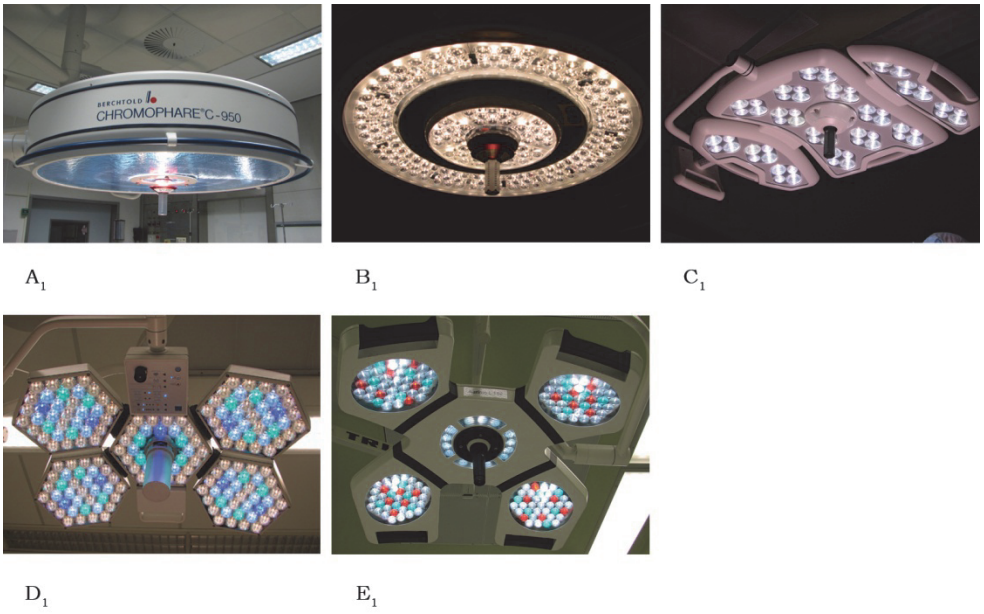

Figure 3.2. An overview of the luminaires A_1 to E_1 measured in this study, as defined in Table 2. Both D_1 and E_1 consist of four or five segments, slightly rotatable to adjust the luminaire's focus. The coloured LEDs of luminaires D_1 and E_1 are clearly visible.

3.2.3 Data processing

For each luminaire the measured illuminances were processed using software developed in Matlab 7.5 (The Mathworks Inc, 2007). The data processing contained the following steps for each luminaire:

1. For Scenario S1: Determine the maximum illuminance E_c and normalize the illuminance distribution such that the point of maximum illuminance is 100% E_c (IEC 2000). This normalized E_c is the reference value for the Scenarios S2 to L4.

2. For each scenario: Interpolate the illuminance distribution along each line to determine the radial locations where the illuminance is 50% or 10% E_c (IEC 2000). The distances between those points of 50% and 10% E_c are the light field diameters $d_{50,i}$ and $d_{10,i}$ along line *i* respectively. Calculate the light field diameters d_{50} and d_{10} in each scenario by averaging $d_{50,i}$ and $d_{10,i}$ over the 4 lines (IEC 2000).

3. For each scenario: Calculate the variation of the light field shape by dividing the maximum diameter by the minimum diameter in the light field found on any of the 4 lines.

4. For each scenario: Normalize the light field diameters with respect to the light field diameters found in Scenario S1.

The CIE 1931 (x,y) chromaticity co-ordinates, the colour rendering index R_a (CRI Ra), and the correlated colour temperature (CCT) were computed from the measured spectral data, according to their definitions (Schanda 2007).

3.3 Results

3.3.1 Illuminance measurement results

Figure 3.3 presents the influence of the different scenarios on the maximum illuminance E_c, the light field diameter d_{10}, and the light field diameter d_{50} for each luminaire relative to that luminaire in Scenario S1. Figure 3.3a shows that changing scenarios resulted in changing maximum illuminances for the different luminaires. The maximum illuminance is therefore shown to be scenario dependant. Figure 3.3b visualizes that the d_{10} light field diameters did change during these varying scenarios, and moreover that, especially in the large light field scenarios (L1 to L4), significant differences in light field sizes between luminaires were introduced. The d_{10} light field diameter was shown to be scenario dependant. Figure 3.3c displays the change of the d_{50} light field diameters. Note that from scenario S4 to L4 hardly any luminaire was able to generate a light spot having at least 50% of the maximum illuminance measured in scenario S1. It is illustrated clearly in Figure 3.3 that the maximum illuminance is not the only parameter that changes during the various measured scenarios and that also the light field diameters d_{10} and d_{50} are scenario dependant.

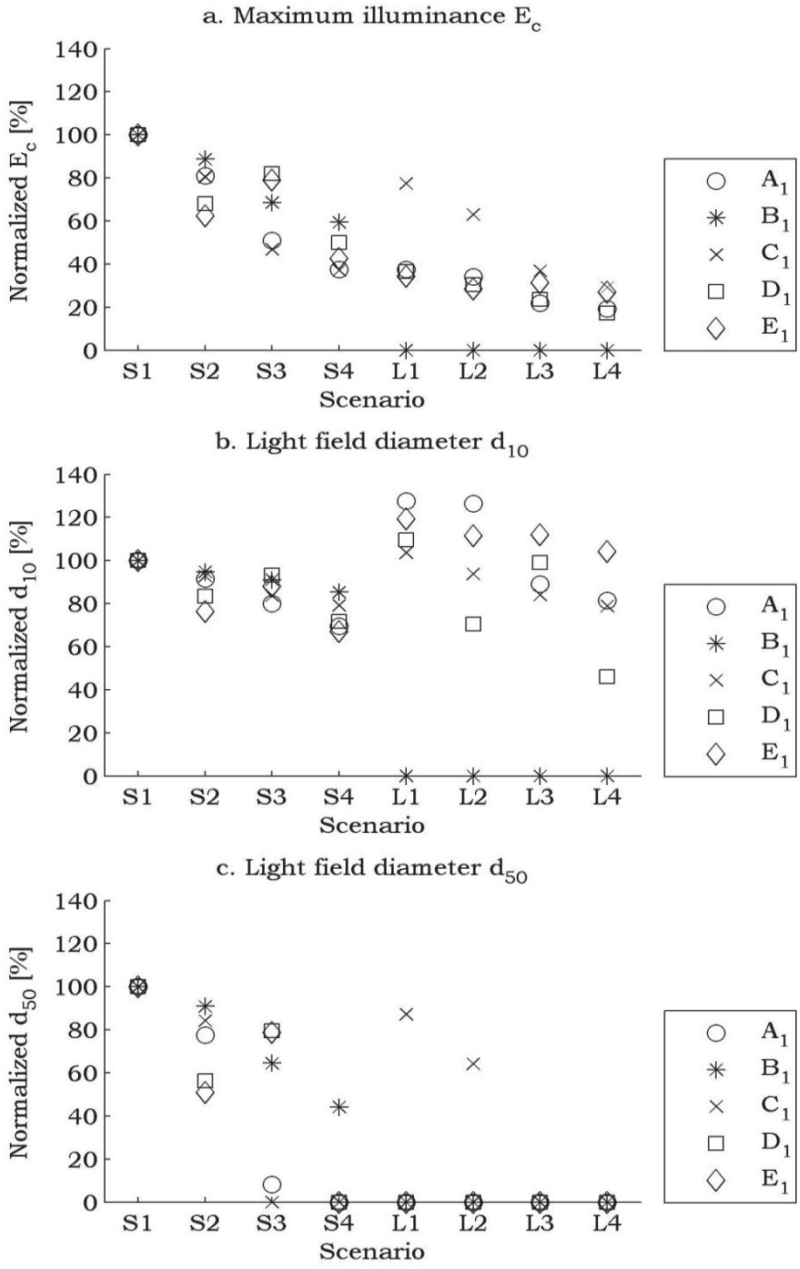

Figure 3.3 (a). The normalized maximum illuminance E_c, (b) the normalized light field diameter d_{10} and (c) the normalized light field diameter d_{50} in various scenarios. The legend labels the data points to luminaire types. As luminaire B_1 had no option to focus the light beam, its values for Scenario L1 to L4 are set to zero. The legend labels the data to luminaire types (Table 3.2).

Figure 3.4 shows the normalized changes of the light field diameters d_{10} and d_{50} as function of the corresponding normalized changes of illuminance E_c. The standard (IEC 2000) only requires measuring and reporting the change of illuminance in the different scenarios. This implies that change in light field diameter is either zero or equal to the change of illuminance. Therefore, Figure 3.4 shows the line of equal changes in light field diameter to changes in illuminance $d=E_c$ and the line of constant light field diameters d=100%. Figures 3.4a and 3.4b visualize the relation between the changing illuminance and the changing light field diameter d_{10} for both the small and large light field size. The figure clearly shows that the d_{10} light field diameter did change as the data points are not on the line d_{10}=100%, and that the diameter changes were less than the illuminance changes, as all data points are above the line $d_{10}=E_c$. These changes were found for both the small and the large light field size. Figures 3.4c and 3.4d visualize the same aspects as Figures 3.4a and 3.4b but now for the d_{50} light field diameter. Here it is shown that d_{50} was also subject to changes under varying scenarios. The changes of the d_{50} light field diameter were larger than the changes in illuminance, as most data points are situated below the line $d_{50}=E_c$. As Figure 3.3 supported the finding that the maximum illuminance E_c and the light field diameters d_{10} and d_{50} were scenario dependant, Figure 3.4 demonstrates that there was no evident relation between the illuminance and the light field diameters.

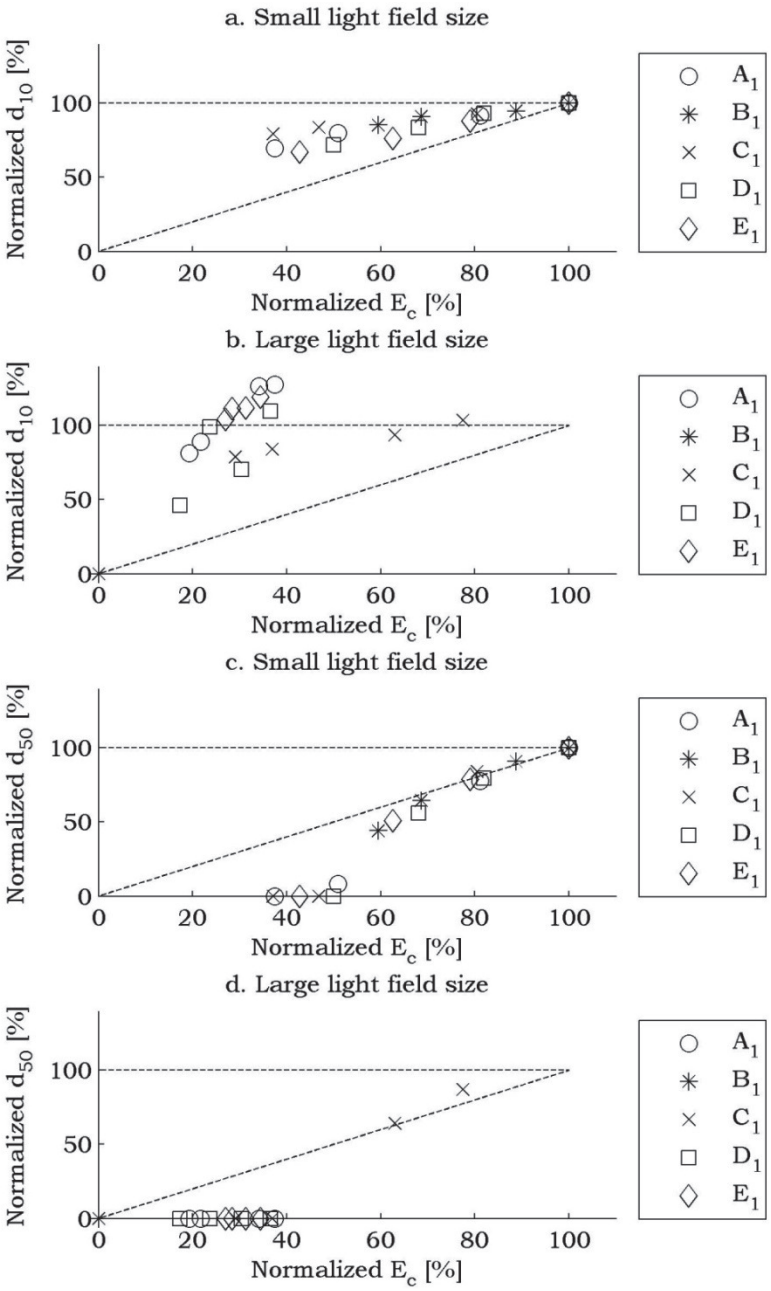

Figure 3.4 (a) Light field diameter d_{10} versus the maximum illuminance, for the smallest light field size, (b) light field diameter d_{10} versus the maximum illuminance, for the largest light field size, (c) light field diameter d_{50} versus the maximum illuminance, for the smallest light field size, (d) light field diameter d_{50} versus the maximum illuminance, for the largest light field. The dashed line is the relation $d=E_c$. The legend labels the data to luminaire types (Table 3.2).

Figure 3.5 represents for each measured luminaire the variation of the light field geometry for varying scenarios, displayed as the ratio of the maximum diameter over the minimum diameter found within the d_{10} light field during that scenario. The variation of the light field shape and the ratio differences between luminaires are most prominently visible for the large diameter Scenarios L1 to L4. The differences between the luminaires are the largest for Scenario L4, with the smallest and the largest ratio being 1.02 and 3.27 respectively.

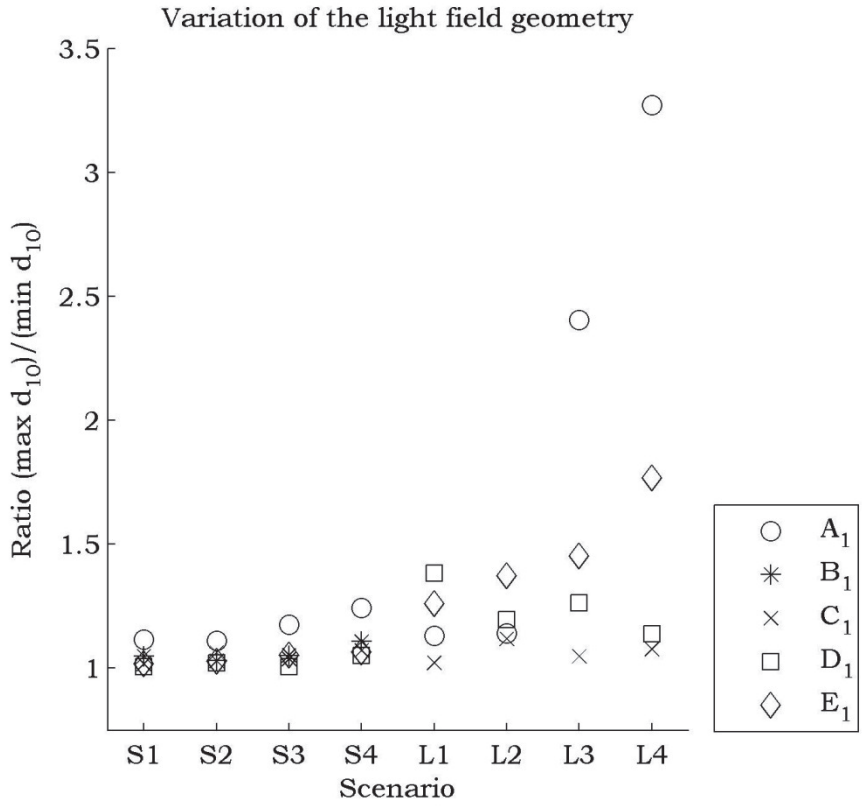

Figure 3.5 Variations of the light field geometry in different scenarios, represented as ratio of the maximum and minimum light field diameter found within the d_{10} light field. A ratio of one represents an identical sized light field shape in all measured directions.

3.3.2 Unexpected results

Besides the measured illuminance distributions a number of unexpected observations were noted. Figure 3.6 shows a photograph of the illumination distribution of luminaire E_1. Multiple illuminance peaks at the illuminated measurement surface are clearly visible. This phenomenon occurred when the focus of both luminaires D_1 and E_1 were adapted to the large light field. Luminaires D_1 and E_1 both consist of (four or five) segments that are completely packed with LEDs (Figure 3.2). Adapting the luminaire's

focus is done by slightly adapting the orientation of those individual segments. Each luminating segment creates its own illuminance distribution. For the smallest light field, the summated illuminance peaks of all individual segments overlap, thereby creating a single illuminance peak. Adapting the luminaire's focus shifts the illuminance peaks of each segment outward from the LFC, thereby creating the observed multiple illuminance peaks.

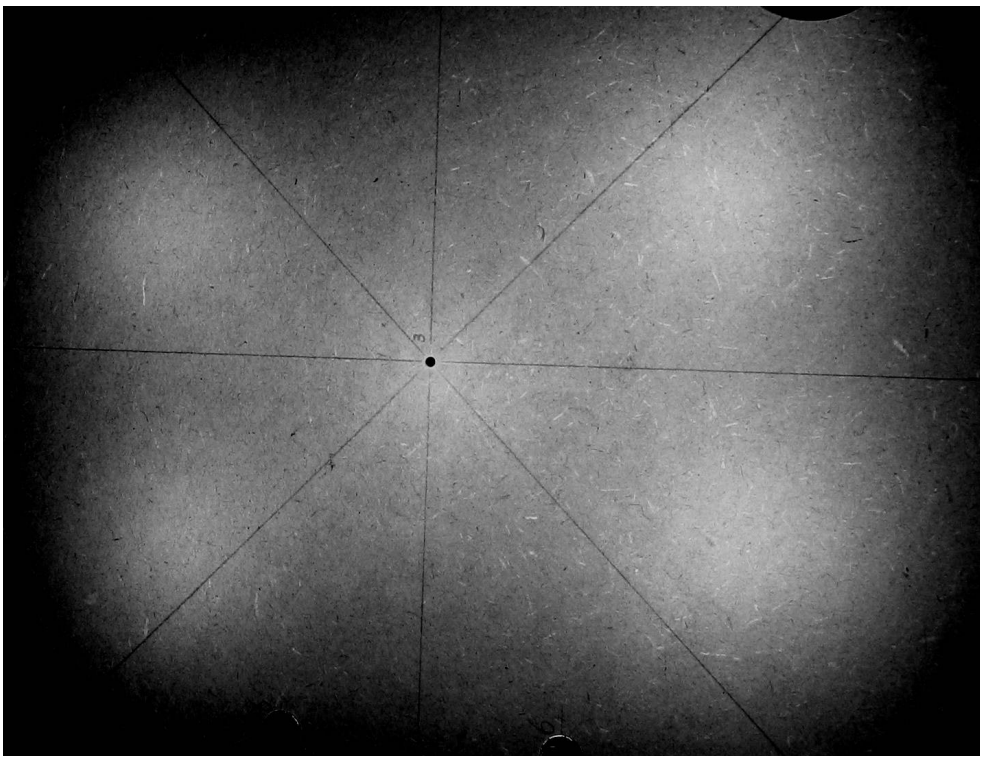

Figure 3.6: Photograph of multiple illuminance peaks on the measurement surface, as seen with luminaires D_1 and E_1 when using the large light field setting of the luminaire. Just visible are the 4 measurement lines drawn at the lighted surface. Note that the centres of the illuminance peaks lie next to these lines.

Light colour variations in the illuminated field were noticed when using luminaires that contain differently coloured LEDs, either as separate LED units or as differently coloured chips in one LED unit. During the first encounter with such a luminaire (C_1) the colour variations were noticed with the bare eye, showing reddish and bluish areas within the illuminated field. Table 3.3 shows the spectral characteristics of the luminaires with differently coloured LEDs, derived from the measured spectra. These luminaires were measured at different luminaire settings and at different locations within the illuminated field. Note that these spectral characteristics were different when the measurements were performed at different locations in the light field, or in different settings of the light field size.

Table 3.3 Light colour variations for luminaires containing differently coloured LEDs. All luminaires were measured in the small light field diameter, and at maximum power, unless stated otherwise. Shown are the correlated colour temperature (CCT), the colour rendering index (CRI R_a), and the colour co-ordinates according to the CIE 1931 (x,y) chromaticity co-ordinate system.

Luminaire	Setting	Location	CCT [K]	CRI R_a	CIE 1931 colour co-ordinates (x,y)
C_1	3800K	2 cm outside LFC	3740	93.3	(0.3798, 0.3450)
C_1	3800K, large light field	As previous	3906	92.8	(0.3722, 0.3372)
C_1	3800K, oval along Line 1	As previous	3802	92.6	(0.3760, 0.3394)
C_1	3800K, oval along Line 3	As previous	4021	93.2	(0.3688, 0.3367)
D_1	5000K	LFC	5292	93.2	(0.3369, 0.3394)
D_1	5000K	5 cm outside LFC	4600	94.2	(0.3564, 0.3570)
E_1	-	LFC	4713	93.5	(0.3547, 0.3681)
E_1	Large light field diameter	As previous	4992	85.9	(0.3471, 0.3748)

Another aspect of using differently coloured LEDs in luminaires is shown in Figure 3.7. This phenomenon was observed when shadow casting objects were placed between the luminaire and the illuminated field. The cast shadows showed a wide variation of colours, varying from reddish for C_1, from violet to orange for D_1, and from green to red for E_1 (Figure 3.7). The variation in colours of cast shadows depends on the selected coloured LEDs in the luminaire.

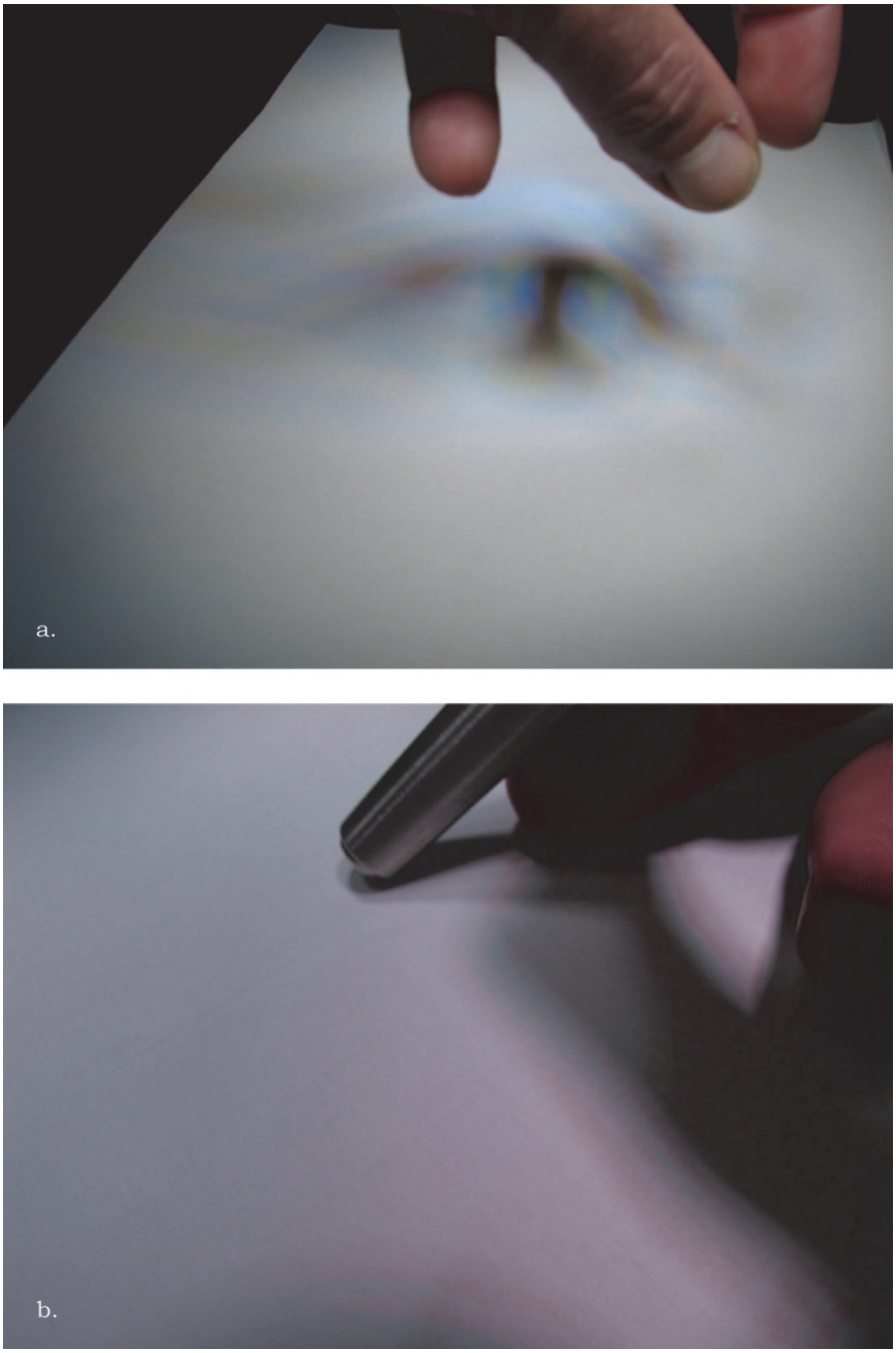

Figure 3.7 An example of coloured shadows projected on a white sheet of paper, (a) violet, blue, green and orange coloured shadows by luminaire D_1, and (b) red and green shadows by luminaire E_1. The shadow casting object was a human hand.

3.4 Discussion and analysis

The primary aim of this study was to evaluate whether presenting the maximum illuminance E_c for Scenario S1, the remaining relative illuminances for Scenarios S2 to S4, and the absolute light field diameters d_{10} and d_{50} for both Scenarios S1 and L1, as laid down in the current standard (IEC 2000), results in a sufficient description of surgical luminaire performance. It was shown that, besides the maximum illuminance, also the light field diameters and even the shape of the light field did vary considerably in the various measured scenarios, both for the small and the large light field. Measuring and presenting only the illumination characteristics, as currently required by the international standard, is therefore not enough to assess the performance of a luminaire for the scenarios measured in this study. In order to supply proper and complete information to users, the international standard should require measurement and publication of the light field diameters and shapes in the different scenarios in addition to the reported change in maximum illumination, both for the small and large light field size. Stating these issues directly in the standard provides more incentive to address these in the optical design.

The secondary aim of this study was to evaluate whether measuring the spectral characteristics at the light field centre is sufficient to describe the spectral characteristics for LED luminaires. In this study it was demonstrated that the spectral characteristics may vary across the illuminated area. These variations are shown to be present in luminaires that contain combinations of different coloured LEDs. The variations occurred as slight colour differences across the illuminated area or as clearly distinguishable differently coloured cast shadows. Since true colour rendering of tissue is an important aspect of surgical lighting (Dain, Hood et al. 1998; Hadrot 1999) the spectral properties of the light source are important factors for luminaire quality. Tissue colour rendering and correct tissue recognition might be more difficult in those situations. Ideally, the standard should provide colour variation limitations, both under various shadow conditions and across the full pattern area, to set specific, generally accepted design goals for manufacturers, and to raise awareness with potential customers.

During the illuminance measurements multiple illuminance peaks were observed for luminaires D_1 and E_1. Apparently, the standard that requires a radially tapered illuminance distribution (IEC 2000) is not met for the large light field. Note that not all these illuminance peaks were located on one of our four measurement lines. This might have influenced the outcomes of the computed light field diameters and the maximum illuminances for these luminaires in Scenarios L1 to L4. Although luminaires D_1 and E_1 were marketed as having a small and large light field adjustment option, this feature might be better suitable to provide variable focus depths of the light beam.

The international standard requires multiple measurements with the two masks placed above each of the four measurement lines, to average the differences that might occur when asymmetric luminaires are measured (IEC 2000). The standard also requires placement of one mask above the centre of the light field. For this study, only 2 masks

above Line 3 were used. Luminaires that are not rotational symmetric, like C_1, D_1 or E_1, may have been penalized or favoured because of such simplifications. However, a quick check on luminaire C_1 with the masks placed above Line 3 and above Line 1 showed hardly any difference in light field diameter d_{10}. A 20% difference was observed for the d_{50} light field diameter and the shape of the light field was slightly affected. The presented data should not be used to make a definite judgement between luminaires, but as a starting point to discuss the current standard on surgical lighting.

3.5 Conclusions

The results of this study show that the current international standard for surgical luminaires is not covering all possibly relevant aspects that provide useful information on the illumination performance of these luminaires. Information on the light field diameters and light field shape in different simulated surgical conditions as well as information on the spectral variation and the appearance of coloured shadows using coloured LEDs is currently insufficiently provided. Adding obligatory measurements to the standard to quantify the change of the light field diameters and the light field geometry would provide more complete information for hospitals that are opting for new surgical luminaires. Furthermore, the standard should be extended with guidelines on the use of coloured LEDs in surgical luminaires to minimize the negative effects (like coloured shadows and light colour variations) that are introduced by using this technology. Manufacturers should be forced to minimize these effects before launching new products on high-end markets like operating room lighting.

3.6 References

Beck WC. 1978. Lighting the surgical suite. Contemp Surg. 12(1): p 9-16.

Beck WC. 1981. Operating room illumination: The current state of the art. Bull Am Coll Surg 66(5): p 10-15.

Dain SJ, Hood JW, et al. 1998. A method for evaluating the acceptability of light sources for clinical visual evaluation of cyanosis. Colour Res Appl 23(1): p 4-17.

Gregory MM. 1987. Surgical lights. Making a purchase decision. AORN J 46(5): p 904-918.

Hadrot L. 1999. L'eclairage au bloc operatoire. Ann Chir 53(9): p 883-889.

[IEC] International Electrotechnical Commission. 2000. International standard - medical electrical equipment - part 2-41 particular requirements for the safety of surgical luminaires and luminaires for diagnosis. Geneva. IEC Publication No. 60601-2-41 2000. 38 p.

Loonam JE and Millis DL. 2003. Choosing surgical lighting. Comp Cont Educ Pract 25(7): p 537-543.

Quebbeman EJ. 1993. Preparing the operating room. Care of the surgical patient: A publication of the committee on pre and postoperative care. Sci Am 5: p 1-13.

Schanda J (2007). Colorimetry: Understanding the cie system. Hoboken, Wiley.

Chapter 4

Illumination Characteristics of State-of-the-Art Surgical Lights

Arjan J. Knulst, Laurents P.S. Stassen, Kees A Grimbergen, Jenny Dankelman

Choosing Surgical Lighting in an LED Era. Surgical Innovation, Volume: 16 Issue: 4 Pages: 317-323, 2009

The aim of this study is to evaluate the illumination characteristics of LED lights objectively to ease the selection of surgical lighting. The illuminance distribution of five main and four auxiliary lights was measured in eight clinically relevant scenarios. For each light and scenario, the maximum illuminance Ec [kilolux] and the size of the light field d10 [millimetres] were computed. The results showed: that large variations for both Ec (25-160 klx) and d10 (109-300mm) existed; that using auxiliary lights reduced both Ec and d10 with up to 80% and 30%; that with segmented lights uneven light distributions occurred; and that with coloured-LED lights shadow edges on the surgical field became coloured. Objective illuminance measurements showed a wide variation between lights and a superiority of main over auxiliary lights. Uneven light distributions and coloured shadows indicate that LED lights still need to converge to an optimal design.

4.1 Introduction

For many years, choosing surgical lighting has been a challenging process for both surgeons and hospitals. The challenge of choosing surgical lighting has further been increased since the recent introduction of the expensive Light Emitting Diode (LED) Operating Room (OR) light in the operating room as an emerging lighting technology. Several studies, as reviewed in (Balaras et al. 2007), have pointed at the surgical OR-light as a source of laminar air flow disturbances. Increased sizes and heat loads of OR-lights have been mentioned to introduce more undesirable effects to the laminar air flow compared to smaller sizes and heat loads. Although clinical evidence has still been lacking, these effects might compromise the sterility of the wound by bringing more contaminating airborne particles to the surgical site. Therefore, hospitals tend to choose small-sized auxiliary-lights-only lighting systems instead of large-sized main lights in an attempt to minimize air flow distortion and to save money. In order to assist hospitals in the purchase processes of OR-lights, surgeons' requirements for surgical lighting have been described by several authors (Anonymous 1970; Beck 1980; 1981; Back and Heimburger 1973; Condon and Quebbeman 1988;Ersek and Lelihei 1972; Geisse 1994; Hadrot 1999; Lonam and Millis 2003). Several important aspects of surgical lighting have been reported, for example, light quantity, shadow reduction, light beam directionality, heat production and light colour. Obtaining the proper light quantities and the correct light colours at the surgical site in all circumstances is important, as these aspects have been shown to influence the performance of visual tasks (Boyce 2003, Dain et al. 1998).

The reported lighting requirements of surgeons have been converted to objective guidelines and measures and formulated in a standard for surgical lighting (IEC 2000). This standard describes the range of different light colour characteristics and the range of the light quantities to which OR-lights should comply. Furthermore, it describes test scenarios in which the maximum light quantity is to be measured. These scenarios are based on clinical situations like surgeons' heads partly blocking the light beam, or light penetration into deep cavities. Although surgical OR-lights comply with the mentioned standard, complaints about the light quality and ergonomics still remain (Matern and Koneczny 2007; Patkin 2003).

The aim of this study is to compare extensively the lighting quality of main and auxiliary surgical OR-lights that use state-of-the-art LED technology. In addition to the tests described by the standard, which only requires the measurement of the maximum light quantity in different situations, the current study also measures the light field sizes and distribution of light across the illuminated field in all above mentioned situations. The light field sizes are expressed in a comparable, clinically relevant way to enable comparison between OR-lights. The study further highlights some phenomena that can be introduced to the surgical field by the use of the new LED lighting technology.

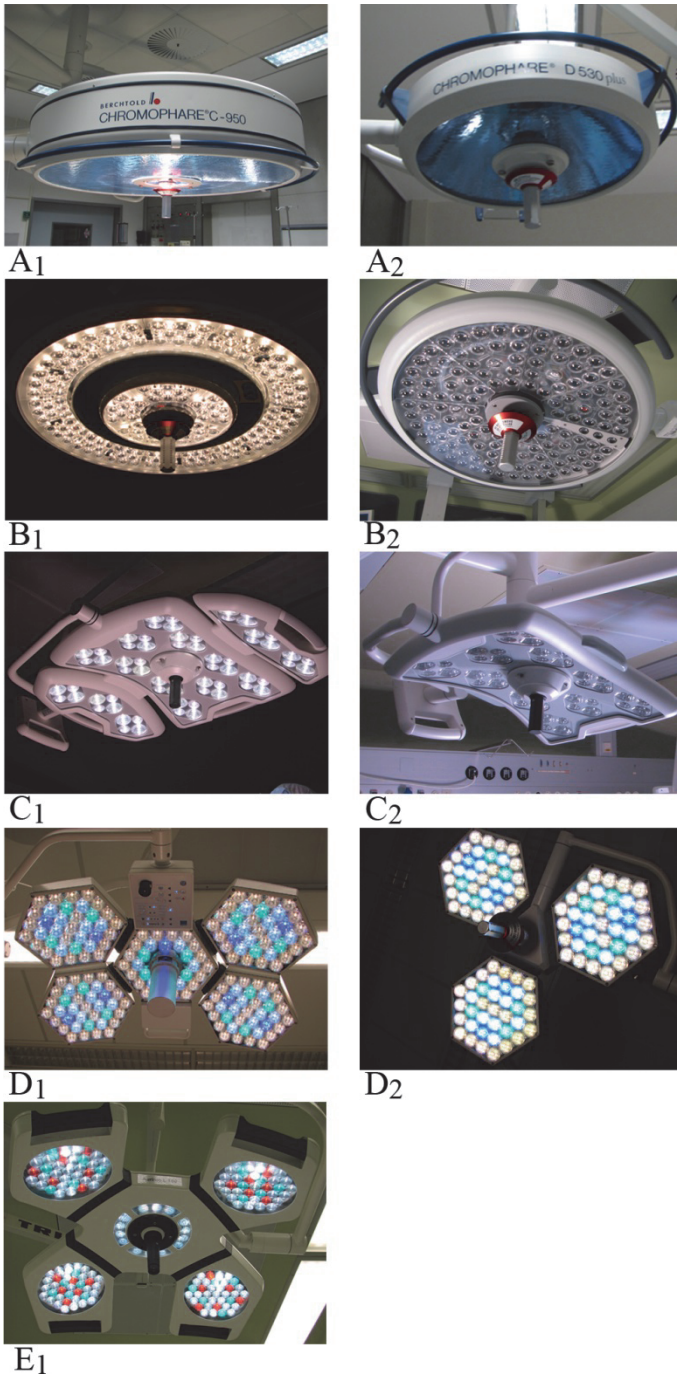

Figure 4.1 An overview of the assessed main OR-lights (A1 – E1) and auxiliary OR-lights (A2 – D2). OR-lights D1, D2 and E1 consist of four or five segments, slightly rotatable to adjust the OR-light's focus. The coloured LEDs of OR-lights D1 and E1 are clearly visible.

4.2 Materials and methods

The OR-lights that were assessed in this study are listed in Table 4.1 and are shown in Figure 4.1. These OR-lights were installed in Dutch operating rooms during the assessments. A main (A1) and an auxiliary (A2) OR-light, equipped with halogen light technology, were included as reference for the LED OR-lights. These lights were chosen because this type is a common type in especially non-academic hospitals. The LED OR-lights had different designs (Table 4.1 and Figure 4.1): some OR-lights had only white LEDs, others a mixture of white and coloured LEDs; some OR-lights had a fixed colour temperature, others the option to vary the colour temperature; and most OR-lights had the functionality to focus the light beam, others a fixed focus.

Table 4.1 Overview of the main properties of the assessed OR-lights and the labels used to refer to the corresponding OR-lights. The column 'Light source technology' distinguishes between halogen lights and LED lights.

Label	Light source technology	Colour temperature*	Focusable light beam	Manufacturer (label)	Type
Main luminaires					
A_1	Halogen	4500K	Yes	Berchtold (A)	C950
B_1	LED, cool white LEDs	3750K	No	Maquet (B)	PowerLED 700
C_1	LED, multicolour chip LEDs	3800K - 4800K	Yes	KLS-Martin (C)	MarLED V16
D_1	LED, mixture of white and coloured LEDs	3500K - 5000K	Yes	Trumpf (D)	iLED 5
E_1	LED, mixture of white and coloured LEDs	4700	Yes	Trilux (E)	Aurinio L160
Satellite luminaires					
A_2	Halogen	4500K	Yes	Berchtold (A)	D530+
B_2	LED, cool white LEDs	3750K	**No**	Maquet (B)	PowerLED 500
C_2	LED, multicolour chip LEDs	3800K - 4800K	Yes	KLS-Martin (C)	MarLED V10
D_2	LED, mixture of white and coloured LEDs	3500K - 5000K	Yes	Trumpf (D)	iLED 3

* The correlated colour temperature is the closest match of the measured light colour to the colour temperature located on the locus of a Planckian black body, reported in degrees Kelvin (K).

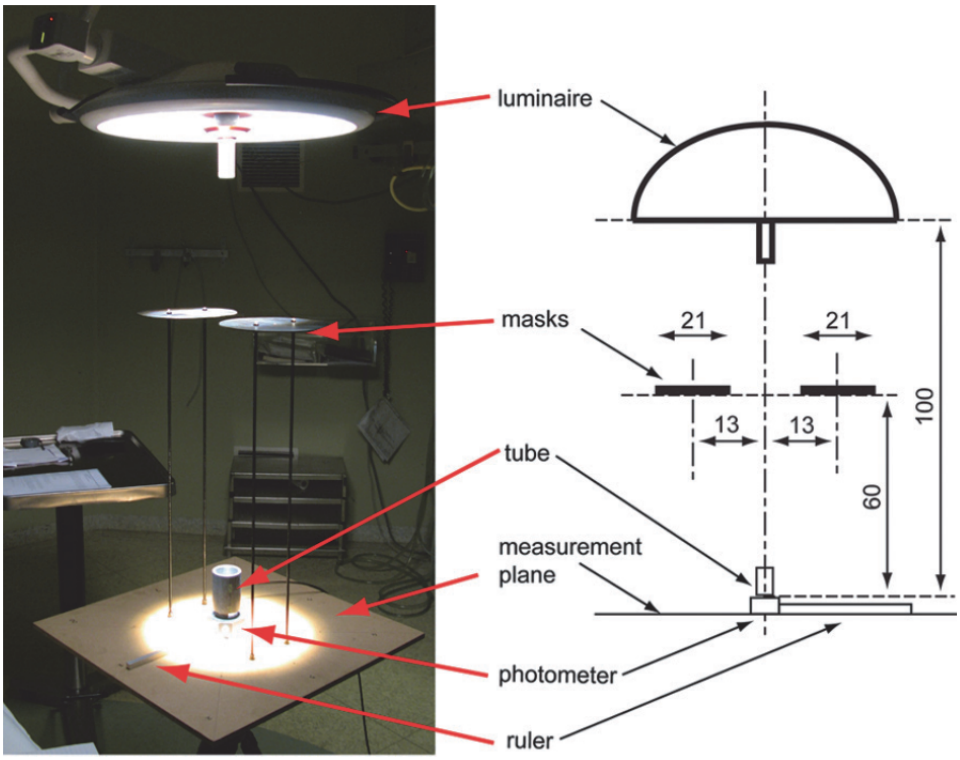

Figure 4.2 A photograph (left) and schematic representation (right) of the illuminance measurement setup showing OR-light positioning, and masks and tube placement. To vary the scenario, either the masks, the tube or both masks and tube were removed from the setup. The photometer was moveable along a ruler, and the ruler could be positioned on each measurement line. All dimensions are given in cm.

In order to assess the illumination characteristics of the OR-lights, a setup was developed (Figure 4.2) according to the requirements of the International Electrical Commission (IEC) standard for surgical OR-lights [13]. The light beam of the OR-light was aimed perpendicular at a horizontally oriented flat plate on which four measurement lines were drawn, lying 45° apart and crossing each other at the centre of the plate. The plate carried a calibrated photometer, with a 13 mm diameter sensor area, that was moveable along each measurement line. The photometer measured the quantity of light (illuminance, reported in units of kilolux [klx]) at multiple locations along each measurement line, and the measured data was stored to a computer. The OR-light was positioned 100 cm above the photometer head during the measurements.

Eight different scenarios were defined, taken from the international standard [13], and for each of these scenarios the illuminance distribution was measured. The scenarios were combinations of adding or removing the following obstacles in different OR-light settings (Figure 2): (a) a tube placed over the photometer, simulating deep wound

penetration, (b) two circular masks placed 60 cm above the photometer, simulating two surgeons' heads as obstacles for the light beam, or (c) changing the light field diameter to the minimal and maximal light field size by adapting the OR-light's focus (Table 4.2). Both geometry and locations of the masks and tube were defined following the IEC standard [13]. The standard defines additional scenarios to be evaluated than those used in this study, such as using one centrally placed mask instead of two masks or varying the location of the two masks. For time reasons, these scenarios were not included in this study.

Table 4.2 The definition of the measured scenarios, defining the use of: (a) the tube, (b) the masks, and (c) the light field size.

Scenario	Tube (a)	Two masks (b)	Light field diameter (c)
Small 1 (S1)	No	No	Smallest
Small 2 (S2)	Yes	No	Smallest
Small 3 (S3)	No	Yes	Smallest
Small 4 (S4)	Yes	Yes	Smallest
Large 1 (L1)	No	No	Largest
Large 2 (L2)	Yes	No	Largest
Large 3 (L3)	No	Yes	Largest
Large 4 (L4)	Yes	Yes	Largest

For each OR-light and scenario the maximum illuminance (Ec), and the light field diameters (d10 and d50) were computed along each measurement line, as defined in Figure 4.3. By definition, d10 or d50 are the distances between the points on the measurement line where the measured illuminances reach 10 or 50% of the maximum allowable illuminance E100 (160 klx [13]). These three variables were computed for each of the four measurement lines and averaged to obtain the mean values of Ec, d10 and d50 for the OR-light and scenario in question. The standard uses a slightly different definition of the light field diameters: instead of computing E10 and E50 as 10 and 50% of the maximum allowable illuminance E100, the maximum illuminance Ec of the measured OR-light in that specific scenario has to be used as a reference. As the maximum illuminance differs between OR-lights and between scenarios, the absolute values of E10 and E50 change as well, yielding incomparable and thus clinically irrelevant light field diameters. In contrast to the standard, the definition used in this study results in absolute values for the 10% and 50% illuminance boundaries, and therefore gives clinically relevant light field diameters that are comparable between OR-lights

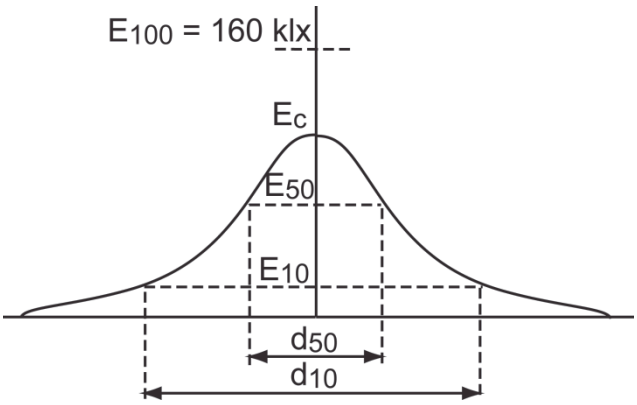

Figure 4.3 The definition of the maximum illuminance (Ec) and the light field diameters d10 and d50 derived from a typical illuminance distribution over one of the four measurement lines. The maximum allowable illuminance (E100) is 160 klx [13]. The d10 and d50 light field diameters are defined by the distance between the points where the illuminance is 10% (E10=16 klx) and 50% (E50=80 klx) of E100, respectively.

4.3 Results

Table 4.3 shows the maximum illumination of the five main and four auxiliary OR-lights as function of the eight evaluated scenarios. When obstacles were added to the setup or when the scenarios were changed to the maximum light field size, the maximum illuminances clearly decreased. Note the variation in maximum illuminance between individual OR-lights: some OR-lights evidently performed better in certain scenarios than others, showing higher light intensities. Most LED OR-lights showed a higher illuminance than the halogen OR-lights (A1 and A2) that were used as references.

Table 4.3 Maximum illuminances (Ec) of main and auxiliary OR-lights, expressed in kilolux [klx] units, measured for Scenarios S1 to L4. Lights B1 and B2 had no option to adapt the focus of the light beam to Scenarios L1 to L4. The auxiliary lights were only measured in Scenarios S1, S3, L1 and L3, as the influence of placing the tube was shown to be negligible.

Scenario:	**S1**	**S2**	**S3**	**S4**	**L1**	**L2**	**L3**	**L4**
Label					**Main lights**			
A_1	133	108	68	50	50	46	29	26
B_1	109	97	75	65	-	-	-	-
C_1	160	129	75	60	124	101	59	47
D_1	157	107	129	79	58	48	37	28
E_1	160	101	127	69	56	46	51	44

	Auxiliary lights							
A_2	81	-	49	-	47	-	30	-
B_2	117	-	52	-	-	-	-	-
C_2	101	-	58	-	80	-	47	-
D_2	125	-	72	-	44	-	41	-

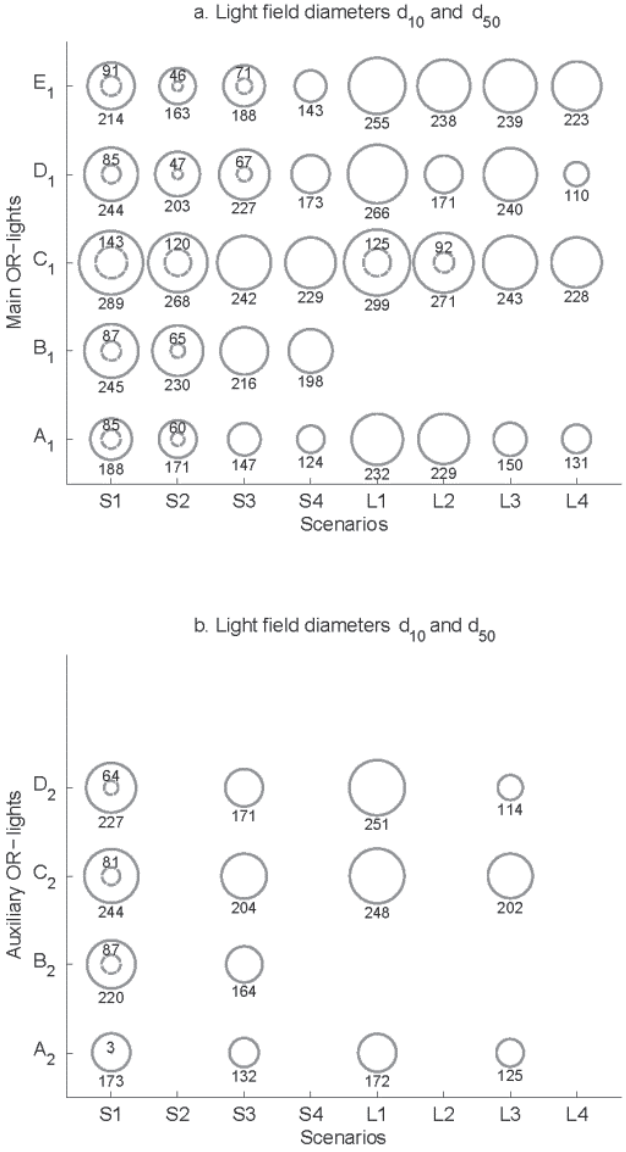

Figure 4.4 The light field diameters of (a) five main OR-lights (A1 – E1, A1 being the halogen reference main OR-light) and (b) four auxiliary OR-lights (A2-D2, A2 being the halogen reference auxiliary OR-light), measured in eight scenarios (S1 – L4). The different lights are depicted on the y-axis, the different scenarios are placed on the x-axis. The d10 light field diameters are plotted as solid circles and its diameters (in mm) are printed below the solid circle. The d50 light field diameters are plotted as dashed circles and its diameters (in mm) are printed above the dashed circle. As OR-lights B1 and B2 had no option to focus the light beam, its values for Scenarios L1 – L4 are set to zero. The auxiliary OR-lights were only measured in Scenarios S1, S3, L1 and L3.

Figure 4.4a depicts the computed light field diameter d10 (solid lines) and d50 (dotted lines) for each main OR-light as function of the measured scenarios. The data showed a large variation in light field size between different OR-lights. Most main LED OR-lights produced a larger light field than the halogen OR-light (A1) that was used as reference. Note that from Scenario S3 and upward, almost none of the OR-lights were able to produce a light field with an intensity higher than 80 klx (50% of 160 klx). From this data set, industry presents only the (incomparable) light field diameters for Scenarios S1 and L1.

The auxiliary OR-lights showed the same effects of the changing scenarios on the maximum illuminance and the light field diameter as was seen with the main OR-lights. In Figure 4b, the data of four auxiliary OR-lights is presented in the same way as was done for the main OR-lights in Figure 4.4a. Halogen OR-light A2 was used as a reference. Only data for Scenarios S1, S3, L1 and L3 was acquired, as a pilot study had shown that placing the tube over the photometer had negligible influence on the illuminance distribution of the auxiliary OR-lights and therefore had hardly any noticeable influence on Ec and d10.

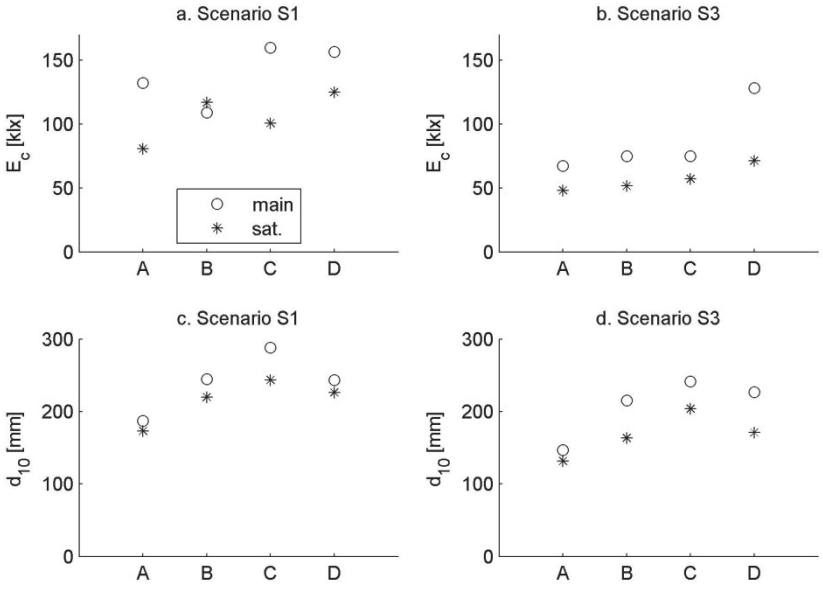

Figure 4.5 A comparison between main (circles) and auxiliary (asterisks) OR-lights per manufacturer for Scenarios S1 and S3. Two parameters are compared: the maximum illuminance Ec, and the light field diameter d10. The different OR-light manufacturers (Table 1) are shown on the x-axis.

Figure 4.5 displays the differences in maximum illuminance and light field diameter between main and auxiliary OR-lights of different manufacturers (A – D) for two Scenarios (S1: no obstacles, and S3: two masks). The data showed that the

performance of main OR-lights was better than the performance of auxiliary lights: the main OR-lights' maximum illuminances were generally higher, and the light field diameters were larger in all measured scenarios.

4.3.1 Other phenomena introduced by using LED OR-lights

Figure 4.6 presents two photographs of the illumination distribution of OR-light D1. One image shows the illumination distribution when the OR-light was focused to its smallest light field size; the other image displays the illumination distribution of the same OR-light when it was adapted to its maximum light field size. Because of the design of the OR-light, in the latter case, the illuminance distribution no longer radially decreased (as the standard [13] requires) but showed multiple illuminance peaks within the illuminated field. The same effect was observed for OR-light E1, whose design also consisted of a number of light emitting areas (see Figure 4.1) that were slightly reoriented by the OR-light to focus the light beam.

a.

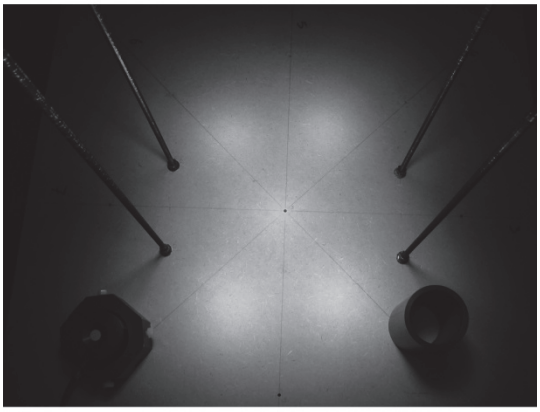

b.

Figure 4.6 Illuminance distribution of OR-light D1 with the OR-lights light field size adapted to (a) the smallest possible and (b) the largest possible. The same illuminance pattern was shown for OR-light E1.

Figure 4.7 shows a phenomenon that is specifically related to LED OR-lights using multiple differently coloured LEDs, like C1, D1 and E1. Because two heads and a hand that were placed in the light beam distorted the mixture of the different light colours, coloured shadows were introduced onto the illuminated field. The colours of the shadows varied depending on the mixture of light colours in the OR-light: OR-light C1 showed reddish shadow colours; OR-light D1 produced greenish, yellowish and bluish shadow colours; and OR-light E1 displayed reddish and greenish shadow colours. Note that the white sheet of paper in Figure 4.7 locally turned its appearance into greenish and bluish coloured paper.

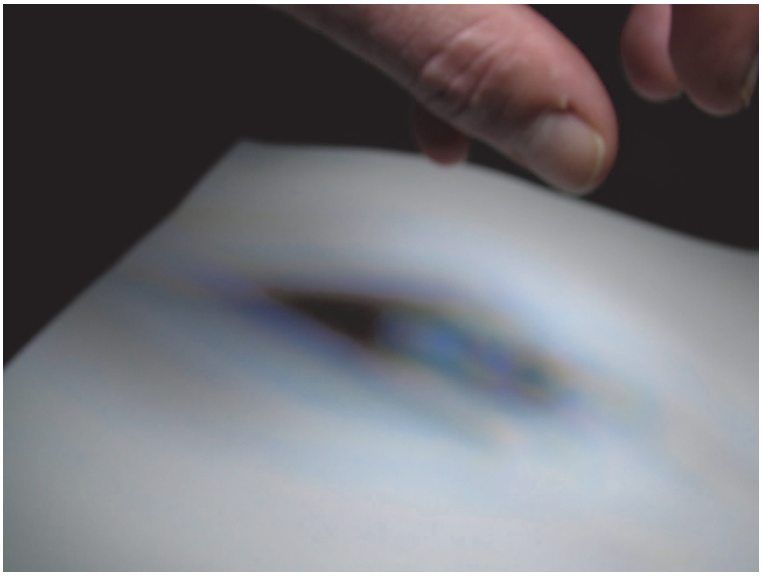

Figure 4.7 An example of coloured shadows cast on a white sheet of paper with a human hand as shadow casting object, as seen with OR-light D1. The shadow colour effect was also visible for OR-lights C1 and E1.

4.4 Discussion

Several hospitals tend to choose small-sized (auxiliary) LED OR-lights to minimize the possible laminar air flow disruption and to save money. Therefore, the aim of this study was to perform a comparative assessment of the lighting quality of main and auxiliary surgical OR-lights that use LED technology. To this end, the illuminance distributions of different LED main and auxiliary OR-lights were studied in eight varying scenarios. Firstly, it was reported that large differences existed for the maximum illuminances and the light field diameters between different OR-lights. Secondly, it was shown that the maximum illuminances and light field diameters for most main OR-lights were superior to those of the auxiliary OR-lights. Finally, it was observed that the use of LED OR-lights that contain differently coloured LEDs introduced coloured shadows cast to the surgical field.

In all scenarios defined by the standard, the only effect of changing scenarios that should be measured is the change in the maximum illuminance for Scenarios S2-S4 relative to Scenario S1. According to the requirements of this standard, industry only presents these relative changes in maximum illuminance to the user, whereas surgeons are interested in clinically relevant parameters like the absolute quantity of light instead of some relative changes. This study provides the absolute illuminances in a wide range of scenarios, even for scenarios with the OR-light adapted to the largest possible light field size.

As defined by the standard, the light field diameter in Scenario S1 is by definition dependent on the maximum illuminance of the OR-light. The light field diameters of different OR-lights are therefore not comparable when they have different maximum illuminances. In other words, this light field diameter -as defined by the standard and as presented by industry- has no clinical relevance. The current study uses a different, absolute definition of the light field diameter that is independent of the maximum illuminance. This property gives comparability between lights and is therefore expected to be more clinically relevant. Industry should present independent and clinically relevant light field diameters to hospitals to improve the comparability of different OR-lights, either voluntarily or on a surgeon's request.

In the measurements as defined by the standard, the variation of the light distribution in different scenarios is not presented to the user. In this study, the changes of the light distribution in the different scenarios are evaluated using the absolute and clinically relevant definition of the light field size. The results show that the size of the light field changes considerably when scenarios are changed, and that considerable differences between OR-lights exist. Industry is not communicating these changes in light field sizes to the surgeons, although these changes occur. Hospitals will be able to make a more objective trade-off between OR-lights if these light field size changes are presented to hospitals by industry.

Several hospitals opting for LED OR-lights tend to choose a configuration with auxiliary OR-lights only. This configuration might reduce the distortion of the laminar air flow, and moreover, is less expensive than a configuration with a main and an auxiliary OR-light. In general, the disturbance of laminar air flow by the surgical light is influenced by its electrical power, its surface area, its shape, its position above the operating table and its angulation. For LED-lights, most of these aspects are comparable with halogen lights, only the surface area and the shape might be slightly better for the air flow. Small-sized auxiliary OR-lights have less electrical power and less surface area than large main OR-lights, thus are expected to have a reduced disturbing effect on laminar air flow. However, this study shows that the illumination performance of the studied auxiliary OR-lights is inferior to the measured main OR-lights. Thus, purchasing only auxiliary OR-lights will save money and might increase laminar air flow performance, but will inevitably be at the expense of illumination quality at the surgical site.

An important aspect of the new LED technology is that the development of the OR-lights is still in its early stage and that the designs have not been converged to an

optimal design yet. Manufacturers use fundamentally different designs for their OR-lights, resulting in varying functionality and performance. Some OR-lights, for example, provide functionality to adapt the colour temperature of the light to the surgeon's preference, whereas other OR-lights lack, for instance, functionality to adapt the focus of the OR-light to the size of the wound. To what extent the presence or absence of those functionalities is advantageous or disadvantageous needs to be investigated. For now, it is observed that the use of coloured LEDs has its drawbacks as it introduces coloured shadows cast to the illuminated field. As the colour appearance of objects is dependent on the colour of the light –remember the local changes of the white sheet of paper into greenish and bluish colours- the appearance of tissue colours within these coloured shadows might be compromised as well. To which extend this effect is clearly visible on human skin or anatomy should be investigated. In summary, the light provided by LED OR-lights would better fit the needs for operating theatre use after the reported aspects of the current generations of surgical LED OR-lights have been improved.

4.5 References

Anonymous, 1970, Operation lighting. A surgical odyssey, Journal of the Illuminating Engineering Society. 65(1):25-30

Balaras CA, Dascalaki E and Gaglia A, 2007, Hvac and indoor thermal conditions in hospital operating rooms, Energy and Buildings. 39(4):454-470

Beck WC, 1980, Choosing surgical illumination, American Journal of Surgery. 140(2):327-331

Beck WC, 1981, Operating room illumination: The current state of the art, Bulletin of the American College of Surgeons. 66(5):10-15

Beck WC and Heimburger RF, 1973, Illumination hazard in the operating room, Archives of Surgery. 107(4):560-562

Boyce PR, Human factors in lighting. 2nd revised edition ed. 2003: Taylor & Francis Ltd

Condon RE and Quebbeman EJ, 1988, Preparing the operating room, Care of the Surgical Patient. 2:82-85

Dain SJ, Hood JW, Montano S, et al., 1998, A method for evaluating the acceptability of light sources for clinical visual evaluation of cyanosis, Colour Research and Application. 23(1):4-17

Ersek RA and Lillehei RC, 1972, A simple solution for the complex problem of surgical lighting, AORN journal. 15(1):68-72

Geisse JK, 1994, The dermatologic surgical suite, Seminars in Dermatology. 13(1):2-9

Hadrot L, 1999, L'eclairage au bloc operatoire, Ann Chir. 53(9):883-889

IEC, International standard - medical electrical equipment - part 2-41 particular requirements for the safety of surgical luminaires and luminaires for diagnosis. 2000, Geneva: International Electrotechnical Commission. 38. IEC Publication No. 60601-2-41 2000

Loonam JE and Millis DL, 2003, Choosing surgical lighting, Compendium on Continuing Education for the Practicing Veterinarian. 25(7):537-543

Matern U and Koneczny S, 2007, Safety, hazards and ergonomics in the operating room, Surgical Endoscopy. 21(11):1965-1969

Patkin M, 2003, What surgeons want in operating rooms, Minimally Invasive Therapy and Allied Technologies. 12(6):256-262

Chapter 5

The Use of Shadows in Surgical Pointing Tasks

Arjan J. Knulst, Jesse van Dongen, Marco W.M. Groenewegen, Elisabeth D. Kaptein, Jenny Dankelman

The effect of shadows on performing stereo visual pointing tasks: Is shadow-free open surgery ideal? LEUKOS 8(2): 111-122, 2011

Surgical overhead lights and head-mounted lights are important tools for surgeons. For undisturbed vision the design of these lights is focused on providing shadow free light. However, shadow is reported as an important cue for depth perception in mono-visual as well as in stereo-visual situations. As surgeons repeatedly touch delicate tissue with their instruments, their depth-perception should not be hampered. This study evaluated the influence of shadow on human performance when executing stereo-visual pointing tasks. Two experiments were performed; Experiment 1 studied the effect of the existence of shadows, Experiment 2 studied the effect of the direction of shadows. Subjects were instructed to point random sequences of virtual targets accurately under different shadow situations. The subject's performance was described by the spatial error E (distance to target [mm]). Experiment 1 showed that both large and small high-contrast shadows gave a significantly smaller spatial error E (4.8, 4.6 mm, respectively) than either low-contrast shadows (5.6 mm) or no shadows (6.3 mm). Experiment 2 showed that the Error varied (2.1 to 3.2 mm) for different illumination directions. The Error decreased with an increasing angle between the line-of-sight and line-of-light. Illuminating from the centre or from the left side of the observer gave better results than from the right side. Surgical lights should provide a clear shadow from a light source that illuminates from within the vertical plane through the line-of-sight, and with a 90° angle with respect to the line-of-sight to maximize the depth-perception of a surgeon.

5.1 Introduction

Visual feedback is an important pathway for visual information during both open and minimally invasive surgery (Stassen, Dankelman et al. 1999). To obtain optimal visual information good illumination of the wound is required. Therefore, many different requirements have been defined in the past (Bartlett 1978; Beck 1981; Geisse 1994; Loonam and Millis 2003), among which a minimal presence of cast shadows. These requirements have led to surgical lights that illuminate wounds with multiple overlapping beams to minimize shadows and to provide high-intensity illumination (Knulst, Stassen et al. 2009; Knulst, Stassen et al. 2009). In some situations even more focused light was required, leading to the development of head-mounted lights that supply focused and shadow-free light to the wound (Rohrich 2001). However, complaints about illumination conditions during surgery still have been reported until today (Patkin 2003; Matern and Koneczny 2007; Knulst, Mooijweer et al. 2010), possibly because of the unavailability of ergonomic knowledge about illumination in the operating room or because of the lack of implementing ergonomic knowledge in the operating room (Berguer 1996; Berguer 1997; Berguer 1999).

It is known that shadow is an important cue for the interpretation of visual information, especially to obtain depth-information (Mamassian, Knill et al. 1998). During minimally invasive surgery the surgeon works in mono-visual conditions -as visual information is obtained from a monitor- and lacks different cues for depth-perception. In this situation shadow was reported to have significant influence of the task performance of surgeons (Breedveld, Stassen et al. 1999; Mishra, Hanna et al. 2004). During open surgery, surgeons work in stereo-visual conditions and have different depth cues operational. The lack of shadows could thus possibly have no significant influence on task performance as many depth cues still are available.

The goal of this study is to evaluate the effect of the presence and direction of shadow on the human performance of executing 3D target pointing tasks during stereo-visual conditions. Subjects had to point at targets in a 3D space under different illumination conditions that influenced the occurrence, the appearance and the direction of shadows. The error subjects made was used as a metric to judge the subjects' task performance during the different illumination conditions.

5.2 Method

Two experiments were performed to study the effects of shadow on human performance during a pointing task. The first experiment was designed to study the effect of the presence of shadow. The second experiment was designed to study the effect of the direction of the shadow.

5.2.1 Experiment 1: The effect of shadow

SETUP 1

Setup 1 was developed to control different experimental conditions for Experiment 1 and to acquire measurement data during Experiment 1. The setup (Fig.5.1) consisted of: 1. a head-rest, 2. a target area containing targets, 3. a pointer device, 4. three light

spots at different positions, 5. a data acquisition system (Qualisys Oqus 3 motion tracking system) and, 6. a control-centre. The complete setup –except the control centre- was placed in a darkened room. The head-rest was used to fixate the position of a subject's head relative to the target area. From the control centre the experiments were controlled by adapting the illumination settings of the three lights, by running the data acquisition, and by instructing the subjects.

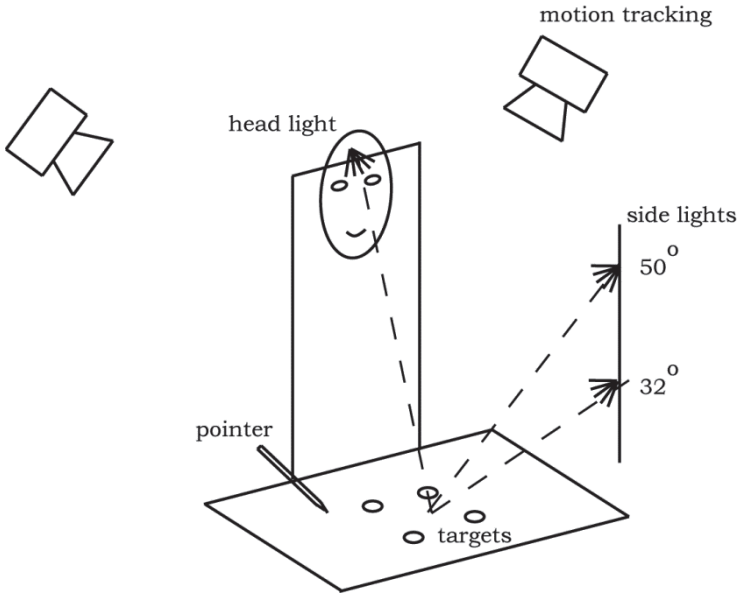

Figure 5.1 The setup used in Experiment 1. A target area contains four targets that need to be indicated by the subjects using the pointer. The headrest fixates the subjects head relative to the target area. Three light sources provide the different illumination situations. All pointer movements were tracked using a motion tracking system.

The target area measured 420 by 300 mm and contained four objects on a known location. The objects were of different heights to prevent any influence of muscle memory or other proprioceptive effects. The objects had a surface parallel to the target area on which a point was marked. Five mm above this point, a virtual target was defined. All objects could be seen by the subjects using stereo-vision and all objects were equally illuminated. The target area and objects were painted matte white. Three infrared passive markers indicated the position of the target area relative to the tracking system.

The pointer device was a 20 cm long, pointed pencil shaped object made of wood, and had three infrared markers attached to it to track the position of its tip. Six infrared cameras of the motion tracking system were placed around the setup and could accurately track the motions of the pointer.

Three LED light spots were used to control the direction and intensity of shadows. One light spot was placed at the head-rest, approximately between the eyes of the subject. This light provided the subject shadow-free light. The two other light sources were placed at different heights outside the right side of the target area, one at an incident angle of 32° with respect to the target area, and one at 50°. These lights projected a long or a short shadow of the pointer to the target area, respectively.

Four different illumination/shadow situations were created by changing the intensities of the light sources (Table 5.1). An illumination sensor was used to measure the resulting illumination at the centre of the target area, and at the centre of the shadow. The illumination at the centre was kept constant for all situations.

Table 5.1 The characteristics of the four different shadow situations Light1 to Light4.

Label	Description	Centre illumination (lux)	Shadow illumination (lux)	Incident angle
Light1	Shadow free	1600	-	-
Light2	Long, high-contrast shadow	1600	900	32
Light3	Short, high-contrast shadow	1600	900	50
Light4	Short, low-contrast shadow	1600	1380	50

PROTOCOL 1

Twenty students were included in Experiment 1. All included subjects were right-handed and had accurate vision and depth perception. After inclusion, subjects were trained to get familiar with the setup and protocol. Subjects were instructed to 'point the virtual targets as precise as possible and freeze motion if the virtual target was reached' in the sequence that was instructed from the control centre.

The sequence of targets was randomized for each condition, and the sequence of conditions was randomized for each subject. Each test contained each condition two times, and each condition contained all four targets.

ANALYSIS 1

The data obtained from the tracking system contained information on the location of the markers on the pointer, and of the location of the target area. From this data a temporal distance profile was computed: the position of the pointer-tip relative to the targets. Using this distance profile a metric was computed to describe the performance of the subjects for each target: the Error. The Error was defined as the distance between the pointer-tip and the target at the moment subjects indicated to have

reached the target by freezing their motion. A repeated measures ANOVA was performed to test the effect of the illumination condition on the Error.

5.2.2 Experiment 2: The effect of shadow direction

SETUP 2

For the second experiment Setup 1 was adapted to fit to the needs of Experiment 2 (Fig. 2). The head-rest was placed 35 cm away from and 50 cm above the centre of the target area. A circular arc with a radius of 90 cm was mounted above the centre of the target area of Setup 1. Four LEDs -pointing at the centre of the target area- were divided along the arc, (α=0°, 20°, 40°, 60°).. Each LED could be switched on/off individually. The complete arc was rotatable around the vertical axis, its rotation indicated by β. Eight different settings for β were defined (β=0°, 45°, 90°, 135°, 150°, 210°, 270°, and 315°).

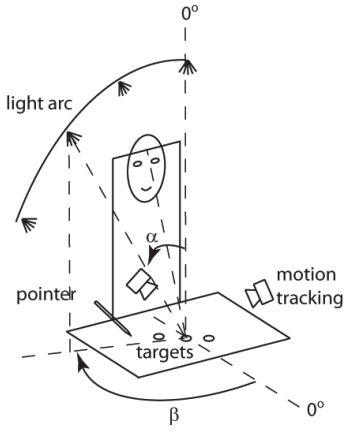

Figure 5.2. The setup used in Experiment 2. A target area contains three targets that need to be indicated by the subjects using the pointer. The headrest fixates the subjects head relative to the target area. Four light sources on a rotatable arc provided illumination from different directions defined by α and β All pointer movements were tracked using a motion tracking system.

As the arc was rotatable, a tracking system should either be inside the hemisphere defined by the arc, or outside this hemisphere to prevent interference with the arc. Tracking from outside the hemisphere would create line-of-sight issues, when the arc would be in between the pointer and the tracking camera. To track the motions from inside the hemisphere a compact tracking system is needed. As the tracking system used for Experiment 1 was too bulky to include it in the hemisphere a system using 2 webcams was used to track the position of the pointer.

The target area contained 3 different objects with a target: the top of a pyramid, a dot and the centre of a ring floating 5 cm above the target area. Data was only gathered for the pointing task at the floating ring object.

PROTOCOL 2

Twelve students were included in Experiment 2. All included subjects were right-handed and had accurate vision and depth perception. After inclusion, subjects were trained to get familiar with the setup and protocol. Subjects were instructed to 'point the three targets as precise as possible and freeze motion if they thought that the target was correctly pointed' in a random sequence that was instructed from the control centre.

Each condition was a combination of α and β. As for α=0 the rotation of the arc would have resulted in the same light position, the conditions for α=0 were restricted to β=0 only. The sequence of targets was randomized for each condition, and the sequence of conditions was randomized for each subject. Each test contained each condition three times. After each condition the subject was allowed 5 minutes rest.

ANALYSIS 2

The distance between the pointer and the centre of the ring at the moment of freeze was computed as the Error in x, y, and z-direction. The total Error was computed from these three orthogonal error components. A repeated measures ANOVA with two factors (α,β) was used to compare the Errors in the different conditions. As α=0° was only tested for β=0°, it could not be tested by the repeated measures ANOVA and was therefore excluded from the ANOVA test.

The angles α and β were transformed to co-ordinates α and β that defined the line-of-light relative to the observer's line-of-sight (Table 5.2). To understand this definition one should imagine a cone with its axis aligned with the observer's line-of-sight (Fig.5. 3). The top of the cone is positioned at the target. A light source is positioned somewhere at the outer shell of the cone, pointing the light towards the target. The position of the light source can be defined by the half top angle of the cone (θ) and the angle of rotation of the line-of-light around the cone's axis (ϕ), measured from the vertical plane through the line-of-sight. This transformation allowed the representation of the mean Error as function of θ and ϕ.

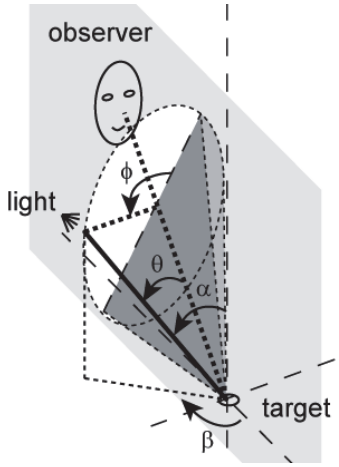

Figure 5.3. Definition of the transformation of light source's line-of-light relative to the observer's line-of-sight. The angles α and β defining the direction of the line-of-light relative to the setup are transformed into angles θ and ϕ defining the light source's direction relative to the observer's line-of-sight.

5.3 Results

5.3.1 Experiment 1

Figure 3 shows the effect of illumination condition on the Error. High-contrast shadows (Light 2 and Light3) gave a significant reduction of the Error, both compared to no-shadows (Light1) or low-contrast shadows (Light4). Long (Light2) or short (Light3) high-contrast shadows were not significantly different, and shadow-free (Light1) and low-contrast (Light4) shadows were not significantly different as well. Light3 gave the largest increase in performance: a reduction of the mean Error by 28%.

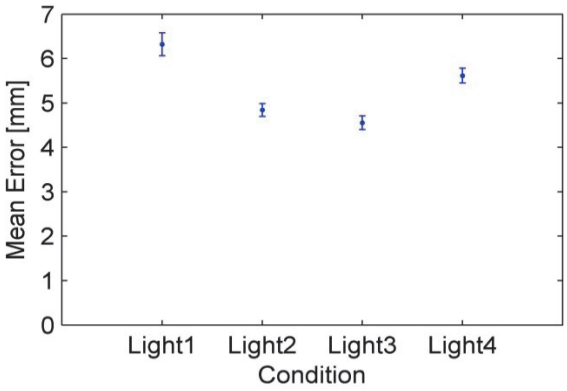

Figure 5.4. The mean Error for the different illumination situations.

5.3.2 Experiment 2

Table 5.2 shows the 25 illumination conditions specified by α and β,, and gives the corresponding transformed angles θ and ϕ and the measured mean Error over all subjects.

Table 2. Mean Error over all subjects and the transformed angles θ and ϕ.

Condition	α [°]	β [°]	θ [°]	ϕ [°]	mean Error [mm]
1	60	0	95.0	0.0	2.14
2	60	45	86.6	37.8	2.50
3	60	90	65.8	71.7	2.74
4	60	135	40.5	109.3	2.70
5	60	150	32.9	127.1	3.10
6	60	225	40.5	-109.3	2.55
7	60	270	65.8	-71.7	2.75
8	60	315	86.6	-37.8	2.62
9	40	0	75.0	0.0	2.45
10	40	45	68.5	29.2	2.92
11	40	90	51.1	55.7	3.07
12	40	135	27.3	81.6	2.88
13	40	150	18.8	93.0	3.17
14	40	225	27.3	-81.6	2.50
15	40	270	51.1	-55.7	2.68
16	40	315	68.5	-29.2	2.73
17	20	0	55.0	0.0	2.66
18	20	45	50.9	18.2	2.93
19	20	90	39.7	32.4	2.88
20	20	135	24.7	35.4	2.93
21	20	150	20.0	30.0	2.83
22	20	225	24.7	-35.4	2.50
23	20	270	39.7	-32.4	2.75
24	20	315	50.9	-18.2	2.61
25	0	0	35.0	0.0	2.92

Figure 5.5 shows the effects of the angles α and β on the mean Error. The effect of β was small, although ANOVA computed the Error at 20° and 60° to be significantly different. More effect was introduced by angle β, with a maximum Error reduction of 20% (from β=150° to β=0°) Significant differences were found for both β=0° and 225° between all other angles except 315°. The significantly different pairs are listed in Table 5.3.

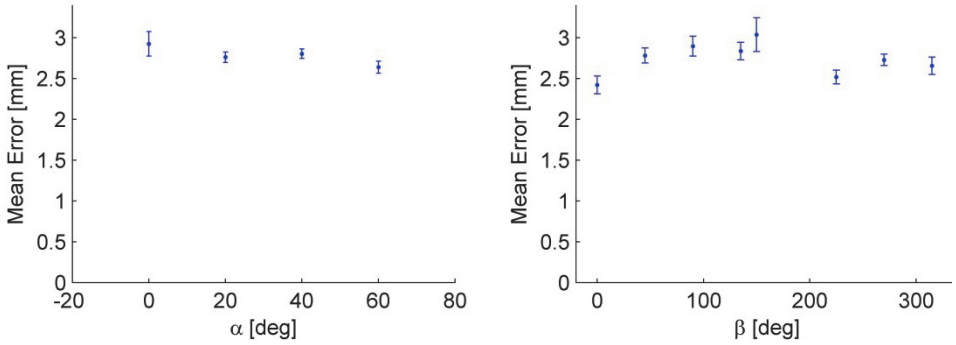

Figure 5.5. The effect of α on the mean Error (left panel) and the effect of β on the mean Error (right panel). The significantly different pairs are identified in Table 3.

Table 5.3 p-values of significantly different mean Errors for angles and .

α	20	40	60
20	-		0.016
40		-	
60	0.016		-

β	0	45	90	135	150	225	270	315
0	-	0.013	0.002	0.003	0.000		0.017	
45	0.013	-				0.04		
90	0.002		-			0.008		
135	0.003			-		0.012		
150	0.000				-	0.001	0.013	0.003
225		0.04	0.008	0.012	0.001	-	0.046	
270	0.017				0.013	0.046	-	
315					0.003			-

Figure 5.6 shows the effects of the transformed angles θ and ϕ on the mean Error. Overall, the negative angles ϕ caused lower Errors than the positive angles. Further, increasing the angle θ seemed to reduce the mean Errors. Best performance was reached at (θ,ϕ)=(95°,0°).

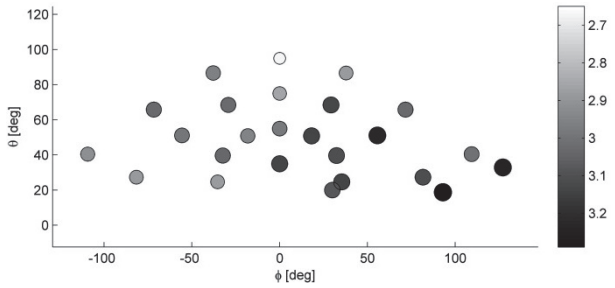

Figure 5.6. The mean Error for light positions relative to the observer's line-of-sight. The mean Error is specified by the shade of the circles according to the shade bar [mm].

5.4 Discussion

The results of the first study indicated that shadow has an effect on the 3D depth estimation of subjects during stereo-visual conditions. The presence of clearly visible shadows reduced the error of depth estimation by 28%, compared to the no-shadow situation. Estimating depth is thus easier done with sharp shadows than without shadows. Moreover, the results of the second study showed that certain illumination directions provided shadows that were more helpful for precise pointing than other directions. Pointing errors were reduced by 20% when comparing the results of the worst case to the best case.

The illumination angles (α, β) from our second study were transformed into illumination angles relative to the observer's line-of-sight (θ, ϕ). This transformation showed the trend that the mean Error reduces with an increasing angle ϕ. This corresponds with the results of the first study, where a light source placed in line with the line-of-sight produced significantly larger errors than when placed at an angle to the line-of-sight. The transformation also showed that the mean Error was smaller for negative angles ϕ than for positive angles. These positive and negative angles ϕ correspond to illumination from the right and the left side of the subject, respectively. As all subjects were right-handed, illuminating from the right side was apparently resulting in less useful or less visible shadows.

The best performance was shown for illumination from a location in the same vertical plane as the observer's line-of-sight (ϕ=0°) and with a large angle between the line-of-sight and the line-of-light (θ=95°). In this situation the shadow is projected on the line between the target and the observer, resulting in good visibility of the shadow.

Illumination from a point on the observer's vertical plane (ϕ=0°) and from an angle θ=90° might be optimal, as light in line with the line-of-sight (θ=0°) and (θ=180°) produces no visible shadow.

A study on optimal illumination direction for minimally invasive surgery (Mishra, Hanna et al. 2004) showed that for mono-visual conditions any shadow gave better performance than no shadow. This corresponds for the current study were stereo-visual conditions with clear shadows gave a better performance than without shadows. In the same previous study, 'overhead illumination' gave surgeons better performance than 'side illumination'. The current study also showed that illumination from the vertical plane through the observer's line-of-sight (β=0°) gave better performance than illumination from the left side (β=270°). Moreover, the current study showed that illumination from the right side (β=90°) was even worse than from the left (for right handed task execution). In contrast to the previous study, the current results showed that incident light should not be aligned with the vertical axis, but should have a large angle between the line-of-light and the line-of-sight.

For good illumination, especially into deep wounds, surgeons tend to place the overhead lights behind their heads (Beck 1980) and/or to use head-mounted lights (Rohrich 2001). In both cases the light source's line-of-light is placed in line with or close to the line-of-sight. Shadows are thus invisible for the surgeon and depth perception will be hampered. For better depth perception the angle between line-of-light and line-of-sight should be increased. Of course, the trade-off here is between good vision and good depth perception, since a deep wound would limit the available lighting angles that still will provide proper illumination. Good vision will be more important, but the issue of depth perception should be kept in mind when positioning overhead lights, using head-mounted lights, or when designing new lighting systems that provide good illumination while respecting the need for depth perception.

All included subjects had right-hand dominance, leading to right-handed task execution. Left-hand dominant subjects might achieve better performance for left-sided illuminance. To what extend eye dominance plays a role was not studied. However, it could have an effect and should be studied as eye and hand-dominance do not have the same prevalence.

The current experimental conditions did not fully resemble surgical conditions, and thus the clinical significance of the findings is not proven. The current study could be expanded to realize a closer match to real clinical conditions. For instance, to explore the effect of shadow direction in deep wounds a view limiting aperture might be added to Experiment 2. A different addition could be to change the experimental environment from a white to a multi-coloured background with lower colour contrasts that resembles the appearance of a surgical wound. Increasing the experimental resemblance of surgical conditions would probably yield to results that have a direct clinical relevance. Although the effects of illumination direction on depth perception in the current experiments would be expected to occur during clinical conditions as well, the size of the effects could be different during clinical conditions.

5.5 Conclusion

This study has shown that the presence of shadows significantly improves depth perception of human subjects during stereo-visual conditions, as the pointing task was completed with significantly less error. Moreover, it was shown that the best depth perception was reached with a light source located in the same plane as the observer's vertical plane, and placed at an angle of 95° between the observer's line-of-sight and the light source's line-of-light. Although the clinical relevance of the findings has not been investigated, the translation of the experimental findings to surgical lighting indicates that the effect of illumination position relative to the observer should be taken into account when positioning surgical lights, using head-mounted lights, and when designing new lighting devices.

5.6 References

Bartlett D. 1978. Operating theatre lighting. NATNews 15(11): 24-30.

Beck WC. 1980. Choosing surgical illumination. Am J Surg 140(2): 327-331.

Beck WC. 1981. Operating room illumination: the current state of the art. Bull Am Coll Surg 66(5): 10-15.

Berguer R. 1996. Ergonomics in the operating room. Am J Surg 171(4): 385-386.

Berguer R. 1997. The application of ergonomics in the work environment of general surgeons. Rev Environ Health 12(2): 99-106.

Berguer R. 1999. Surgery and ergonomics. Arch Surg 134(9): 1011-1016.

Breedveld P, Stassen HG, et al. 1999. Theoretical background and conceptual solution for depth perception and eye-hand coordination problems in laparoscopic surgery. MITAT 8(4): 227-234.

Geisse JK. 1994. The dermatologic surgical suite. Semin Dermatol 13(1): 2-9.

Knulst AJ, Mooijweer R, et al. 2010. Indicating shortcomings of surgical lighting systems. MITAT in press(doi: 10.3109/13645706.2010.534169).

Knulst AJ, Stassen LP, et al. 2009. Choosing surgical lighting in the LED era. Surg Innov 16(4): 317-323.

Knulst AJ, Stassen LPS, et al. 2009. Standards and Performance Indicators for Surgical Luminaires. Leukos 6(1): 37-49.

Loonam JE and Millis DL. 2003. Choosing surgical lighting. Comp Cont Educ Pract 25(7): 537-543.

Mamassian P, Knill DC, et al. 1998. The perception of cast shadows. Trends Cogn Sci 2(8): 288-295.

Matern U and Koneczny S. 2007. Safety, hazards and ergonomics in the operating room. Surg Endosc 21(11): 1965-1969.

Mishra RK, Hanna GB, et al. 2004. Optimum shadow-casting illumination for endoscopic task performance. Arch Surg 139(8): 889-892.

Patkin M. 2003. What surgeons want in operating rooms. MITAT 12(6): 256-262.

Rohrich RJ. 2001. Why I hate the headlight ... and other ways to protect your cervical spine. Plast Reconstr Surg 107(4): 1037-1038.

Stassen HG, Dankelman J, et al. 1999. Open versus minimally invasive surgery: a man-machine system approach. Trans Inst Meas Contr 21(4-5): 151-162.

Chapter 6

Enhanced Visual Performance and Comfort

Arjan J. Knulst, Jenny Dankelman

The effect of luminance ratios on visual performance and comfort in a surgical setting. Submitted.

Light is important for surgeons to obtain good vision. This study aims to assess the effect of the luminance ratio of the wound and its direct surroundings on the visual performance and comfort of humans. Visual performance (Score and Threshold) and perceived Comfort were tested on 40 subjects during 7 Luminance ratios (0.1 to 7.0) using a contrast discrimination task at the Centre and Edge of the wound. Highest scores, lowest thresholds, and highest comfort were obtained for Luminance ratios around 1. The colour difference between wound and surroundings seemed to have a dominant effect as the Edge Score was reduced by a factor 0.8, and the Edge Threshold was increased by a factor 2.2 compared to the Centre. For good surgical illumination both luminance and colour need to be balanced to obtain maximum visual performance and comfort, invariant to the task location within the wound.

6.1. Introduction

Light, delivered by surgical lights, is important for surgeons to obtain useful visual information from the wound. Many authors have described different aspects of requirements for good surgical illumination (Anonymous 1970; Bartlett 1978; Beck 1978; Beck 1980; Beck 1981; Gregory 1987; Condon and Quebbeman 1988; Oostlander 1988; Galassini 1990; Bourke, Yee et al. 1993; Quebbeman 1993; Geisse 1994; Berguer 1997; Hadrot 1998; Loonam and Millis 2003; Brogmus, Leone et al. 2007; Litorja, Brown et al. 2007; Okoro, Patel et al. 2007; IEC 2009; Knulst, Stassen et al. 2009; Knulst, Stassen et al. 2009; Knulst, Dongen et al. 2011), ranging from characteristics of the illumination to manoeuvrability of the light head. Despite those requirements the usability of the surgical light has led to complaints from the user (Patkin 2003; Matern and Koneczny 2007; Knulst, Mooijweer et al. 2011). It appeared that surgical lights needed frequent adaptation of position during surgery, dominantly because of insufficient illumination at a new working location after a change in working location within in the wound. These adaptations can be quite cumbersome because of bad mechanics of the light (Knulst, Mooijweer et al. 2011; Knulst, Mooijweer et al. 2012) and can disrupt the visual feedback with the wound (Stassen, Dankelman et al. 1999). Headlights or light sources in the wound (Knulst, Santos et al. 2011) were suggested to reduce the number of adaptations during surgery.

Surgical lights provide highly focused, concentrated light to the wound (Knulst, Stassen et al. 2009; Knulst, Stassen et al. 2009). The effect can be a difference in luminance within the wound: some areas are brightly lit, whereas other areas are less brightly lit. Besides that, surgical lights project not only light on the wound itself, but also on the surroundings of the wound. As the surrounding skin and drapes reflect light two to three times better than the wound (Beck 1981), the effect is a difference in luminance between the wound and its surroundings: the wound appears dark compared to the skin and drapes. The human eye adapts to the average luminance within about 20° of the fixation point (Boyce 2003). Variations in luminance across the visual field might thus reduce the visual performance and comfort of the surgeon (Boyce 2003) and, therefore, lead to the need for adaptations of the light. Thus, an alternative approach to reduce the number of adaptations might be to create a better balance in luminance across the wound and surroundings.

Literature on contrast thresholds during different luminance conditions to determine if something is *not* visible is generally available, however, the effect of changing luminance conditions on how well something is visible is not generally available (Boyce 2003). Therefore, this study evaluates the effect of differences in luminance between the wound and the surroundings of the wound on the human visual performance and visual comfort. It is expected that a balanced luminance will lead to the highest performance and comfort, and thus to equal performance on different locations across the wound. The visual performance and the perceived comfort of subjects were assessed by colour contrasts discrimination tasks located at the centre and at the edge of a wound under different luminance conditions.

6.2. Methods

6.2.1 Setup

A setup was build consisting of a screen that contained a wound area and a surgical drape area, two target locations within the wound area, two beamers to provide illumination, and a headrest and a seat for the subjects (Fig. 6.1). The subject was positioned 70cm away from the centre of the screen. The (1.20x0.55 m) screen was made of wood, and completely covered with standard surgical drapes. Only at the centre a 15 cm diameter circle was not covered by drapes, corresponding to 12.2° visual angle. Instead, a red printed piece of paper covered this circle. The red circle was defined as the 'wound area', a 10 cm band around the wound area, corresponding to 53.1° visual angle, was defined as the 'surgical drape area', and the remaining part of the screen was defined as the 'environment. Two 2x2 cm square target locations were cut in the wound area, one at the Centre and one at the right Edge of the wound area. Two circular discs were placed behind the screen, such that the edge of a disc covered a target location. Each disc hosted 63 colour contrast samples, visible to a subject at one of the target locations. By rotating a disc a series of different contrast samples could be presented to a subject to assess the subject's visual performance.

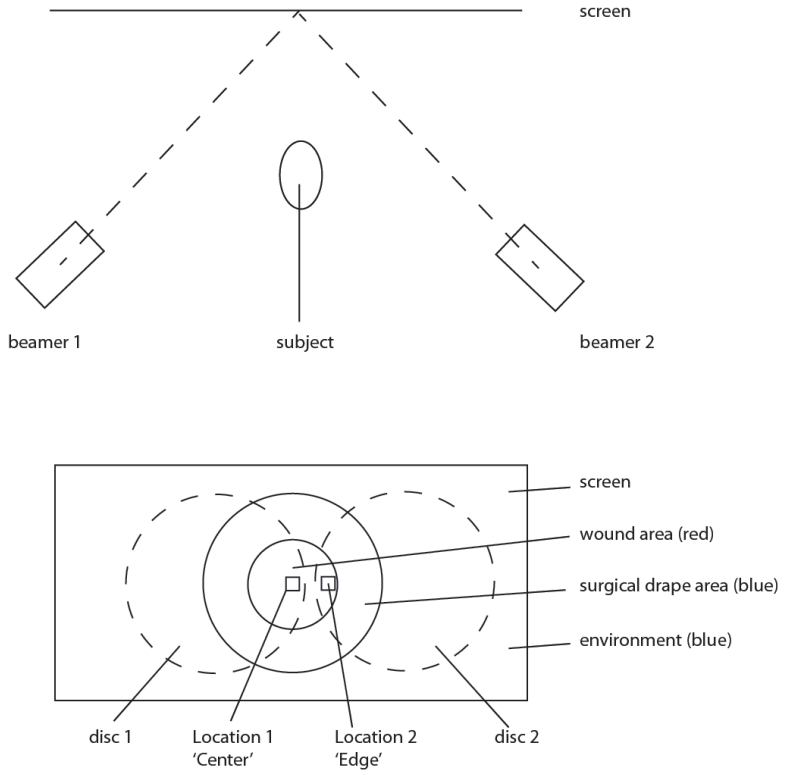

Figure 6.1 Schematic picture of the setup, showing a top-view (upper picture) and a front-view (lower picture) of the setup.

6.2.2 Colour contrasts samples

The colour contrast samples were made of red printed paper in the same colour as the 'wound' with one or more stripes in a slightly different shade of red, thus creating a colour difference between stripes and background. From a wide selection of samples 7 different colour contrast samples were selected, ranging from easy to hard to discriminate. Each colour contrast sample had 9 variations: one to three stripes with a left diagonal, vertical or right diagonal orientation. The colour contrasts were computed as Colour differences using a Matlab algorithm that computes the CIEDE2000 colour difference (Sharma ; Sharma, Wu et al. 2005). The colours of the background and samples were obtained from one photograph that showed all different colour contrast samples using Photoshop. Table 1 presents the Colour difference for each colour contrast sample.

Table 6.1 Colour difference of the colour contrast samples.

Colour contrast sample	**1**	**2**	**3**	**4**	**5**	**6**	**7**
Colour difference to background	0.7	1.5	2.2	2.8	8.0	8.2	9.0

6.2.3 Luminance conditions

The beamers were used to project varying amounts of light on different parts of the screen using images that contained varying shades of gray. Each image had three concentric areas whose projection corresponded with concentric circles on the wound area, the surgical drape area, and the environment area. By changing the gray value of each area the amount of light on each part of the screen could be varied. The resulting luminance of each area on the screen relative to the other areas as seen from the subject's position was measured. The Luminance ratio (L_W/L_D) of the wound area (L_W) to the surgical drape area (L_D) was computed. Also the Luminance ratio (L_W/L_E) of the wound area to the environment (L_E) was computed. The images were adapted until a set of seven different Luminance ratios L_W/L_D was created for a fixed 0.03 ratio of L_W/L_E. In other words: the luminance of the surgical drape area was varied while keeping the luminance of the wound area and the surrounding environment constant. Table 2 lists the luminance conditions and corresponding Luminance ratios.

Table 2 Definition of the luminance conditions.

Luminance condition	1	2	3	4	5	6	7
Ratio L_W/L_D	7.1	5.1	2.1	1.0	0.5	0.2	0.1

6.2.4 Protocol

Forty subjects were included in the experiment and were assigned to four groups for later data-analysis. Thirty subjects (age: 21±1) were randomly assigned to groups 1 to 3, and ten subjects (age: 52±5) were assigned to group 4. All subjects had normal colour vision, determined with the Ishihara colour test. Each subject was to be seated

in front of the setup. Subjects were instructed to read the number and orientation of the contrast stripes for the Centre and Edge location consecutively.

For each subject the sequence of luminance conditions was determined randomly. For each luminance condition a series of colour contrast samples was presented in random sequence to the subject at each location. Each series had a fixed order: starting at the highest colour contrast and ending at the lowest colour contrast. Each series was repeated twice per luminance condition. The orientation and number of the stripes of each presented sample was randomly selected. The answers of the subject for each sample and each location were recorded as 'correct' or 'incorrect', which was converted to a score of '1' and '0' respectively. At the end of each contrast test subjects were asked to rate the current visual Comfort on a 5-point Likert scale ranging from bad to good visual Comfort.

6.2.5 Data analysis

Visual performance

Visual performance was assessed using the score data. For each of the four groups the group Score was computed for each colour contrast sample during a certain luminance condition and location, resulting in a group Score between 0 and 1 with 0.05 resolution. The group Score was defined as the ratio of correctly identified colour samples over the number of tested colour samples. A sigmoid psychometric function with two parameters (a and b) as function of the Colour difference (x) (Eq. 6.1) was fitted to the group Score for each Luminance condition, each Location, and for each Group to define the parameters *a* and *b*, and to compute the Threshold value (Eq. 6.2). The Threshold value defines the minimal Colour difference that is required to achieve a Score that is more than chance. For both group Scores and Thresholds the difference between the Centre and Edge location was computed. Group Scores, Thresholds, Score difference, and Threshold difference were tested using a repeated measures ANOVA in SPSS with Location and Luminance condition as factors.

$$score(x) = \frac{1}{1 + e^{a \cdot x + b}} \qquad \textit{(Eq. 6.1)}$$

$$threshold = b / a \qquad \textit{(Eq. 6.2)}$$

Comfort

Comfort was assessed using the subjective comfort rating data. Comfort scores of each subject were normalized to the average Comfort score of that subject. A non-parametric Related-Samples Friedman's Analysis of Variance by Ranks was used to test the effect of luminance conditions on the experienced comfort, because the obtained Likert-scale was an ordinal scale.

6.3. Results

Figure 6.2 shows the fitted Score of each group for the Centre and Edge location under different Luminance ratios as function of the Colour difference. Three main effects can be seen when comparing the figures. Firstly, the lines for the different luminance conditions are not on top of each other, but are slightly different. Secondly, for all groups and luminance conditions the slopes of the lines are steeper at the Centre than for the Edge location. And thirdly, Group 4 had a less steep curve than the other groups for both the Centre and the Edge location.

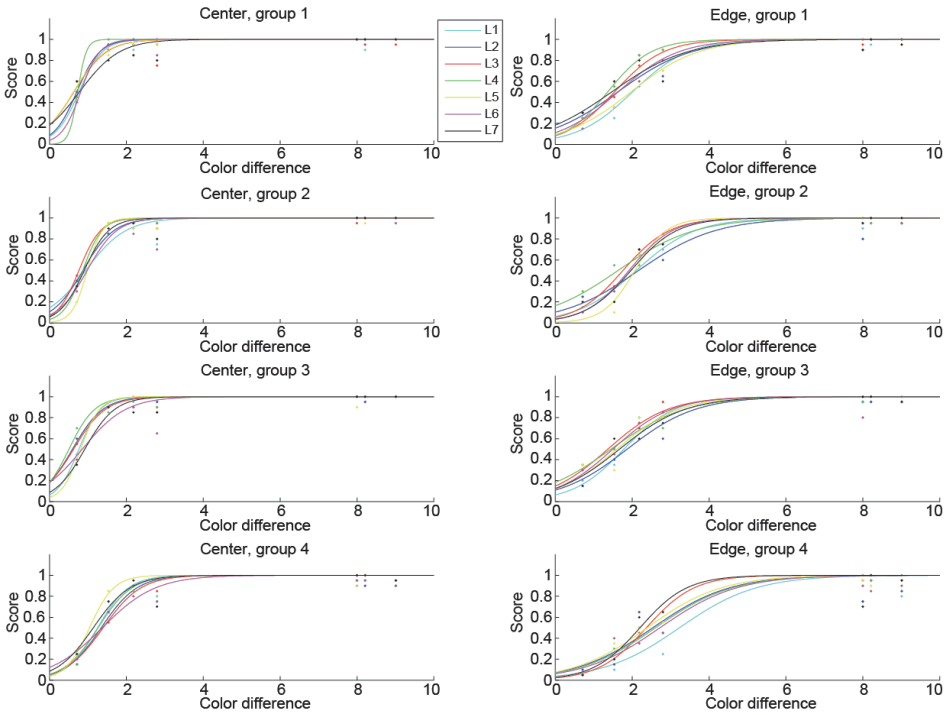

Figure 6.2 Scores and fits for the Centre location (left panels) and Edge location (right panels) for the four groups (upper to lower panels) during the tested Luminance ratios (separate lines). L1 to L7 indicate the luminance conditions 1 to 7.

Table 6.3 lists the significance of the overall effects of the factors Location, Luminance ratio and Colour difference on the metrics Score, Threshold, Score difference between Locations, Threshold difference between Locations, and Comfort.

Table 3 Significance (p-value) of the factors Location, Luminance ratio and Colour difference on the metrics Score, Threshold, Score difference, Threshold difference, and Comfort.

	Score	Threshold	Score difference	Threshold difference	Comfort
Location	0.000	0.000	n.a.*	n.a.*	n.a.*
Luminance ratio	0.000	0.001	0.015	0.034	0.000
Colour difference	0.000	n.a.*	n.a.*	n.a.*	n.a.*
* n.a.: factor is not applicable on this metric.					

Figure 6.3 shows the effect of Colour difference on the Score over all groups and over all luminance conditions for each Location. Clearly, the Edge location scores lower than the Centre location. Samples with a small Colour differences were harder to see correctly than samples with large Colour differences. Only the samples at 2.2 and 2.80 and at 8.2 and 9.0 had no significant difference.

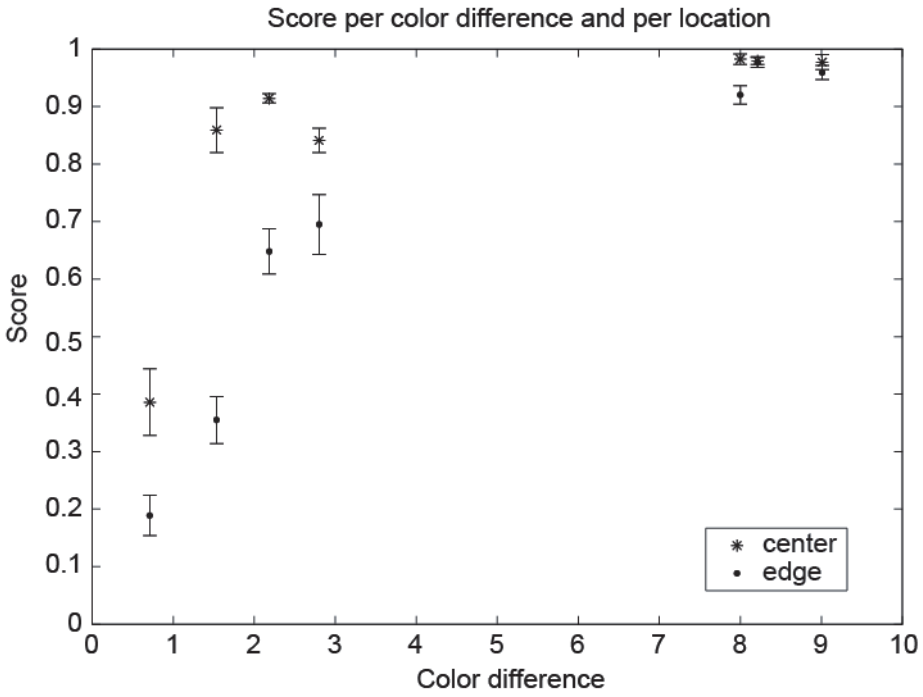

Figure 6.3 Effect of Colour difference and Location on Score.

Figure 6.4 (left panels) shows the effect of the Luminance ratios on the Score (upper panel) and on the estimated Thresholds (lower panel) for the two Locations. Overall, the difference between the two Locations was large. The Thresholds were doubled at

the Edge location compared to the Centre and the Score was reduced by 20%. The highest Score was obtained for the Luminance ratio 1.0, although it was not significantly different from Luminance ratios 0.5 and 2.1. The lowest Threshold was also obtained for Luminance ratio 1.0, although again it was not significantly different from 0.5 and 2.1. The results show that the visual performance in terms of Scores and Thresholds significantly decreased for Luminance ratios larger than 2 and smaller than 0.5.

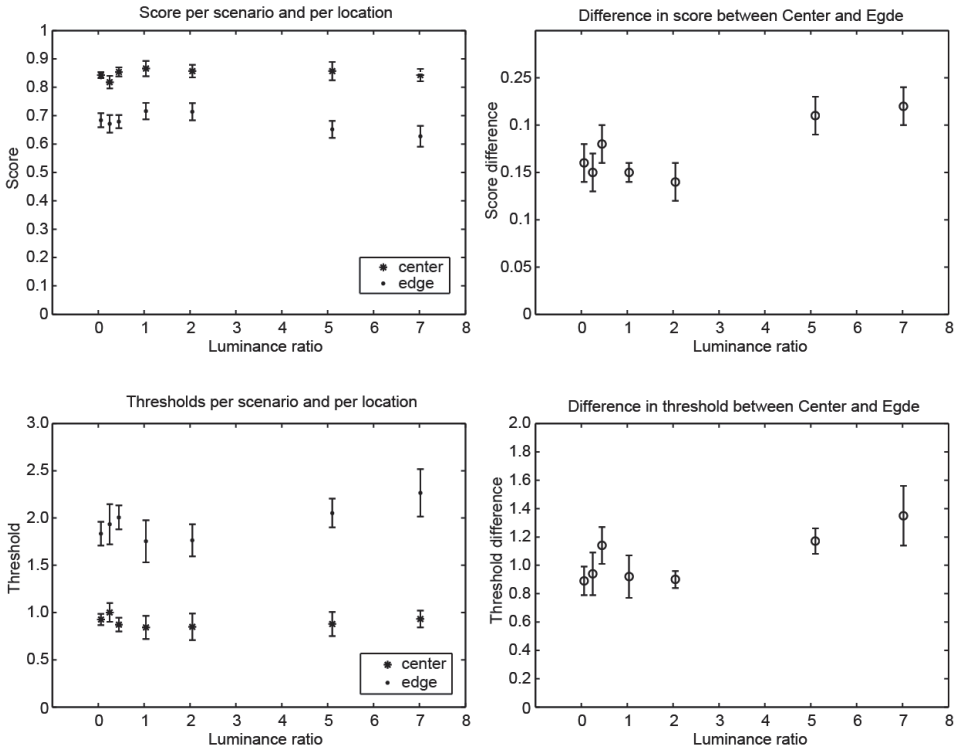

Figure 6.4 Effect of Luminance ratio and Location on Score, Threshold, Score difference, and Threshold difference.

Figure 6.4 (right panels) shows the effect of the Luminance ratios on the differences in Score (upper panel) and Threshold (lower panel) between the two Locations. The smallest differences for both Score and Threshold were obtained for Luminance ratios between 0 and 2, without any significant differences within this range. Significant effects were found between Score and Threshold differences for Luminance ratios in this range and differences for Luminance ratios larger than 2.

Figure 6.5 shows the effect of the Luminance ratios on the perceived Comfort of subjects. Luminance ratio 1.0 had the highest median Comfort, although it was not significantly different from 0.5 and 2.0. The Comfort was significantly reduced for Luminance ratios smaller than 0.5 or larger than 2.0.

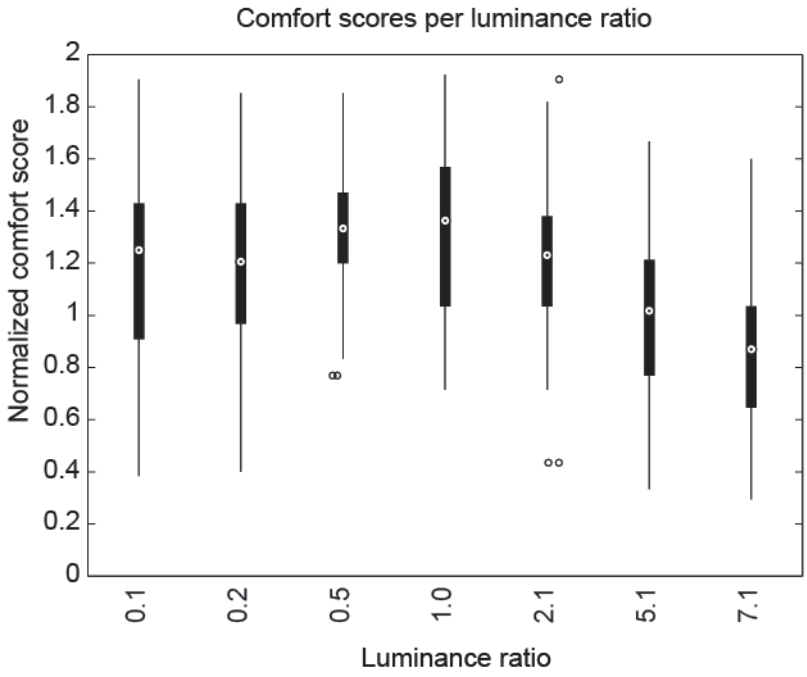

Figure 6.5 Comfort Scores per Luminance ratio, normalized to the mean Comfort Score of a subject.

6.4. Discussion

The results of this study showed that the Luminance ratio (luminance of the wound divided by the luminance of the direct surroundings of the wound) has significant influence on visual performance and comfort. Besides the Luminance ratio, also the Location of the visual task within the wound was shown to have a large and significant influence on visual performance. The difference between the visual performances at the two Locations was significantly affected by the Luminance ratio. What do these findings mean, and how can these be implemented in good surgical lighting?

It was hypothesized that a uniform luminance distribution (the Luminance ratio equals one) will lead to the highest Score, to the lowest Threshold, to a zero, and minimum difference in Score and Threshold between the Centre and the Edge of the wound, and to the highest perceived Comfort. In that case visual performance would be optimal and equal across the whole wound, minimizing the need for adaptations of the light. The results of this study confirm most of these expectations. Only the difference in Score and Threshold between the Centre and Edge did not become very small, although a minimum was found. Also, the effect of an increasing Luminance ratio was not the same as that of a decreasing Luminance ratio, showing asymmetry in the results. The improvements in Score were mainly because of the decrease in Threshold

and/or the increase in Score at small Colour differences. These findings can improve the illumination of wounds.

It is clear that a uniform luminance pattern across the wound and its surroundings will improve the visual performance and the perceived Comfort of surgeons. However, it was not expected that the effect of a difference in luminance between wound and surroundings is larger for a 5 times higher luminance of the surroundings than for a 5 times lower luminance of the surroundings. It seems that the human eye can better see in a relatively bright area than in a relatively dark area. Therefore, for good visual performance and comfort the surroundings of the wound can better be lit too less than too much, although of course, equal luminance is to be preferred.

The difference in Scores and Thresholds between the Centre and the Edge location did not completely behave as expected. The effect of a minimum difference for a Luminance ratio around one was clearly found. At the Edge, best visual performance was clearly obtained for a Luminance ratio of one. However, the minimum difference was not as small as expected. For uniform luminance the minimum difference was expected to become close to zero, leading to equal visual performance across the complete wound, thereby minimizing the need for adjustments of the surgical light. Obviously, another factor than the Luminance ratio played an important role here.

Besides adaptation to luminance, the eye also adapts to colours changing the perception of colours depending on the environment. The Centre location was completely surrounded by red paper, whereas the Edge location was surrounded by red paper at the left side, and by blue surgical drapes at the right size. At this location, the ‘settings’ of the eye were not optimal for discrimination of small reddish colour contrasts, but at a compromise between red and blue. Presumably, this difference in colour adaptation caused a different perception of the colour contrast samples, leading to a far worse visual performance. It might also have influence on the perceived Comfort. Thus, to create better equality in visual performance across the full wound, it might not only be useful to balance the luminance of the direct surroundings of the wound, but also the colour.

The behaviour of the group of senior subjects showed some trends, although not significantly tested. Firstly, their Thresholds were higher and their Scores lower than the younger subjects’, especially for the highest and lowest Luminance ratios. Secondly, their Comfort Scores for the highest and lowest Luminance ratios were lower than the younger subjects’. As many surgeons are aged closer to this senior group than to the younger group, the effects of luminance and colour difference on visual performance and comfort might even be stronger than reported in this study. Proper illuminance might thus be even more important when optimizing illumination for surgeons.

6.5. Conclusion

This study showed that visual performance and comfort of subjects is significantly affected by the Luminance ratio of the wound and the surroundings of the wound. For optimal visual performance and comfort the luminance should be balanced. This study also showed that the visual performance is not equal across the wound: close to the Edge of the wound both Thresholds and Scores were significantly worse than at the Centre. Although the Luminance ratio had some effect on this difference, the main cause is thought to be the difference in colour of the wound and the surgical drapes. Besides the Luminance ratio also the colours seem to require a certain balance. Implementation of these findings in surgical lighting will increase the surgeon's visual performance and Comfort, and might lead to a reduced amount of adaptations of the surgical light during surgery.

6.6. References

Anonymous. 1970. OPERATION LIGHTING. A SURGICAL ODYSSEY. 65(1): 25-30.

Bartlett D. 1978. Operating theatre lighting. NATNews 15(11): 24-30.

Beck WC. 1978. Lighting the surgical suite. Contemp Surg. 12(1): 9-16.

Beck WC. 1980. Choosing surgical illumination. Am J Surg 140(2): 327-331.

Beck WC. 1981. Operating room illumination: the current state of the art. Bull Am Coll Surg 66(5): 10-15.

Berguer R. 1997. The application of ergonomics in the work environment of general surgeons. Rev Environ Health 12(2): 99-106.

Bourke DL, Yee K, et al. 1993. Severe burn caused by an operating room light. 79(1): 171-173.

Boyce PR (2003). Human factors in Lighting, Taylor & Francis Ltd.

Brogmus G, Leone W, et al. 2007. Best Practices in OR Suite Layout and Equipment Choices to Reduce Slips, Trips, and Falls. 86(3): 384-398.

Condon RE and Quebbeman EJ. 1988. Preparing the operating room. 2: 82-85.

Galassini A. 1990. Lighting system for operating rooms-Criteria and norms. 77: 1153-1158.

Geisse JK. 1994. The dermatologic surgical suite. Semin Dermatol 13(1): 2-9.

Gregory MM. 1987. Surgical lights. Making a purchase decision. AORN J 46(5): 904-918.

Hadrot L. 1998. Surgical light. 20(3): 9-15.

IEC (2009). International Standard - Medical electrical equipment - Part 2-41 Particular requirements for the safety of surgical luminaires and luminaires for diagnosis. Geneva, International Electrotechnical Commission: 38.

Knulst AJ, Dongen Jv, et al. 2011. The effect of shadows on performing stereo visual pointing tasks: Is shadow-free open surgery ideal? 8(2): 111-122.

Knulst AJ, Mooijweer R, et al. 2012. A simulation model that predicts handling forces required to reposition surgical lights. Journal of medical engineering & technology 36(3): 174-179.

Knulst AJ, Mooijweer R, et al. 2011. Indicating shortcomings of surgical lighting systems. MITAT 20(5): 267-275.

Knulst AJ, Santos ALR, et al. 2011. Evaluation of a New Surgical Light Source for Difficult Visibility Procedures. 18(3): 214-222.

Knulst AJ, Stassen LP, et al. 2009. Choosing surgical lighting in the LED era. Surg Innov 16(4): 317-323.

Knulst AJ, Stassen LPS, et al. 2009. Standards and Performance Indicators for Surgical Luminaires. Leukos 6(1): 37-49.

Litorja M, Brown S, et al. (2007). Development of surgical lighting for enhanced colour contrast. Progress in Biomedical Optics and Imaging - Proceedings of SPIE, San Diego, CA.

Loonam JE and Millis DL. 2003. Choosing surgical lighting. Comp Cont Educ Pract 25(7): 537-543.

Matern U and Koneczny S. 2007. Safety, hazards and ergonomics in the operating room. Surg Endosc 21(11): 1965-1969.

Okoro SA, Patel TH, et al. 2007. Who needs the surgical headlight? 44(2): 126-128.

Oostlander K. 1988. Potentials and risks of lighting technic in the operating room. 26(1-2): 14-19.

Patkin M. 2003. What surgeons want in operating rooms. MITAT 12(6): 256-262.

Quebbeman EJ. 1993. Preparing the operating room. Care of the surgical patient: A publication of the committee on pre and postoperative care. Sci Am 5: 1-13.

Sharma G. "http://www.ece.rochester.edu/~gsharma/ciede2000/." Retrieved November, 2011.

Sharma G, Wu WC, et al. 2005. The CIEDE2000 colour-difference formula: Implementation notes, supplementary test data, and mathematical observations. 30(1): 21-30.

Stassen HG, Dankelman J, et al. 1999. Open versus minimally invasive surgery: a man-machine system approach. Trans Inst Meas Contr 21(4-5): 151-162.

Chapter 7

Illumination from within wounds

Arjan J. Knulst, Ana Laura R. Santos, Richard H.M. Goossens, Jenny Dankelman

Evaluation of a new surgical light source for difficult visibility procedures.
SURGICAL INNOVATION, 18(3): 214-222, 2011

A new lighting device for open surgery of difficult access wounds was designed: the Extender add-on. The performance of the Extender is evaluated and compared with the conventional solutions used in the operating room (OR) on illumination quality. A cylindrical setup was built to measure the distribution of light in a simulated pelvic wound. The light was provided by a head-mounted light, an OR light, and a pair of Extender prototypes. The results showed that the Extender prototypes provided 12.2 lumens inside the wound, whereas the head-mounted light gave 5.7 lumens. The Extenders provided smoothly angular distributed light from 0° to 180°, whereas the head-mounted light and OR light only provided light from 115° to 180°. The Extender prototypes had a promising performance in terms of light distribution. It is expected that a more accurately produced Extender will increase performance in terms of illumination quantity and illumination distribution smoothness even further.

7.1 Introduction

Visualization of surgical wounds depends mainly on 3 factors: good illumination, non-obstruction, and efficient retraction (Beck 1981). Open surgical procedures (e.g., deep pelvis and thorax (Knulst et al. 2010) involve wounds of difficult access and are characterized for their poor visibility conditions (Matern and Koneczny 2007; Satos et al. 2009). Head-mounted lights are frequently used as a complement to main operating lamps in order to establish sufficient illumination of the field. However, the performance of these conventional lighting solutions is not always efficient because they require unpractical and sometimes annoying adjustments that are time consuming and require concentration (Knulst et al. 2010). Furthermore, they do not provide steady illumination, and they limit the mobility of the surgeon (Knulst et al. 2010, Matern and Koneczny 2007; Santos et al. 2009; Patkin 2003). In addition, strong glare and the presence of harsh shadows significantly reduce the visualization and focus of the surgeon (Ersek and Lellehei 1972).

An alternative solution to illuminate narrow and deep wounds is proposed: the Extender add-on (Figure 7.1). The device was designed to use during pelvic procedures to project light into depth and extend the effect of retraction. The main advantages offered by this design include the operator independence, its additional retraction function, modularity allowing the adaptation to different procedures and variety of choice for instruments application. Furthermore, it is a cable-free solution of safe and environment-friendly disposable. The main claimed assumptions are the ability to reach deep in the wound, to provide a uniform light distribution, and to provide reduced shadow intensity.

In this study, the illumination performance of a pair of Extenders is compared to conventional lighting sources and evaluated on illumination quantity, distribution and depth, using a specially built wound model.

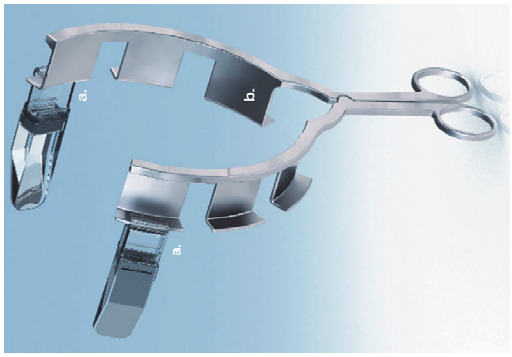

Figure 7.1: Artist's impression of the Extender add-on: (a) the Extender add-on and (b) a rectal retractor

7.2 Methods

7.2.1 Setup

A setup was built to systematically compare the different lighting solutions in a standardized wound simulation (Figures 7.2 and 7.3). This setup is composed of 6 important components: (1) a wound model, (2) illumination sensors, (3) 2 Extenders, (4) a head model, (5) a head-mounted light (Karl Storz Type 094053, Tuttlingen, Germany), and (6) an operating room (OR) light (Berchtold Chromophare D650, Tuttlingen, Germany).

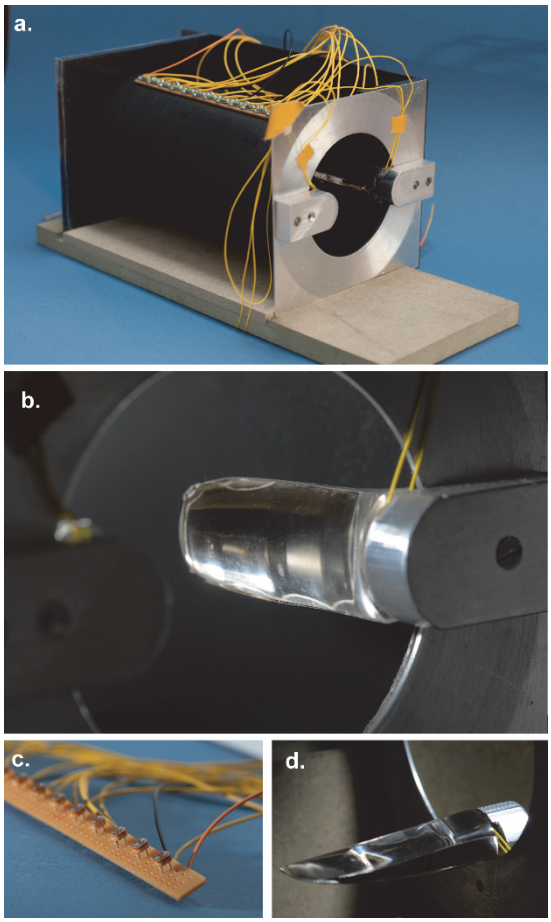

Figure 7.2: Components of the experimental setup: (a) the wound model, (b) a mounted extender inside the setup, (c) a detailed picture of the light-dependent resistors used as light sensors, and (d) an Extender in detail.

The wound model (Figures 7.2a and 7.3) was made from a matte black polyvinyl chloride (PVC) cylindrical tube of 70 mm in diameter and 150 mm in depth, according to anatomic measurements of the deep pelvic cavity during surgery, after resection of the rectal tumour (Gordon and Nivatvongs 2007). To mimic the high absorption of light

by haemoglobin and tissue and thus prevent reflections of light within the wound, the matte black PVC material was chosen for the tube. The cylinder was supported horizontally but was rotatable about its axis.

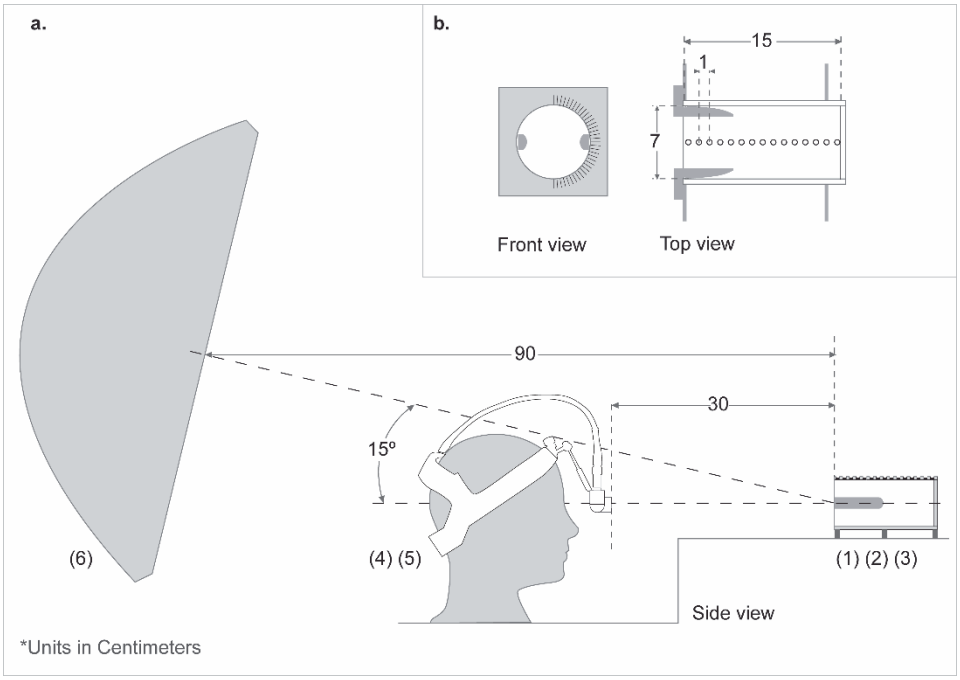

Figure 7.3: Schematic overviews of the setup: (a) a side view and (b) a front and top view of the wound model The numbers between brackets refer to the setup components as mentioned in the text.

An array of 15 light dependent resistors (LDR VT935G group A) was inserted through 15 holes in the wall of the cylinder, with 10-mm spacing between the sensors to measure the illuminance in the wound at different points of depth (Figures 7.2c and 7.3). The 4.8-mm diameter resistors were individually calibrated by measuring their resistance at different light levels (from 535 to 5380 lx). The calibration results were used by the measuring program (LabVIEW) to compute the illuminance. All readings of the resistors had an error in light level less than 10% and were stored to a computer via an analogue to digital converter.

A human head model (Figure 7.3a) was used to support the head-mounted light, to create a realistic obstacle for the illumination produced by the OR light, and to provide a centreline between eyes. The axis of illumination output of the headset was aligned with the axis of the wound model, and positioned at a distance of 30 cm from the wound surface (Figure 3c). This alignment should provide best possible illumination in the deep part of the wound, although it is not always realistic since the wound is often lower than the surgeons' heads and the surgeons do not maintain a permanent

position. The OR light axis of illumination was aligned with the axis of the wound, with a vertical angle of 15° with respect to the wound axis (Figure 3c), to provide best possible illumination into the deep part of the wound.

One Extender consists of a set of 2 battery-powered add-ons, mountable in symmetric pairs to different retractors. An add-on integrates 2 disposable acrylic parts—a lens, which spreads the light and extends the retraction of the wound, and a grip to attach to a common retractor blade—which snap together in a watertight and sterile connection. The modular configuration of this add-on allows a versatile production of different size components.

For this study, the Extender lenses were designed, analysed, and optimized for their illumination performance in LightTools, a software package for illumination design and evaluation (Optical Research Associates, Pasadena, CA). The optimization goal was a uniform illumination distribution across the full half-wound, with the same illumination level at any point of the half cylinder. For this simulation, only a half cylinder and one Extender were used because of assumed symmetry. The optimization design process resulted in the following Extender design: An Extender consisted of a light-emitting device (LED; Lumileds Luxeon Rebel. Philips Lumileds, San Jose, CA), a heat sink to dissipate heat, a specially shaped lens (Figure 7.4 and Table 7.1), and a reflective adhesive (ReflecTech, Arvada, CO) on the back of the lens. The poly(methyl methacrylate) lens was CNC-machined and hand-polished.

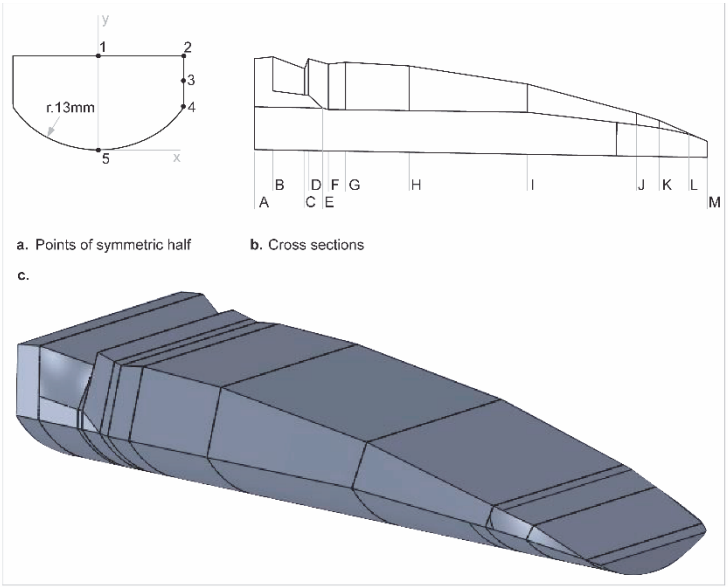

Figure 7.4. The geometry of an Extender lens: (a) a symmetric cross-section with points 1 to 5 defined, (b) the locations of the different cross-sections A to M, and (c) a 3-dimensional visualization

Two Extenders were mounted at the front of the cylinder, opposite to each other, and glued to the heat sink (Figures 7.2a, 7.2b, and 7.2d). An aluminium plate was placed in front of the cylinder to attach the Extenders' heat sinks and to simulate the reflective environment around the wound caused by skin, gauzes, and instruments. The Extenders were connected in series to a power source driving the LEDs at 350 mA.

Table 7.1. x, y, z Coordinates (mm) of Points 1 to 5 (Figure 4a), in Cross-Sections A to M (Figure 4b)

	1		2		3		4		5	
	x	y	x	y	x	y	x	y	x	y
A:z 0.000	-10.00	0.00	-10.00	10.00	-6.45	10.00	-4.70	10.00	0.00	0.00
B:z 2.000	-10.20	0.00	-10.20	10.00	-6.45	10.00	-4.66	10.00	0.04	0.00
C:z 5.500	-8.90	0.00	-8.90	8.00	-6.00	10.00	-4.60	10.00	0.10	0.00
D:z 5.900	-10.00	0.00	-10.00	8.24	-6.00	10.00	-4.59	10.00	0.11	0.00
E:z 7.478	-9.57	0.00	-9.57	8.33	-4.57	10.00	-4.57	10.00	0.13	0.00
F:z 8.100	-9.40	0.00	-9.40	8.37	-4.41	9.88	-4.41	9.88	0.14	0.00
G:z 10.000	-9.60	0.00	-9.60	8.28	-4.38	9.88	-4.38	9.88	0.18	0.00
H:z 17.000	-9.20	0.00	-9.20	8.31	-4.29	9.91	-4.29	9.91	0.30	0.00
I:z 30.000	-7.20	0.00	-7.20	8.21	-4.10	9.94	-4.10	9.94	0.53	0.00
J:z 41.204	-4.21	0.00	-4.21	7.96	-2.81	8.91	-2.81	8.91	0.72	0.00
K:z 44.500	-3.20	0.00	-3.20	7.53	-2.31	8.41	-2.31	8.41	0.78	0.00
L:z 48.931	-1.27	0.00	-1.27	7.10	-1.27	7.10	-1.27	7.10	0.86	0.00
M:z 49.796	-0.89	0.00	-0.89	6.51	-0.89	6.51	-0.89	6.51	0.87	0.00

7.2.2 Measurement Protocol

To compare the performance of the new lighting solution to conventional solutions, 4 experimental scenarios were defined in each of which a different light source was used: Extenders, headlamp, OR light, and ambient level. For each of the scenarios, the illuminance on the inner surface of one half of the cylinder was measured from 0° to 180° at a 5° resolution and along the full depth at 5 to 145 mm at a 10-mm resolution. The result was an illuminance matrix over half the wound, measuring 15 values deep and 37 values wide. Only one half of the cylinder was measured because of symmetry in the setup. Each measurement was repeated 3 times to increase the measurement accuracy. The OR light was measured at minimum power, because of limitations of the illumination sensors, as this has no effect on the relative distribution of light. The ambient light level was solely measured at a limited number of angles to estimate if any measured values needed to be compensated for ambient light. The alignments of

the OR light and headlight were not changed during the experiment, as the goal of the Extenders was to provide better lighting without any adaptation when the area of the surgeon's attention shifts across the wound, whereas the traditional lights do need these changes because they offer very localized light.

7.2.4 Data Analysis

The data analysis was done in Matlab 2007. First, the 3 repetitions were averaged and compensated for ambient light. The total amount of light in the wound was computed by numerical integration of the measured illuminances over the whole half-cylinder. Next, 2 boxplots were computed for the Extender simulation and for each lighting concept to visualize (1) the illumination distribution at different angles across all depths and (2) the illumination distribution at different depths across all angles. It is important to note that the boxplots do not represent the variation in data at one location because of measurement inaccuracy, measurement noise or any other measurement disturbance as boxplots normally do but represent the variation in the distribution of light along the wall of the cylindrical wound in a certain direction: (1) in axial direction and (2) in angular direction. If the distribution of light is perfectly smooth then the spread will be zero. If there is more variation in light distribution, but the variation is symmetric then the spread will grow, and the median will be in the middle of the boxplot. If the distribution is not symmetric then the median will tell the symmetry of the variation by moving to one of the boxplot's borders. Thus, the spread in the boxplots characterizes the smoothness of the illumination distribution across either all angles or across the full depth, and the median visualizes how balanced the illumination distribution is over either all depths or all angles.

7.3 Results

Table 7.2 lists the total amount of light in the wound for each lighting concept. The Extenders provided in the wound more than twice the total amount of light of the headlight. The OR light provided more light in the wound than the Extenders, even when running on minimum power. For all measurements, the maximum error between the 3 repetitions of each sample was less than 0.05%.

Table 7.2. Total Amount of Incident Light Inside the Half Wound for Different Lighting Concepts, in Units of Lumen (lm)

Lighting concept	Total luminous flux inside the wound [lm]
Extenders	12.2
Headlight	5.7
OR-light (minimum power)	17.3

Figure 7.5 displays for each lighting concept the illumination distributions along the full depth of the wound at different, constant angulations in the wound, visualized by boxplots. Figure 5a displays the results of the LightTools simulation of the Extenders

design, Figures 7.5b to 7.5d show the results of the Extenders, Headlight, and OR light measurements, respectively. Regarding the spread in the boxplots, the variation of the illumination distribution across the depth of the wound was smaller for the simulated Extenders than for the measured Extenders. The Extenders (Figure 7.5b) provided light at every angle in the wound (although not highly uniform in depth), whereas the headlight (Figure 7.5c) and the OR light (Figure 7.5d) only provided light where they were aimed at. At 75° until 105°, the spread is larger because there was hardly any light on the cylinder wall as it was blocked by the extenders.

Figure 7.6 shows for each lighting concept the illumination distributions along the full hemi cylinder at different depths visualized by boxplots. Each boxplot visualizes the variation in illumination along the hemi cylinder at the depth specified on the x-axis. Figure 6a displays the results of the LightTools simulation of the Extenders design, Figures 6b to 6d show the results of the Extenders, headlight, and OR light measurements, respectively. The simulation of the Extenders again displays a smaller variation of the distribution of illumination across the depth of the wound and is also more constant over the different angles. Figure 6b shows that the Extenders provided more illumination in the shallow part of the hemi cylinder than in the deep part of the hemi cylinder. However, in the deepest parts of the wound, the Extenders still provided approximately identical median illumination levels compared with the headlight and the OR light (Figures 6c and 6d, respectively).

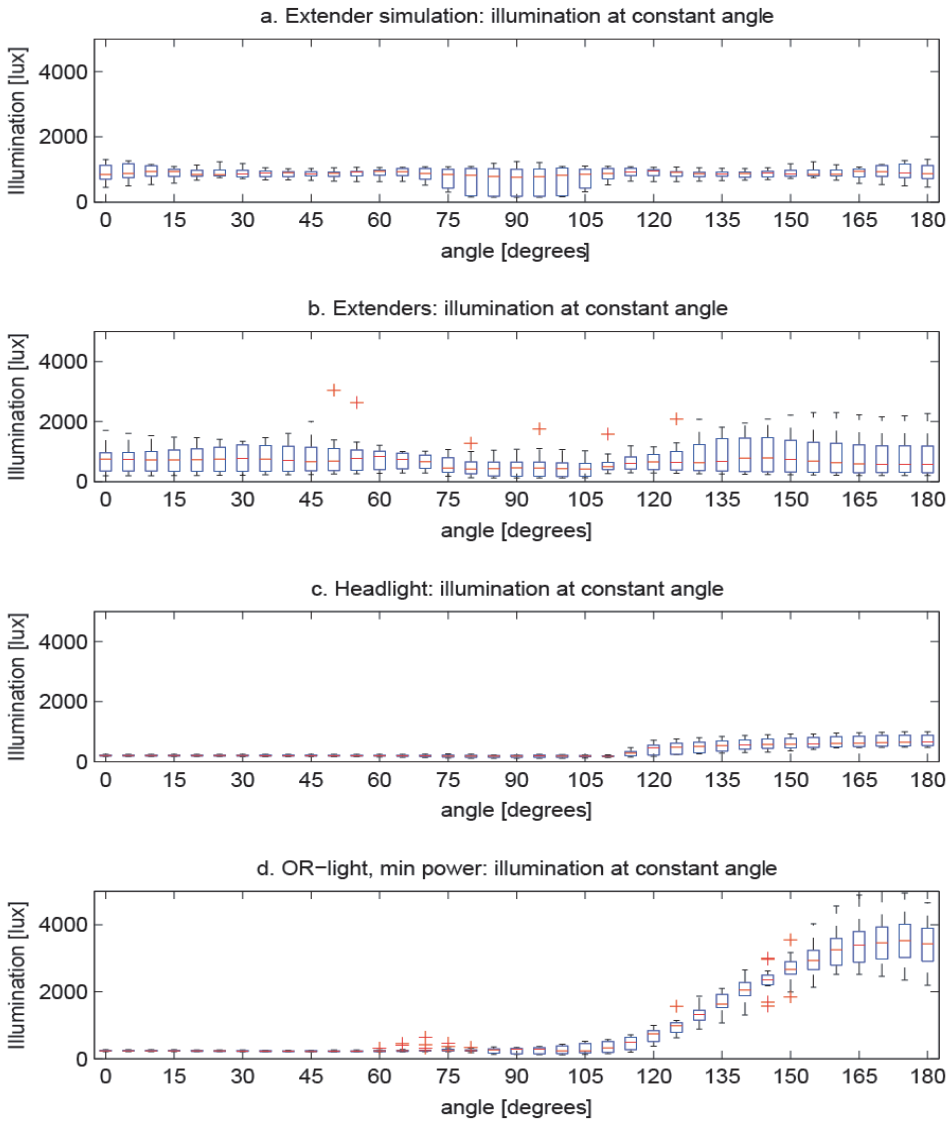

Figure 7.5. Boxplots representing the illumination distribution at different angles inside the wound for the different lighting concepts

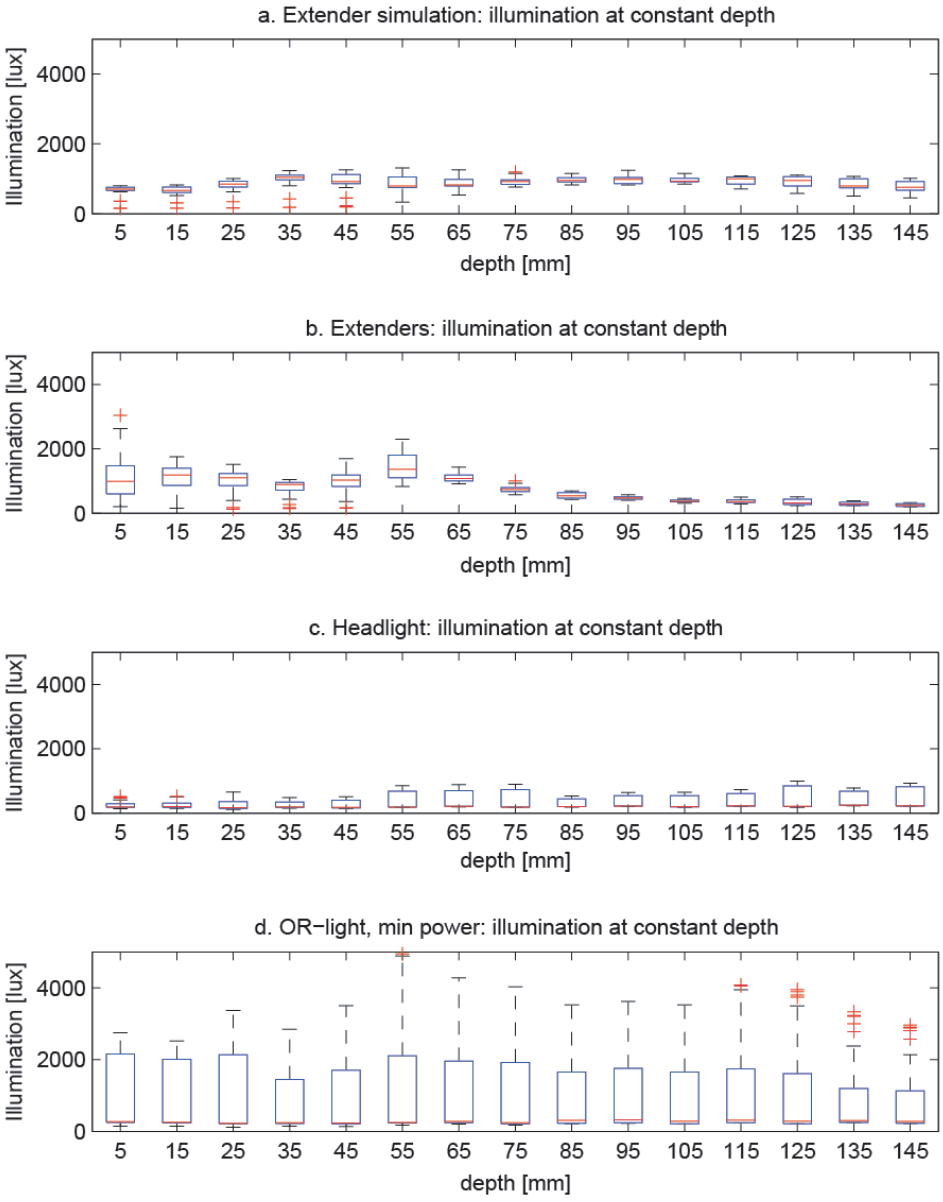

Figure 7.6. Boxplots representing the illumination distribution at different depths inside the wound for the different lighting concepts

From Figures 7.5b to 7.5d and Figures 7.6b to 7.6d it can be seen that the Extenders provided evenly distributed illumination along the hemi cylinder at a certain depth, as the medians in Figure 6b were approximately in the middle of the boxplot, in contrast to the medians of the headlight or the OR light (Figures 7.6c and 7.6d, respectively).

7.4 Discussion

Sufficient illumination of deep wounds during surgery was reported as hard to accomplish with conventional OR lights and headlights (Beck 1981, Knulst et al. 2010, Matern and Koneczny 2007; Ersek and Lillehei 1972) and therefore the Extenders concept was proposed. This research compared the illumination performance of the Extenders with an OR light and a headlight on the total amount of light in the wound and on the distribution of light across the total wound surface. It was shown that OR lights provided the most light in total inside of the wound, and the headlight the least. More important, it was shown that both the OR light and the headlight produced locally very concentrated light, whereas the Extenders produced well-distributed light across the whole wound surface, both in depth as in the angular direction. This implies that both the OR light as well as the headlight need to be redirected during surgery to keep proper illumination when the area of interest of the surgeon is shifting or when the surgical site changes in shape or orientation because of the surgeon's manipulations. The Extenders, however, require no extra handling after correct placement in the wound. The Extenders thus objectively showed to offer potential for illumination of deep surgical sites.

Visual inspection also showed better shadow-dissolving capability of the Extenders over the OR light or headlight. This makes sense, as the light that needs to enter the wound from an external light source is obstructed easily, whereas the light that is generated at multiple locations inside the wound is harder to block. However, this aspect was outside the scope of this study and as such, the setup used in this study did not allow for a standardized check to confirm this visual observation. The shadow-dissolving capability should be studied more thoroughly.

The evaluated Extender prototype did not exactly resemble the simulated performance with the virtual model: the illumination decreased with increasing depth and was also more irregularly distributed. In the LightTools simulations there was a better illumination into deep areas and a smoother illumination distribution. In the simulation only one light emitting Extender was incorporated in the model, whereas the other Extender was just a passive obstacle in the wound. Furthermore, in the simulation only one half of the cylinder—opposite the emitting Extender—was used to measure the light output. This information was used to optimize the Extender design for illumination distribution smoothness. However, modifications of the simulation model showed that the second Extender also emits light in the same half of the cylinder. This emittance formed 2 peaks just beside the second Extender. This emittance pattern was not incorporated in the simulations and turned out to be irregularly distributed. Figure 7.7 shows the boxplots of the data of the adapted simulation with the 2 Extenders incorporated. The same trends as during the measurements can be distinguished: more illumination and more variation in the first part of the cylinder than deep in the wound, and more variation in illumination beside the Extender (0° to 45° and 135° to 180°) than in the original simulation. The emittance over the full cylinder should be incorporated in the design process of a next-generation prototype.

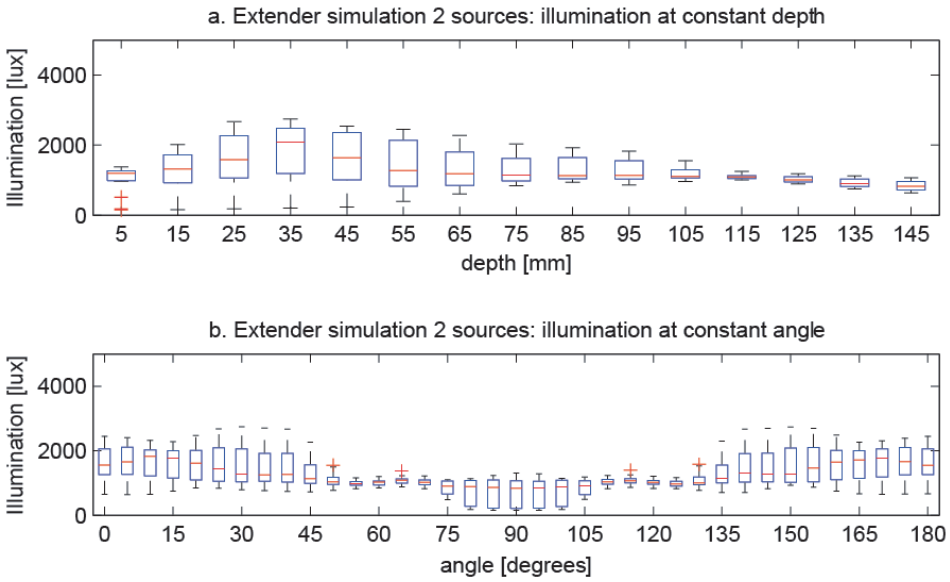

Figure 7.7. Boxplots representing the illumination distribution of the adapted simulation with 2 Extenders: (a) at constant depths and (b) at constant angles

The adapted simulation still does not exactly resemble the measurements. This performance mismatch was most probably caused by small differences between the prototype and the simulation model: CNC machining is less accurate than injection moulding, the reflective adhesive layer on the backside of the lens hardly replaces a metal coating because of its glue layer, the connection between LED and lens was not of precise fitting, and the surface finishing of the lens and its material grade did not match the required optical quality. These prototype shortcomings were caused by limited fabrication facilities available for this study.

An important aspect of illumination is the perceived illumination quality. Both headlights and OR lights not only produce light inside the wound but also illuminate directly at the skin around the wound. As such, the reflected light levels around the wound might be higher than the reflected light levels inside the wound. Such contrast ratios are known to hamper the visual performance and increase fatigue if their ratio is too high (Berguer 1997; Rohaly and Wilson 1999). As the Extenders only provide light inside the wound the contrast ratio during their use might be better for human visual performance and comfort. This study did not include this aspect but focused merely on objective, measureable illumination characteristics. How the illumination quality of the different lighting approaches is perceived by surgeons should be studied, together with usability evaluation, using a higher quality prototype and a different setup.

The tested Extender prototype had a promising performance in terms of illumination distribution and usability potential. For special wounds that are difficult to illuminate, the dedicated local illumination approach seems useful and promising. Earlier research

mentioned a top 4 of types of surgical working areas that were problematic to illuminate according to surgeons: transthoracic (23%), (deep) pelvic (21%), rectal (15%), and deep abdominal (15%). As the current Extender lens design was optimized for a deep cylindrical and relatively narrow wound, the design optimization needs to be redone when, for example, designing for a transthoracic procedure that is characterized by a large, dome-shaped wound. Also, the retractors used in these procedures might require a different design of the grip that connects the Extender to the retractor. So, dedicated designs need to be made for different types of deep wounds and retractors. It is expected that the illumination of these types of hard-to-illuminate wounds will improve and thereby minimize the need of repositioning of overhead OR lights or headlights.

7.5 References

Beck WC. Operating room illumination: the current state of the art. Bull Am Coll Surg. 1981;66(5):10-15

Berguer R. The application of ergonomics in the work environment of general surgeons. Rev Environ Health. 1997;12:99-106.

Ersek RA, Lillehei RC. A simple solution for the complex problem of surgical lighting. AORN J. 1972;15:68-72.

Gordon P, Nivatvongs S. Principles and Practice of Surgery for the Colon, Rectum, and Anus. New York, NY: Informa Healthcare; 2007.

Knulst AJ, Mooijweer R, Jansen FW, Stassen LP, Dankelman J. Indicating shortcomings in surgical lighting systems [published online ahead of print November 17, 2010]. Minim Invasive Ther Allied Technol. doi:10.3109/13645706.2010.5 34169.

Matern U, Koneczny S. Safety, hazards and ergonomics in the operating room. Surg Endosc. 2007;21:1965-1969.

Patkin M. What surgeons want in operating rooms. Minim Invasive Ther Allied Technol. 2003;12:256-262.

Rohaly AM, Wilson HR. The effects of contrast on perceived depth and depth discrimination. Vision Res. 1999;39:9-18.

Santos AL, Jakimowicz J, Goossens R. Lighting Pelvic Surgeries. Delft, Netherlands: Delft University of Technology, Faculty of Industrial Design; 2009.

Chapter 8

Lightfield adaptable surgical luminary

Jeroen Kunst, Arjan Knulst

Based on MSc Thesis of Jeroen Kunst.
Lightfield adaptable surgical luminary, July 2014

Submitted.

Visual performance and visual comfort are a combined effect of the lumination characteristics and the illuminated objects. Current surgical lighting systems have a fixed shape lumination pattern whereas the wound and surroundings have a variable shape and characteristics. A lighting system that is able to adapt its shape and light distribution to the characteristics of the wound might improve visual performance. This chapter describes the development of a new concept for lighting using bendable strips with LEDs. The basic idea of placing LEDs on a bendable surface is very simple and elegant. To achieve a functional system it is important to investigate the effects of the different design choices, such as shape of the stripes, number of LEDs, number of stripes, and LED power. The influence of these choices will be evaluated by simulation using a computational model to identify the optimal parameters for the design. The final design is evaluated using the computational model and a physical prototype consisting of one luminaire segment. The system is able to produce light fields that can have fairly complex shapes at a good range of different sizes. It was possible to give recommendations about aspects like spot size and strip number. The physical test model indicates that the calculated system seems to function in a way that is close to how it would in a real-life situation. Given the results it can be concluded that a system, which is able to modify the light field in real time and that requires minimal control effort, can be a good addition to the operating room.

8.1 Introduction

Proper lighting is an essential factor during a surgical procedure [NEN, 2009]. Many different luminaire systems are available on the market that all provide lighting in a generally comparable manner. These current surgical luminary systems often consist of a large central light source, sometimes accompanied by one or two satellite light sources and they are manually moved into position. These systems are able to project light towards the surgical field. The shape of the projected light field is determined by the luminary output of the system, the shape of the illuminated surface and the orientation that the luminaire and the target surface have in relation to each other. One set of parameters that control the properties of the projected light field is determined by the suspension arm system by which the luminary is connected to the ceiling. The range of motion of the suspension system determines under which angles the light is able to be projected and what the distance of the light source can be to the surgical area. Another set of parameters is determined by the light source itself. Typical properties of the light source are; the surface area of the light emitting surface, the shape of that surface, the focus point of the light beam, shape of the beam, spectral bandwidth and many more. These properties of the light source determine the shape and light distribution of projected light field and luminance of the illuminated surface.

Vision is a complex and dynamic sensory function. How well a person can see is largely determined by the lighting conditions that affect the illuminated object. Current surgical lighting systems project a round light field onto the surgical field that has a more or less a circular Gaussian distribution. Because wounds are often not round in shape it is thought that a circular Gaussian distribution is in many circumstances not the optimal lighting condition. Visual discomfort might arise from the fact that unnecessary areas inside the operating field are being illuminated. Everybody has experienced the effect of trying to look at a dark region when there is brightly illuminated region in front of it. It is difficult to see until you block the bright region, e.g. with your hand. This effect is also applicable to the situation in the operating room [Beck 1971, 1980]. Even though complete blinding might not occur, the situation is often far from optimal. Surgical drapes have reflective properties of 35%, whereas the reflective properties of the wound area are around 8% [Beck 1980]. This creates a ratio of 4.3:1 which is larger than the recommended ratio below 3:1. The only solution that the surgeon has to compensate for this, is to manipulate the luminary during surgical procedures to redirect the light away from the high intensity areas, or cover high reflecting surfaces.

A light field that is able to adapt its shape according to wound dimensions might provide a better lighting condition and thereby decreasing visual strain and increasing the performance of the surgeon. The main goal of this study is to design a system that is able to provide greater adaptability of the light field, which is able to use information about the wound shape. This must be done without compromising the quality of the luminary in other important areas. Typical areas where the system should provide improvements compared to current systems are; less light projection on unnecessary areas, better uniformity of the light field in relation to the shape of the wound.

In this chapter a new concept for lighting will be presented using bendable stripes with LEDs. To achieve a functional system it is important to investigate the effects of the different design choices, such as shape of the stripes, number of LEDs, number of stripes, and LED power. The influence of these choices will be evaluated by simulation and with a test prototype of one stripe.

8.2 Method

8.2.1 Concept

During a concept analysis a design solution was chosen that makes use of multiple LEDs as light source (see MSc Thesis report Jeroen Kunst for concept analysis). These LEDs are mounted on flexible strips. These strips will be used to alter the direction of the LEDs which are attached to its surface. This way it is possible to control the direction of several LEDs by manipulating a single strip. By combining multiple strips it is possible to create light fields that have more complex shapes. Placing these strips in a radial alignment creates a system that can move the spots over a large surface area beneath the luminaire. An example about what such a system will look like can be seen in Figure 8.1. The strips can bend to modify the direction of the LEDs. The angle of the strips must be adjustable to position the light field on the surface.

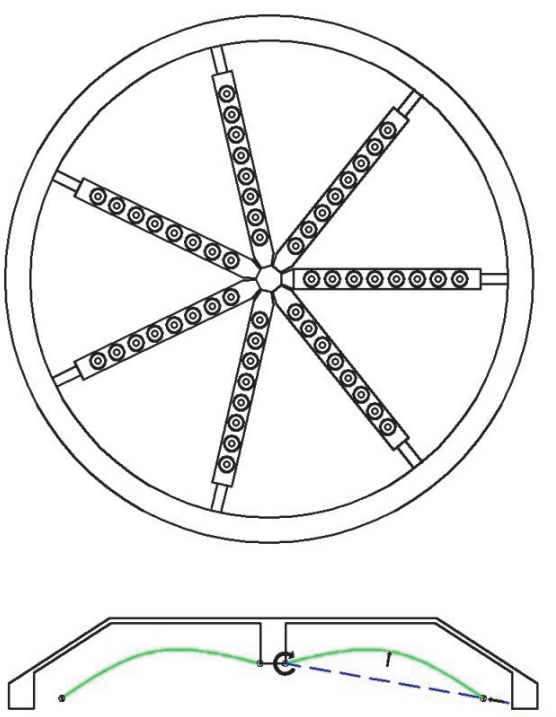

Figure 8.1: Bottom view and cross section of a luminaire that uses bendable strips.

8.2.2 Model simulation with LightTools

The system has been modelled in LightTools to get more insight in how the luminaire system functions in reality. LightTools is a software package that uses models of the real LED-lens combinations and uses them to render light rays that hit a surface which acts as a receiver. The LightTools software is controlled from Matlab. The individual spot locations and orientations that were calculated in the optimisation are used for this analysis. The LightTools code in Matlab connects to the software and translates the coordinates, orientations and power values into instructions that is understood by LightTools. LightTools calculations and returns the results in the form of a two dimensional matrix.

LEDs

The LED is a fairly simple light source. Figure 8.2a show a spot shape with a peak power of 1 cd and a spot width of 1 mm. When the spot hits a surface at an angle, the shape of the spot will become oval and the centre point of the spot will shift slightly away from the middle, as can be seen in Figure 8.2b.

It is needed to adjust the intensity of each LED individually in order to maintain a good light distribution inside the combined light field. Hence, the intensity of these light sources should be controlled. In the final design (not in this thesis) it is the idea that this device will receive the input image and translate this into a new system state that makes the new light field possible.

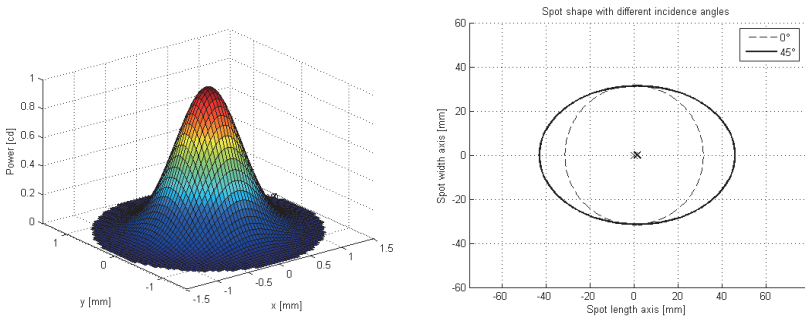

Figure 8.2: a) Basic spot shape, b) Spot shape at angle.

Strip functionality

Each strip has two parameters that determine its functionality. The first parameter is the curvature. By curving the strip it is possible to control the spread of the focus points of the individual LEDs. The second parameter is the orientation of the strip. This orientation is controlled by the angle between the horizontal plane and the line that intersects both endpoints of the strip. By changing this angle it is possible to position the combined light field along a linear path. The combined light field will be a result from the curvatures and angles of the individual strips and the intensity of each LED.

The directions of the LEDs are determined by the deformation of the strip. The shape of this deformation depends on the construction of the strip and the way it is actuated. To reduce construction complexity and to keep the calculations simple, a very basic deformation method was chosen for this project. Each strip will be connected to the luminaire body by a hinge at both ends. Deformation is initiated by moving a point in the middle of the strip upwards. It is now possible to stabilise the system against vibrations and unwanted deformations, because the strip is handled in the middle as well as at the end points.

Each strip can be modelled as a thin straight beam that is supported in its endpoints. The hinge on the proximal end of the strip allows rotation and the hinge on the distal end allows both rotation and horizontal displacement. As the ends of the strip start to move together, the strip curves upwards (Figure 8.3).

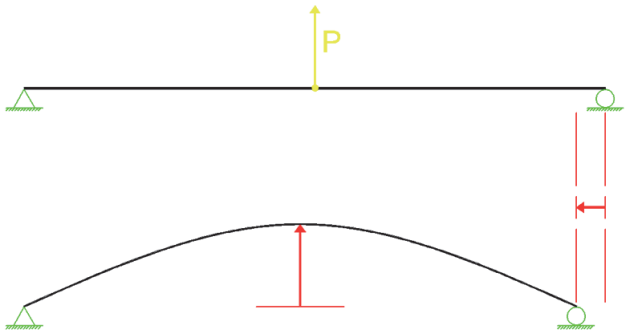

Figure 8.3: Bending shape with a central point load

The shape of the deformation is similar to a scenario where a concentrated load is applied in the middle of the strip in perpendicular direction. The deformation formulas for a beam under similar loading conditions give Equation 8.1 for the deflection of a point somewhere on the strip

$$y_{strip}(x) = P \frac{x}{48EI}(3Lstrip^2 - 4x^2) \quad (8.1)$$

The directions of the LEDs are perpendicular to the surface of the strip, so the derivative of this function gives the direction of the LED somewhere on the strip. During the optimisation process, the position and direction of each LED is calculated many times. Therefore, it is desirable to simplify this formula to speed up the calculations. The strip in the final design will be thin compared to its length. In that case the deformation will take a shape that is very close to the shape of the positive half of a sine wave.

LED positions

When a strip curves upwards, an LED that is attached to its surface follows this movement. Since the LED is fixed to the strip, the location of the LED is determined by

the curve length of the strip section which starts at the hinge point and goes up to the position of the LED. When the x-position is known the y-position can be determined.

Combined beam shape

Each LED has a specific direction in which it emits its light. This creates a line that determines where the brightest point of the spot will be located on an intersecting surface. These lines need to intersect to create the desirable narrow waist in the area between the luminaire and the surface.

When the strip curves the direction of the individual LEDs are altered and the lines start to intersect. The distance of the intersecting point of two LEDs decreases as the curvature increases. Because of the sine shaped curvature there will not be a true focus point where all directional lines intersect. The effect can be seen in Figure 8.4. The green dots indicate where two opposite lines intersect. For curve heights larger than 25 mm the intersecting lines create a waist somewhere between the surface and the luminaire. This waist is desirable because it gives room to the working area of the surgeon where no light will be blocked. Because the lines do not intersect, the final light field will always be slightly larger than a single spot.

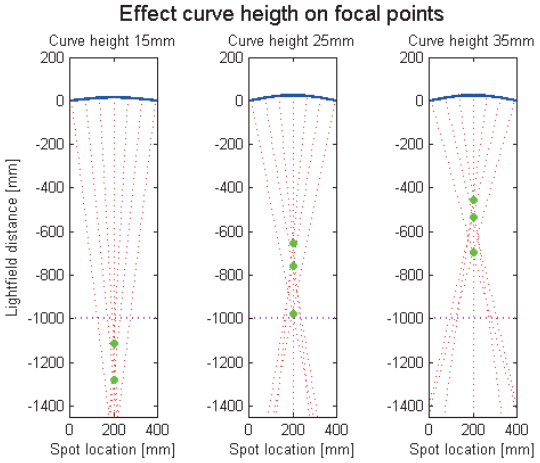

Figure 8.4: Effect of strip curvature on LED focus points

Strip angle

To move the combined light field of a single strip inside the total light field, it is needed to alter the angle of the strip. Modifying the angle moves the distal point of the strip up or down. This change in orientation modifies the spatial location and direction of the LEDs. The primary effect is that the locations of the projected spots are shifted along the surface. Another effect is that the angle of incidence changes for each of the LEDs. A 3rd effect is that the distance to the target surface is altered. The secondary effects of an elliptical spot shape and the change in spot diameter are not used in the optimisation. Incorporating these effects would mean a major increase in

computational complexity with only minor effects on the resulting outcome. The optimisation procedure can be found in the MSc thesis of Jeroen Kunst. An example of an outcome is given in Figure 8.5.

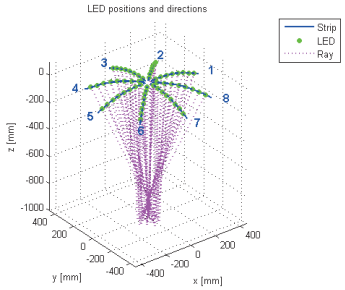

Fig. 8.5 Example of a system state that creates a narrow beam

8.3 Results

Multiple design choices such as strip number, LED number, LED power, Spot size, and LED strip position need to be made to come to a properly functioning luminaire system. A thorough examination of these different options is needed to be able to tell the effect they have on the way the device will function. Two examples will be given here.

The produced light field data are given in Figure 8.6. The Z-axis can be normalized like in Figure 8.6a, or it can show the actual luminous intensity like in Figure 8b. For the normalized representation the generated intensity values have been divided by the target luminous intensity. This makes it easier to compare settings with different target intensities.

The black line inside the graph shows the outline of the target light field which helps to judge how well the generated light field matches target light field. A text box inside the graph shows several settings that were used to generate the light field.

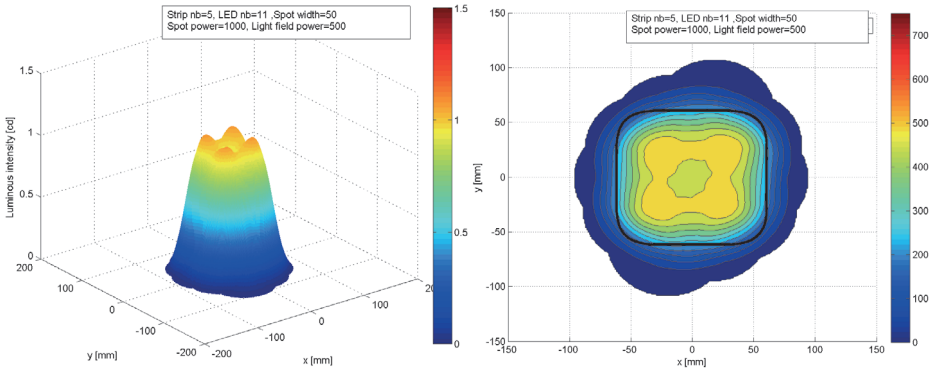

Figure 8.6 Simulated light field data. a) Light field isometric; b) Light field contour

Figure 8.7a shows the error between the generated light field and the target light field. This figure can be represented normalized or regular, like the figures for the generated light field. In the optimal case this figure would be empty except for the outline of the target light field. A text box shows the largest positive error value, the largest negative error value and a total error value. The total error value is the summation of the error field, divided by the number of pixels. Figure 8.7b shows the positions of the individual spots inside the light field. A blue dot is the centre point of a spot. The green lines connect the spot locations that are projected by LEDs which are attached to the same strip. The number next to a green line shows the specific strip number. The text box inside the graph gives the average power of all the LEDs.

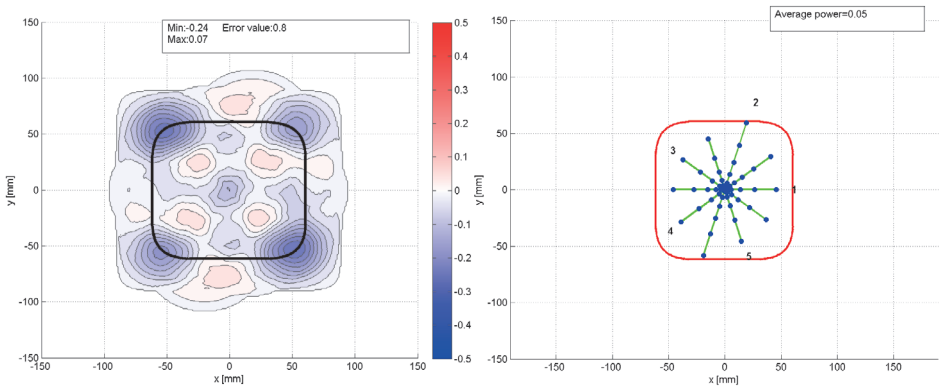

Figure 8.7. Simulated light field, a) Error field, b) Spot locations

Whether or not a setting or result is feasible is not of major interest at this point of the analysis. The main goal is to analyse the effects of certain settings. The power of the used LEDs, for example, is often unrealistically high. This way errors cause by other effects than lack of power become better visible. At a later stage of the design process an analysis will be made to see what the limits of a realistic system will be.

After examining the effect of the previously listed design choices, an analysis will be done to determine the effect of several input factors on the system's performance. Several factors can be examined, e.g. target light field shape, target light field size, target light field rotation, target light field position.

8.3.1 Strip number

The number of used strips is a primary factor in the resulting light field. Each strip is only capable of placing its spots close together, or creating an elongated light field. The orientation of this light field inside the combined light field depends on the radial alignment of the strip. Assuming that equal angles are used between the strips, then it makes sense to use an uneven number of strips. An even number of strips would have the negative effect that the axis over which two opposite strips can position their light field would coincide. This reduces the number of axis that cross the target light field by

a factor 2, as can be seen in Figure 8.8 where using 6 strips gives the same number of axis as when using 3 strips. The higher the number of axis, the better the luminaire is able to spread the light over the target light field. The effect that an added strip has on the performance reduces as more and more strips are used as can be seen in figure 8.8b. The blue line shows the resulting error value when an uneven number of strips is used and the red line when an even number is used. As expected the performance with an uneven number of strips is much better. The blue line is no longer decreasing when more than 7 strips are used. These error values are generated using the same setting and target field, with only the strip number varying. The complexity of the target light field and the diameter of the LEDs will also influence these results. This means that it might be beneficial in other situations to use more than 7 strips. On the other hand, using a high number of strips increases the complexity of the system. Another limit to the number of used strips that can be used is the space it takes inside the luminaire. For most following settings a strip number of 7 is used.

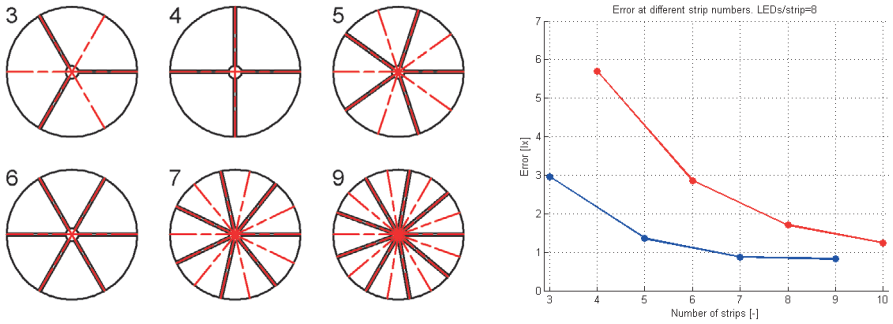

Figure 8.8: Effect of strip number on illumination axis, a) configuration for different number of strips, b) Effect of strip number on illumination axis

8.3.2 Led Power

The user input consists of a shape and a target intensity. Whether the system is able to achieve this target intensity largely depends on the power of the LEDs. The available power is still one of the main challenges during development of this system, although LEDs are becoming more and more powerful. The way the system functions is different from current multi LED systems in that, with an adaptable light field, not all LEDs point at the same spot. This means that a single LED will have to provide a bigger contribution to the illumination of a certain part of the combined light field. A light field has been generated at a range of different LED peak powers to analyse what illumination levels can be expected of the system.

The target light field is set at a value of 500 lux. Figures 8.9 and 8.10 show the produced light and error fields. At low power levels of 50 and 100 lux the system is clearly unable to fill the fairly large target light field. The required levels are only reached in the centre of the light field where many spots are located close together

due to the crossing of the strip's illumination axis. At 200 lux and higher the system is able to produce a much better image.

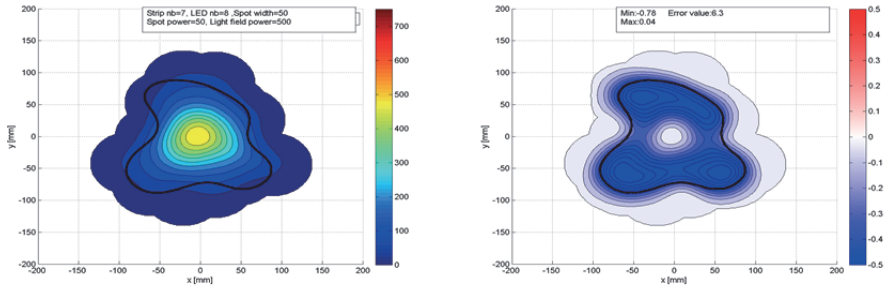

Figure 8.9: a) Light field at power = 50; b) Error at power = 50

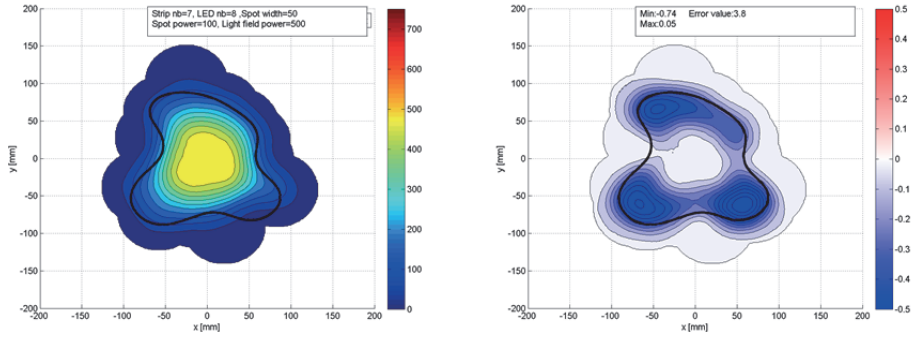

Figure 8.10: a) Light field at power=100, b) Error at power=100

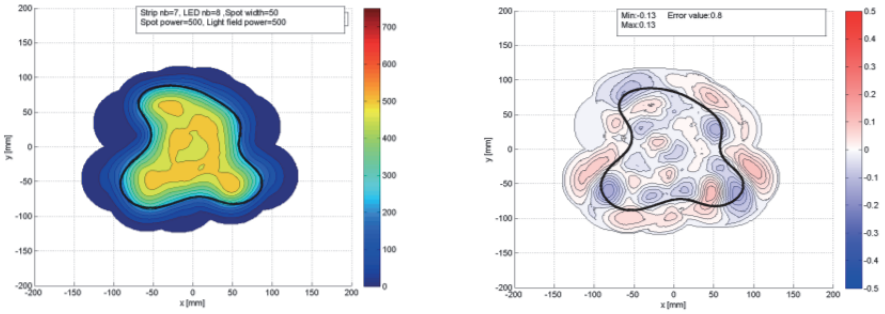

Figure 8.11: a) Light field at power=500, b) Error at power=500

Table 1 Selected variable values

Variable	Value
Strip number	7
Number of LEDs per strip	8
Target spot size at 1 m	50mm

8.4 Experimental validation

A physical model of one of the strips has been built to evaluate the model (Figure 8.12). The decision to build only one strip and not the entire luminaire is made to reduce the building cost of the test setup. It is not essentially needed to analyse a system with all strips because each strip functions as an individual entity inside the luminaire. The light field that is produced by an individual strips is simply summed with the light fields of the other strips to form the main light field. The modification of the shape of the strip is done by hand. The orientation in space of the strip is done using a tripod. The brightness of the LEDs is controlled using a micro controller (see J Kunst for detail control of voltage and compensation for variation in LEDs).

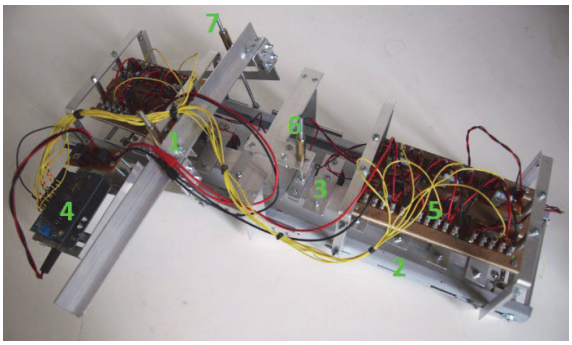

Figure 8.12:
Model top view, 1:Stationary frame, 2:Rotating frame, 3:LED holder, 4:Micro controller, 5:Constant current source, 6:Height rod, 7:Angle rod.

The chosen combination of an LED with a certain lens is a very important aspect of the luminaire system. It is also a very limited choice because it depends on what type of lenses and optics are available. It became clear that most LED-lens systems project a much bigger spot size. Only a few combinations came close enough and of those systems only one type was generally available. The LED light source is a Cree XP-C high power LED with a 26.5 mm Narrow Spot Plain TIR lens from Carclo-optics.

The first setting is set at a curve height of 0 mm, so the strip is completely flat. This gives a very long light field, as can be seen in Figure 8.13b. The light field that was created by the system does not look as smooth as the light field created in Matlab (Figure 8.13a). This is mainly caused by the directional errors of the LEDs. The result of these errors is that some spots overlap more than others, which causes a higher intensity value on one side of the spot and a lower intensity value on the other side. It is also clear that the light field is a little bit wider in vertical direction than the

computer generated light field. This is caused by the slightly wider spots and also misalignments of the LEDs in y direction. The resulting light field clearly shows these differences in width and smoothness.

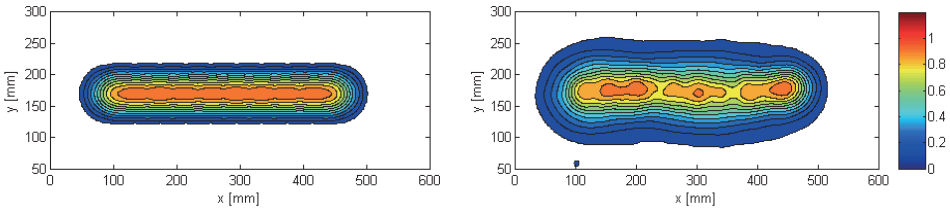

Figure 8.13: Light field comparison at curve height 0mm. a) Calculated light field, b) Photograph

Increasing the curve height to 22 mm moves the spots closer together (Figure 8.14). This improves the smoothness of the light field. There is still clearly a difference in the width of the LEDs. The resulting light field shows that there are no longer areas where the intensity is lower than the calculated value.

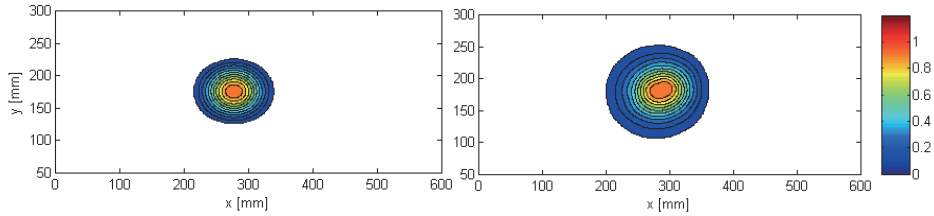

Figure 8.14: Light field comparison at curve height 22mm. a) Calculated light field, b) Photograph.

8.5 Conclusion

In this chapter a new concept for an adaptable surgical light is presented and evaluated. During the project it became clear that many different aspects come into play when a system is designed that can modify the shape of a light field. The basic idea of placing LEDs on a bendable surface is very simple and elegant. From this simple idea a system evolved with many different subsystems and variables that all influence the functionality in their own way. Each subsystem on its own is not complex, but the complexity comes from the interdependency between them. It was clear that each subsystem had to be examined individually to see the influence it has on the system. During these analyses the abilities of the system became visible. The system is able to produce light fields that can have fairly complex shapes at a good range of different sizes. It was possible to give recommendations about aspects like spot size and strip number. The physical test model indicates that the calculated system seems to function in a way that is close to how it would in a real-life situation. Given the results it can be concluded that a system, which is able to modify the light field in real time and that requires minimal control effort, can be a good addition to the operating room.

8.6 References

Beck, WC (1971), Lighting the operating room- criteria and choice . AORN Journal, Volume 14, Issue 4, Pages 46–49,

Beck, WC (1980), Choosing Surgical Illumination. The American Journal of Surgery, Volume 140, Issue 2, Pages 327–331

Kunst J, Lightfield adaptable surgical luminary. MSc Thesis TU Delft, July 2014, p1-99

[NEN-EN-IEC 60601-2-41, (2009), Medical electrical equipment(2009). Particular requirements for the basic safety and essential performance of surgical luminaires and luminaires for diagnoses.

Chapter 9

A Model of the Mechanics of Surgical Lights

Arjan J. Knulst, Rik Mooijweer, Jenny Dankelman

A simulation model that predicts handling forces required to reposition surgical lights. Journal of Medical Engineering & Technology. 36:174—179, 2012

High handling forces of surgical lighting systems limit their usability. To make improvements to the mechanical design of the system the behaviour of the system should be understood. Therefore, this study presents a model that predicts handling forces of the system. Geometry and joint friction torques of a real lighting system were measured and implemented in a validated force model. Mean, standard deviation within the spatial region, minimum and maximum forces were computed for 3 different regions of the working area. The mean (standard deviation within the spatial region) forces were 129 (106) N in the centre region, and 61 (14) N and 60 (17) N in more off-centre regions. The simulation results showed high handling forces in the central region, explaining the observed repositioning patterns of the surgical light during surgery. The model can also be used to compare different lighting systems, or to evaluate the effect of design changes.

9.1. Introduction

Most surgical lights are large and heavy units suspended from the ceiling by a two-linkage pendant system. This pendant system is intended to give the light manoeuvrability and to make its use flexible: it is usable at any position within its working range. This adjustability is required as the surgical light provides strongly focused illumination (Knulst et al. 2009a,b), whereas the location and size of the wound might vary during surgery. Several studies have indicated ergonomic shortcomings in the operating room (OR) or have formulated requirements for the OR (Barlet 1987; Beck 1978;1980;1981;Berguer 1996;1997;1999;Geis 1994;Knulst et al. 2011; Matern and Koneczny 2007; Patkin 2003;Quebbeman 1993; Rohrich 2001). Some of these studies (Kunst et al. 2011; Matern and Koneczny 2007; Patkin 2003; Quebbeman 1993) have indicated that the manoeuvrability of the Surgical Lighting System (SLS) takes too much effort: surgeons complained about high handling forces and immobility of the lights, which troubled one-handed or even two-handed positioning of the light.

An observation study (Knulst et al. 2011) has shown that repositioning of the light is frequently needed –on average every 7.5 minute- during surgery, and that in 10% of these cases the forces were so high that immobility of the light was the result. In 56% of the repositioning tasks the light was not moved along the shortest possible route in 3D space, indicating that in some areas the forces required for repositioning were too high. It was shown that such complications during repositioning of the light double the time required for repositioning.

As these repositioning tasks were mostly done by surgeons, the surgeon's attention was frequently drawn away from his/her core task towards the SLS, thereby disconnecting his/her visual feedback from the core task (Stassen et al. 1999). The observed high handling forces, immobility and elongated routes were not shown everywhere within the working area of the SLS, but only in a limited region close to the ceiling mount where 80% of the repositioning actions took place. It was suggested that these problems were related to the characteristics of the mechanical system.

In such case, the required handling forces were dependent on the position of the light unit and on the direction of motion. To make any improvements to the design of the lighting system possible the behaviour of the mechanical system should be understood, and the most important parameters in the design that influence the behaviour should be identified. Measurements of the required forces for any movement across the working area are complicated in the OR. It requires OR time which is expensive, it requires a flexible and robust measurement system, and it has some sterility issues. Therefore, this study uses a limited set of measurements on a real lighting system to formulate a validated simulation model that can predict the required handling forces for any motion of the lighting system within its working area.

9.2 Methods

9.2.1 Measurements

A particular SLS was used to for the model: the Berchtold Chromophare C950 as it was installed in the Reinier de Graaf Hospital in Delft. Knowledge about: 1) the geometry and mass of the system and 2) the frictional behaviour of each joint were required to formulate a mechanical model. The geometry of the SLS was partly obtained from the Operating Instructions of the SLS, and partly measured on the actual system. The mass was estimated as part of the total system mass with help of the geometrical properties of each part. The obtained data was implemented in the rigid body model.

The frictional behaviour of each individual joint of the SLS was measured in the OR. A calibrated force sensor (Feteris Scaime ZFA loadcell 100kg) was connected at a known location on a pendant arm, 0.82m from the joint's centre. While all other joints were fixated the pendant arm was rotated at a constant low speed of about 8°/s for 4.5s by gently pulling the force sensor manually. This process was repeated 18 times for all five joints. The force data was stored to a computer at a sample rate of 10 kHz. Next, the force data was multiplied by the 0.82m moment arm to obtain friction torques. For each joint 9 measurements were randomly picked from the set of 18 and averaged to be used for modelling the frictional behaviour (T_{model}), the remaining 9 measurements were averaged and stored to be used for the validation of the model ($T_{validation}$).

For total model validation purposes the threshold force required for motion of the luminaire was measured at 4 luminaire positions: 0, 30, 60 and 180° angle between the two main pendant arms for 4 movement initiation directions: x^+, x^-, y^+, y^-. The pulling force was measured at the handgrip of the luminaire using a force sensor. The pulling force was slowly increased until luminaire motion was started. Three repetitions were performed. The measured maximum force for each position and direction averaged over the 3 repetitions ($F_{threshold}$) was stored.

9.2.2 Model

A rigid body model was made using the ADAMS software package (MSC ADAMS 2005r2, USA). Figure 9.1 shows the geometrical layout of the model with numbered main parts (1-6) and joints (A-E). Part 1 is fixed to the co-ordinate axes of the simulation, part 6 is the luminaire, and parts 2-5 belong to the pendant system. To avoid curved shapes some parts were constructed from multiple straight segments that were rigidly connected as if they were welded (Figure 9.1, symbol W). All parts had weights and sizes and in each joint a frictional behaviour was implemented.

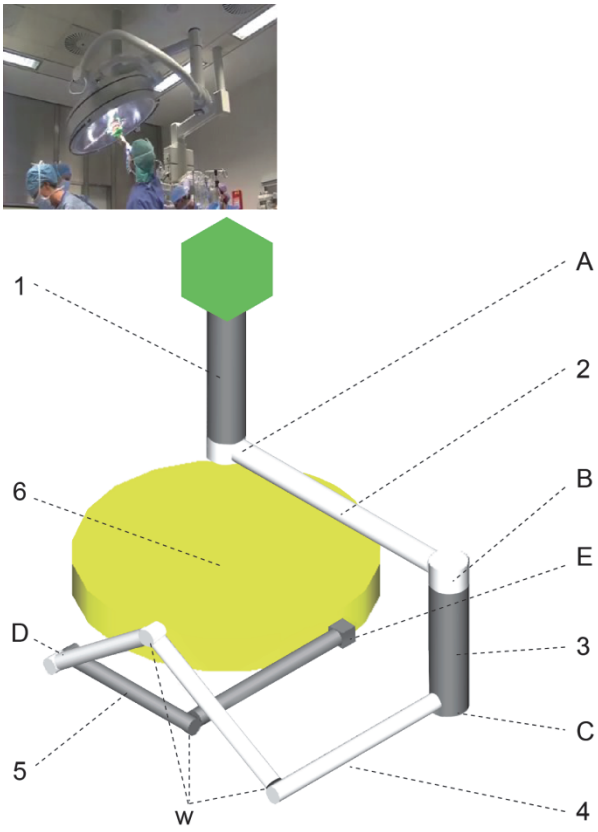

Figure 9.1 Schematic representation of the modelled lighting system, with labelled main parts (1-6) and labelled joints (A-E). To approximate the curved tubes of the real system two or three straight tubes were rigidly connected (W). The squared box represents the ceiling mount, the large disc represents the surgical light. The inset shows the real system during use.

Each joint had a resistance torque T_r implemented using the ADAMS STEP-function. The ADAMS STEP-function uses a polynomial to approximate an S-shaped change between two function values (torques T_1 and T_2) at two instants (joint speeds v_1 and v_2) as function of joint speed vi. Two combined STEP-functions approximated the measured friction Tmodel using a friction model:

$$T_r = STEP(v_i, v_0, T_{r,0}, v_1, T_{r,1}) + STEP(v_i, v_2, T_{r,2}, v_3, T_{r,3}) \quad (9.1)$$

Here, the friction torque T_r at joint speed v_i is defined by the torque $T_{r,0}$ at joint speed v0 that changes into torque $T_{r,1}$ at joint speed v_1 and by the torque $T_{r,2}$ at joint speed v_2 that changes into torque $T_{r,3}$ at joint speed v_3. So, the parameters of the STEP-functions determined the values and the instants of the static and dynamic friction torques as function of joint velocity v_i. Each joint also had an applied torque Ta implemented using the ADAMS SPLINE-function. The SPLINE-function imports exactly the measured

force T_{model}. In an iterative process the parameters of the STEP-function were altered until actuation of the joint by means of the applied torque resulted in a simulated joint velocity approximately equal to the measured joint velocity.

9.2.3 Validation

For validation of the model two steps were made. 1) The applied torque was changed, using the validation data set $T_{validation}$ as input for the SPLINE function. The resulting joint velocity was compared to the joint velocity obtained when using T_{model} as input for the SPLINE function. The resulting joint velocities were applied to the model to measure the resulting torque response. The resulting torque response was compared to the measured friction torques. 2) The force required to initiate movement of the luminaire in the four different defined positions and four directions (requiring movement of the complete mechanical system) was compared between simulated and measured forces.

9.2.4 Experiments

Once a validated model has been formulated a simulated experiment was performed. In the experiment the luminaire was positioned in a series of different initial conditions, and the luminaire handle was translated along a straight horizontal line at a constant speed of 0.1 m/s while the required handling forces (F_x, F_y) were predicted by the simulation. Eighteen different initial conditions were formulated by variation of joint angle A from 0 to 170° in steps of 10 degrees to cover the complete working area of the SLS. The initial angle of joint B was kept at 170°. All other initial joint angles were kept identical. The translation experiment was executed in both positive x and y direction of motion.

The two handling force components were combined into one total handling force: $F_t = \sqrt{F_x^2 + F_y^2}$. The total handling force across the working area of the SLS was visualized by a force map created by a contour plot fit on the simulated data. The total handling force was further analysed in Matlab (The Mathworks, USA) for three regions of the working area defined by their distance R from the ceiling mount: 1) the central work field (0≤R<50 cm), 2) the mid work field (50≤R<100 cm), and 3) the outer work field (100≤R<150 cm). The most outer part (150≤R<190 cm) was removed from the data as forces increased rapidly once the edge of the working area was reached. For each region the mean force, standard deviation within the spatial region, the minimum and the maximum force were computed.

9.3 Results

9.3.1 Measurements

Table 9.1 lists the segments, dimensions and masses of the different parts as applied in the SLS model. Table 9.2 displays the measured threshold forces for motion into four directions at four different positions in the working area of the SLS.

Table 9.1 Dimensions and weights of parts of the SLS model (Figure 9.1).

Part	Segment	Dimensions [m] (length x diameter)	Mass [kg]
1	1	0.51 x ø 0.063	21.9
2	1	0.08 x ø 0.063	3.4
	2	0.83 x ø 0.063	14.6
	3	0.08 x ø 0.063	3.4
3	1	0.63 x ø 0.03	19.7
4	1	0.63 x ø 0.03	6.2
	2	0.57 x ø 0.03	4.8
	3	0.06 x ø 0.03	0.5
	4	0.38 x ø 0.03	3.2
	5	0.06 x ø 0.03	0.5
5	1	0.06 x ø 0.03	0.7
	2	0.39 x ø 0.03	4.4
	3	0.54 x ø 0.03	6.1
	4	0.06 x 0.06 x 0.06	0.9
6	1	0.12 x ø 0.48	25.5

Table 9.2 Measured threshold forces for motion of the luminaire.

	Mean $F_{threshold}$ **per direction (n=3) [N]**			
Angle B [°]	x^+	x^-	y^+	y^-
0	>>100*	>>100*	34	34
30	80	80	27.5	27.5
60	58	61	32.5	27.5
180	32.5	32.5	>>100*	>>100*
* force above maximum of force sensor				

Figure 9.2a shows for all joints the averaged measured friction torques (T_{model}) used for the estimation of the friction model of the joints. In general, the measured friction torque increases rapidly in time to its maximum value, and after that, the measured friction torque gradually decreases until a constant level is reached. Note that the friction torque decreases for more distal located joints. Figure 9.2b shows the averaged measured friction torques used for the validation ($T_{validation}$) of the model response.

9.3.2 Model

Figure 9.2c shows the friction behaviour of each joint depending on joint velocity as computed using the ADAMS STEP-function. Table 9.3 shows the corresponding ADAMS STEP-function parameters for each joint.

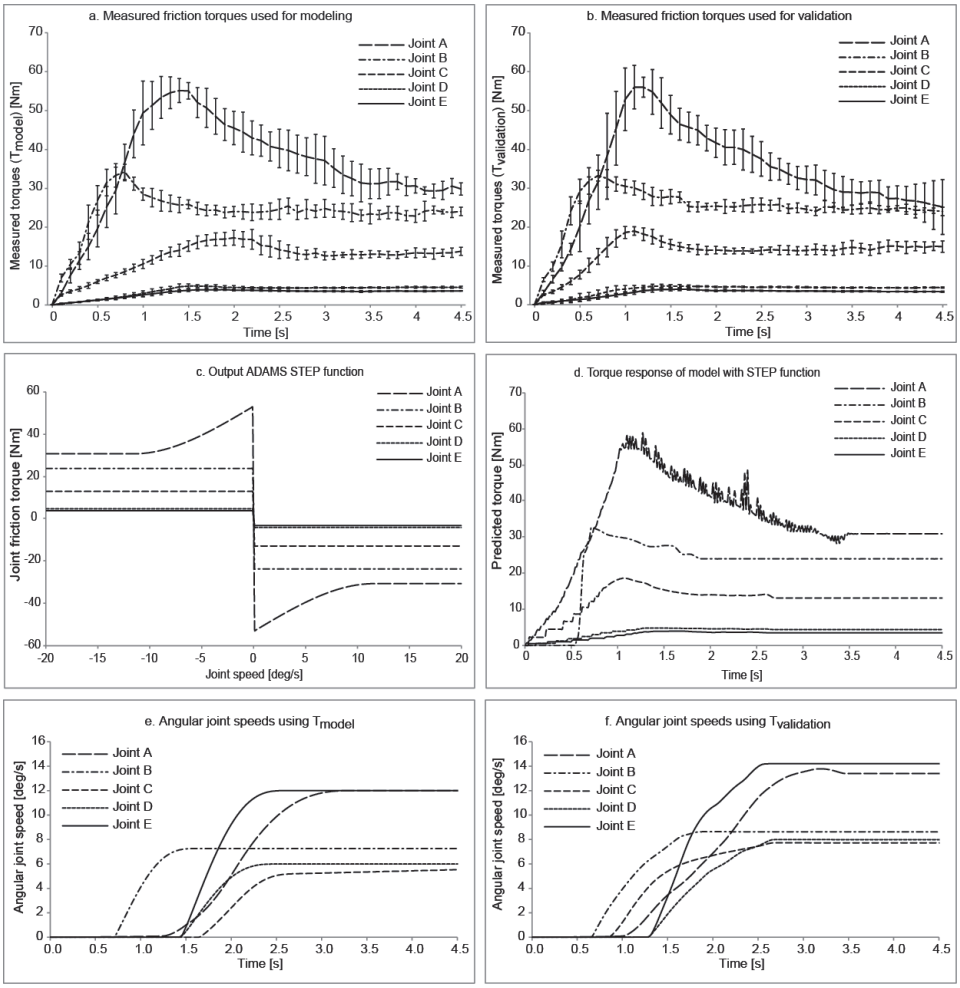

Figure 9.2 a. Averaged measured joint friction torques Tmodel for each joint. b. Averaged measured joint friction torques Tvalidation for each joint. c. Implemented friction behaviour (STEP function) per joint. d. Simulated torque response of the model. e. Joint speeds resulting from application of the measured torques Tmodel on each joint. f. Joint speeds resulting from application of the measured torques Tvalidation on each joint.

Table 9.3 The STEP model parameters that defined the friction model (Figure 9.2c).

	v_0	$T_{r,o}$	v_1	$T_{r,1}$	V_2	$T_{r,2}$	V_3	$T_{r,3}$
Joint A	-0.01	53.25	0.01	-53.25	-11.55	-22.45	11.55	22.45
Joint B	-0.01	33.4	0.01	-33.4	-0.03	-9.5	0.03	9.5
Joint C	-0.01	18.4	0.01	-18.4	-0.03	-5.3	0.03	5.3
Joint D	-0.01	4.75	0.01	-4.75	-0.03	-0.35	0.03	0.35
Joint E	-0.01	3.8	0.01	-3.8	-0.03	-0.3	0.03	0.3

9.3.3 Validation

Figure 9.2e and 9.2f show the joint velocity response of all joints using T_{model} or Tvalidation as input, respectively. This validation step allows comparison of the joint speeds resulting from comparable, but slightly different applied torques. The velocity profiles showed comparable behaviour, but had higher end values (on average 30% higher). Figure 9.2d shows the response of each joint in time when set in motion according to the speed profiles of Figure 9.2f. The resulting torque responses are quite comparable to the measured responses (Fig. 9.2a and 9.2b). Only Joint B showed unexpected behaviour, perhaps because of numerical instability. The second validation step compared the predicted and measured forces required to set the luminaire in motion. The model showed on average a 20% overestimation of the measured required force (Table 9.2).

9.3.4 Experiments

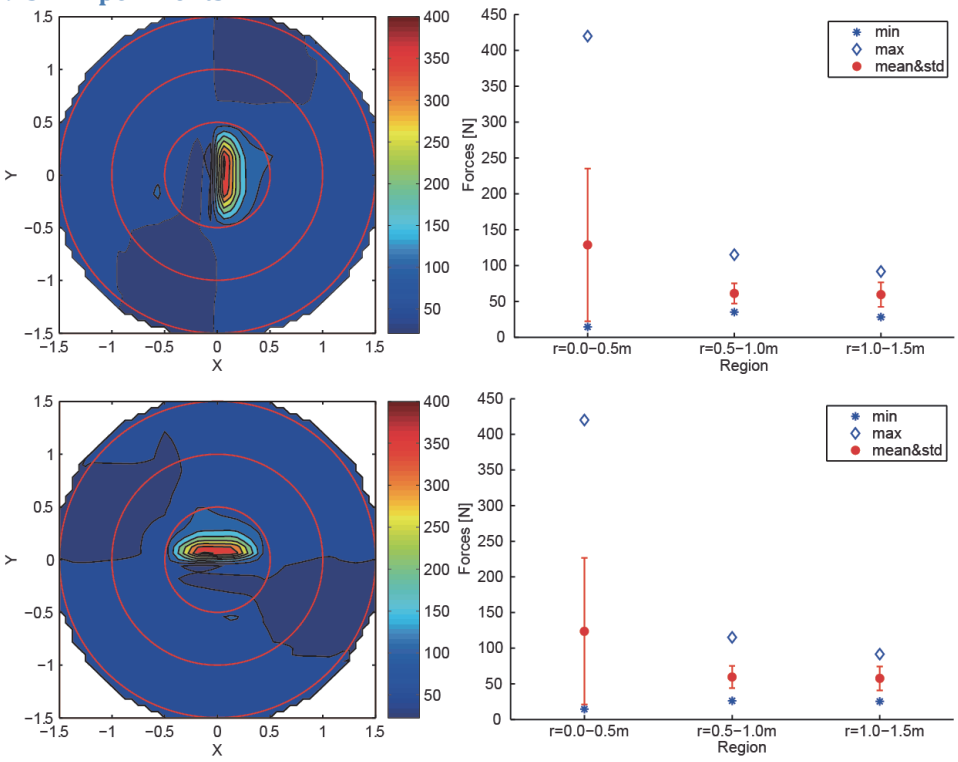

Figure 9.3 The simulation force results for movement in positive x-direction (upper panels) and positive y-direction (lower panels), showing handling forces indicated by colour (left panels) and the force characteristics for the different regions (right panels). The red circles indicate the outer boundaries of each of the different regions. The ceiling mount was located at (0,0).

Figure 9.3 (left panels) shows the resulting force maps of the simulation experiments for both directions of motion (upper panels: x-direction, lower panels: y-direction). As visible, a force peak occurred in the central region. The shape of the force map was

hardly influenced by the movement direction, except for the orientation of the force map. Forces were the highest in the central region and lower outside this region. This behaviour is illustrated by Figure 9.3 (right panels) where characteristics of the force map are depicted for each spatial region of the force map. Characteristics were: the mean force and standard deviation within each spatial region, and the minimum and maximum force. Mean, standard deviation within the spatial region and maximum force were the highest in the centre region (r=0.0-0.5m). Although all other areas show lower forces, still the mean force was 60N.

9.4 Discussion

The goal of this study was to formulate a simulation model that predicts handling forces during the repositioning of surgical lights. The model showed an elliptical area of high forces within the area spanned by a 0.5m radius around the ceiling mount. The orientation of this elliptical area was shown to depend on the direction of movement. Average forces in this area were 129N, and the maximum force even increased to 420N. Outside this area average forces were about 60N. This area of high forces explains the usability problems that users experienced with manoeuvrings of surgical lights (Knulst et al. 2011).

The model was built in ADAMS based on handling force measurements of an installed lighting system. A validation test showed that the model overestimates handling forces on average by 20%. Possible causes for this deviation might be the uncertainties in the manually performed joint torque measurements, mismatches between measured joint torques and the fitted Coulomb friction model, joint friction differences that might occur at different positions of the luminaire than the position in which the joint friction was measured. Although this overestimation occurred, the model was able to predict the force behaviour correctly, showing high and low forces at locations and in directions where these were experienced or measured, making the model a valuable tool to study the behaviour of the pendant system and study the effect of changes to the system.

The area of high forces explains the immobility of the light and the strange movement patterns through the working area that were observed in (Knulst et al. 2011): instead of taking the shortest route between point A and B through the central region, users avoid this central region by taking alternate routes. The explanation might be that human beings simply have difficulties to produce the required amount of force. In ergonomic literature (Burandt 1978) limits are set to the push/pull forces that human beings can possibly exert with their hands into different directions and at different locations relative to the body. The lowest force limit was reported as 60N. The same work also specified a scaling factor that scales the maximum forces to a force level perceived as suitable for a certain application. For perceiving comfortable forces this scaling factor was approximately 0.10 to 0.20, with a maximum of 0.40, yielding a maximum comfortable force level of 6-12N with a maximum of 24N for comfortable movement in any position and any direction. Average handling forces were above comfortable force levels across almost the complete working area, and in the central

region even above maximum force levels. When the central region needs to be crossed when moving the luminaire from location A to B, this central region will be avoided because of forces above human capabilities, as observed in the previous study by Knulst et al. 2011.

The current standard for surgical lights (IEC 2009) gives only limited guidelines to the maximum allowable forces. Force limits are only set for vertical movement of the luminaire, and for rotations of the luminaire around its own axis. However, no limits are set for translational movements of the luminaire in the horizontal plane. As these translational movements introduce very high forces and even immobility of the light, intra-operative safety might be compromised. The standard should adopt metrics to describe and limit the maximum allowable forces anywhere across the working area. These metrics could follow the force map characteristics like the one used in the current study, or describe forces required for motion at different locations and in different directions of motion.

The model can be used in different ways. In the current study only the forces required for 2-dimensional movements along straight lines across the working area at one height were estimated. A constant speed along a straight path was dictated to the handgrip of the luminaire and the required handling forces to maintain that path and speed were recorded. Another way of use could be defining 3-dimensional paths for a number of frequently occurring manipulations of the luminaire as observed during the observation study (Knulst et al. 2011) and record the required forces. The model can also be used as a design tool to study the effect of changes in the characteristics of the design; for instance a different frictional behaviour, a different geometry of one of more pendant arms, a different location of the ceiling mount, a different number of pendant arms, a different weight (distribution) of the system, etc. The modelling procedure can be used to define models with adapted characteristics for different surgical lighting systems to compare the handling forces between them.

9.5 Conclusion

This study presents a software simulation model that predicts the handling forces for repositioning of a surgical light. The model was used to show the handling forces for movements at constant speed at different locations across the working area of the lighting system. It was shown that the handling forces differed depending on the location in the working field, and that forces were the highest and most varying in an area of 0.50m radius around the ceiling mount. The simulated forces explain the observed problems during repositioning of the lighting system by the surgical team. The model might also be used to compare different surgical lighting system, evaluate certain repositioning tasks, or evaluate the effect of design changes in the lighting system.

9.6 References

Knulst AJ, Stassen LP, Grimbergen CA, Dankelman J. Choosing surgical lighting in the LED era. Surgical Innovation 2009;16(4):317-23.

Knulst AJ, Stassen LPS, Grimbergen CA, Dankelman J. Standards and Performance Indicators for Surgical Luminaires. Leukos 2009;6(1):37-49.

Bartlett D. Operating theatre lighting. NATNews 1978;15(11):24-30.

Beck WC. Lighting the surgical suite. Contemporary Surgery 1978;12(1):9-16.

Beck WC. Choosing surgical illumination. American Journal of Surgery 1980;140(2):327-331.

Beck WC. Operating room illumination: the current state of the art. Bulletin of the American College of Surgeons 1981;66(5):10-15.

Berguer R. Ergonomics in the operating room. American Journal of Surgery 1996;171(4):385-386.

Berguer R. The application of ergonomics in the work environment of general surgeons. Reviews on Environmental Health 1997;12(2):99-106.

Berguer R. Surgery and ergonomics. Archives of Surgery 1999;134(9):1011-1016.

Geisse JK. The dermatologic surgical suite. Seminars in Dermatology 1994;13(1):2-9.

Knulst AJ, Mooijweer R, Jansen FW, Stassen LP, Dankelman J. Indicating shortcomings of surgical lighting systems. Minimally Invasive Therapy and Allied Technologies 2011;20(5):267-275.

Matern U, Koneczny S. Safety, hazards and ergonomics in the operating room. Surgical Endoscopy 2007;21(11):1965-1969.

Patkin M. What surgeons want in operating rooms. Minimally Invasive Therapy and Allied Technologies 2003;12(6):256-262.

Quebbeman EJ. Preparing the operating room. Care of the surgical patient: A publication of the committee on pre and postoperative care. Scientific American 1993;5:1-13.

Rohrich RJ. Why I hate the headlight ... and other ways to protect your cervical spine. Plastic and Reconstructive Surgery 2001;107(4):1037-1038.

Stassen HG, Dankelman J, Grimbergen CA. Open versus minimally invasive surgery: a man-machine system approach. Transactions of the Institute of Measurement and Control 1999;21(4-5):151-162.

Burandt U. Ergonomie fur design und entwicklung. Koln: Schmidt; 1978. 154 p.

IEC. International Standard - Medical electrical equipment - Part 2-41 Particular requirements for the safety of surgical luminaires and luminaires for diagnosis. Geneva: International Electrotechnical Commission; 2009. Report nr IEC Publication No. 60601-2-41 2009. 38 p.

Chapter 10

Evaluation of a multiple-joint approach

Arjan J. Knulst, Jenny Dankelman

Evaluation of Simulated handling forces of surgical pendant systems – an improved design. Submitted

The usability of surgical lights is hampered by high handling forces. The purpose of this study was to investigate whether a three- or four-arm pendant design could improve the performance in terms of mean, maximum and variation of handling forces for different parts of the working area. A validated simulation model was used to compare two-, three-, and four-arm designs on the mean, maximum and variation of handling forces across different parts of the working area. In the most frequently used area, the three-arm design reduced the mean force by 3.8x and the variation of force 19.4x. The locations of the maximum forces were shifted to less frequently used areas. The four-arm design did not outperform the three-arm design. The three-arm design improved the performance and usability of the pendant system as handling forces were reduced in the most intensively used part of the working area. However, the singularities were not completely annihilated, so a more fundamentally different mechanism might be required.

10.1. Introduction

Traditionally, most surgical lights are large and heavy units suspended from the ceiling by a two-linkage pendant system. This pendant system is intended to give the light manoeuvrability and to make its use flexible: it is usable at any position within its working range. This adjustability is required as the surgical light provides strongly focused illumination [1, 2], whereas the location, orientation and size of the wound might vary during surgery. Several studies have indicated ergonomic shortcomings in the operating room (OR) or have formulated requirements for the OR [3-14]. Some of these studies [10-12] have indicated that the manoeuvrability of the light is not good enough: surgeons complained about high handling forces and immobility of the lights, which hampered one-handed or even two-handed positioning of the light. An observation study [10] has shown that repositioning of the light is frequently needed – on average every 7.5 minutes- during surgery, and that in 10% of these cases the forces were so high that immobility of the light was the result. These repositioning tasks were mostly done by surgeons.

The same observation study [10] also showed that 80% of the repositioning tasks took place in a relatively small circular area (50 cm radius) centred at the ceiling mount of the pendant system. Cases in which the handling forces were too high also occurred in this small centre area. Hence, with current pendant systems the positioning is the hardest in the area where it is used the most. The underlying problem is related to the position of the end-point of the pendant system –where the light is mounted to the pendant- and the configuration of the pendant arms. When the end-point comes close to the ceiling mount then the moment arm induced by the handling force acting on the end-point becomes small, requiring high forces to overcome friction of the system. This phenomenon is called a mechanical singularity. The location of this singularity at the centre of the working area of the pendant system is inherently connected to the construction of the pendant system.

A possible way to decrease the impact of this problem could be by shifting the location of the singularity away from the centre to a part in the OR where the light is used less frequently. Simply shifting the location of the ceiling mount limits the working range of the lights, and therefore, two ceiling mounts and two sets of lights would be needed to cover the complete working area. A pendant system that includes three or even four arms may result in a similar the working range, and in shifted singularity. To investigate the consequences of the number of arms on usability and performance, a software model was developed that predicts the handling forces and singularities across the working area of three different pendant designs. The behaviour of the software model was validated by measurements on a hardware model.

10.2. Materials and Methods

10.2.1 Software and hardware setup

Three different pendant designs (type A, B, and C, Fig. 1) were compared. The difference between the models was the number of arms and joints, and therefore, the number of degrees of freedom. The total length of each type was 3.0 m and the total mass was 20 kg. Each of the three pendant designs were modelled both in software, scale 1:1 and in hardware, scale 1:10. The hardware models were used to validate the behaviour of the software models and the software models were used to compare the three different pendant designs. For the validation the friction parameters of all joints of the software models were individually adapted to the averaged measured parameters of the hardware models. For the pendant comparison the friction parameters of the software models were adapted to create comparable situations, and also a 25 kg mass -resembling a light- was attached to each endpoint.

10.2.1.1 Software model

The three pendant designs were modelled with a software package (Working Model 2D, Design Simulation Technologies). The pedant arms were connected to each other by joints. As the initiation of the pendant motion was not of interest, only dynamic friction was incorporated in the model. Each joint contained a simple friction model (Eq. 11.1) that generated a friction torque (M_f) counteracting the rotation in case of the slightest rotational motion of the joint ($\dot{\varphi}$). The amplitude of the torque (M_f) was defined by the radius of the joint (r) –creating a moment arm for the friction force- and the friction force defined by the friction coefficient (μ) and the normal force (F_N). A small offset (0.01) was used in the denominator to prevent the model from dividing-by-zero errors. The normal force on each individual joint was varied to set the average friction torque as measured in the hardware model.

$$M_f = -\mu \cdot r \cdot F_N \cdot \frac{\dot{\varphi}}{|\dot{\varphi}| + 0.01} \qquad \text{(Eq.11.1)}$$

During the software simulations the end-point of the pendant model was moved at a constant low speed of 0.1 m/s along a straight line located at different X-locations separated by 0.1 m. Meanwhile, the forces to keep this trajectory at a constant speed were computed, and the model was sampled at 10Hz to store data to a file. The defined working area of 3x3 m was simulated three times for each pendant model.

10.2.1.2 Hardware model

Three 1:10 scaled pendant models were manufactured in the workshop according to the before mentioned designs (Fig. 11.1). Each model was made of an aluminium bar, having a 10x10 mm square cross-section. A 2 mm thick friction material layer (Vulka SA-80/10, friction coefficient 0.41) was glued to a pendant arm surface facing a 10 mm diameter aluminium cylinder that was glued to the surface of next pendant arm. A 4 mm diameter silver steel axis was extended through all these layers. The axis fixated the different parts of the pendant models to each other and allowed rotation around

its axis. To get a certain level of friction between two pendant arms, a nut on the silver steel axis was used to change the normal force between two pendant arms. The friction in each joint was set to withstand a 0.24 Nm torque at an angular position of 0 degrees. To measure the average friction of each joint the torque to initiate motion was measured three times at 8 equiangular orientations of the joint, ranging from 0 to 360 degrees, and averaged to obtain the mean friction of the joint.

A measurement setup was build. It consisted of a calibrated 6 DOF force sensor [15] placed on a XY-movable platform, a pendant mounting point fixed to a rigid frame above the movable platform, and three hardware pendant models. The pendant mounting point functioned as a ceiling mount for the pendant models. The movable platform with force sensor functioned as an operator of the pendant model end-point. The force sensor was sampled at 10 Hz and the data was stored. To prevent damage to the setup in case of a singularity, the force sensor and the pendant model end-point were magnetically connected, such that the connection would fail in case of high forces.

During the validation experiment the platform was moved in Y-direction at constant speed of 10 mm/s along straight lines located at different X-locations separated by 10 mm. At the beginning of each run, the initial configuration of the pendant system was defined by specifying the end-point of the pendant and the angulations of some pendant arms. For each initial end-point position, angles α_b, α_c and β_c were set to 90° (Fig. 1). The resulting data grid covers a 300x300 mm square measurement area with a 1x10 mm resolution and resembles the total force required to maintain a constant end-point speed in a fixed direction. Along each line the forces were measured.

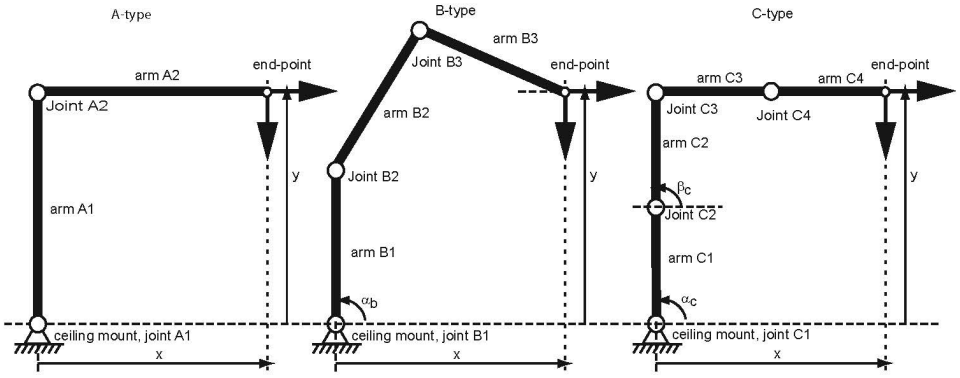

Figure 10.1. A schematic representation of the three pendant designs (A, B and C) with labelled arms (A1-A2, B1-B3, C1-C4) and joints (A1-A2, B1-B3, C1-C4). The position of the end-point is represented in x,y-coordinates relative to the ceiling mount joint (A1-C1).

10.2.1.2 Pendant comparison

For the comparison of the three different pendant designs, the friction parameters of the software model were adapted to create comparable friction torques. The normal

forces of all ceiling joints were set to 1200N, giving a 22.4Nm friction torque in the joint, requiring a 7.5N end-point force for constant motion. The normal forces of all other joints were set such that the friction torques resulted in the same required end-point forces in case of a fully extended pendant configuration. In this way, the pendants will have a tendency to move more distal pendant arms first. The normal force of the ceiling joint was adapted such that the friction torque of the ceiling mount resembled the real pendant system's ceiling joint (Berchtold Chromophare C950, unpublished data, measured at the Reinier de Graaf hospital, Delft). The simulation protocol used was identical to the simulation protocol used during validation.

10.2.2 Metrics

Data from the hardware and the simulation measurements were analysed in Matlab R2009b (The MathworksTM). The measured force vectors in X and Y direction (Fx, Fy) were summed to obtain the magnitude of the resultant total handling force (Ft). Each dataset resulted in a force map of the total handling force magnitudes over the full working area.

Four circular subareas were defined for the working area of the pendant systems by an increase of radius of 0.5m: Centre, Ring 1, Ring 2, and Periphery. The Centre area corresponds to the area in which 80% of all light position manipulations were observed. Next, the force map of the complete working area was cut into four subsets for each subarea. For each subarea the mean force, the standard deviation of force, and the maximum force were computed to describe the resulting force map.

In case of a failure of the magnetic connection due to singularities, no data was recorded for the remaining part of that platform path. As the simulation did not have such force limitation build in, the simulated data at locations where no measured data was available were not included in the validation. In this way, both datasets were again comparable.

10.3. Results

10.3.1 Friction data

Figure 2 shows the measured friction torques for the different joints of the hardware model for different angulations of the joint. The friction was highly variable for some joints, and for other joints the variation was low. The friction data was averaged per joint, and used as friction torques of the joints in the software model by adapting the normal forces. Table 1 lists the average and the standard deviation of the friction torques of the joints in the hardware model. Also, the table lists the normal forces used in the software model for the validation procedure, and the friction torques obtained by these normal forces. Finally, Table 1 shows the settings of the normal forces used in the software model for the pendant comparison procedure.

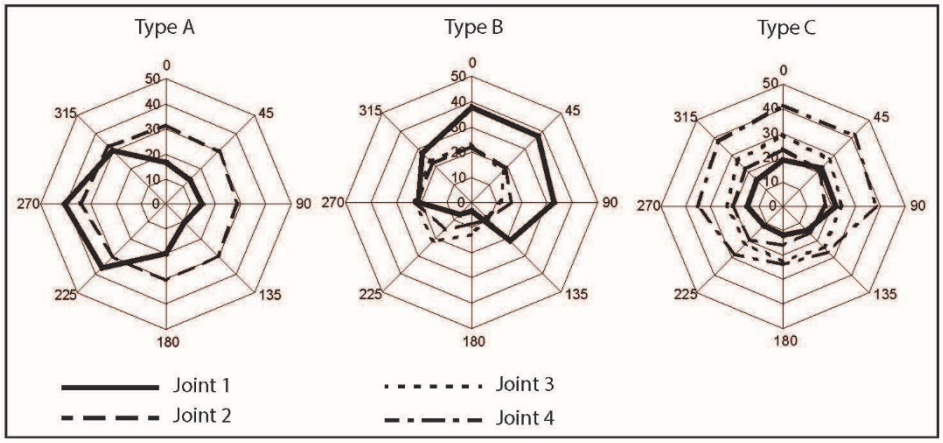

Figure 10.2. Variation of friction torques [Nm] of each hardware model (two-, three-, and four-arm pendant system, left to right panels), measured per joint in different angular directions (0-315 degrees). Each line represents one joint.

Table 10.1 Friction torques and normal forces used in different hard- and software models.

	Hardware[1]		Model validation[2]		Pendant comparison[3]	
Joint	**M_{mf} [Nm][4]**	**$M_{mf,std}$ [Nm][5]**	**F_n [N][6]**	**M_f [Nm][7]**	**F_n [N]**	**M_f [Nm]**
A1	0.23	0.11	1144.5	22.6	1200	22.4
A2	0.31	0.02	1557.0	30.8	600	11.2
B1	0.18	0.06	892.2	17.6	1200	22.4
B2	0.17	0.06	840.5	16.6	800	14.9
B3	0.24	0.13	1191.0	23.5	400	7.5
C1	0.19	0.03	972.4	19.2	1200	22.4
C2	0.16	0.04	817.3	16.2	900	16.8
C3	0.25	0.03	1245.3	24.6	600	11.2
C4	0.34	0.07	1711.3	33.8	300	5.6

[1] values measured in the hardware model
[2] values implemented in the software model for validation of the model.
[3] values implemented in the software model for pendant comparison.
[4] average friction torques per joint, measured over 8 joint orientations.
[5] standard deviation of measured joint friction torques.
[6] normal forces per joint, used to set the required friction torques.
[7] required friction torques per joint.

10.3.2 Model validation

Figure 3 shows the force maps of the simulated and measured results obtained during the validation procedure. The obtained force maps show that force peaks occurred at approximately equal locations for both measurements and simulations. The white areas indicate the areas where the magnetic connection between sensor and pendant failed in the hardware model. The simulated and hardware four-arm pendant models (Figs. 3 left lower panel and right lower panel) showed the largest difference in behaviour.

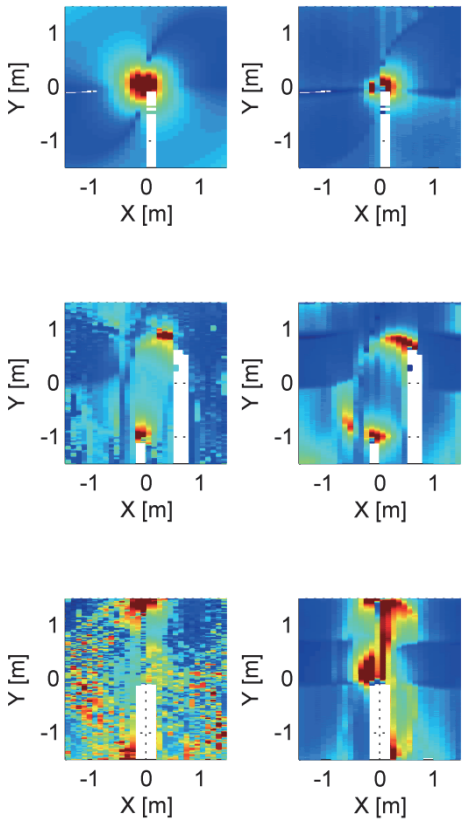

Figure 10.3. Validation force maps of the working area of *simulated* (left panels) and *measured* (right panels) data for the two-, three-, and four-arm pendant systems (upper to lower panels). The colour scale from blue to red indicates 0 to 100 N.

10.3.3 Pendant design comparison

Figure 4 shows the force maps as obtained with the three pendant simulation models. The two-arm pendant showed an area of high forces in the centre, around the ceiling mount, and low forces in the remaining area. The three-arm pendant showed some peaks of high forces on a radius of 1 meter around the ceiling mount, equalling the length of a pendant arm. Low forces were shown in the remaining area, especially inside a 1m radius area around the ceiling mount. The four-arm pendant showed high forces in the centre area, and at the top and bottom edge. Low forces were found in the upper half of the working area, and high forces in the bottom half.

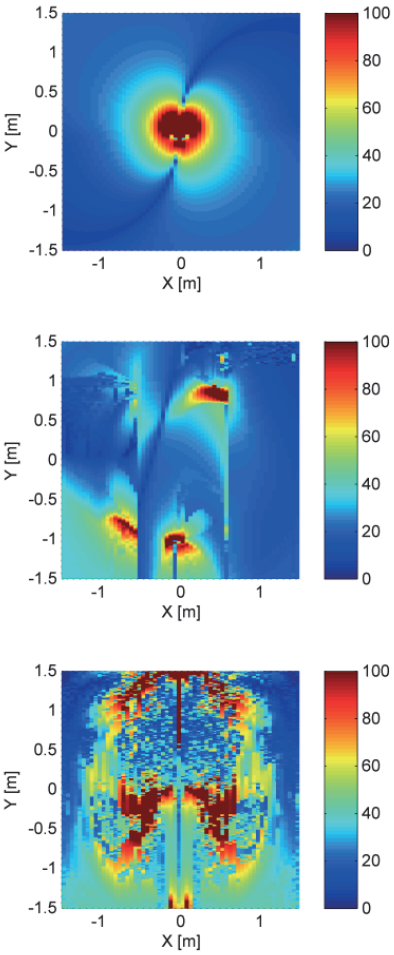

Figure 10.4. Reality resembling force maps of the working area of three *simulated* pendant designs. Depicted are the two-, three-, and four-arm pendants (upper to lower panels). The colour scale visualizes computed forces in Newtons.

Figure 5 displays the effect of different pendant designs on the force map described by the mean force (Fig. 5 upper panel), the maximum force (Fig. 5 middle panel) and the variation in force (Fig. 5 lower panel). The upper panel shows that the mean forces were high in the Centre area and that they decrease with increasing distance from the centre mount for the two-arm design. The three-arm design showed a mean force reduction of a factor of 3.8 for the Centre area. The mean forces of the four-arm design were in between the two- and three-arm design. The middle panel shows that the force peaks found in the two-arm design were shifted from Centre to Ring 1 and 2 in the three-arm design. The four-arm design moved the peaks further to the Periphery. The lower panel shows that the variation in force was also shifted from the Centre to the Ring 1 and 2 areas for the two- and three-arm designs, respectively. Furthermore, the variation in force was reduced by a factor 19.4 compared to the two-arm design. The forces in the four-arm design were higher compared to the three-arm design.

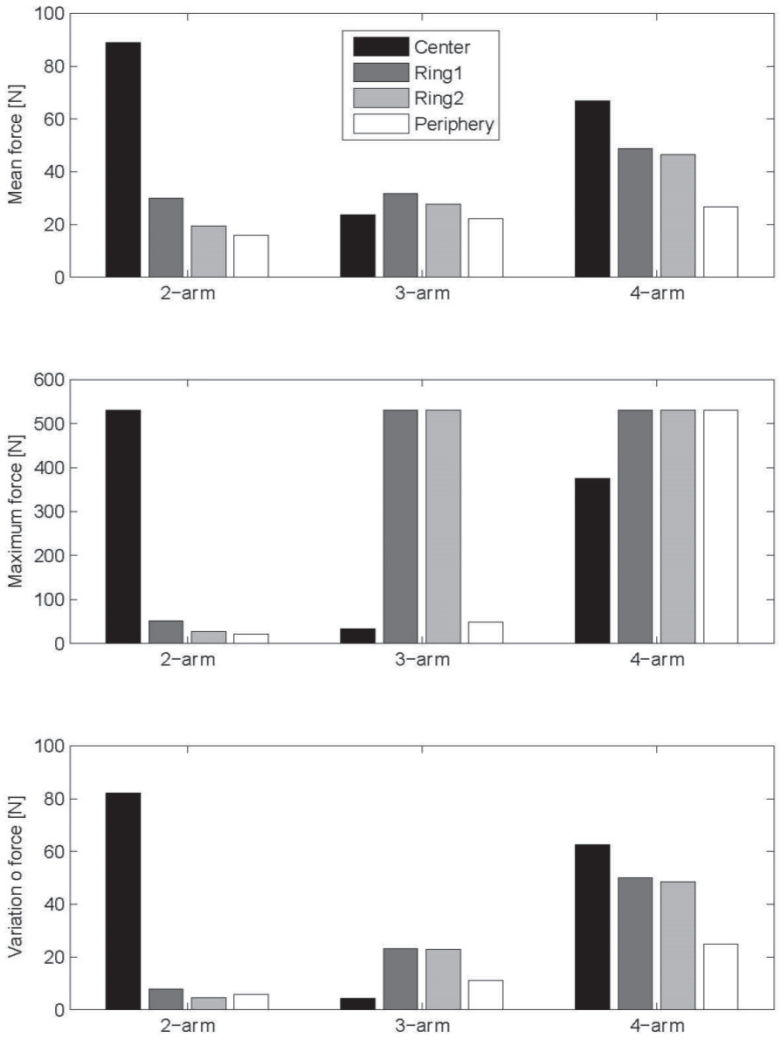

Figure 10.5. Mean force, maximum force and variation in force per area for the three different designs. Simulated mean (upper panel), peak (middle panel), and variation (lower panel) are given per area.

10.4. Discussion

The goal of this study was to compare the handling forces of two-, three-, and four-arm pendant design using a validated simulation model. This study has shown that a three-arm design improved the handling forces compared to a two-arm design: the mean force in the most frequently used Centre area was reduced by a factor 3.8, because the locations of the maximum forces were shifted to the less frequently used areas Ring 1 and Ring 2. Also, the variation in force in the Centre area was reduced by a factor 19.4.

The four-arm design showed force reductions, but to a far less extend. Using a three-arm pendant will thus have important improvements on handling forces compared to the current situation by shifting locations of high forces to less frequently used locations.

The simulation results for the two-arm pendant show much higher forces in the centre area than in the remaining part of the working area. In an observation study [10] it was observed that most problems with high handling forces occurred in the centre area. It was also noticed that during repositioning of the light this centre area was being avoided, although the shortest possible route between the original and the new location would have been through the centre area. Apparently, forces were above comfortable (max. 24N) or even above maximum (60N) force levels in this area [16].

The simulation models showed deviations from the hardware model measurements. These deviations had a number of sources. The most important source is expected to be the shortcomings of the hardware model that had high variations in friction torques for some joints. This is clearly visible when comparing the force maps of the simulated and measured two-arm pendants. The simulated system showed symmetrical behaviour between the left and the right part of the working area, whereas the measured system showed a strong asymmetry between the left and right part of the working area. Furthermore, in the friction model of the joints, only dynamic friction was included, whereas in reality there is also a static friction component. The difference between static and dynamic was kept as low as possible by choosing a friction material that had a low difference between static and dynamic behaviour (ratio dynamic/static 0.9). Finally, the models with three or four pendant arms were under-defined: there are more possible pendant arm positions that lead to the same end-point location. Combined with the high angular variations of the friction torques of the hardware model, this under-defined construction might have led to the rather large differences between simulated and measured four-arm pendant systems.

Despite these deviations, still the resulting force peaks occurred at the same locations compared to the measured situations, and variations of forces across the working area showed sufficient resemblance, except for the four-arm model. It can be concluded that the behaviour of the two- and three-arm pendants can be predicted with sufficient confidence to compare both designs. The four-arm pendant had large deviations from the measurements, and its simulation results were therefore less reliable.

The force behaviour of a pendant model is highly dependent on the orientation of the pendant arms. Multiple initial pendant arm orientations would have led to the same initial end-point location, but in different force levels. Because of the under-defined configuration, this initial orientation needed to be defined. The initial position was defined such that a worst case scenario was the result. Therefore, the initial position was kept identical with the first arm (for the three-arm) or the first two arms (for the four-arm) in forward direction. Having other initial positions might have shown force peaks at different locations, but would still have shown the same effect, as the three-

arm system would still have created low forces in the Centre area. Moreover, the under-defined characteristic enables the system to suffer less from singularities as the possibility of getting stuck in a high force area is lower.

Both measurements and simulations confirmed that a different pendant design can shift the locations of singularities from a frequently used area to a less frequently used area such that its impact on the performance of the system and the perceived handling forces is largely reduced. A full-scale prototype will allow usability testing involving users to verify the impact of a three-arm pendant on the perceived performance of the system. However, the singularities were not completely annihilated, so a more fundamentally different mechanism might be required.

10.5. Conclusion

In conclusion, a three-arm pendant design reduces mean handling forces in the most frequently used area by 4x and the variation in force in this area by 19x compared to the two-arm pendant design. This improved design shifts the singular points with high forces to less frequently used areas, thereby minimizing the impact of singularities. This design improvement has major effects on the performance of pendant systems and it is expected that the three arm pendant design could lead to a reduced amount of distractions of the surgical team. However, the singularities were not completely annihilated, so a more fundamentally different mechanism might be required.

10.6 References

Knulst, AJ, Stassen, LP, Grimbergen, CA, and Dankelman, J, Choosing Surgical Lighting in the Led Era. Surg Innov. 2009; 16: 4: 317-23.

Knulst, AJ, Stassen, LPS, Grimbergen, CA, and Dankelman, J, Standards and Performance Indicators for Surgical Luminaires. 2009; 6: 1: 37-49.

Bartlett, D, Operating Theatre Lighting. NATNews. 1978; 15: 11: 24-30.

Beck, WC, Lighting the Surgical Suite. Contemp Surg. 1978; 12: 1: 9-16.

Beck, WC, Choosing Surgical Illumination. Am J Surg. 1980; 140: 2: 327-31.

Beck, WC, Operating Room Illumination: The Current State of the Art. Bull Am Coll Surg. 1981; 66: 5: 10-5.

Berguer, R, The Application of Ergonomics in the Work Environment of General Surgeons. Rev Environ Health 1997; 12: 2: 99-106.

Berguer, R, Surgery and Ergonomics. Arch Surg. 1999; 134: 9: 1011-6.

Geisse, JK, The Dermatologic Surgical Suite. Semin Dermatol. 1994; 13: 1: 2-9.

Knulst, AJ, Mooijweer, R, Jansen, FW, Stassen, LP, and Dankelman, J, Indicating Shortcomings of Surgical Lighting Systems. MITAT. 2010; in press: doi: 10.3109/13645706.2010.534169:

Matern, U, and Koneczny, S, Safety, Hazards and Ergonomics in the Operating Room. Surg Endosc. 2007; 21: 11: 1965-9.

Patkin, M, What Surgeons Want in Operating Rooms. MITAT. 2003; 12: 6: 256-62.

Quebbeman, EJ, Preparing the Operating Room. Care of the Surgical Patient: A Publication of the Committee on Pre and Postoperative Care. Sci Am. 1993; 5: 1-13.

Rohrich, RJ, Why I Hate the Headlight ... And Other Ways to Protect Your Cervical Spine. Plast Reconstr Surg. 2001; 107: 4: 1037-8.

Horeman, T, Rodrigues, S, Jansen, F, Dankelman, J, and van den Dobbelsteen, J, Force Measurement Platform for Training and Assessment of Laparoscopic Skills. Surg Endosc. 2010; 1-7.

Burandt, U, Ergonomie Fur Design Und Entwicklung. Koln, Schmidt, 1978, 154.

Chapter 11

Optimizing Joint Configurations for Luminaire Suspensions

Jouke Harms, Arjan J. Knulst

Based on MSc thesis of Jouke Harms.
Surgical Lighting in Motion
MSc Thesis TU Delft, May 2012

During surgical operations usability issues have been observed in luminaire repositioning. These difficulties are related to the kinematics of the translational subsystem of the suspension mechanism, specifically the possibility of singularity. The required force for luminaire repositioning can be high and depends on the spatial arrangement of the mechanism. The goal of this study is to design a surgical luminaire suspension system that improves luminaire repositioning. A computer aided method was devised to optimise the mechanism kinematics to the required movement space in the operating room. This resulted in 13900 serial combinations of revolute joints, prismatic joints and links. Based on a scoring routine, a selection of concepts was made and further assessed. The resulting concept is an adaptation of the translational subsystem of the conventional suspension mechanism and is considered most feasible. The adaptations consist of a rail system from which the mechanism is suspended and a wrapping pair that couples the two vertical rotations of the pendant-type mechanism. As a result, the horizontal movement space is improved and described without singularity.

11.1. Introduction

Several studies have indicated ergonomic shortcomings of surgical lights in the operating room (OR). It has been observed that because of the size of the luminaire and the kinetics of the suspension system, repositioning the system is not always a straightforward task. Results of questionnaires held among surgical personnel and complaints made by surgeons between (Patkin 2003; Matern and Koneczny 2007; Knulst et al 2010), demonstrate dissatisfaction with surgical lighting. This is confirmed by a recent observational study, which concludes that most problems are caused by the repositioning of the surgical luminaire (Mooijweer 2010). The indicated complications range from collisions with equipment or personnel to the system not being able to move because of the spatial arrangement of the suspension system. The majority of these complications can be led back to singularity in the two-arm pendulum type suspension system, combined with the suspension generally being operated close to singularity. This results in extra steps in one in four luminaire actions (LA) that take more than 8 seconds, up to a recorded maximum LA time of 30 seconds (Mooijweer 2010).

Mechanical singularity in a double pendulum type system is a spatial configuration in which the end-effector loses the ability to move over one direction (the singular direction) and can only move back and forth in the orthogonal direction. In a frictionless world this state is only reached in the singular points (i.e. when the two arms are exactly in line). However, due to friction in the suspension system joints, movement in a certain angle around the singular direction becomes difficult or even impossible when the system is near the points of singularity. Moreover, movement of the end-effector over a small distance in or near the singular direction will result in large movements of the mechanism. As a result, in practice the luminaire is rarely moved to its new location over the shortest possible route.

Several patents show designs for surgical luminaire suspension systems that are very different from the current system and can potentially remove singularity issues [5-8]. These designs seem to have some benefits over the current suspension design, particularly concerning the repositioning of the luminaire. However, when compared with the current simple and robust system, these alternatives pose some practical drawbacks. This is probably why none of these suspension systems is currently successfully applied.

The control of the luminaire causes interference with surgical tasks, because it disrupts the visual feedback from the surgical area and perceptive feedback from the patient or instruments. This finding is supported by observational data; two thirds of the LAs are performed by the personnel performing the surgery, and in two thirds of the LAs the surgery is interrupted (Knulst et al. 2010).

The suspension mechanism causes difficulties during repositioning and this systematically interrupts surgery, therefore, the overall goal of this research is to design a surgical luminaire suspension system without singularity that improves luminaire repositioning. We are aiming for a solution that can easily be implemented in

current OR's, therefore, the focus will be on the design of a passive serial suspension system that can easily be actuated manually. In this chapter the results of an analysis of the (problems with) current hardware and its functions, regulations together with the results of research in the field of surgical luminaire suspension systems, will be translated into a list of requirements for this task. This is followed by the conceptual design phase in which the functions are determined based on the requirements. A custom solution-searching method is developed. From these resulting principal solutions, a realisable module structure (or concept) is created.

11.2. Methods

11.2.1 List of requirements

The requirements for the design of an improved luminary suspension system are based on the observed problems in the usage of the current suspension mechanism and the current operating room standards and regulations.

Movement area. The operating table is by default positioned in the centre of the operating room (OR). A survey of the current operating tables [9] shows that these offer great positioning flexibility so that the wound can always be positioned in the centre of the operating room regardless of where the wound is on the operating table. This is especially the case when the table stand is not fixed to the OR floor.

Although modern ORs are equipped with very flexible operating tables, the wound cannot be positioned at any given location in the OR. According to regulations the amount of colony forming units (CFUs) in the air directly surrounding the wound have to be lowered to certain boundaries (Zoon 2007), which are especially low for OR's that host surgery involving big wounds (e.g. transplant surgery) (10 CFU/m3 according to DIN 1946). The wound has to be positioned in the centre of the air column (plenum of minimally 9 m2, according to DIN 1946) for minimal influence of air column disturbance, which is in the centre of the operating room by default.

An overview of recent commercially available luminaires (Knulst et al. 2009) shows that the centre of the focal area (or depth of illumination) is by default located at 1 m distance from the luminaire, which is also the default distance at which the maximum luminance (Ec) is to be measured according to the European standard (NEN 2010). Two positioning extremity measures are distinguished by the standard; the distance over which the luminaire can be moved closer to the wound until it reaches 60% of Ec (L1) and the distance over which the luminaire can be moved away from the wound until it reaches 60% of Ec (L2). The total distance (L1+L2) is the depth of illumination, the luminaire manufacturers do often not supply a specific number, and the distances do not always describe the point of 60% Ec. However, L1 is always smaller then L2, and the total distance is found to be between 0.5-1.0 m.

Modern operating tables also have great height flexibility, to accommodate for the surgeons height and posture. The height range of 0.725 m to 1.215 m of the Alpha Maquet 1150 (Maquet 2012) coincides roughly with the 5th-95th percentile of the

elbow height in standing Dutch adults age 20 to 60, which is 0.949 m to 1.219 m. Therefore, the luminaire also has to be able to direct its light at angle in a height range of 0.5 m, which means that the total variability in height has to be approximately 1.5 m.

- **Requirement 1:** The end-effector of the suspension mechanism should be able to move around any wound in a spherical volume at a distance of approximately 0.8 m to 1.3 m. Where it was assumed that the wound on the operating table can be positioned within a horizontal area of 2.4 m by 1.2 meter around the centre of the operating room, with a variability in height of 0.5 meter. This results in a required movement space of 4.4 by 3.2 by 1.5 meters.

Degrees of freedom. Current surgical grade luminaires produce a cone shape light beam that has a certain direction and shape [14], depending on the lighting settings, position and orientation of the luminaire this results in a circular or oval illuminated spot around the wound (focal point, F in Figure 11.1). The focal point requires five degrees of freedom to be positioned at any surgical wound from every possible direction.

Three translational degrees (along x,y and z in Figure 11.1) of freedom to move around the wound in a 3D space and two rotational degrees of freedom (ϕ and q in Figure 11.1) to take on the correct orientation in a certain position, so that the light enters the wound at a convenient angle. Because the focal point is positioned perpendicular to the illuminated surface of the luminaire at a default distance of 1 m, the required degrees of freedom of the focal point translate directly to the luminaire.

For the development of a new luminaire that is capable of producing an asymmetric focal point, an additional rotational degree of freedom of the light beam around its own axis is needed.

- **Requirement 2.** The suspension has to provide 6 independent degrees of freedom at the end-effector. Three translational degrees and three rotational degrees of freedom.
- **Requirement 3.** The axes of the three rotational degrees of freedom have to intersect at one point along the axis of the light beam.

Kinematics. Most modern ORs feature two surgical luminaires that are meant to be used simultaneously. Because the movement space is shared by many actors and medical equipment, interference of the luminaires with each other or with other suspended medical equipment is likely to occur.

The suspension facilitates the required luminaire movement between positions, and its orientation within the defined space. The kinematic properties of the system define the route that the end-effector can travel between any set of two positions, and how

the mechanism will move to facilitate this movement. A user has to be able to manually steer the luminaire with the suspension system within the shared space without the need to constantly monitor the suspensions movement. Therefore, the suspension movement has to occur in reserved space or should be conform to the movement of the luminaire and thus not deviate from the luminaire's direction and speed as can occur in the current solution.

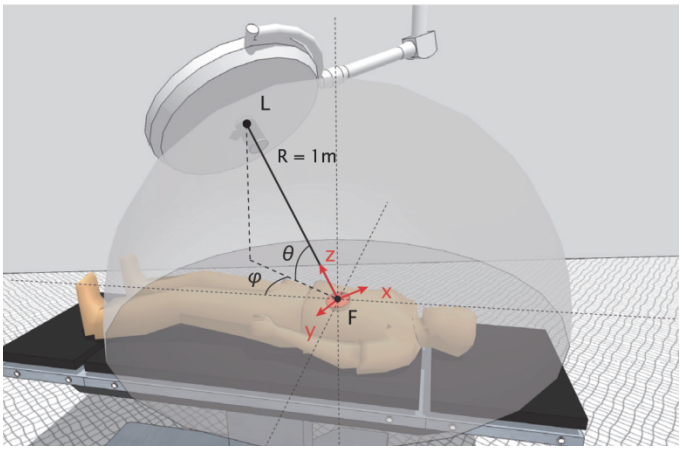

Figure 11.1 The five degrees of freedom of the focal point, three translational (x, y, z) and two rotational (ϕ, q).

During an operation most of the movement will occur around the (main) surgical site, by default at a 1 m distance. Much larger movements occur less frequently. A large movement that can be distinguished is in and out of a parking position that lies outside the plenum.

- **Requirement 4.** The mechanism can passively support a luminaire of 10-20kg and keep it perfectly still (sufficient stiff ness).
- **Requirement 5.** The end-effector of the mechanism can travel in a straight line between any two positions in the defined movement space or along the great circle over the sphere surrounding the focal point of the luminaire.
- **Requirement 6**. Two suspension systems can be installed in one OR and can both be used during one procedure without interfering with each other.
- **Requirement 7.** The direction and speed of any part in the suspension is conforming to the direction and speed of the luminaire.

Actuation speed and accuracy

The movement of the luminaire has to be fast and accurate to facilitate the surgeon's workflow. Therefore the actuation should provide a wide speed range and high accuracy. The observed mean luminaire action time of approximately 5 s (Knulst et al. 2010) is taken as a guideline; all possible movements around the wound should be

completed within this time (the longest route around the wound is half a circle with a 1 m radius). The accuracy of the focal point position is mainly dependent on the accuracy of the luminaire rotations, as 1^{o} rotation results in a position difference of 17 mm at 1 m distance. As a general rule of thumb the inertia and movement speeds should be kept as low as possible [(Haddadin 2009).

- **Requirement 8**. The suspension system has to be able to complete a maximal movement of π meter (half a circle at 1 m radius) with a 20kg luminaire in 5 s.
- **Requirement 9.** The focal point can be positioned at sub-cm accuracy. The suspension system has to be able to rotate a standard luminaire at the accuracy of half a degree. The suspension system has to be able to position the luminaire at sub-cm accuracy.

Human factors. The surgical luminaire has to be movable by hand and therefore has to be reliable, conform regulation (NEN 2010) and respect relevant ergonomic values that are neglected in the current system.

- **Requirement 10**. The manual operating force required to translate the luminaire in any direction from any posture does not exceed 59N (Burandt 1978).
- **Requirement 11**. The manual operating force required to rotate the luminaire in any direction from any posture does not exceed 25N [(NEN 2010)).
- **Requirement 12**. The required manual operating force is independent of luminaire position and movement direction.

General requirements. Besides the new requirements that are aimed at improvement, the design should also meet the requirements that are met by the current system, and those that are set for medical hardware in general. Furthermore the researched interaction method should be made applicable to the suspension system.

- **Requirement 13**. The weight of the complete system including a 20kg luminaire should be less than 140kg (weight of the Maquet system).
- **Requirement 14**. The suspension should offer room for at least two cables 9mm each (for e.g. power, camera) (Orchis-Maquet.com).
- **Requirement 15.** The suspension has to conform to standard EIC60601 Medical electrical equipment – general requirements for safety.
- **Requirement 16.** The suspension has to conform to standard ISO13485 Medical Devices - Quality management systems.

11.2.2 Functions of conceptual design

Based on the analysis of the required functions, a custom computer aided solution-finding method is developed for the task of generating working principals. This has resulted in several mechanisms that are optimised for the required movement space. These mechanisms are tested against the list of requirements, to select a realisable structure for further development.

Analysis of the OR-lighting system gives that the following sub-functions are required:

- Rotation (over 3 axis)
- Translation (over 3 axis)
- Actuation (manually)
- Brake (manually)
- Position holding (i.e. gravity compensation)

The design task specifies that the mechanism is a serial configuration, which means that the behaviour of the mechanism depends on the order in which the modules are placed between the ceiling and the luminaire. Figure 11.2 gives a schematic representation of a standard suspension system. In the system the rotation function is placed at the end-effector of the module responsible for translation, because it is required that the luminaire can be rotated at any position in the movement volume independent of luminaire movement. The actuation and brake functions are executed by the person that moves the luminaire, by exerting forces and torques on the luminaire handle. The position holding function is to compensate gravity, therefore, this subfunction is part of the module responsible for translational and rotational functions of which the movements are subject to gravity. Based on these specifications, and because the translational subsystem is the cause of the singularity issues in current suspension systems, it is chosen to focus the design process on the translational subsystem. A rotational subsystem will be connected at the end-effector of this translational subsystem.

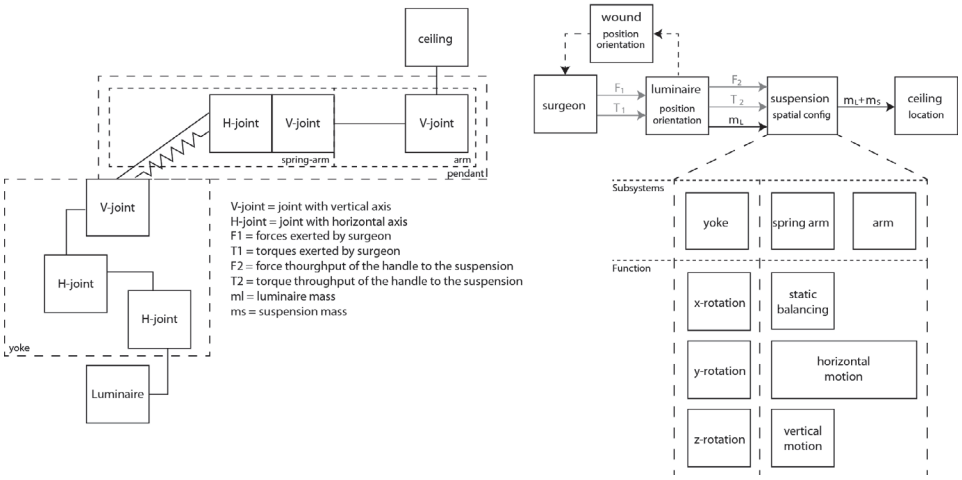

Figure 11.2 Schematic representation of current serial suspension mechanism (left). The luminaire is connected to the ceiling and consists of three subsystems (right) each having specific functions. The yoke facilitates rotations and the pendant facilitates translations. The spring-arm stores the energy put into the system by gravity during vertical movement, thus keeping the vertical movement static in every position. All of the other movements are not influenced by gravity and are kept static by the friction in the joints.

11.2.3 Building blocks

The movement of a mechanism is defined by the type of joints, the number of joints and the dimension of the connections between the joints. Therefore, the design process of a mechanism can be separated in three consecutive steps; type, number and dimension synthesis [18]. The function of the mechanism and the list of requirements constrain the amount of possibilities for joint types, the amount of joints and the dimensions that are viable. Hence, defining the 'building blocks' that can be used in each of the three synthesis steps.

Joint types. Two links connected by a joint are called a kinematic pair. In a kinematic pair, the joint constrains the motion that two links can perform relative to each other, and thus limits their relative degrees of freedom (DOFs). Kinematic pairs can be classified in lower and higher kinematic pairs by the type of contact within the connecting joint (Hartenberg and Denavit 1964). Higher pairs are specifically meant for the transmission of motion (e.g. Cams, belts and sprockets) and are excluded from this synthesis, as motion transmission is not a function of the suspension mechanism. Lower kinematic pairs are connected by one of the following joints:

- Prismatic joint (translation over 1 axis, 1 DOF) [P]
- Revolute joint (rotation over 1 axis, 1 DOF) [R]
- Screw joint (coupled rotation-translation over 1 axis, 1 DOF) [S]
- Cylindrical joint (rotation and translation over 1 axis, 2 DOFs) [C]
- Spherical joint (rotations over 3 orthogonal axes, 3 DOFs) [S]
- Planar joint (translation over 2 orthogonal axes and rotation around an axis orthogonal to the translation plane, 3 DOFs) [P]

From the requirements it follows that the end-effector of the suspension has six DOFs relative to the base of the mechanism, three translational and three rotational. Translational movement can be effectuated by a prismatic joint or by a revolute joint in combination with a link. In the latter case the translation will follow a curved path. Rotation can be acquired by a revolute joint or a prismatic joint moving along a curved path. This means that both motions can be created by the right combination of any of the lower kinematic pairs.

Number of joints. The amount of DOFs that a kinematic chain has relative to its base depends on the type, amount and placement of joints and links in the mechanism. In serial mechanisms, the amount of DOFs at the end-effector is equal or less to the sum of the amount of DOFs of all kinematic pairs in the mechanism. Therefore, the required amount of DOFs at the end-effector defines the minimal number of joints and link combinations in the suspension's kinematic chain.

The maximum amount of kinematic pairs is not defined by the requirements directly. However, the required amount of DOFs of the end-effector is equal to the maximal amount of DOFs anybody can have relative to a 3D reference frame. Therefore, a greater amount of kinematic pairs in the mechanism than minimally required, will not result in more DOFs at its end-effector, but it will influence the kinematics of the mechanism. A surplus of kinematic pairs in a purely serial mechanism will result in

interaction between kinematic pairs, which cannot be controlled by steering the end-effector. Also, the amount of possible spatial configurations in which the mechanism can reach a certain end-effector position and orientation increases, thus making the mechanism less predictable. In the synthesis of a suspension system for the surgical luminaire, it can be theorized that the number of links and joints should be chosen close to the minimum.

Dimensions and links. When Joints translate, they move along a certain axis over the dimension of the joint. Thus the joint dimension defines the span of the joint. Joints that rotate are dimensionless and facilitate rotation around a certain axes. The span of a movement induced by rotations is created by the relative position of the joints, the end-effector and the axes. This is determined by the dimension of links or translational joints.

The required movement space of the end-effector of the suspension system is 4.4 x 3.2 x 1.5 m. The end-effector has to be able to be set at any position within this space and take on any rotation at any position. Thus the dimensions of the links and translational joints should be in the order of about 1 to 3 m. In the current mechanism a donut-shaped movement space is reached with three joints and two arms that both measure about 1 m (Figure 11.3).

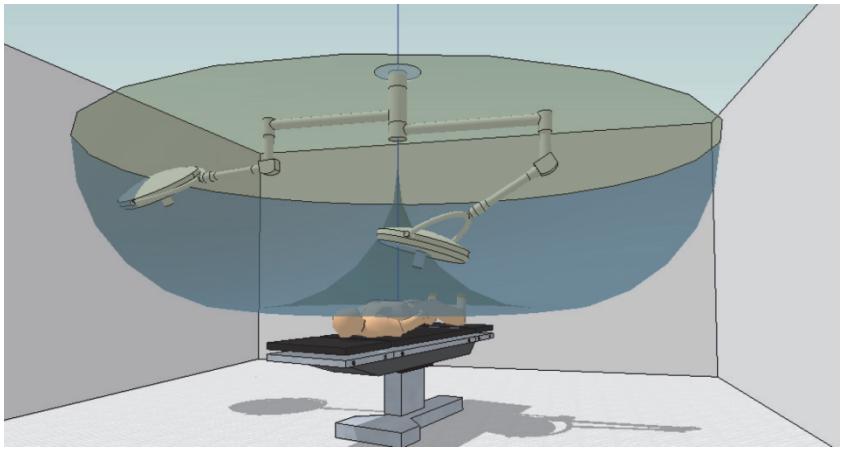

Figure 11.4 The shape of the movement area, which is reached by the current suspension mechanism. This mechanism features a base link, two links of 1 m length and three revolute joints. The base (ceiling) is connected to the first link with a revolute joint around the vertical axis. The second link is connected to the first link with two revolute links, one with a vertical axis and one with a horizontal axis.

11.2.4 Design method

Although the definition of building blocks has limited the design space for the translational subsystem, a vast amount of conceivable mechanisms remains. Among

these mechanisms are many designs that do not meet all the other requirements. Thus, the challenge is to create a combination of building blocks that best meets the requirements.

For the translation subsystem, the size of the movement space can be set as the primary design requirement. Therefore, the synthesis can be approached as an optimization problem: to find a mechanism that is optimised to span the required movement space. This is a tedious task, if done by hand, however, because of the well-defined design space this process can be automated, so that the complete design space is considered. This mathematical optimization of the translation subsystem, can be performed in two ways.

1. Less exhaustive: a recursive algorithm that takes a certain starting configuration and varies the components in such a way that the performance measure improves, until changes do not result in improvement anymore, and a local or global optimum is found.
2. Exhaustive: A brute-force algorithm that creates every possible combination and tests its performance.

The first would be the preferred method, for its efficiency in finding the optimal solution. However, the mechanism with the best movement space does not necessarily meet the other requirements, and the mechanism that does can well be absent in the convergence towards the optimum. The second method will result in a selection of mechanisms that best fit the required movement space out of the entire design space. Such an overview is preferred in a design process, in which all requirements need to be taken into consideration to select a successful concept. Thus the second method is used.

Mathematical mechanism synthesis. The movement of a mechanism and thus the movement space, can be described by kinematic equations. The input for such equations is the degrees of freedom of each joint and the dimensions of the links. The output is the position and orientation of the end-effector.

The Denavit-Hartenberg representation (1964) is used as method to calculate kinematic equations. This method allows for “mathematical assembly” of mechanisms. The position of the end-effector in a global coordinate system is described by the product of local coordinate system transformations induced by links and joints.

A local 3D coordinate system is defined on each link and joint, the transformation of adjacent local coordinate systems is expressed by a 4x4 transformation matrix with parameters that represent joint degrees of freedom. The complete product results in a symbolic equation of the transformation of the end-effector relative to the base-link’s global coordinate system, with all the mechanism’s DOFs as input parameters. Thus allowing for the mechanism assembly to be varied by replacing or adding transformation matrices.

In the transformation matrix of the Denavit-Hartenberg representation, parameters can be set for three rotations, three angles, and three translation, three distances. Therefore all lower kinematic pairs can be modelled (Figure 11.3).

- The revolute joint has one parameter; an angle.
- The prismatic joint has one parameter; a distance.
- The cylindrical joint is a prismatic joint combined with a revolute joint, thus two independent parameters; an angle and a distance.
- The spherical joint is a combination of three revolute joints, thus three independent parameters; three angles.
- The planar joint is a combination of two prismatic joints and a revolute joint, thus three independent parameters; an angle and two distances.
- The screw joint combines the rotation of a revolute joint with a translation of a prismatic joint, thus two dependent parameters; an angle and a connected distance.
- A link spans a certain distance depending on the dimensions, a free-formed link can translate the coordinate system over three dimensions, thus three parameters; three distances.

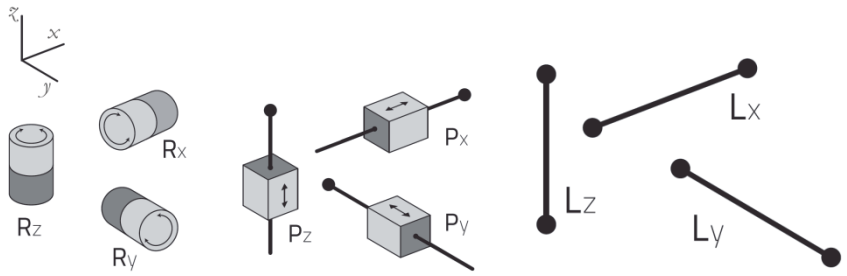

Figure 111.4 The building blocks that are represented using the Denavit-Hartenberg representation [18] are prismatic joints (P), rotational joints (R) and links (L). All of which can be defined over the 3 axis. By combining joints and links a mechanism can be assembled.

Only the screw joint cannot be represented with this method. However, it can be argued that the screw joint is not suited for the translation of the luminaire. The translation of the luminaire has to be independent of the rotation of the luminaire, to enable the luminaire to illuminate any wound from all directions. The connection of a rotational DOF with a translational DOF is not useful in a purely translational mechanism. Therefore, the screw joint is omitted from the optimization. A link is a translation over a fixed distance, which can also be represented by a transformation matrix. Links other than a simple straight link can be modelled as two or three translations in one or several transformation matrices. The same holds for longer and shorter links.

The product of a set of transformation matrices results in equations for the x, y and z coordinate of the mechanism's end-effector, relative to the global origin. For a surgical luminaire suspension system, the global origin, or base-link, is the ceiling of the operating room. Thus the mechanism's movement space is the portion of the movement space below this x-y plane at z=0.

Performance measure. With the proposed Denavit-Hartenberg representation every serial mechanism within the design space can be virtually synthesized as a sequence of transformation matrices, with links along three axis (Lx, Ly and Lz), revolute joints about three axis (Rx, Ry and Rz) and prismatic joints along three axes (Px, Py and Pz). However, to incorporate dimension synthesis, the link and prismatic joint dimensions also have to be varied resulting in an enormous amount of variation. Therefore, the dimension of every serial link is standardised to a total reach of two meters. This was based on the reach of the current mechanism. The optimal configuration of joints and links would have a movement space that fits the required movement space. Using the standardised dimensions however, the fit of the required movement space has to be measured proportionally.

To compare the mechanisms based on the required movement space, a performance measure is devised that measures the fit of the required movement space in the mechanism's movement space. This performance measure is derived by fitting a volume that is proportional to the required movement space inside the boundaries of the mechanism's movement space. The percentage of the mechanism's movement space that is covered by the fitted volume is a dimensionless measure of how well the combined motion of the mechanism can cover the required movement space.

Mechanism boundary computation. The boundaries of a mechanism's movement space can be derived from the kinematic equations, and are characterised by the DOFs reaching a minimal or maximal value, or the singularity in the equation. However, methods that use mathematical singularity to define the boundaries of a mechanism's movement space require engineering insight for interpretation and are therefore not applicable in an automated process (Abdel-Malek et al. 1997).

A less elegant but more robust method is to obtain the movement space boundaries from a map of the complete movement space. Using the Denavit-Hartenberg representation, the movement space can be mapped by consecutively stepping through the entire movement range for all degrees of freedom or equation parameters (Figure 11.5 left). This results in a 'cloud' of possible end-effector positions, of which the resolution is defined by the step-size. This cloud can be sampled over the x-y plane to find the maximal and minimal z values for each sample, and thus define the boundaries of the movement space cloud. The sample resolution is set depending on the step-size.

Box fitting routine. The box fitting algorithm starts by identifying three maximal distance values between the upper and lower boundary, inserting a small box halfway

between these boundaries. Then the box is increased in size while maintaining its proportions, until a boundary is hit by any of the six sides. In case of a hit, the box is moved away from that boundary and further enlarged, until no increase in size is possible anymore (Figure 11.5 right). This process is started at a coarse enlarging size, which is lowered to 1/32 of the starting size in a total of 5 iterations.

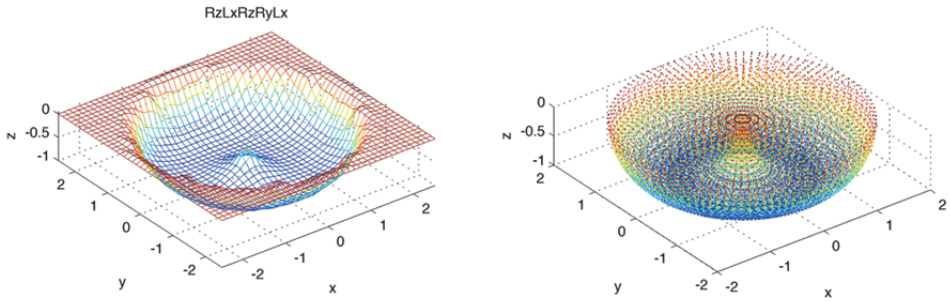

Figure 11.5. Left: The sampled lower boundary of the current suspension system model, with the proportional required movement area fitted inside. Right: visualisation of the cloud of end-effector positions of the 75th mechanism (Rz-Lx-Rz-Ry-Lx) in the 9th sequence (R-LR-R-L). This is the modelled version of the current suspension mechanism. The position on the Z-axis is colour coded from red (0) to blue (lowest point).

11.2.5 Implementation

The virtual mechanism synthesis and performance measurement is executed using MATLAB®. Both methods apply brute force methods, which makes the routines computational intensive. The amount of calculation steps that are needed to span the movement space is the step resolution to the power of the amount of joints. Therefore, the resolution and the number of joints in the mechanism were limited. Analysis has shown that lowering the step resolution for mechanisms with more joints has a significant influence on the performance measure. Therefore, it was decided to fix the resolution for all mechanisms at 32, which gives good results in boundary computation. To keep computation time of all mechanisms within a few hours at a resolution of 32 steps per joint, the following constraints were set.

- The design space is limited to mechanisms that have a total 3 or 4 degrees of freedom. Three DOF is the minimum and more than 4 joints is not computational feasible. Also, as argued before, adding more joints will probably result in less intuitive mechanisms.
- The total length of the combined links is set to 2 m
- A pendant mechanism with two links of unequal length will result in a movement space with a gap in the centre, therefore a link cannot be connected to another link in the sequence.
- A prismatic joint is a translation, therefore the combination of a prismatic joint followed by a link or vice versa is omitted.

- A revolute joint has a translational effect if it is followed by a link or prismatic joint, therefore a revolute joint can never be the last component in the serial mechanism.
- The only way of spanning a rectangular shaped movement space, like the required movement space, is by a combination of three perpendicular prismatic joints. This can be taken into account without simulation, thus the maximal amount of sequential prismatic joints is set to two.
- Because there are only three possible rotations, the combination of more than three translational joints is omitted.
- Combinations that result in a transformation matrix with a rank lower than three span a movement space with less than three dimensions and are therefore omitted.

Statistical analysis of the complete dataset is done in SPSS to generate tables with relevant measures and compare groups using ANOVA test.

For visual assessment the data set is sorted descending on score and filtered, because one mechanism is created in several combinations (e.g. RzLxRzRyRx is the same as RzLyRzRyLx), all mechanisms that score equal within the same sequence are omitted except for the first occurrence of that score.

11.3. Results

A total of 40 viable sequences were created, of which 11 sequences with three joints and 29 sequences with four joints. 834 combinations were made with the three joints sequences and 13908 combinations with four joints sequences. The chain length in these sequences varied from three to seven components. To keep computation time within a few hours for all combinations, the step resolution was chosen at 32 steps for every joint. Computation of all steps with the forward kinematic equations resulted in about 20GB of 3D position data.

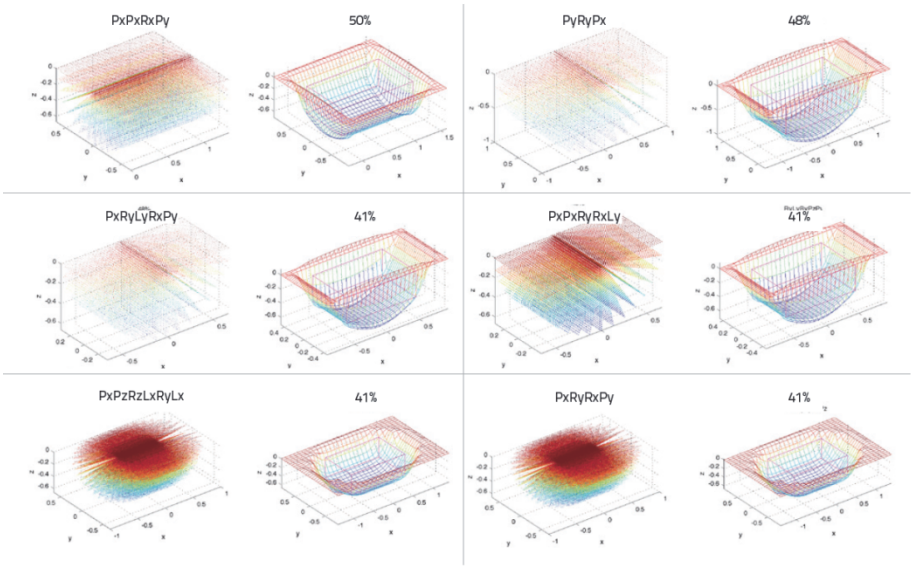

Figure 11.5 An overview of the six best scoring movement spaces that are created by 34 combinations from 14 sequences. For each movement space the end-effector positions cloud is depicted left to the derived boundary of the movement space with the fitted box. One of the combinations that create each movement space and the rounded score of the fitted box is denoted above the plots.

11.3.1 Visual assessment

Visual assessment of the movement spaces (Figure 11.5) of the highest scoring combinations shows that the scores are dependent on the shape of the movement spaces.

Within the sequences it is observed that several combinations yield equal scores, because sometimes the orientation of a building block does not affect the resulting mechanism and thus also not the movement space it creates (Figure 11.6 left). Such cases can be filtered out by discarding all equal scores within a sequence except for the first occurrence.

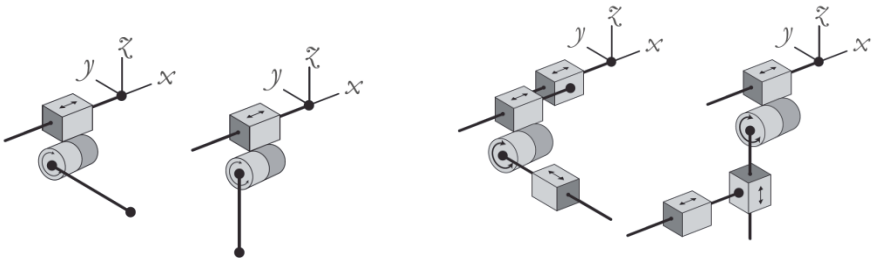

Figure 11.6 Left: An example of two combinations in one sequence that result in an equal movement space. Therefore, the scores are filtered, so that only the first occurrence of a score within a sequence is considered. Right: An example of two combinations from different sequences that both yield the highest scoring movement space. These two combinations form unique mechanisms with different kinematics that should both be assessed for concept selection.

Among different sequences, the scores can also be equal, for instance due to a shifted rotational joint (Figure 11.6 right). These double scores are not filtered out, because the configurations from different sequences result in completely different mechanisms with different kinematics. Furthermore it can be seen that several completely different movement space shapes have scores that are very close to each other (or even equal when rounded off). Only the first two scores of 50% and 48% are uniquely for one movement space shape and are significantly higher than the rest of the scores. After these, the score gradually declines from 41% to 0%, and each rounded score is shared by several movement space shapes.

After filtering the 14742 combinations 2402 remain, of which the top 200 are assessed. This is done on paper, so that the mechanism layout can be quickly drawn next to a printed plot of the movement space. During this assessment the following observations
were made.

- The shape of the movement space on the x-y plane at z=0 depends heavily on the first joints. If the first joint is a revolute joint, then the movement shape is likely to be round. If the first joint is prismatic, then the movement shape has at least one straight side.

- The two highest scoring movement space shapes are square on the x-y plane at z=0, because they contain at least two prismatic joints in a perpendicular configuration.
- The best scoring movement spaces are either square or have a long side along the x-axis. Which is logical as the required movement space also has a long side along the x-axis.
- The highest scoring shortest sequence is in the second movement space shape [PyRyPz].
- The translational subsystem of the current suspension mechanism is not among the 200 best scoring combinations.

11.3.2 Statistical analysis

The data set spans the complete design space at one resolution, thus resulting in a data set that can only be analysed using descriptive statistics. Comparison of the mean, median, variance and maximal values of certain groups within the data set, gives insight in how chain length, chain components and component positions influence the score of the mechanism. The significance of certain differences can be checked using the ANOVA method as long as the distribution is close to normal and variances between groups are comparable.

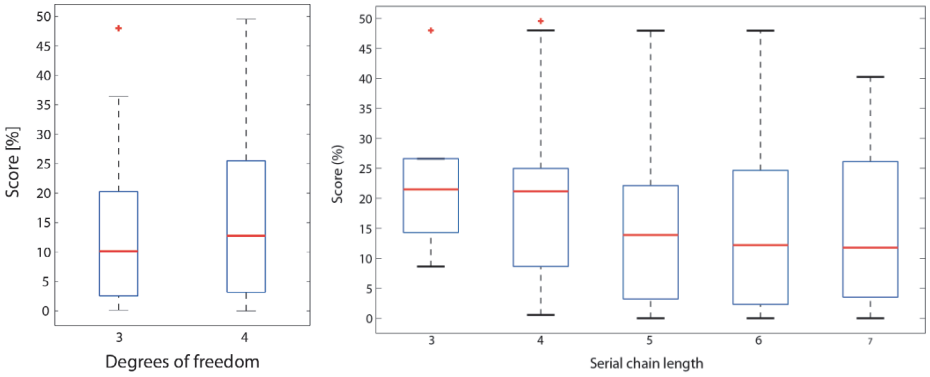

Figure 11.7 Boxplots of the scores for all mechanisms grouped on the degrees of freedom (left) and grouped on kinematic chain length (right) of the mechanism. Apparently the median score drops for longer chains.

Degrees of freedom

The data set can be divided in two groups, based on the degrees of freedom (joints) in the mechanism. This shows that mechanisms with four joints generally score higher then mechanisms with three joints (Figure 11.7 left). However, six mechanisms with the sequences [PRP] and [RPP] describe the second scoring movement space. These mechanisms are an outlier to the group of mechanisms with three joints.

Statistical analysis of the complete data set indicates that the influence of the amount of joints on the score is significant. However when the same test is performed on only the 5000 best scoring mechanisms, the influence becomes insignificant ($p>0.05$).

Chain length

By grouping the mechanisms on the sequence chain length and comparing the scores in a box plot representation, it seems that shorter chains tend to score higher overall (Figure 11.7 right). However, the maximal values and outliers are equal up until a chain length of seven components.

Statistical analysis shows that the scoring in populations with different chain lengths is significant different ($p<0.05$). However, a Tukey post-hoc test shows the scores of mechanisms with chain length three and four are not significant different ($p>0.05$) and that the scores of mechanisms with chain length five, six and seven are in a homogeneous subset, as the scores of mechanisms with chain length of five and six ($p>0.05$), six and seven ($p>0.05$) and five and seven ($p>0.05$) are all not significant different.

Chain components and their positions

If the scores of combinations that contain a prismatic joint and those without prismatic joints are compared, it can be concluded that mechanisms without prismatic joints generally score higher. Among the 200 highest scoring combinations 71 do not contain a prismatic joint, of which 69 contain 4 revolute joints and 51 of those have a sequence length of 7.

The variance of scores of all mechanisms that have a specific component at a specific position could show successful positions for certain locations. components. It appears that only for the prismatic joint a clear trend exists, the median score becomes higher towards the fourth position in the kinematic chain. Both revolute joints and links show some small variations in score distribution between the positions. The maximum score values are not effected by specific components at specific positions.

Statistical analysis shows that the variance in score between components at every location differs significantly. However, a post-hoc test results do show scores are not significant different for some components at certain locations.

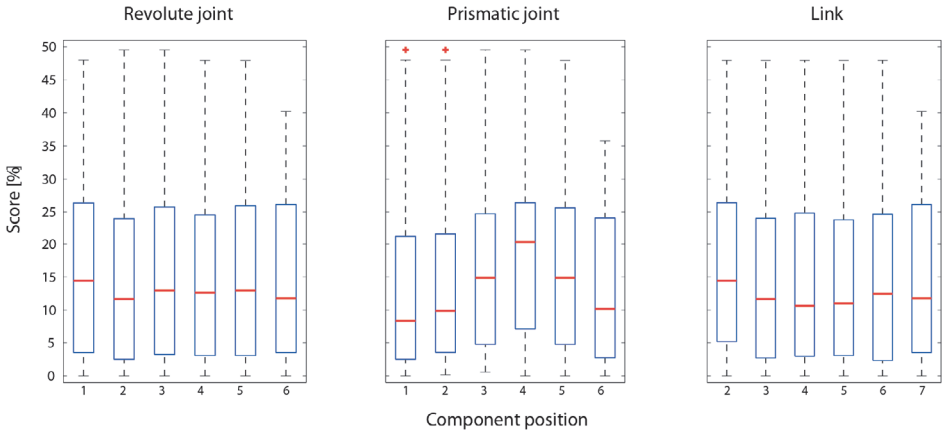

Figure 11.9 Groups of boxplots of the scores for all mechanisms grouped on component type and their location in the chain length. This means that one combination is in several groups. Notable is that the score distribution for the prismatic joint seems to shift upward towards a prismatic joint at the fourth location and that prismatic joints at the first two positions generally score low.

11.4. Concept selection

The results show that mechanisms with revolute kinematic pairs are generally better suited for the required movement space. However, the top ten scoring mechanisms all contain a prismatic joint. Thus, with regard to the movement space, the conclusion from previous research is confirmed; serial mechanisms containing a prismatic joint are the most promising for improvement of the surgical luminaire suspension system. However, with regard to the other requirements, most systems that contain a prismatic joint are unfeasible.

In this paragraph, a high scoring mechanism is selected that best meets all requirements. This is done in two stages. First, a rough selection is made from the 200 best scoring combinations via exclusion. Secondly, the selection is rated on the compliance to relevant requirements.

11.4.1 Mechanism exclusion

Combinations are excluded based on useless joints and on the following two categories.

Kinematics. A configuration with prismatic kinematic pairs can better meet the requirements set for the kinematics than combinations of kinematic pairs based on revolute joints. A prismatic joint can only move over a straight line, thus two perpendicular placed prismatic joints (i.e. a planar kinematic pair) can describe every movement in a plain equally well, independent of the spatial starting configuration. Moreover, no singularity issues exist if a plane is described by two perpendicular prismatic pairs. Therefore, mechanisms without prismatic kinematic pairs and mechanisms that contain conflicting revolute pairs in one plane are excluded. Furthermore, a short kinematic chain is preferred, longer kinematic chains are more

liable to singularity and the control by manipulation of the end-effector is likely to be difficult.

Passive weight compensations. The mechanism is required to passively compensate its own weight and the weight of the luminaire. This compensation is only necessary over degrees of freedom that are affected by gravity, which can be done in various ways. However, the difficulty of weight compensation for revolute joints increases with every degree of freedom that has to be compensated. Therefore mechanisms with more than 2 joints affected by gravity or 2 joints after a gravity affected joint are discarded. To compensate a vertical prismatic joint is easier and independent of its position in the kinematic chain, however it is not desirable to have a complete mechanism move up and down. Therefore every mechanism that starts with a vertical prismatic joint (Pz) is discarded.

11.4.2 Mechanism selection

The mechanism exclusion resulted in a selection of 7 mechanisms, these mechanisms are further assessed and rated. This assessment focuses mainly on detailed kinematics, feasibility in the OR and minimizing inertia by position the joints closely together near the base.

Feasibility in the OR. Compared to the 'closed' revolute joints that are applied in the current suspension systems, the prismatic joint is an 'open' joint. Therefore the prismatic joint is not commonly applied in the sterile environment of the operating room. Despite of this, several systems with prismatic joints have recently been developed for the positioning of equipment in the operating room. Based on these references, it is estimated that the prismatic joint is feasible in the OR as long as it is positioned well away from the surgical site and out of sterile airflow. Therefore, all mechanisms that contain prismatic joints near the end of the kinematic chain get a negative rating on feasibility.

11.4.3 Firming up the concept

From the exclusion and selection process no clear winner emerges and the best rated mechanism does not meet all criteria. However, there are a two features that seem promising regarding the results and the research, these features should be further investigated and firmed up to generate a concept.

- A rail along the long side of the movement space is both feasible in the OR and results in high scoring movement space shapes.
- A prismatic movement further along the kinematic chain, specifically the fourth location according to statistics, results in promising mechanisms. However, due to contamination hazard this cannot be a common rail or piston type joint, also passive weight compensation and actuation of this joint is difficult. Therefore, the embodiment possibilities of such a joint should be further looked into.

Rail in the OR. Current examples of the hybrid OR proof that it is possible to suspend the luminaire from a rail. However, the chosen design involves a rail system that is positioned in the centre of the movement space thus directly above the patient and the wound, which is an unfeasible location. One of the examples shows an integration of the rail and a 2T-plenum through a small separation of the plenum fields. Such integration does not move the rail too far out of the centre of the OR and compared to the rail systems that are used for catheter visualisation equipment, a rail for a luminaire suspension is less bulky and can therefore be much better integrated. According to an expert in the field of plenums (Rob van den Berg from Telstar Medical) such integration is perfectly feasible. However, it should be taken into account that any gap between the plenum fields is to be closed in a dust tight fashion. This is already used in closed rail systems for imaging equipment in the Hybrid-ORs.

Fig. 11.10 Lego models. Left: Rail concept, middle: Scissors concept, Right: Coupled joints

Conceptual kinematics. The best rated mechanism (Rail concept) does not meet two of the tested requirements, because of singularity and the inability of travelling along a straight line due to the same singularity. To further investigate this problem a Lego model has been constructed (Figure 11.10 left). In this model the prismatic and revolute joint has very low friction characteristics, whereas the friction of the prismatic joint depends on the angle of the link relative to the rail. The singularity also depends on this angle and occurs when the angle is 90°. In practice this means that the model can only be fully controlled if the angle remains below approximately 25°, mostly due to the friction.

In theory the friction of the prismatic joint in the OR could be less than the model, thus the angle at which the mechanism can be positioned could increase. However, due to the singularity the angle can never be larger than 45°, unless a torque can be transferred through the control handle, which is impossible due to the required rotational degrees of freedom of the luminaire. Therefore, the realistic movement space of this mechanism becomes a lot smaller, which drastically decreases the feasibility of this concept.

The selected concepts that do not contain a singularity problem are very similar to the best rated mechanism, the only difference is a prismatic joint at the fourth position in the chain instead of a revolute joint with a vertical axis at the third position. Besides the absence of singularity, these concepts also have the highest scoring movement space shapes. However, the problem is that ‘open’ joints are not feasible near the

wound, due to contamination hazard. Therefore, a feasible concept for a prismatic joint based on closed joints has to be invented.

The only joint that is closed and accepted to function near the wound is the revolute joint. Thus the best solution seems a mechanism consisting of links and revolute joints, of which the end-effector can only move over a straight path.

Concept 1: scissors. A well-known mechanism that combines a series of links and revolute joints to move over a straight path is the 'scissor lift'. Such a mechanism seems extremely well fit for this design problem, as it also features a rail at the base. Further development of the idea shows that the kinematics of the idea work very well, a Lego model shows that the end-effector of the mechanism can move over two perpendicular lines that can both be controlled from the end-effector without the need of transferring a torque. However, the construction's 'bulkiness' decreases its feasibility in the OR and it is difficult to compensate gravity in the rotational degree of freedom that allows the mechanism to move over the vertical axis.

Concept 2: four bar mechanism. Other and more 'elegant' mechanisms exist besides the scissor lift that aims to constrain the motion of the end-effector, so that it can only move along a straight path (Seitz 1965). For example the principal applied in the harbour crane, which is a pendant mechanism with a guide link. Further development of this type of solution shows that the resulting mechanism resembles the current pendant type suspension system, which makes it highly feasible. The path that is described by the end-effector of the system depends on the dimensions of the arms. A limitation to this mechanism is that the components have to align if the end-effector passes to the other side of the rail. Therefore the precision in dimensions is very high, depending on the play in the joints.

Concept 3: Coupled joints. The coupling of rotations of two revolute pairs can be done with the addition of lower kinematic pairs, such as a guide link. However, it can also be done by a higher kinematic pair that transfers the motion. Examples of higher kinematic pairs that transfer rotation to rotation are a chain, a belt or sprockets. For the end-effector of a pendant with links of equal length to travel over a straight line, the ratio between the angles of rotation is 2 on 1. This idea has also been modelled in Lego (Figure 11.10 Right), in which the motion transfer works and the end-effector moves over a straight line as a result. However, the friction in the rail and the play in all the sprockets make it impossible to move the rail if the end-effector is further away from the rail. Never the less, it can be observed that the sprockets lock whenever the force on the end-effector is in parallel direction to the rail.

11.4.4. Final concept

The Lego models served as an important estimation tool in the assessment of the three kinematic concepts, which were tested on the requirements that were also used in the first exclusion and selection process. This resulted in the selection of the third concept for further development. In essence this concept is the current suspension with a very simple adaption and an added rail system. Both of which are currently applied in the

OR, thus considered highly feasible. The mechanism meets the requirements and features a high scoring movement space. To further firm up the working principal, an improved scale model was build (Figure 11.11).

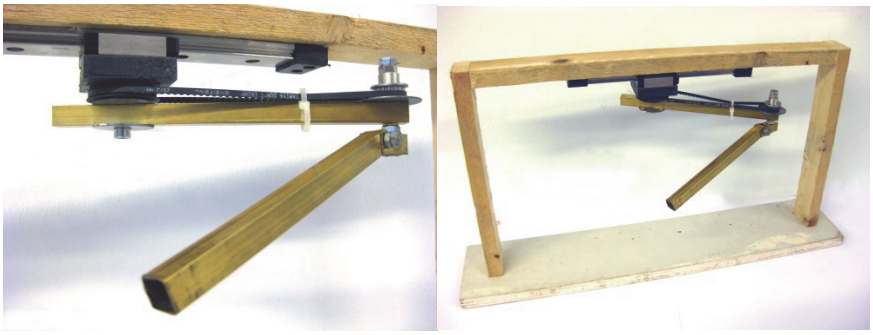

Fig. 11.11. A scale model of the final concept, the arms in this model are approximately 150mm in length and the rail is about 200mm in length. The toothed belt and pulleys have been bought at a model building shop and because their axes cannot move, the belt is tensioned with a tie wrap.

The arms in the improved scale model feature a wrapping pair (two pulleys and a belt) for the transmission of the motion and the rail features a linear ball bearing with very low friction. As a result, the mechanism functions perfectly and all forces on the end-effector parallel to the rail are transferred to rail movements independent of the end-effector position. However, due to play in the wrapping pair, there is some play at the end-effector, which should be solved by a tensioning mechanism in a final design.

Kinematics. The end-effector in the final concept moves in two perpendicular directions in the horizontal movement area, which is facilitated by the coupled arms and the rail (Figure 11.11 right). These movement characteristics are constant throughout the complete movement area, thus no singularity issues exist. The vertical movement is provided by the spring-arm, which is also applied in the current suspension mechanism and compensates the weight of the luminaire.

In the operating room. Two types of rail integration have been observed in the current operating room (OR); along the sides of the plenum or integrated between plenum fields. The latter option allows for a smaller and less conspicuous mechanism, which is preferred. Also, because the plenum with several fields is expected to be standardize in the future OR, integration with the lighting system seems a promising solution.

In a 2T or 3T plenum, two rails can be integrated alongside the central plenum field and the best configuration would be to suspend one luminaire from both rails, in a mirrored configuration. The luminaires are then able to pass one another with minimal interference. The rail should be dimensioned longer then the plenum, to allow for a luminaire to be parked outside the surgical area if obsolete. Also, a secondary (small) luminaire can be suspended from one of the rails as well, in a mirrored configuration.

In this rail integration, room remains for the suspensions for other equipment along the sides of the plenum.

11.5. Discussion

To optimise the mechanism kinematics of OR lights to the required movement space in the operating room, a computer aided method was devised, resulting in 13900 serial combination of revolute joints, prismatic joints and links. A scoring routine, followed by a selection process, resulted in a concept which is an adaptation of the translational subsystem of the conventional suspension mechanism.

It can be questioned what the added value of the applied computer aided design method really is and how valuable the result is compared to results that can be obtained with more conventional solution generating methods, such as the morphological matrix. A computer can never replace the designer, because a designer can consider a complete range of requirements and has insight in the design problem, whereas the computer bluntly creates combinations within a set of constraints and is confined to a standardized scoring method. However, the designer can use computer generated results as an input in much focused design problems.

In the case of the translational subsystem of the surgical luminaire suspension system, the preconditions offered sufficient framework which supported the assumption that a successful design should be optimised for the required movement space. The outcome is a selection of serial mechanisms out of 13900 mechanisms that perform best in spanning the required movement space. This seems to be a sufficient result compared to the amount of combinations that are normally created through conventional methods.

The challenge is to select the best concept from the enormous amount of mechanisms. From the statistical analysis, it can be concluded that, although there are certain factors that cause differentiated groups of mechanisms to gain a higher overall score, in each group the maximum score approximates the overall maximum value of 50%. Thus, no specific recipe exists for an optimised serial configuration for the required movement space. Therefore, it was decided that the best approach to selecting a concept is by manual assessment of the best scoring mechanisms on their feasibility of application in the operating room.

11.5.1. Recommendations

In hindsight it might be argued that minor changes to the constraints and scoring method could greatly alter the outcome of the computer aided design method as it was applied. For instance, it is not clear how much influence the absence of dimension synthesis in this method has on the outcome, as the movement space ratio of some mechanisms can be greatly influenced by varying the dimension of certain components.
Therefore, it can be recommended that a computer design tool should allow for easy variation in constraints, such as in this case dimensions, maximal chain length and the amount of joints. With that in mind, it can also be recommended to use a more

performance oriented programming language for this kind of computer aided design methods, so that the result of the variation in constraints can be quickly reviewed.
The selected system, which is an adaptation of the translational subsystem of the conventional suspension mechanism, needs further evaluation with users. This will be done in the next chapter.

11.6 References

Abdel-Malek K., F. Adkins, H.-J. Yeh, and E. Haug, “On the determination of boundaries to manipulator workspaces,” Robotics and Computer-Integrated Manufacturing, vol. 13, no. 1, pp. 63–72, 1997.

Burandt U., “Ergonomie fur design und entwicklung,” no. Koln: Schmidt, p. 53, 1978.

Haddadin S., A. Albu-Schaffer, and G. Hirzinger, “Requirements for Safe Robots: Measurements, Analysis and New Insights,” The International Journal of Robotics Research, vol. 28, no. 11, pp. 1507–1527, Nov. 2009.

Hartenberg and J. Denavit R. S., “Kinematic Sythesis of Linkages,” ebooks.library.cornell.edu, 01-Jan.-1964. [Online]. Available: http://ebooks.library.cornell.edu/k/kmoddl/toc_hartenberg1.html. [Accessed: 03-Oct.-2011].

Knulst A. J., L. P. S. Stassen, C. A. Grimbergen, and J. Dankelman, “Choosing Surgical Lighting in the LED Era,” Surgical Innovation, vol. 16, no. 4, pp. 317–323, 2009.

Knulst A, R. Mooijweer, and F. Jansen, “Indicating Shortcomings in Surgical Lighting Systems,” Minimally Invasive Therapy & Allied Technologies, 2010.

Maquet 2012, “Overview positioning possibilities operating table system Alphamaquet 1150,” maquet.com.

Matern U and S. Koneczny, “Safety, hazards and ergonomics in the operating room,” Surgical endoscopy, 2007.

Mooiweer R., “The surgical lighting problem,” MSc Thesis TU Delft pp. 1–82, Oct. 2010.

NEN, 301062, “NEN-EN-IEC 60601-2-41 Medical electrical equipment - Part 2-41: Particular requirements for basic safety and essential performance of surgical luminaires and luminaires for diagnosis (IEC 60601-2- 41:2009,IDT),” pp. 1–52, Jan. 2010.

Patkin U, “What surgeons want in operating rooms,” Minimally Invasive Therapy & Allied Technologies, 2003.

Seitz E.-O., “SURGICAL ILLUMINATING APPARATUS,” 05-Apr.-1965.

Chapter 12

Evaluation of an Improved Suspension System

Jan Jouke Harms, Jenny Dankelman, Arjan J. Knulst

Based on MSc thesis of Jouke Harms. Surgical Lighting in Motion
MSc Thesis TU Delft, May 2012

Surgeons have indicated ergonomic problems with the surgical luminaire, which have been observed to occur during repositioning. The possibility of singularity, within the movement space of the translational subsystem of the current double-arm suspension systems, is confirmed to be the cause of these problems. In this study a redesign of the translational subsystem - without the possibility of singularity - is compared to the conventional translational subsystem in a user experiment with 14 participants. The experiment is performed outside the operating room, with one setup that can be altered between two designs; an uncoupled state with the kinematics of the conventional subsystem, and a coupled state with the redesigned kinematics. The work cost of a movement in the conventional uncoupled state is confirmed to depend on the spatial orientation of the mechanism, which is not the case in the new coupled state. Due to these different kinetics the movement patterns with the coupled mechanism are more consistent between participants, the duration of movements is shorter, less problems occur and participants are able to better control the movements. This result validates the redesign and confirms the hypothesis that a translational subsystem without the possibility of singularity within its movement space will improve luminaire repositioning.

12.1. Introduction

Complaints of surgeons regarding the usability of surgical lighting (Patkin 2003; Matern and Koneczny 2007) have been supported with recent observations of difficulties in luminaire repositioning during surgical procedures (Knulst et al. 2010). These difficulties have been confirmed to be related to the kinematics of the translational subsystem of the current default double-arm suspension system. Due to the possibility of singularity, the force required to reposition the luminaire is dependent on the spatial arrangement of the mechanism (Knulst 2012).

Based on these findings, the goal has been set to design a surgical luminaire suspension system that improves luminaire repositioning. It was hypothesised that a suspension mechanism without the possibility of singularity will improve luminaire repositioning. The resulting design is an adaptation of the translational subsystem of the conventional suspension mechanism, which is optimised for the required movement space.

The adaptations consist of a rail system from which the mechanism is suspended and a wrapping pair that couples the two vertical rotations of the pendant-type mechanism. As a result, the mechanism does not contain singularity within its movement space. The rail mechanism can be integrated between the air inlets of current state-of-the-art two (or three) temperature plenums and the pendant-type mechanism currently present in the OR. Therefore, the design is considered most feasible.

The goal of this experiment is to validate the design of the new mechanism and the hypothesis, by answering the following two research questions;

1. Are the forces required to reposition the luminaire in the new mechanism consistent with movement velocity and independent of the spatial configuration?
2. What is the reduction in repositioning duration and problems if repositioning forces are consistent with movement velocity and independent of the spatial configuration?

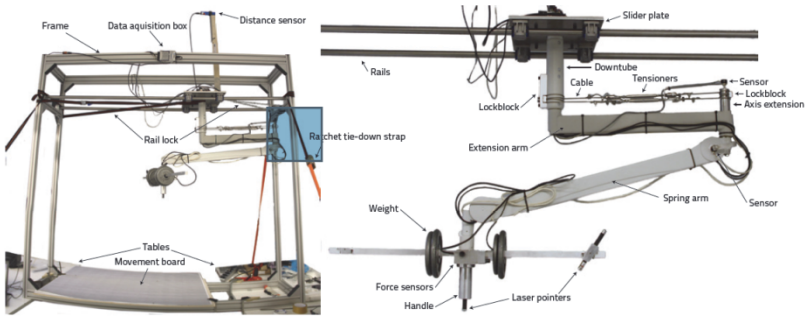

Figure 12.1 The experimental setup on the left and a close-up of the prototype on the right. The experimental setup is photographed in the conventional uncoupled state. The close-up is of the coupled state.

12.2. Methods

Data on repositioning duration and problems with the current suspension were derived from observations of luminaire usage during surgical procedures (Knulst et al. 2010). Due to regulations and restrictions it was not possible to test a conceptual system during a surgical procedure or in the OR. Thus, improvements in usage were validated outside the OR-environment and measured relative to the current standard.

12.2.1 Setup

The prototype was built using the Acrobat 2000 suspension mechanism supplied by the German manufacturer Ondal. This mechanism consists of a ceiling flange with a down-tube of approximately 350 millimetre (mm) in length (10.6 kilogram), an extension arm of 600 mm in length (2.6 kg) and a spring arm with a length of 910 mm (6.2 kg).

A wrapping pair was added to the suspension mechanism and the assembly was suspended from an existing linear joint test rig. These adaptations were designed in such a way that the prototype can be easily switched between two states: the conventional uncoupled state and the conceptual coupled state. (Figure 12.1).

Frame & Linear joint

The ceiling flange of the Acrobat mechanism was fixed to an aluminium slider plate that moves with four SKF linear rolling bearings on two steel bars with a diameter of 25 mm, 1900 mm in length and was spaced at 400 mm. The bars were suspended at a height of approximately 1600 mm in an aluminium frame of Minitec profiles that measures 2000 x 2000 x 460 mm. The frame was set on top of two tables at a height of 850 mm, to elevate the centre of the vertical movement area to approximately 1700 mm from the floor. The frame was fixed to the tables at both ends by clamps and ratchet tie down straps, for lateral stability.

In the uncoupled state the rail is locked by fixing the slider to the frame, this is done by a chain on one side and a ratchet tie down strap at the other side. This ensures that the slider is always locked at exactly the same position.

Joint coupling

In the coupled state, the two vertical rotations in the Acrobat suspension system were coupled with a steel cable wrapping pair, consisting of a 3 mm diameter cable (7x19 AISI 316) and two rigging screws for tensioning and easy disconnection. The cable was wrapped around the suspensions down-tube and secured with a custom lock block. At the other end of the extension arm, the axis of the spring arm was extended with a custom made axis extension to which the cable was locked in a similar fashion. The diameter of the down tube was 60 mm and the diameter of the axis extension was 32 mm, which was the optimal ratio for the chosen suspension dimensions. Before usage the cable was pre-stressed, so that the system response was sufficiently stiff and added joint friction remained within limits.

End-effector

In the OR, the suspension translations are operated through a large luminaire with a sterile handle that can be rotated around two or three axis. To imitate such an input device, the designed end-effector could rotate around the vertical axis and was equipped with a handle and a crossbar. The end-effector featured only one rotation as the improvement - and thus the experiment - was limited to the translation subsystem . The handle featured a blue laser pointer and was dimensioned with a diameter of 41 mm and a grip length of 100 mm. The crossbar was 900 mm in length, to imitate the diameter of a surgical luminaire. At one end of the crossbeam, a red laser pointer was connected that could be rotated between two pre-set angles. Weight was added to the crossbar to stabilise the gravity compensating mechanism in the spring-arm and to imitate the inertia of a luminaire. The total weight of the end-effector was approximately nine kilograms.

Movement board

Four black dots with a diameter of 10 mm were printed on the grey movement-board in rectangular pattern of 500 mm by 800 mm (Figure 12.2). The two laser pointers in the end-effector were directed at this surface placed on top of the frame profiles below the end-effector. The crossing point of the red and blue laser beams imitated the focal point of a surgical luminaire. The distance between this focal point and the centre of the handle was determined by the two pre-set angles of the red laser pointer. The first at which the spring arm is slightly below horizontal, and the second at which the spring arm slightly above the lowest setting. In both settings, up or down movement of the end-effector causes the laser dots to move apart on the movement-board.

Data acquisition

All degrees of freedom in the prototype were outfitted with a sensor, to measure positions of the end-effector. Also the handle was outfitted with two force sensors, to measure all control forces in the horizontal plane.

- The four rotations of the mechanism were measured by four potentiometers (Altheris fcp22e 5kΩ ~3%), which were connected to a 9 volt battery and map the angle within the nine volt range at a linearity of ~0.5%. The potentiometers were connected to the setup with sticky tape and glue.
- The translation of the rail system was measured with an ultrasonic distance sensor (PIL P43-T4V-2D-1C0-130E), which was aimed at the wall next to the setup. The ultrasonic sensor was powered by a standard 24 volt DC adapter.
- The forces at the end-effector were measured by two force sensors (Scaime ZFA 25kg and ZFA 100kg) that were mounted perpendicular between the handle and the end-effector, in such a way that the sensors did not interfere and measure all forces in the horizontal plane.

The potentiometers and the distance sensor were connected to a National Instruments USB-6008 data acquisition device and the force sensors were connected to a National Instruments USB-9162 data acquisition device running at high-speed timing mode.

Both devices were connected to a Dell Latitude E6510 laptop which was running the National Instruments DAQmx drivers and the LabVIEW data acquisition software. The LabVIEW programme sampled all sensor output at a rate 100Hz and generated a tab separated file format. Furthermore, all the user experiments were captured on 1080p video, using a Canon EOS 650D DSLR camera. This camera was setup to capture the movement board and suspension system in one shot, for later reviewing of the participant's performance.

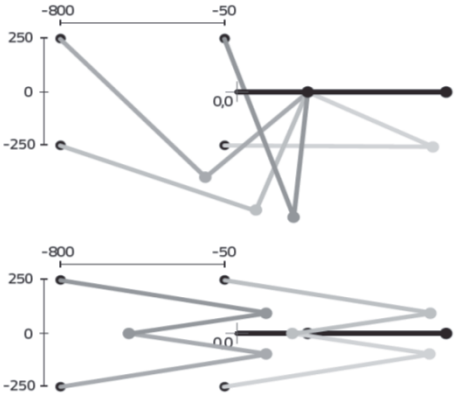

Figure 12.2 The movement-board measures 500 by 800 millimetres. The board is positioned 50 millimetre left of the calibration point (0,0), and underneath the rail that moves along the horizontal axis. Five spatial configurations of mechanism are depicted for the conventional uncoupled state (above) and the conceptual coupled state (below). Four configurations for each of the markers and the calibration configuration. The latter is a singular position for the uncoupled system state. In this report the markers are referred to as top-left, top-right, bottom-left and bottom-right.

12.2.2. Experiment

The experiment was designed to capture human interaction with all three degrees of freedom of the suspension's translational subsystem.

Task

The participant was asked to position both laser dots in one of the black markers on the movement board and to confirm when that position could be maintained without releasing the handle. Hereafter, the next marker was specified and the subject was signalled to start the movement to the next position. A complete sequence existed 12 movements, containing every movement between all four points (three categories); four movements along the x-axis (from left to right and vice versa), four movements along the y-axis (from top to bottom and vice versa) and four diagonal movements. The movement-board was located 50 mm left of the point of singularity (0,0 in Figure 12.2) and was orientated with the x-axis parallel to the rail. Therefore, only diagonal movements required simultaneous control of both degrees of freedom in the coupled mechanism, and the uncoupled mechanism was only operated close to singularity at the right side of the movement board (Figure 12.2).

There were two movement sequences, one for a standing posture and one for a sitting posture (Figure 12.3). In the complete task both sequences were performed twice, once with the suspension system in the coupled state and once with the suspension in the uncoupled state. For the sitting posture a laboratory chair with caster wheels was

used at a height setting that was preferred by the subject and the spring arm was lowered by approximately 400 mm. This shortened the length of the spring arm in the horizontal plain and thus changed the system's kinetics.

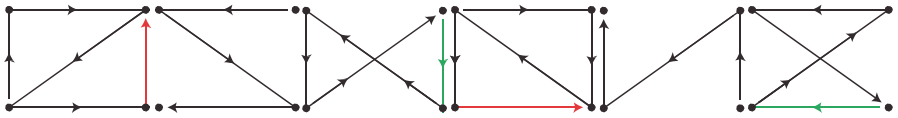

Fig. 12.3 From left to right, the sequence of the 12 movements that are performed twice by all subjects, once with the suspension system in uncoupled state and once with the suspension system in coupled state. The left sequence is performed in a standing posture, the right sequence is performed in a sitting posture. The green arrow is the first movement, the red arrow is the last movement. Both sequences contain the same movements that can be divided in three types of movement; diagonal, x and y.

Before the start of each sequence the subject was asked to practice until he or she perceived to have reached the optimum in speed of movement within their control. The assignment was not further specified to prevent the subject from optimising their performance on a certain goal, so that the intuitiveness of the system is captured in the experiment. During the task, the subject was not allowed to touch the table or any part of the setup other than the handle and the movements were performed single handed.

Participants

The group of participants existed of ten male students, two female students, a male surgeon specialised in the field of gynaecology and a male surgeon specialised in the field of neurology. All participants enrolled in the experiments voluntarily. The participants were subdivided in two groups of five male students, one female student and a surgeon. The first group used the system in the uncoupled state first and the second group used the system in the coupled state first. So that the learning effects are equal in both mechanisms.

Questionnaire

After completion of the task with the system in one of both states, the participants were asked to complete a short questionnaire de-tailing the usage experience. The questionnaire was based on the NASA Task Load Index and assessed the workload on six different subscales: Mental Demand, Physical Demand, Temporal Demand, Performance, Effort, and Frustration (Hart and Staveland 1988). After the experiment all participants were asked to complete a second questionnaire that asked the overall experience and relevant demographics.

Data analysis

The obtained data-files were analysed using MATLAB®. The position data was calibrated with values obtained in the calibration configuration (Figure 12.2) at the start of every sequence and filtered with a third order Butterworth low-pass filter with a cut-off frequency of five hertz. This data was used to calculate the positions and

rotations of the end-effector relative to the movement-board with forward kinematic equations of the setup. To check the results, the setup movements were plotted in a top-view and compared with the captured video of the experiments. The data of the force sensors was also filtered with a third order Butterworth low-pass filter with a cut-off frequency of five hertz and corrected for the rotations of the end-effector. Every movement in the sequence was isolated based on a marker value in the data set, which indicates the signal given to start a movement and the confirmation of arrival signal given by the participant. This value was manually updated during the measurements relative to the movement board.

Indicators

To answer the first research question, force (f) and movement velocity (ds/dt) are used as indicators. These indicators are combined in the work (W) measure (Equation 1), which calculates the energy cost of a movement in Joule. A paired measure (W_p) of one movement in opposite directions by one participant (W_1 and W_2) for both mechanism states and both postures is compared (Equation 2). If the required forces for repositioning are consistent with movement speed and independent of the suspension's spatial configuration, it is expected that equal movements in opposite directions cost similar amounts of energy for one participant. Thus, that the paired measure is zero or close to zero.

$$W = \int (f \cdot (ds/dt)) \cdot dt \qquad (1)$$

$$W_p = W_1 - W_2 \qquad (2)$$

The second research question refers to previous research, in which outliers in movement duration are an indicator of problems that occur during positioning. The duration of a movement (t_m) is defined as the end-time (t_{end}) minus the start-time (t_{start}) of that movement. Outliers are registered and inspected in the video capture of the experiments, the observed problems and relevant measurements are discussed. Furthermore, several theoretical models exist that describe human hand movement for assessment of motion disorders and movement quality (Campos and Colado 2009). Although no publications have been found that connect usability to a movement quality indicator, the indicators are aimed to reveal information about healthy unconstraint point to point motion and it can be theorised this is the preferred motion for humans.

An early and influential descriptive model is the minimum-jerk model, which is based on the observation that - in unconstraint point to point movements in the horizontal plane - humans strive to "generate the smoothest motion to bring the hand from the initial position to the final position in a given time" (Flash and Hogan 1985). Such motion is characterised by a bell-shaped velocity profile, which is acquired by the minimization of the jerk cost function (CF). The cost function is the integral of the squared jerk (change in acceleration over time) in all directions (x, y and z) over the interval of the movement (Equation 4).

$$CF = \int ((d^3x/dt^3)^2 + (d^3y/dt^3)^2 + (d^3z/dt^3)^2) * dt \qquad (4)$$

Statistics

The analysis was performed using the statistics toolbox of MATLAB® 7.14. The data were paired on participant and movement, grouped by the three movement types (diagonal, x and y) and compared on two factors (state and posture), by means of a two-way repeated measures analysis of variance. The same paired data, grouped by movement type and state (or posture), was also compared on posture (or state), by means of a repeated measures ANOVA and a Wilcoxon signed rank test. Furthermore, three comparisons were done within each posture-state combination, between the movement types, by means of a t-test and a Wilcoxon signed rank test. The result of the Wilcoxon is used in cases of insufficient normality, which is tested by means of a Lilliefors test. $p < 0.05$ is considered significant.

12.3. Results

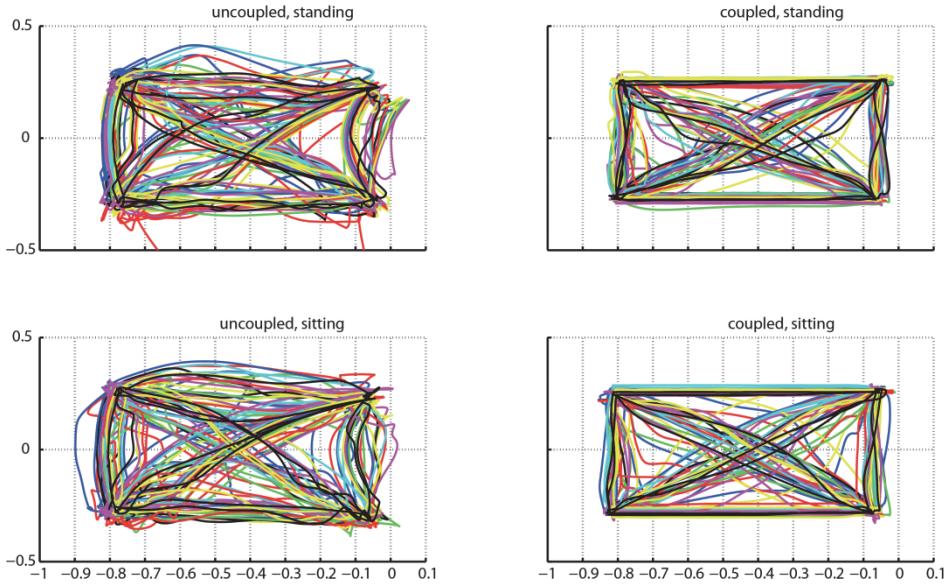

Figure 12.4 The movement paths of the end-effector of all participants, plotted on the movement board. The movements with the conventional uncoupled mechanism are plotted at the left and with the conceptual coupled mechanism at the right. The upper figures are of the movements performed in a sitting posture and the lower figures of the performance in a standing posture. It can be observed that the perpendicular translations in the coupled mechanism create straight movement paths, whereas the uncoupled mechanism is moved along curved paths.

A plot of the movements of all participants gives an overview of the difference in movement paths between participants, postures and mechanism states (Fig. 12.4). It can be observed that the movements with the uncoupled mechanism are less consistent and contain several radical outliers. The parts in which most participants

seem to perform equal are mostly circular shaped segments with the uncoupled mechanism, and straight segments with the coupled mechanism. No specific differentiations can be seen between the postures.

A visualisation of the input forces along an exemplary movement path shows the difference in force magnitude and direction between the two system states (Figure 12.5). It can be observed that the forces in the uncoupled system are much larger and seem arbitrary in direction, whereas the forces in the coupled mechanism show acceleration in one direction and deceleration in the opposite direction. No outstanding differences can be distinguished between the performance of an expert (surgeon) and that of a novice (student).

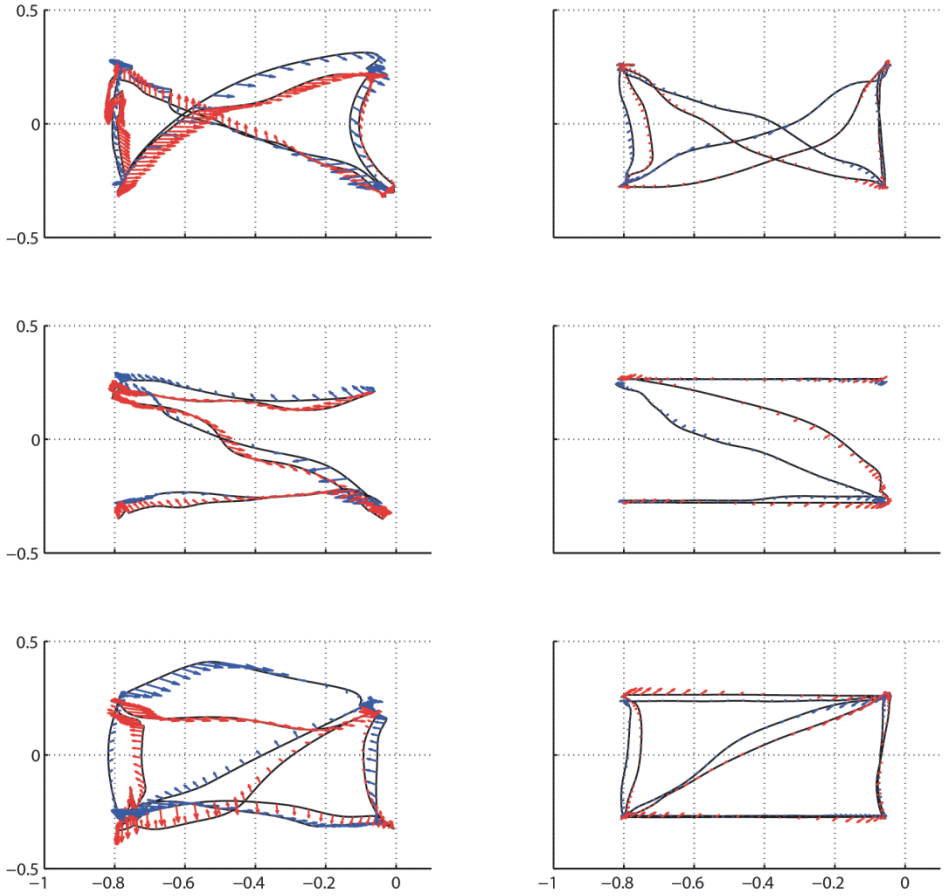

Figure 12.5 Force magnitude and direction along a couple of travelled paths for a Surgeon (Red arrows) and a Student (Blue arrows). Uncoupled (left panels) and coupled (Right panels).

Work

The average work is calculated for every participant per movement type (diagonal, x and y) with both mechanism states and in both postures, thus 12 sets of 14 values (Figure 12.6). In a comparison of the movements in equal mechanism states (between postures) no difference occurs in the uncoupled state ($p>0.05$).

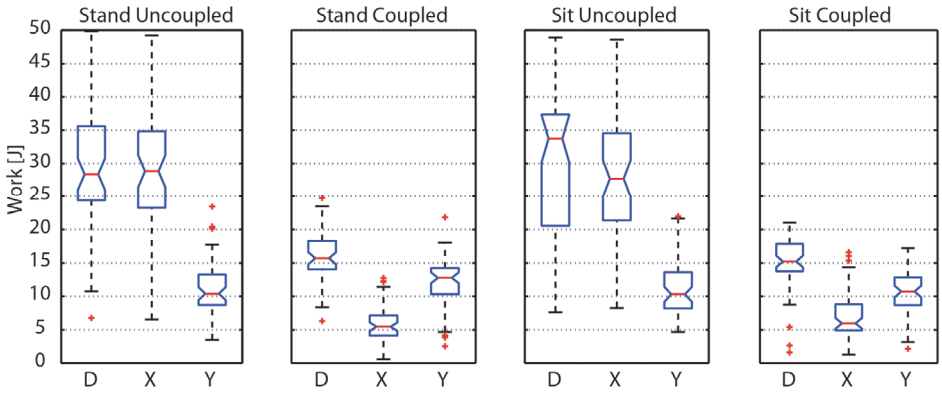

Figure 12.6 The average work values in Joule for all participants, grouped by posture, state and movement type; diagonal (D), X and Y. Non-overlapping notches show that medians differ at a 5% significance level. Thus, it can be observed that there is no difference between postures and that there is difference between system states except for the y movements. As a reference, the work value of 25 Joule is approximately equivalent to lifting 2.5 kilograms to a height of 1 meter.

In the coupled state, the X movements have a lower work cost in standing posture ($f(1,13)=4.92$, $p<0.05$) and the Y movements have a lower work cost in a sitting posture ($f(1,13)=5.12$, $p<0.05$). When movements in the different mechanism states are compared (within postures), the work cost of the diagonal and X movements is less in the coupled state ($f(1,55)=117$ and $f(1,55)=338$, $p<0.01$) and the work cost is of the y movements is equal ($f(1,55)=0.29$, $p>0.05$).

Within each posture-state combination the work cost between movement types is different, except for the diagonal and horizontal movement in the uncoupled state ($f(1,55)=1.79$, $p>0.05$). The paired difference is calculated for all six trajectories in the movement sequence, between the movements in opposite direction, for all four posture-state combinations and for all participants. Thus, resulting in 24 sets of 14 values). Also for this indicator the mechanism states shows great similarities between postures, and a clear difference within postures. For the uncoupled state, in all movement directions the work cost of opposite movements is different ($p<0.05$) except for the Y movement at the right side of the movement board ($t=1.29(13)$ and $t=0.22(13)$, $p>0.05$). For the coupled the results are contrary, for all movement directions the work cost of opposite movements is equal ($p>0.05$), except for the Y

movement at the right side in standing posture (t=4.54(13), p<0.01) and the Y movement at the left side in sitting posture (t=5.11(13), p<0.01).

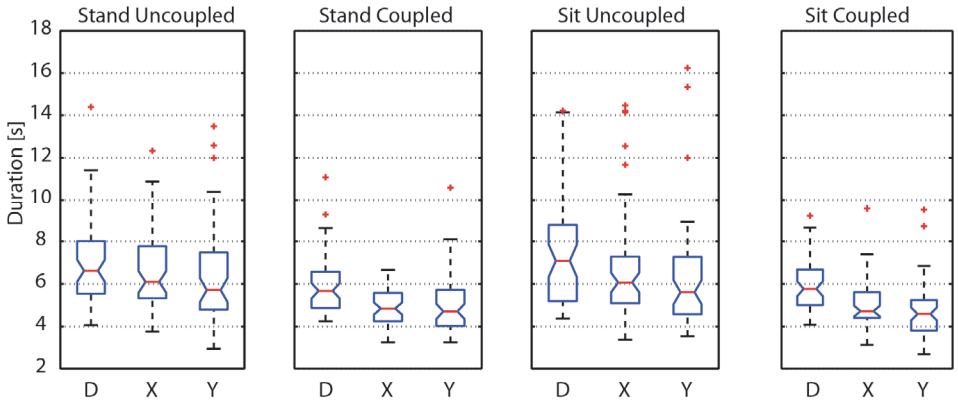

Figure 12.7 The duration of each movement for all participants, grouped by posture, system state and movement type; diagonal (D), X and Y. It can be observed that the duration of movements made with the coupled mechanism is shorter on average. However, the notches denote the 5% significance, which shows that the duration difference is insignificant for y movements. Also it can be observed that the variance in duration and the amount of outliers is generally

12.3.1. Movement duration and problems

The movement duration is calculated for every participant per movement type (diagonal, X and Y) with both mechanism states and in both postures, thus 12 sets of 14 values (Figure 12.7). Also for this indicator the mechanism states are equal between postures (p>0.05), and show a clear difference within postures. The coupled mechanism is positioned within less time than the uncoupled mechanism (p<0.01). Furthermore, it can be observed that the variance in duration and the amount of duration outliers is less for the coupled mechanism (Figure 12.7). This implies that fewer problems are encountered and that the performance of participants is more consistent. This is supported by the selection of movements with a duration longer than nine seconds, in which the uncoupled system state is predominant and both postures are approximately equally represented. In this group it can be observed that two female participants and one male participants are responsible for 67% of the outliers above nine seconds and that both surgeons are present in the other 33% with 5 movements that were executed with the uncoupled mechanism. Through a review of the captured video for the movements with the longest movement durations of several participants, a variety of problems are observed. These problems often cause the participant's attention to shift to the suspension, away from the task at the movement board. Three common causes can be distinguished.

Friction & Precision

The friction in the plain bearing of the rotational joint between the down tube and the extension arm increases when the end-effector is further from the down tube. As a

result, the movements with the uncoupled mechanism at the left side of the movement board (Figure 12.8, left) and toward the right side have an increased difficulty. This specifically causes difficulties during more precise positioning near the end part of the movement, which is a problem that exists in every movement in the uncoupled mechanism.

Collisions

The hand that is holding the end-effector rotates along with trunk of the participant during X movements. This rotation can cause the cross beam to hit the two vertical beams at the left side of the setup. In the worst case, the cross beam is pushed between the two vertical beams in the movement from bottom left to top left (Figure 12.8, right). The mean durations of all y movements at the left side with the uncoupled mechanism is 6.71 (s) and 5.25 (s) with the uncoupled mechanism (f (1,111)=14.9

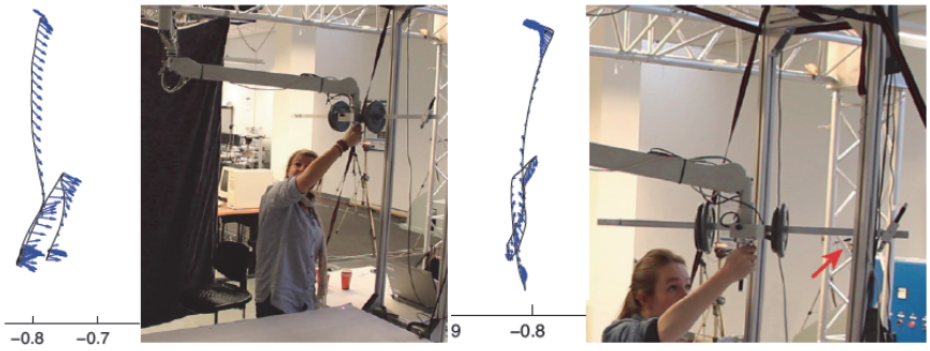

p<0.01).

Figure 12.8 The travelled path is depicted to the left of a video still of two occurring problems; (left) Relative high friction in the suspension causes the participant to repeatedly overshoots the target caused by the build-up of force to overcome friction in precise movements. (right) Rotations of the end-effector causes collisions or entanglement of the cross beam with the setup frame. The depicted case is the most severe, in which the suspension is completely retracted before the movement can be completed.

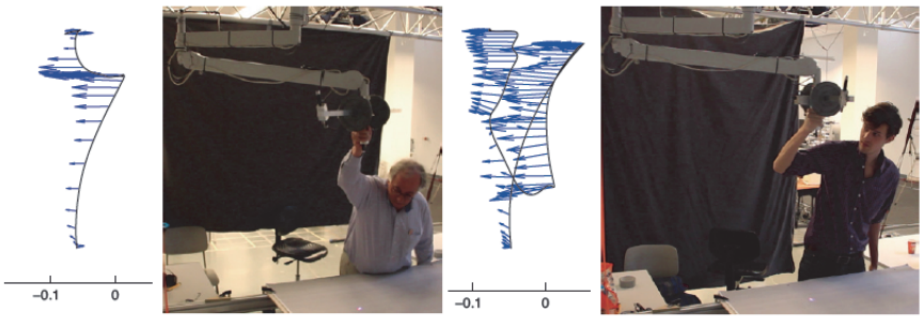

Figure 12.9 Two cases of a longer movement duration caused by singularity; the travelled path is depicted to the left of a video still of the occurrence of the problem. This problem only occurs in the movement from bottom-right to top-right. The situation is often resolved by an increased input of force without looking away from the task (as the neurosurgeon on the left demonstrates). Or the situation is resolved by inspection of the mechanism followed by retraction and a retry on a different path (as the student on the right demonstrates).

Singularity

At the right side of the movement board several participants reach a singular spatial configuration with the uncoupled mechanism, in the movement from bottom-right to top-right. Although this movement does not contain any singular points, the human controller is apparently 'tempted' to follow the rotations of the spring-arm. The resulting (close to) singular configuration is resolved by reversing the movement or by the exertion of an increased amount of force (Figure 12.9). The mean duration of the upward y movements at the right side with the uncoupled mechanism is 6.35 (s) and 4.57 (s) with the coupled mechanism ($f(1,55)=17.2$ $p<0.01$).

Because collisions and singularity occur in the y movements at both sides of the movement board, y movements that take longer than 7.8 seconds (>75th percentile) are analysed; 84% (n=27) of these movements are performed with the uncoupled mechanism and 58% occurred at the left side of the movement board. The three previously mentioned participants are also predominant in this selection with 65% of the movements and again both surgeons are among the other 35% with 4 movements executed with the uncoupled mechanism.

12.3.2. Jerk cost

The jerk cost is calculated for every participant per movement type (diagonal, X and Y) with both mechanism states and in both postures, thus 12 sets of 14 values (Figure 12.10). Again it was observed that performance in the mechanism states is very similar between postures. There are no differences in the coupled state ($p>0.05$). In the uncoupled state, the jerk cost in diagonal and X movement is larger in sitting position ($z=2.10$ and $z=2.19$, $p<0.05$).

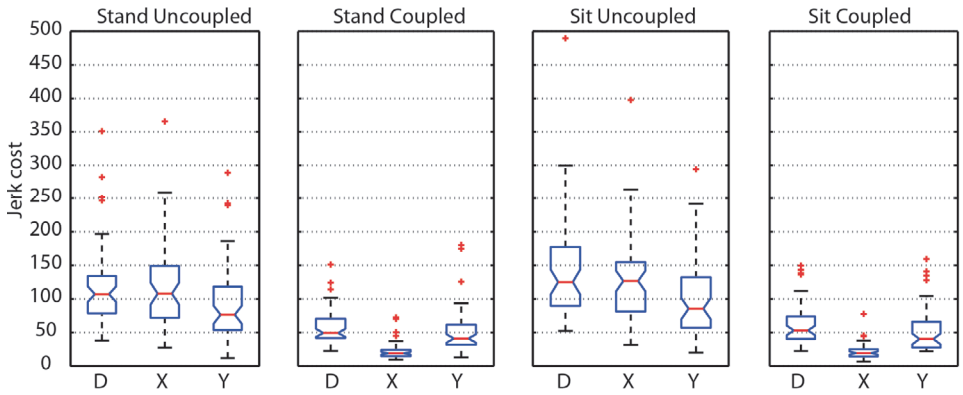

Figure 12.10 Jerk cost over time interval of each movement for all participants.

Within postures, the difference between the conventional uncoupled mechanism and the conceptual coupled mechanism is very distinct ($p<0.01$). For diagonal and Y-movements the jerk cost in the coupled state is approximately half the cost in the uncoupled state. For X movements this is approximately a fifth. Within each posture-state combination the jerk cost differs significantly for the coupled state in both postures ($p<0.01$). For the uncoupled state no difference exists between the jerk in X and Y movements in both postures ($f(1,55)=0.65$, $p>0.05$).

Furthermore, the variance of the distributions is much smaller for the coupled mechanism and its incidence among the highest scoring movements is very low. Based on analysis of the captured video for the highest scoring results, it appears that high friction and singularity are a main cause for a high jerk cost, whereas the movement duration.

Questionnaire results

The results of the questionnaire that was completed after the experiment are very unambiguous and in favour of the coupled system, approximately 93% of the participants answered that the uncoupled system required most force to move and 91% answered to have more control over the movements of the coupled system. The results of the TLX questionnaire are verified using a paired one-sided t-test. According to this test there is no difference in mental demand between the mechanism states ($t=2.07(13)$, $p>0.05$), all other questions are answered in favour of the conceptual coupled mechanism ($p<0.05$).

Also from the answers to a number of other relevant questions the effect of the coupled mechanism appeared to be positive. However the y movements are mainly regarded to be annoying in both mechanism states and with both mechanisms the participants felt that they could improve their performance by practicing for a long period. Furthermore, most participants indicated that movements to the right of the movement board were strenuous in the uncoupled mechanism, due to a large

difference between the friction in the rail and the suspension. Also the low friction in the rail was repeatedly indicated to cause overshoot of the target.

12.4. Discussion

This study shows an explicit difference in manual repositioning performance between the new coupled translational subsystem and the conventional uncoupled subsystem. The movement patterns described with the new mechanism show more efficiency and consistency. This is quantified by the indicator outcome and favoured by the participants.

The aim of this study was to validate the absence of singularity in the redesigned translational subsystem, and to subsequently test the hypothesis that the kinematic change improves repositioning. This was researched via a user experiment with 14 participants. Who executed a sequence of repositioning movements with one test setup, in both the conventional uncoupled state, and the new coupled state.

The results show that the work required for two movements between equal points in opposite directions is inconsistent for the uncoupled mechanism. This is caused by inconsistency in the movement forces and velocity. These are apparently influenced by the differences in the mechanism's spatial configuration over the course of the opposite, but otherwise equal, movements. This effect was expected, because of the uncoupled mechanism's kinematics. The force input at the handle creates a certain torque at each joint, which depends on the spatial orientation of the mechanism. Whereas the friction remains constant, and thus the required movement force depends on the spatial orientation of the mechanism. For the coupled mechanism, the work required for the equal opposite movements is consistent. This demonstrates the absence of singularity within the movement space of the new mechanism design.

Furthermore, results show improvements in repositioning performance with the coupled mechanism, relative to repositioning with the conventional uncoupled mechanism. The movements are performed faster and less problematic situations occur, that cause outliers in the movement duration. Also the jerk cost of the movements is less and the qualitative participant responses are in favour of the coupled system. However, there are two factors that have influenced the experiment and have to be taken into account for correct interpretation of these results; the movement pattern and friction differences.

Friction differences

Movement of the rail mechanism was subject to little friction relative to the rotation of the suspension arms, which greatly reduced the work required for X movements in the coupled mechanism. Although this can be seen as an improvement of the kinetics, it is also of influence on indicators used to describe improvements of the kinematics. As a result, with respect to the kinematics, the only unbiased movement is the Y movement. This is performed with a combination of arm movements in both states. That the friction characteristics are equal for this movement is confirmed by the equal work cost between states in both postures.

The paired work indicator is a comparison within one system state and thus insensitive for interstate friction differences, because the same friction is present in the paired opposite movements. Therefore, the proof for absence of singularity in the new mechanism holds. Furthermore, the jerk cost measures the smoothness of the movement, which is sensitive for variations in the friction and not so much the magnitude (as long as it can be reasonably overcome by human power). Therefore, these indicators are considered to give insight into the effects of the different kinematics. However, the duration indicator is influenced by the difference in friction. Presumably, the duration of movements in the coupled mechanism would decrease when the friction in the revolute joints is lowered.

Movement pattern

The second factor is the movement pattern, which was designed and positioned in such a manner that the degrees of freedom of the coupled system can be assessed separate (y and x movements) and combined (diagonal movements). The effect manifests in the work cost of the movements with the coupled mechanism, in which the work that is required of diagonal movements approximates the sum of the work required for X and Y movements. The uncoupled mechanism can only complete the movements in the movement pattern with a combination of the two arm rotations, resulting in relatively arbitrary work. It can be expected that luminaire movements in the operating room will mostly require a combination of the degrees of freedom. Thus, a representative comparison of mechanism performance between states can only be performed between diagonal movements.

12.4.1. Improvement of repositioning

With consideration of before mentioned factors, it can be concluded that the difference between the mechanism kinematics, in the coupled mechanism, improves the repositioning performance. The y movements with the coupled mechanism are executed 1.5 second faster (6.3-4.8) and, in the conventional mechanism, there is a difference of approximately 20 Joule in opposite diagonal movements between the bottom-left and top-right markers, whereas the work cost for these movements is equal in the coupled mechanism. Furthermore, the significantly lowered squared jerk for the movements with the coupled mechanism shows that the kinematics of the coupled mechanism has resulted in improved usability. The factor two (or more) difference in jerk cost, indicates that participants were able to better optimise the “smoothness” of the repositioning movements with the coupled mechanism. This directly translates to an improvement of usability, under the assumption that the minimal jerk model (Flash and Hogan 1985) is true, as it is regarded the most influential model describing human arm movement control (Campos and Calado 2009). The improvement of usability is supported by the qualitative results. These show that participants significantly favour the coupled mechanism with regard to movement effort, movement control, movement force and the success of the movement. Also participants felt their movements with the coupled mechanism were faster, easier and less susceptible for collisions. However, it has to be taken into account that the lowered input forces that were required for horizontal and diagonal movement in the

coupled mechanism can have contributed in a feeling of more control and a lower required control effort.

12.4.2. Recommendations

The results in this research are obtained outside the operating room, in a controlled environment, with a subsystem of the suspension system and through a task that was abstracted from the actual task of luminaire repositioning - in the operating room during an operation. Therefore, the design is only partially validated. To really improve the actual luminaire repositioning, the proposed mechanism has to be further validated in the operating room environment.

12.5. Conclusion

The significant difference in work cost that is required for a diagonal movement in opposite directions shows that the spatial arrangement influences the velocity and force required to perform a movement in the uncoupled system. In the coupled mechanism there is no significant difference between such movements, hence answering the first research question; the forces required to reposition the luminaire in the new mechanism are consistent with the movement velocity and independent of the spatial configuration.

A significant reduction in duration is observed for the coupled mechanism in movements with equal friction characteristics and the incidence of the coupled mechanism among movements with significantly high duration is low. Therefore, the second research question can be answered as follows; the repositioning duration and problems are significantly lower for a mechanism with movement forces that are consistent with movement velocity and independent of the spatial configuration.

These answers together with the improvement in usability of the redesigned translational mechanism lead to the validation of the hypothesis; a suspension mechanism without singularity does improve luminaire repositioning. Hence, the research goal is accomplished, a suspension mechanism has been designed that improves luminaire repositioning.

12.6 References

Campos F. and J. Calado, “Approaches to human arm movement control--A review,” Annual Reviews in Control, vol. 33, no. 1, pp. 69–77, 2009.

“DINED: Dutch adults,” 2004. [Online]. Available: http://dined.io.tudelft.nl/dined. [Accessed: 30-Jan.-2011].

Flash T and N. Hoban, “The Coordination of Arm Movements – an Mathematical-Model,” J Neurosci, vol. 5, no. 7, pp. 1688–1703, 1985.

Hart S. G. and L. E. Staveland, “Development of NASA-TLX (Task Load Index): Results of empirical and theoretical research,” Human mental workload, vol. 1, pp. 139–183, 1988.

Knulst A., R. Mooijweer, and F. Jansen, “Indicating Shortcomings in Surgical Lighting Systems,” Minimally Invasive Therapy & Allied Technologies, 2010.

Knulst A. J., R. Mooijweer, and J. Dankelman, “A simulation model that predicts handling forces required to reposition surgical lights,” http://dx.doi.org/10.3109/03091902.2012.663052, 2012.

Matern U. and S. Koneczny, “Safety, hazards and ergonomics in the operating room,” Surgical endoscopy, 2007.

Patkin M., “What surgeons want in operating rooms,” Minimally Invasive Therapy & Allied Technologies, 2003.

Chapter 13

An Affordable System for Luminaire Control

Arjan J. Knulst, Eda Emirdag, Jenny Dankelman

Development of an affordable Wii-based tracking system for per-operative marker tracking. MSc Thesis Eda Emirdag, TU Delft

Position adaptions of surgical lights occur frequently and interrupt the surgical procedure. A semi-automatically adaptable lighting system controlled by a wireless pointer could minimize the need for and impact of adaptations. A low-cost pointer and tracking system based on four Wii-remotes™ could be sufficient for such a task. The accuracy and precision of the system were determined using single markers at a known position. The pointer was also evaluated on orientation estimation and wound shape reconstruction. For single markers the absolute accuracy was 2.8mm, and the precision was 0.72mm. The pointer centre location could be estimated with 9.8mm accuracy and 0.27mm precision, and the pointer angle with 2.2° accuracy and 0.7° precision. The location and radius of a 100mm and 220mm diameter wound could be reconstructed with a maximum error of 8mm and 36mm respectively. The tracking system is therefore suitable for low-accuracy tracking tasks underneath the surgical light.

13.1 Introduction

Requirements for good surgical lighting have been described in the past by various authors (Barlet 1978, Beck 1978, 1989, 1981, Berguer, 1997, 1999, Geisse 1994, Loonam and Millis 2003, Quebbeman 1993). However, still some problems with the use of surgical lights have been encountered by surgeons. Surgical lights have been reported to produce much focused circular shaped light beams (Knulst et al. 2009a, b). Combined with a wide variety of wound geometries this leads to frequent adaptations of the spatial orientation of the light head to maintain good visibility at a location of interest in the wound (Knulst et al. 2011a). Together with the limitations of the mechanics of the suspension systems of surgical lights (Knulst et al. 2011a, Mooijweer, 2011) the lighting systems required frequent attention of the surgeons and led to complaints of the medical staff on the ergonomics and usability of the lighting system Knulst et al. 2011a). Surgical illumination should thus be improved, as the current lighting systems frequently draw the attention of the surgeons away from the patient to the repositioning of the lighting system (Knulst et al. 2011a, Stassen et al. 1999). Different approaches to improve the situation during surgery have been suggested in literature. For instance, head-mounted lights that project light along the line-of-sight and, therefore, give almost shadow-free light at the location of interest. However, head-mounted lights do have downsides. They are uncomfortable, limit the dexterity of the surgeon's head and shadow-free light can decrease depth perception (Hanna 2002, Knulst et al. 2001b, Mishra et al. 2004, Rohrich 2001). A different approach mentioned was in-wound, retractor-mounted lights that project light across the complete wound (Knulst et al. 2011c). All these approaches try to minimize the need for adjustment of the spatial orientation of the surgical light.

A lighting system that adapts the properties of the light beam to match the geometry of the wound, and that spatially orients itself by means of semi-automated actuation, could be an alternative approach to minimize the need for and the impact of adaptations. Such system allows for an adapted interaction between the surgeon and the light: the control over the light is no longer provided by means of manual power to a handgrip, but can now be provided by a wireless pointer that can be used in the proximity of the wound. Such pointer can be used to give information to the lighting system about the required position and angulation of the light beam, and even information about the geometry of the wound. The position and orientation of this pointer can be tracked relative to the surgical light. Placing multiple infrared (IR) cameras in a surgical light and multiple IR markers on a pointer would then enable the computation of the 3D position and orientation of the pointer relative to the light.

IR tracking systems are widely used in research and also during surgery in the operating room, e.g., for navigation during computer-assisted surgery (Cheong and Letson 2011, Elfring et al. 2010). However, those systems are very expensive because of their high accuracy and precision (Elfring et al. 2010), and therefore are less suitable for tracking tasks where the demands on accuracy and precision are low. Installing Nintendo Wii Remotes® on the surgical light may provide a simple and cheap solution to track instruments or pointers with sufficient precision and accuracy in the relatively

small volume underneath the surgical light. The use of Nintendo Wii Remotes® has been successfully implemented and evaluated for large tracking volumes (De Amici et al. 2009). However, the accuracy and precision of a small-sized Wii configuration for 3D tracking in a small tracking volume is unknown. This study aims to evaluate the absolute and relative accuracy and precision of a Wii Remote-based system -that is small enough to be installed on a surgical light- for tracking of a single marker, for tracking of a pointer incorporating multiple markers, and for reconstruction of simple wound shapes.

13.2 Methods

13.2.1 Hardware setup

A setup was developed for the evaluation, consisting of four Wii-Remotes® used as IR cameras, two circuit boards each carrying an array of 2x2 IR Light Emitting Diodes (LEDs), a pointer having three IR LEDs and a test platform (Fig. 13.1). The choice for four IR cameras was made to reduce the risk of obstruction of the line-of-sight by for instance the head of a surgeon. The four IR cameras were mounted to a cross-shaped structure at an angle of 40° to the vertical z-axis. To mimic the placement of the cameras in a surgical light the distance between two IR cameras was set to 0.70m, which compares to a typical diameter of a surgical light. All cameras had an overlapping view starting at z=0.42m. The result was a 0.70m cylindrical volume of overlapping camera views starting 0.42m underneath the cross-shaped structure. This volume defined the trackable volume. The IR cameras were connected to a laptop via Bluetooth. A horizontal support was mounted at an adjustable distance underneath the cross. Depending on the experiment the horizontal support could either support the arrays of IR LEDs or the test platform.

The arrays of IR LEDs (Fig. 13.1c) were made of two square circuit boards placed 100mm apart. Each circuit board was equipped with four IR LEDs (Vishay Semiconductors Model TSAL6400, 940nm) that were placed at the corners of a 100x100mm square. The array was mounted on the horizontal, height-adjustable support of the setup.

The pointer (Fig. 13.1b) was made of a 100x100mm circuit board, equipped with three IR LEDs placed at the corners of an equilateral triangle with sides of 86mm. A 250mm long wooden rod with a 6mm diameter was placed at the centroid of the triangle, normal to the plane of the IR LED triangle. A simple holder was constructed to place the pointer somewhere on the test platform. The test platform could be placed on the mounting bar, and had a rectangular grid for alignment of the pointer (Fig. 13.1a).

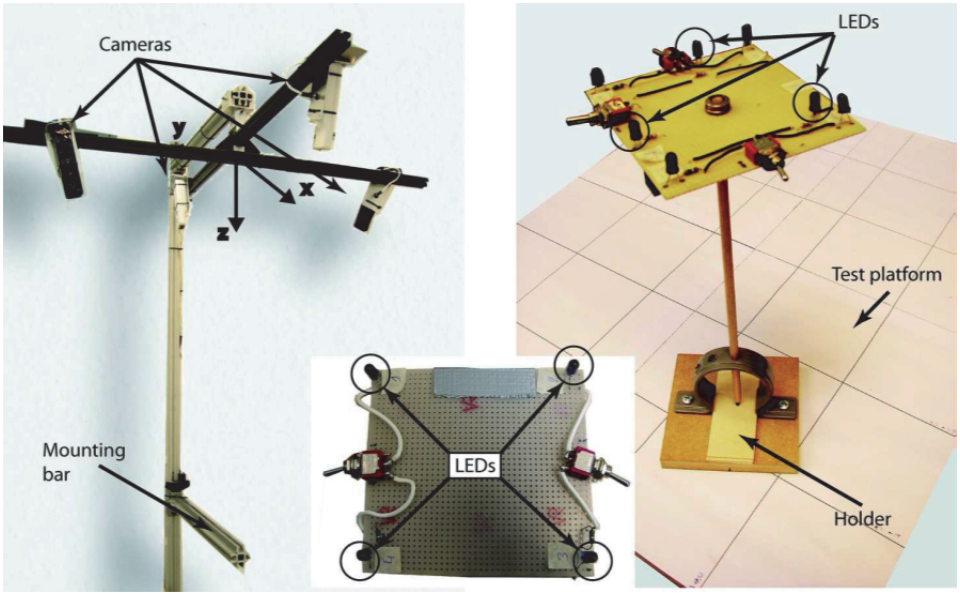

Figure 13.1 a. Test setup with the four IR cameras mounted to a cross-shaped structure and a mounting bar for the placement of the test platform (left panel). b. Pointer prototype with three IR LEDs placed on the test platform (right panel). c. A circuit board with a 2x2 array of IR LEDs (inset).

13.2.2 Software setup

The communication between the Wii Remotes and the laptop was provided using a native C++ Wii-Remote library (WiiYourself! v1.15 RC3) that is publically available (gl.ttr.WiiYourself 2007). For each camera up to four pixel coordinates and point sizes of visible markers, and a unique device identification number were transferred to Matlab for further analysis (Matlab 2010b, The Mathworks, USA).

Calibration of the four cameras was performed simultaneously using an algorithm developed by Svoboda (2005), which is publically available [Svoboda et al. 2010]. The camera positions and orientations were set in the algorithm. The origin of the world coordinate system was placed at the centre of the cross (Fig 1a). A single IR LED was moved slowly through the complete trackable volume while the calibration algorithm was running. 2500 samples were gathered, and the first and last 10% of the samples was removed to eliminate possible start and end effects from the data, such that 2000 samples remained for the calibration. The calibration resulted in a camera calibration matrix for each IR camera.

The position of a marker in the real world was estimated by the Direct Linear Transformation (DLT) triangulation algorithm (Hartley and Zisserman 2004) that uses the output of two cameras. In total six camera pairs were available as the setup had four cameras installed. Therefore, six triangulations could be performed, however, not all triangulations were equally accurate and some triangulations had to be discarded

because of missing data. The principle of epipolar geometry (Hartley and Zisserman 2004) was used to select the camera pair that had the best epipolar match, and therefore, was expected to give the best triangulation estimate.

The last step was to apply corrections to the raw triangulation results. The first correction was to detect and discard cases where epipolar matching failed. As the distance between two markers was known, the estimated distance between every two markers can be compared to the real distance. When the estimated distance was more than 1.5 times the real distance that case was discarded. The second correction was to correct the raw estimated x-,y-, and z-coordinates for calibration inaccuracies. A set of linear functions was fit on each relation between real and raw estimated x-,y-, and z-coordinates. These functions were used to successfully improve the accuracy of the estimated coordinates using the raw estimates.

The pointer was reconstructed by combining the 3D-location of the three IR LEDs. The centroid position could be computed using the positions of the three IR LEDs, and the orientation of the pointer could be reconstructed by computing the normal vector of the plane defined by the three IR LEDs. Combining the centroid position and the pointer orientation allowed the reconstruction of the pointer-tip.

13.3 Experiments

13.3.1 Experiment 1

Experiment 1.1 was designed to evaluate the accuracy and precision of the Wii-based tracking system for a static 3D position estimation of markers. The array of eight IR LEDs was mounted on the horizontal support of the setup. The vertical distance of the array to the origin was varied (0.84, 1.00, 1.14, 1.30, and 1.60m). Three tracking runs of each 300 samples were taken at each height, and the 3D position of each marker was reconstructed based on the selected camera pair. Two errors were computed for each sample: 1. The absolute error between the estimated and real 3D position (E3D), and 2. the relative error between the estimated distance and the real distance between two adjacent markers (Edist). For each of those errors the Root-Mean-Square-Error (RMSE) and the Standard Deviation (STD) were computed per marker/marker pair. The mean and standard deviation were computed for the RMSE and STD. The accuracy of the system was defined by the mean and standard deviation of the RMSE, and the precision was defined by the mean and standard deviation of the STD.

Experiment 1.2 was designed to evaluate the accuracy and precision of the system in a dynamic situation. One of the IR LED arrays with one active LED pair was manually moved around the working volume, meanwhile collecting 1300 samples of all four markers. The RMSE and STD were computed for the relative error (Edist).

13.3.2 Experiment 2

Experiment 2.1 was designed to evaluate the accuracy and precision of the system during a specific application: indicating 3D-positions and angulations by using a pointer, intended for the control of a surgical light. The test platform was mounted on

the horizontal support of the setup, and the pointer was placed in the holder that was positioned at 16 different positions on the platform. The platform was mounted at 4 different vertical distances to the origin (0.84, 1.0, 1.30, 1.60m). The 3D Error was computed between the estimated and the real 3D position of the pointer centroid, the pointer tip, and the pointer angle, as well as the Root-Mean-Square-Error (RMSE) and the Standard Deviation (STD) of the 3D Error. Again, the mean and standard deviation were computed for the RMSE and STD to compute the accuracy and precision of the pointer estimation.

Experiment 2.2 was designed to evaluate the use of the pointer to create a wound shape reconstruction. Two different sized circles (100 and 220mm diameter) were placed on the test platform and the contour of each circle was drawn five times using the pointer. An elliptical fit is applied to the resulting cloud of tip-coordinates. The result of the fit were two radii (a, b) and the origin location (x0, y0, z0) of the fitted ellipse. The error between the fitted radii and origin location and the real radius and origin location was computed for each fit, and averaged over the five repetitions.

13.4 Results

Figure 13.2 shows a comparison of the accuracy and precision of each camera pair relative to the selected camera pair. It shows that the data from selected camera pairs provided highly accurate and precise results, very close to the most accurate camera pair.

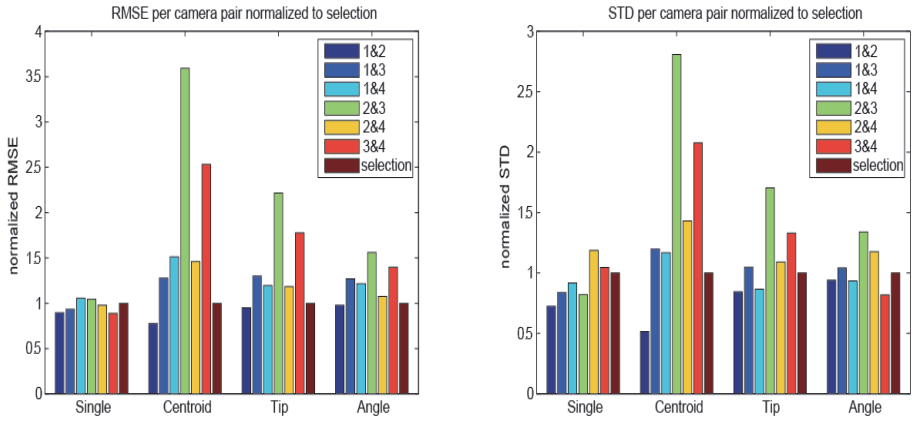

Figure 13.2 The effect of camera selection based on epipolar geometry on the accuracy (left panel) and precision (right panel). The different colours indicate the camera pairs. Each column is normalized on data of the selected cameras.

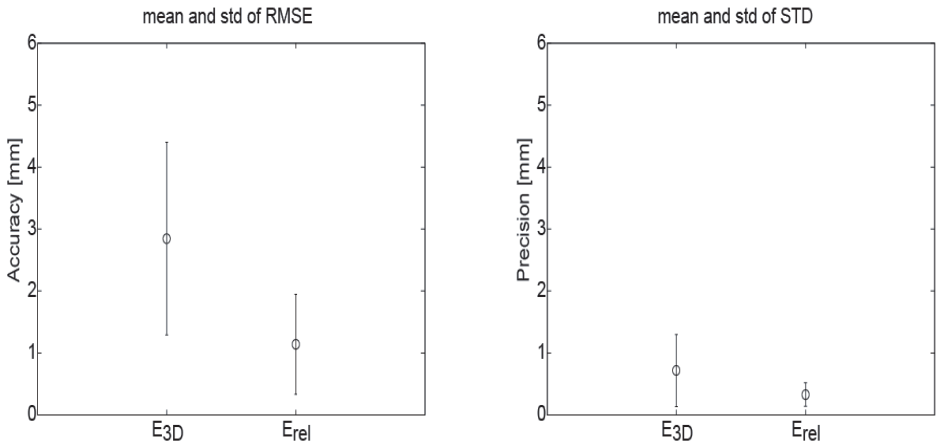

Figure 13.3 Mean and standard deviation of the accuracy (left panel) and precision (right panel) of the absolute 3D error (E_{3D}) and relative error (E_{rel}).

13.4.1 Experiment 1

Figure 13.3 presents the accuracy (mean and standard deviation of the RMSE) and precision (mean and standard deviation of the STD) of Experiment 1.1, using 8 markers at one plane at different distances to the camera system. Absolute accuracy was rather low (2.8±1.6mm), whereas the relative accuracy was higher (1.1±0.8mm). The absolute precision was 0.7±0.5mm, whereas the relative precision was 0.3±0.2mm.

Figure 124 shows the variation of the accuracy and precision at different distances to the tracking system. Clearly, the mean accuracy decreased with increasing distance, both absolute and relative. The precision also varied with the distance, but did not have a clear trend. Again, relative measurements were more accurate and precise than absolute measurements.

The results of Experiment 1.2 using the moving board showed a relative accuracy of 3.3mm and a relative Precision of 3.1mm. The dynamic situation thus influenced both the accuracy and precision compared to the static situation.

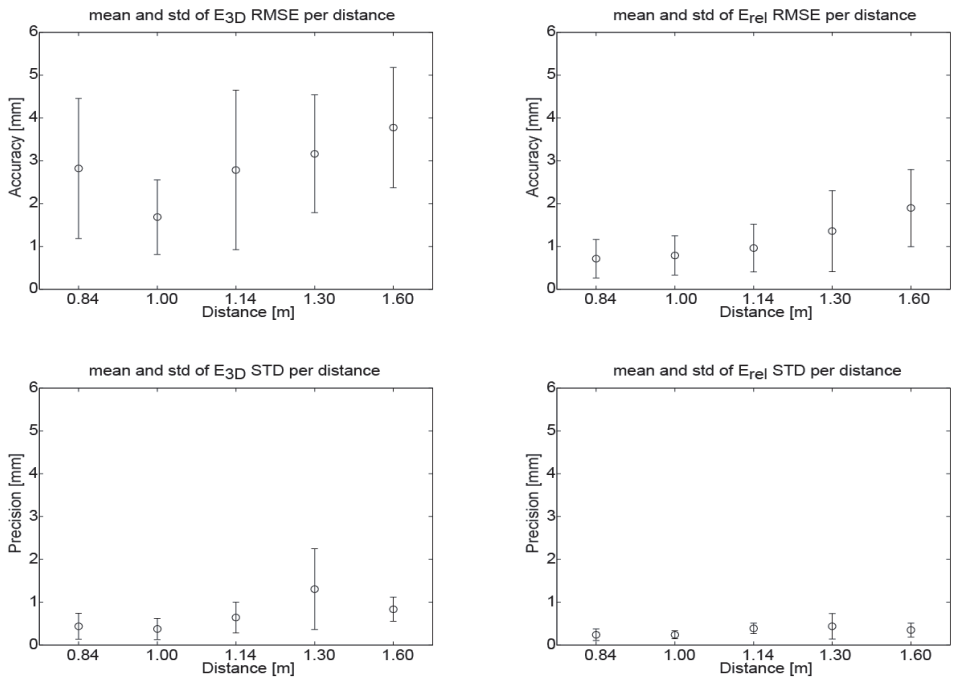

Figure 13.4 Absolute (left panels) and relative (right panels) mean and standard deviation of accuracy (upper panels) and precision (lower panels) as function of distance.

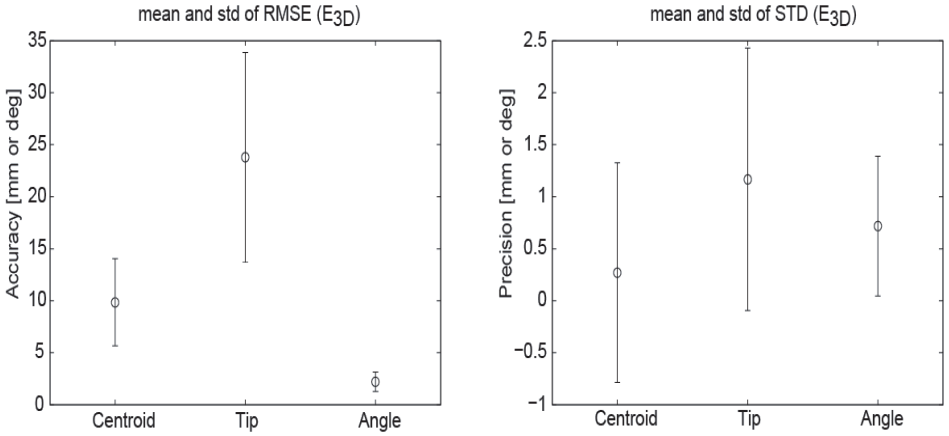

Figure 13.5 Mean and standard deviation of the relative accuracy (left panel) and relative precision (right panel) of the centroid [mm], tip [mm], and angle [°] estimation of the pointer.

13.4.2 Experiment 2

Figure 13.5 shows the mean and standard deviations of both the accuracy (RMSE) and precision(STD) of the centroid, tip and angle location estimation when using the pointer. The centroid location could be estimated with an accuracy of 9.8±4.2mm and

a precision of 0.3±1.1mm. The pointer angle could be estimated with good accuracy (2.2±0.9°) and precision (0.7±0.6°). The tip location estimation was less accurate (23.8±10.0mm) and precise (1.2±1.3mm). The relative accuracy and precision were comparable to the results of Exp. 1.

Figure 13.6 shows the mean and standard deviation of the error of the elliptical fit to both measured circular wound shapes. The radius (a and b) of the large circle was overestimated by 12.6±1.7 to 18.0±0.4mm on average, whereas the radius of the small circle was better estimated, with average errors of -0.34±1.7 to -0.78±2.1mm. The centres (x0, y0, z0) of both the large and small circles had a small mean error (-5 to +8mm) but with a large variation for x0 and y0.

Figure 13.7 illustrates the shape estimation process, from the measured centroid locations to the computed tip location, and down to the (average) shape estimated on the tip location information.

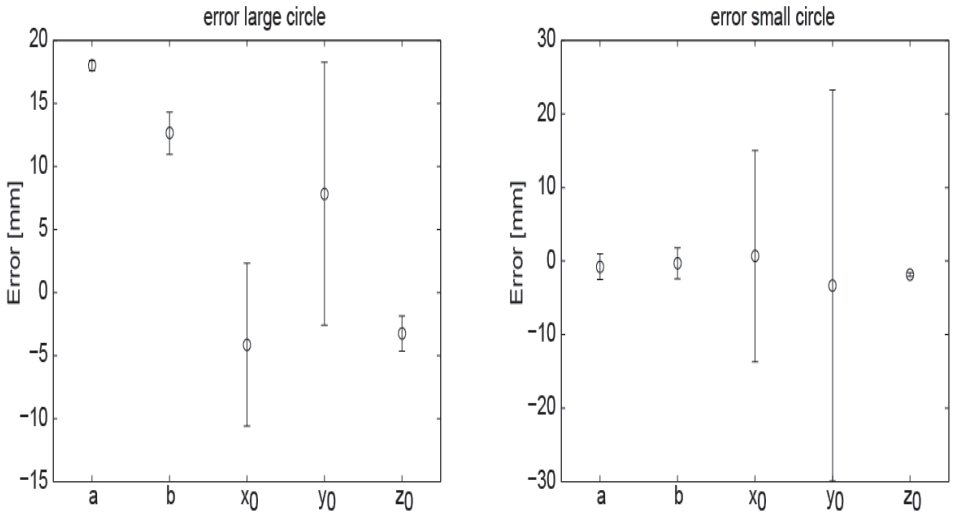

Figure 13.6 Mean and standard deviation of the absolute error of the shape estimate. The error is shown for the ellipse radii (a, b) and ellipse centres (x0, y0, z0).

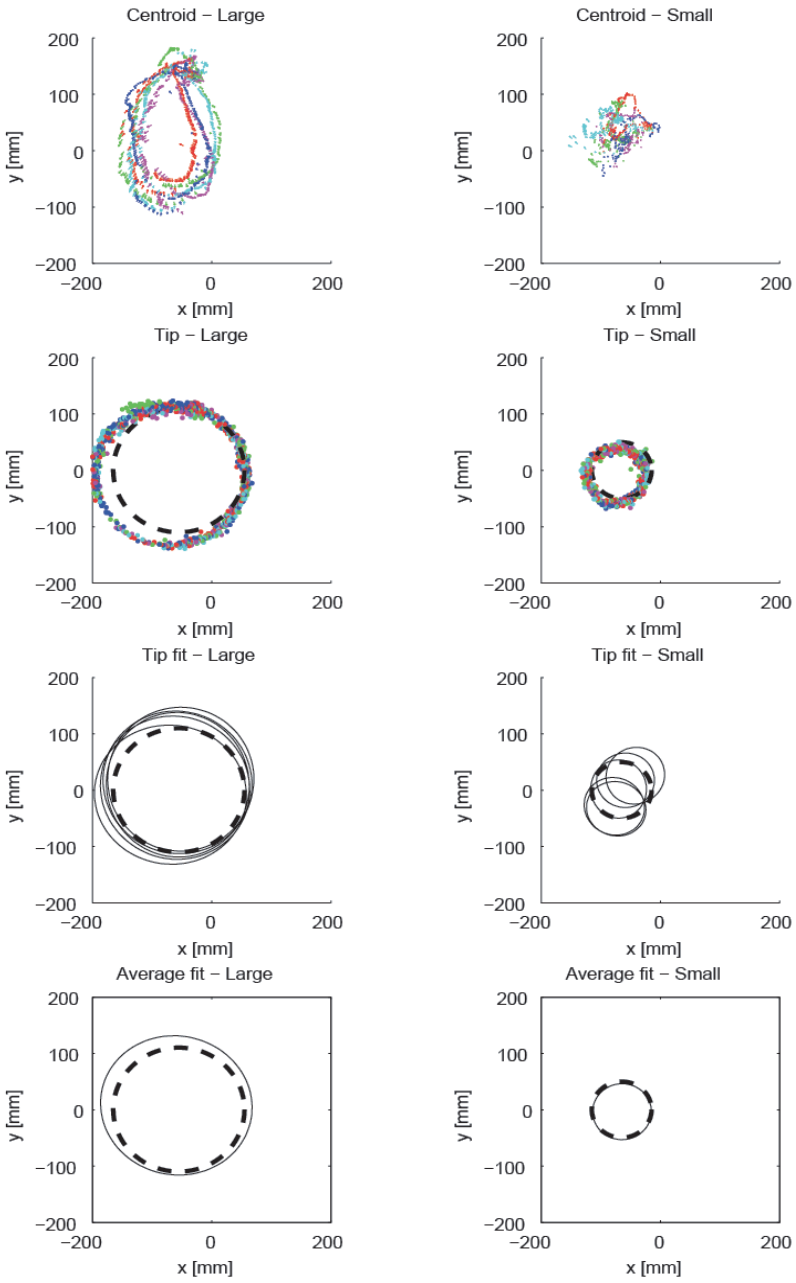

Figure 13.7 Shape estimates for the large (left panels) and small (right panels) circular wound shape. The top row panels show the pointer centroid locations for 5 trials, the second row shows the pointer tip locations for five trials and the real shape (dashed line), the third row shows the estimated ellipses for five trials and the real shape (dashed line), and the bottom row shows the average estimated ellipse and the real shape (dashed line).

13.5 Discussion

This study showed that a small, low-cost tracking system based on Wii-remote IR cameras is capable of tracking IR markers with millimetre accuracy and sub-millimetre precision. The centroid of a pointer carrying 3 IR LEDs could be tracked with centimetre accuracy and sub-millimetre precision. The mean accuracy and precision of the pointer tip estimation were two times less accurate and precise as the centroid estimation, and the angular accuracy and precision were good. The reconstruction of a circular wound shape was rather good: the deviation between the estimated mean radius and real radius was 18mm, and the mean centre of the circle had a maximum error of 8mm. The camera selection based on epipolar geometry proved to be effective. The tracking system is therefore suitable for tracking tasks underneath the surgical light when the requirements for absolute accuracy are low, or when relative tracking is applicable.

Most commercially available surgical tracking systems have a sub-millimetre relative accuracy (Elfring et al. 2010). The absolute accuracy is not reported for those optical tracking systems, as the systems are designed to use a reference frame that relates the measured marker positions to positions in the real world. The mean relative accuracy of a single marker was less accurate than for those commercially available systems. However, commercial systems are far more expensive than the low-cost system proposed in this study. The accuracy and precision of the system used in this study were comparable to the results of another Wii-based system that was designed for large tracking volumes (12.5m3), where distances between Wii cameras were set to several meters (De Amici et al. 2009).

All cameras were aimed at (x,y,z)=(0,0,1). The accuracy and precision decreased for markers with increasing distance to this aiming point. This aiming point should therefore be chosen carefully such that it is located close to the centre of the tracking volume, which might however depend on the application. On the other hand, the variation in accuracy might be introduced by sub-optimal calibration of the cameras. Improved calibration methods might give more consistent results.

As the volume between the surgical light and the wound can be occupied by the heads, arms or instruments of surgical staff, obstruction of the camera's line-of-sight is likely to occur. To minimize the risk of obstruction four cameras were implemented instead of two. This redundancy gave six camera pairs available for triangulation instead of two. Another advantage of camera redundancy is to cope with cameras that fail to see one or more markers. And finally, the redundancy allows for selection of a camera pair that provides the most accurate triangulation.

The camera selection algorithm was based on epipolar geometry. This method proved to be successful, as the selected data had an accuracy and precision comparable to the most accurate camera pair. The algorithm favoured the most accurate camera pair, and only in case of a triangulation failure for that camera pair it favoured a different camera pair. These triangulation failures have no effect on the mean accuracy and precision of one camera pair, but do have an effect on accuracy and precision of the selected data, as the selection algorithm is forced to choose a (normally) less accurate

camera pair. That is why the selected data has a slightly lower accuracy and precision than the most accurate camera pair. The camera selection could successfully select the most confident triangulation result and can, therefore, effectively cope with triangulation failures of a camera pair when their line-of-sight is obstructed or they fail to recognize a marker.

The accuracy and precision of the tip of the pointer was less accurate than that of the centroid. The tip position was simply a mathematical extrapolation based on centroid location and centroid orientation. The longer the tip, the larger the amplification of the error of the centroid. The reported tip error is thus valid for this particular configuration only. A different tip dimension will lead to a different error. The tip used in the current study was rather long (250mm), intended for use in very deep wounds where the bottom of the wound needs to be reached. For less demanding geometries a shorter tip would be sufficient to reach the bottom of a wound, and then the tip error would be smaller than reported in the current study.

The current system was designed primarily to control the position, orientation and light beam size of surgical lights. Therefore, the system should provide information about the location, orientation and geometry of a wound, and about the required angle of the light beam. This study shows that the origin of a circular wound could be indicated using the pointer within 10mm error on average, and had a rather large standard deviation of 5 to 20mm. The size of the wound could be indicated with an error of 0 to 18mm on average, and had a small standard deviation. The large standard deviation on the wound location indicates that the wound should be drawn more than once to obtain a good estimate. The required angle of the light beam could be indicated with a 2.2° high accuracy and 0.7° precision, which is expected to be sufficient.

Other fields of application for this system might be tracking the motions of minimally invasive instruments during surgery or training tasks to assess the surgeon's or resident's performance. Also, dimensions or shapes of a wound or structures within a wound can be recorded using the pointer. However, the accuracy of these measures should not be critical, as the relative accuracy was not at sub-millimetre level.

13.6 Conclusion

Although the accuracy and precision of the low-cost tracking system is lower than that of state-of-the-art surgical tracking systems, the current findings show that a low-cost tracking system offers sufficient accuracy and precision for less critical or less demanding tasks like indicating the control input for surgical lights. The highest accuracy was achieved during relative tracking, where the position of markers is recorded relative to a known reference position. Although the absolute tracking had a lower accuracy and precision, still it is expected to be accurate enough for the control of surgical lights.

13.7 References

Bartlett D. Operating theatre lighting. NATNews. 1978;15(11):24-30.

Beck WC. Lighting the surgical suite. Contemporary Surgery. 1978;12(1):9-16.

Beck WC. Choosing surgical illumination. American Journal of Surgery. 1980;140(2):327-31.

Beck WC. Operating room illumination: the current state of the art. Bulletin of the American College of Surgeons. 1981;66(5):10-5.

Berguer R. The application of ergonomics in the work environment of general surgeons. Reviews on Environmental Health. 1997;12(2):99-106.

Berguer R. Surgery and ergonomics. Archives of Surgery. 1999;134(9):1011-6.

Cheong D, Letson GD. Computer-assisted navigation and musculoskeletal sarcoma surgery. Cancer control : journal of the Moffitt Cancer Centre. 2011;18(3):171-6.

De Amici S, Sanna A, Lamberti F, Pralio B. A Wii remote-based infrared-optical tracking system. Entertainment Computing. 2009;1(3-4):119-24. doi:10.1016/j.entcom.2010.08.001.

Elfring R, de la Fuente M, Radermacher K. Assessment of optical localizer accuracy for computer aided surgery systems. Computer Aided Surgery. 2010;15(1-3):1-12.

Geisse JK. The dermatologic surgical suite. Seminars in Dermatology. 1994;13(1):2-9.

gl.ttr. WiiYourself! Native C++ Wiimote Library. http://wiiyourself.gl.tter.org/. 2007.

Hanna GB, Cresswell AB, Cuschieri A. Shadow depth cues and endoscopic task performance. Archives of Surgery. 2002;137(10):1166-9.

Hartley R, Zisserman A. Multiple View Geometry in Computer Vision. 2 ed. Cambridge University Press; 2004.

Knulst AJ, Stassen LP, Grimbergen CA, Dankelman J. Choosing surgical lighting in the LED era. Surgical Innovation. 2009a;16(4):317-23.

Knulst AJ, Stassen LPS, Grimbergen CA, Dankelman J. Standards and Performance Indicators for Surgical Luminaires. Leukos. 2009b;6(1):37-49.

Knulst AJ, Mooijweer R, Jansen FW, Stassen LP, Dankelman J. Indicating shortcomings of surgical lighting systems. Minimally Invasive Therapy and Allied Technologies. 2011a;20(5):267-75.

Knulst AJ, Dongen Jv, Groenewegen MWM, Kaptein ED, Dankelman J. The importance of shadows during open surgery: effects of shadows on performing stereo visual pointing tasks. Leukos. 2011b;8(2):111-22.

Knulst AJ, Santos ALR, Goossens RHM, Dankelman J. Evaluation of a New Surgical Light Source for Difficult Visibility Procedures. Surgical Innovation. 2011c;18(3):214-22.

Loonam JE, Millis DL. Choosing surgical lighting. Compendium on Continuing Education for the Practicing Veterinarian. 2003;25(7):537-43.

Mishra RK, Hanna GB, Brown SI, Cuschieri A. Optimum shadow-casting illumination for endoscopic task performance. Archives of Surgery. 2004;139(8):889-92.

Mooijweer R. The surgical lighting problem: 'Manipulation problems with the surgical lighting system during surgical procedures'. Master thesis. Delft: Delft University of Technology, Engineering DB;2011 2011-02-18.

Quebbeman EJ. Preparing the operating room. Care of the surgical patient: A publication of the committee on pre and postoperative care. Scientific American. 1993;5:1-13.

Rohrich RJ. Why I hate the headlight ... and other ways to protect your cervical spine. Plastic and Reconstructive Surgery. 2001;107(4):1037-8.

Svoboda T, Martinec D, Pajdla T. A convenient multicamera self-calibration for virtual environments. Presence: Teleoperators and Virtual Environments. 2005;14(4):407-22.

Svoboda T. Multi-camera self-calibration. http://cmp.felk.cvut.cz/~svoboda/SelfCal/. 2010.

Stassen HG, Dankelman J, Grimbergen CA. Open versus minimally invasive surgery: a man-machine system approach. Transactions of the Institute of Measurement and Control. 1999;21(4-5):151-62.

Chapter 14

Discussion

Although research on surgical illumination has not been a topic of much research in the last decades, this thesis shows that there is much to gain in terms of ergonomics, optimal illumination and improved interaction with surgical lights. It was concluded that the frequency of luminaire adjustments and the high adjustment forces of the current system are the main issues encountered during use of surgical lights. The approach of this project was to improve surgical illumination by reducing the frequency of luminaire adjustments through improved illumination techniques and conditions, and by reducing the adverse effects of adjustments for the surgeon through improved mechanics and through an alternative method of illumination control. Although clinical user evaluations have not been done, the functional evaluations have shown that in-wound lights sources and adaptive surgical lights can improve the illumination distribution across the surgical task. Also, functional evaluations have shown that alternative and more intuitive suspension systems for surgical lights reduce the required handling forces for luminaire adjustments. The feasibility of a Wii-based tracking system for control of adaptive, actuated surgical lights was demonstrated. Finally, integration of the knowledge and concepts presented in this thesis is expected to lead to improved surgical illumination.

14.1 Introduction

The main goal of this thesis was to improve the current practice of surgical illumination, as literature indicated that surgical illumination had some flaws (Patkin 2003; Matern and Koneczny 2007). The approach to the main goal was specified by five sub goals:

1. Define the problems associated with the use of surgical lights,
2. Analyse the causes of these defined problems,
3. Gain knowledge required to improve surgical illumination,
4. Implement the obtained knowledge in new ideas,
5. Evaluate these solutions on their functionality and feasibility.

A threefold structure was followed in this thesis. Part 1 started with a study to define the main issues that occur during use of surgical lights. Part 2 focused on the analysis and improvement of illumination to reduce the need for luminaire adjustments. Several directions for improvement were explored and solutions were evaluated. Part 3 focused on the analysis of the suspension system and on the improvement of the interaction between the surgeon and the luminaire to reduce the adverse effects of luminaire adjustments during surgery. Again, several directions for improvement were explored and were evaluated. This chapter will discuss the achievements, the limitations, and recommendations resulting from this thesis, using the thesis goals as guideline.

14.2 Achievements

This section will discuss the achievements with regards to the individual (sub) goals specified in the introduction.

14.2.1 The problems associated with the use of surgical lights defined

This thesis showed that the main problem associated with the use of surgical lights lies in the frequent need for adjustment of the position and orientation of the surgical light, which interrupt the surgical procedure, take time and concentration, and can be quite cumbersome. Most adjustments took place in a 0.5m radius area around the ceiling mount of the light. In the majority of the cases the surgeon made the adjustments, as the surgeon is the only person who can judge the quality of illumination. The main trigger for an adjustment was a changing task location within the wound, resulting in insufficient illumination. The adjustment of the light can require high forces, resulting in two-handed actuation of the light, or even in immobility. These observations were confirmed by the results of a questionnaire among surgical staff. It was concluded that for improvement of surgical lighting the focus of the work should be on reducing the need for adjustments, by providing better and more flexible illumination, and on reducing the adverse effects of adjustments, by improved mechanics of the suspension system or by a changed interaction of surgeon and light.

14.2.2 The causes of the defined problems analysed

The analysis of the causes of the above mentioned problems relates to two topics: the frequency of adjustments and the adverse effects of the adjustments.

The cause of frequent adjustments

The measurements of the surgical lights showed that the light beam is strongly focused, causing high intensity illumination at the centre of the light beam, and strongly decreasing intensities outside the centre. The result of this variation in illuminance is that when the actual task location is slightly outside the centre, the illumination is perceived as insufficient, and the need for an adjustment of the light increases. An example was a long incision that was sutured: the surgeon made many sutures along the incision, and every now and then the light was adjusted to aim the centre of the light beam at his current location of suture.

The cause of adverse effects of adjustments

The current suspension system of surgical lights consists of two pendant arms, connected by rotational joints, and at one end connected to the ceiling above the centre of the operating table. All joints have a certain friction level for position stability of the light. A simulation model was constructed to create force maps that illustrate the force required for adjustment of the light. The model showed acceptably high forces across the full working area of the suspension system, but significantly higher forces inside the 0.5m radius area around the ceiling mount. This explains the high forces, the immobility of the light, and the typical movement patterns of the light during the observed adjustments.

14.2.3. Knowledge for improved surgical illumination

This work has shown that the current standard for surgical lights (IEC 2009) is not covering every aspect than might be necessary to cover. It was shown that LED based surgical lights can introduce coloured shadows to the surgical field. It was also shown that the illuminance characteristics in different surgical conditions cannot be described by only the change of centre illumination; also the size of the pattern changes. Furthermore, it might be wise to relate the descriptive metrics to a standard value to allow better comparison of the performance of different lights.

Most surgical light minimize shadows cast onto the surgical field. Especially when the light is placed behind the surgeon in line with the line-of-sight, or when using a head-mounted light no shadow is visible at all. This thesis showed that shadows not only have a negative contribution in terms of visibility, but also have a positive contribution on the depth estimation and accuracy during pointing tasks. Despite the availability of depth cues like stereo-vision, clearly visible shadows reduced the error on the subjects' pointing accuracy, especially when the angle between the line-of-sight and line-of-light was approximately 90°.

The luminance image of a wound during surgery that enters the eye is the product of the optical properties of the wound, its surroundings and objects within the wound, and the illuminance distribution that the surgical light supplies to this area. It was

shown that variations in luminance within this area affect the visual performance and comfort of subjects. For optimal performance and comfort the variation in luminance should be minimal, and the luminance of the wound and its surroundings should be equal. The size and shape of the illuminating light beam should thus match the size and shape of a wound for optimal visual performance and comfort. This is expected to reduce the need for adaptations of the light.

Besides variations in luminance, also colour differences between wound and surroundings of the wound showed to affect the visual performance. The reddish coloured wound and bluish coloured surroundings of the wound reduced the visual performance for a contrast discrimination task close to the transition. For optimal visual performance the colours of the surroundings of the wound should be matched to the colours of the wound. This is expected to reduce the need for adaptations of the light for tasks close to the edge of the wound.

14.2.4 Evaluation of ideas for improved surgical illumination

This subsection will discuss the concepts developed and evaluated that might contribute to improved surgical illumination, focused on the reduction of the frequency of luminaire adjustments and on the reduction of the adverse effects of adjustments.

Better illumination to reduce frequency of adjustments

To improve the illumination distribution of small, deep wounds a local light source was developed. The idea is to connect multiple of such local light sources to the retractors that keep the wound open. Each light source aims to equally distribute the light across the wound. Therefore, each local light source consists of a high intensity LED and a piece of optics to distribute the light over a large part of the wound. The design of the optics will depend on the shape and size of the wound that is to be illuminated. A functional prototype was developed for tests. These test showed that such local light sources can provide equally distributed illumination across wounds, creating identical illumination at every spot inside the wound. However, current light levels were still too low.

As was shown by the study on luminance balance, the size, shape and illuminance distribution of a light beam of a surgical light should match the size and shape of a wound to create equal luminances across the visual field for optimal visual performance. A surgical light was designed that allows for this functionality using adaptable stripes

Reduced adverse effects of adjustments

Several ideas to reduce the negative impact of luminaire adjustments have been explored. The first attempt was to add one or two extra links to the suspension system. The idea was that the singularities would move away from the centre to the less frequently used parts of the working area, creating a zone of low operating forces around the centre. Although singularities would still exist, their impact would be less as they would be encountered less frequently, and they would be easier to overcome, as

the system would have multiple configurations available to reach one point with the light. This idea has been modelled in a simple simulation model, and materialized in a simple scale model for tests. These tests showed that indeed high peak forces in the central part of the working area can be eliminated and shifted to other regions, creating a better adjustable light in the most frequently used region. However, singularities were not completely annihilated.

Another idea that has been explored is the use of prismatic joints. The most efficient way to allow positioning an object within the rectangular workspace around the surgical table without any singularities is using two orthogonally oriented prismatic joints. One prismatic joint is placed behind the laminar airflow outlet. The other prismatic joint is constructed of a regular two-armed suspension system with coupled degrees of freedom. The result is a system that approximates the kinematics of a prismatic joint. Together, both joints form two orthogonally oriented prismatic joints that allow placement of a light within a rectangular volume without singularities occurring inside that volume. This allows for low-force and intuitive manual repositioning, but also actuation is expected to be easy. A functional prototype was developed for tests and the results showed an improved performance.

A conceptual idea that changes the interaction between the surgeon and the light is an actuated, adaptive system. In such system, the light is controlled by the surgeon from the wound using a wireless handheld device, or even using gestures to interact with the light. The control information provided by the surgeon can be used to adapt the position and orientation of the light, and to adapt the illumination distribution characteristics of the light beam. As a part of such system an adaptive luminaire has been developed, as well as a suspension system that is ready for actuation, and an interaction device for the control of the light.

A pointer whose position and orientation is tracked could be used to provide control information to an actuated, adaptive lighting system. However, most tracking systems are too expensive for use in surgical lights. Therefore, a tracking system based on Wii-Remotes™ was developed. Four Wii cameras were installed as if installed in a surgical light. The four Wii's covered a trackable volume underneath the surgical light. A prototype pointer was made that had three infrared LEDs that were visible to the Wii system. Triangulation is used to reconstruct the position and orientation of the pointer. Using this information the required focal point and direction of the incident light beam can be indicated, and also the geometry of a wound. Test showed that the position and orientation of the pointer can be reconstructed accurate and precise enough for a task like illumination control. Using the pointer the size and geometry of the wound could be reconstructed and thus the characteristics of the light beam can be indicated.

14.3 Limitations

The initial aim of this project was to improve surgical illumination. However, since not much work has been done on surgical illumination, the work presented in this thesis is explorative. The work is aimed to define the important issues associated with surgical lighting, and on finding directions for improvement of surgical illumination. The ideas

that have been explored were, therefore, evaluated rather on functionality then on user-perception. However, despite functional improvements, an idea might have flaw-backs when used in clinical practice by medical personnel.

The observation study focused on one hospital, on one brand of surgical lights, and on a selection of surgical procedures that were likely to show luminaire adjustments. Although the observations were confirmed by the results of a questionnaire, a wider observation study might have led to different frequencies or different adjustment durations. However, the set of adverse effects identified in this research is not expected to change.

The research on knowledge for improved or optimal illumination has mainly been done in laboratory conditions. These conditions were simplified surgical situations or tasks, intended to include aspects of the situations or task that were relevant for the research question under consideration. However, in a clinical situation or for a clinical task, the effects found might be stronger or weaker.

Many of the opposed ideas have been tested on isolated functionality of that particular concept only. However, the individual concepts can be combined or integrated to support each other's functionality. To what extend combining or integrating concepts will result in improved surgical illumination was not studied. This is especially important for the concept of an adaptive, actuated lighting system, were integration is required before functional or even user tests can be performed.

14.4 Recommendations for future work

The limitations mentioned above indicate topics that need further attention to take surgical illumination more steps forward. The individual concepts need to be developed further and integrated into a new, adaptive surgical lighting system before studying their functionality as experience by clinical users. Also, the experiments on optimal illumination need to be done in clinical conditions. Ideally, the developed concepts can be used to adapt the experimental variables in an experiment in a clinical setting.

Extrapolated from the achievements of this thesis, some directions for future work can be specified that are recommended or required for further improvements of surgical illumination. Topics that need attention are listed in this paragraph. The influence of coloured shadows at the surgical field on visual performance needs to be established, both in laboratory as in clinical conditions. The occurrence of coloured shadows needs to be quantified. The reduction of glare at the surgical field needs to be investigated, for instance using low-reflective instruments, low-reflective gloves, or polarized light and goggles. And also, the use of different coloured surgical drapes or different coloured lights that surround a wound needs to be studied to create optimal visual performance and comfort. Knowledge on these topics is recommended to improve the illumination conditions during surgery.

14.5 Conclusions

Although research on surgical illumination has not been a topic of much research in the last decades, this thesis shows that there is much to gain in terms of ergonomics, optimal illumination and improved interaction with surgical lights. It was concluded that the frequency of luminaire adjustments and the high adjustment forces of the current system are the main issues encountered during use of surgical lights. The approach of this project was to improve surgical illumination by reducing the frequency of luminaire adjustments through improved illumination techniques and conditions, and by reducing the adverse effects of adjustments for the surgeon through improved mechanics and through an alternative method of illumination control. Although clinical user evaluations have not been done, the functional evaluations have shown that in-wound lights sources and adaptive surgical lights can improve the illumination distribution across the surgical task. Also, functional evaluations have shown that alternative and more intuitive suspension systems for surgical lights reduce the required handling forces for luminaire adjustments. The feasibility of a Wii-based tracking system for control of adaptive, actuated surgical lights was demonstrated. Finally, integration of the knowledge and concepts presented in this thesis is expected to lead to improved surgical illumination.

14.4 References

IEC (2009). International Standard - Medical electrical equipment - Part 2-41 Particular requirements for the safety of surgical luminaires and luminaires for diagnosis. Geneva, International Electrotechnical Commission**:** 38.

Matern, U. and S. Koneczny (2007). "Safety, hazards and ergonomics in the operating room." Surgical Endoscopy **21**(11): 1965-1969.

Patkin, M. (2003). "What surgeons want in operating rooms." Minimally Invasive Therapy and Allied Technologies **12**(6): 256-262.

Appendix

A - Steerable head-mounted light

A.1 Introduction

Some surgeons use a head-mounted light to provide extra illumination to the surgical site; for instance, during heart surgery, plastic surgery or surgery in deep wounds. Although such a light improves shadow-free illumination into deep wounds as it provides light along the line-of-sight and at the current place of interest, the head-mounted light has some disadvantages. The questionnaire on surgical lights also issued a question on the use and (dis-)advantages of head-mounted lights. The most mentioned reasons for not using the head-mounted light were because of unfamiliarity with such light, because of problems when using such light, and because of discomfort during use.

The dominant advantages of head-mounted lights mentioned were:

- better illumination,
- light at the place you need it, and
- a focused, small light pattern.

The dominant disadvantages of head-mounted lights mentioned were:

- discomfort (weight, pressure on the head, and headaches),
- functionality (only good light for the user of the head-mounted light, limited dexterity because of being wired to the operating room, and because of the light beam being fixated to the head's orientation), and
- usability (hard to set the light properly at start of surgery, and collisions with the light).

This Appendix briefly describes the design of a wireless steerable head-mounted light that automatically keeps the light beam aimed at a certain point of interest within a wound. The idea is to re-establish the surgeon's dexterity because of the automated aiming mechanism and the wireless design, and to improve usability by making the initial position and orientation easier to set.

A.2 Design

The design consisted of an LED and lens and Wii-camera mounted on a steerable platform that was mounted to the adjustment mechanism of a conventional head-

mounted light (Fig. A.1), and one or more battery-operated infrared LEDs that were placed on the sterile drapes nearby the wound. The steerable platform could rotate around two axes to allow steering of the light beam in left-right and up-down directions. The platform was actuated by servo drives that were placed in a casing on a belt around the waist (Fig. A.2), using Bowden cables to connect the servo drives to the platform.

The Wii camera sees the IR LEDs placed nearby the wound, and sends the coordinates of the LEDs with respect to the Wii image to a controller placed in the casing. The controller used this information to aim the light beam to a previously defined set-point. A switch, either manual or voice-controlled, can be operated to define a new set-point in case the light needs to be aimed at a different location. Once set, the light beam keeps aimed at the defined location, allowing the wearer of the light to move his head and body. In this way, the design will help the surgeon to easily aim the light at the beginning and during surgery, and to regain dexterity of the body and head.

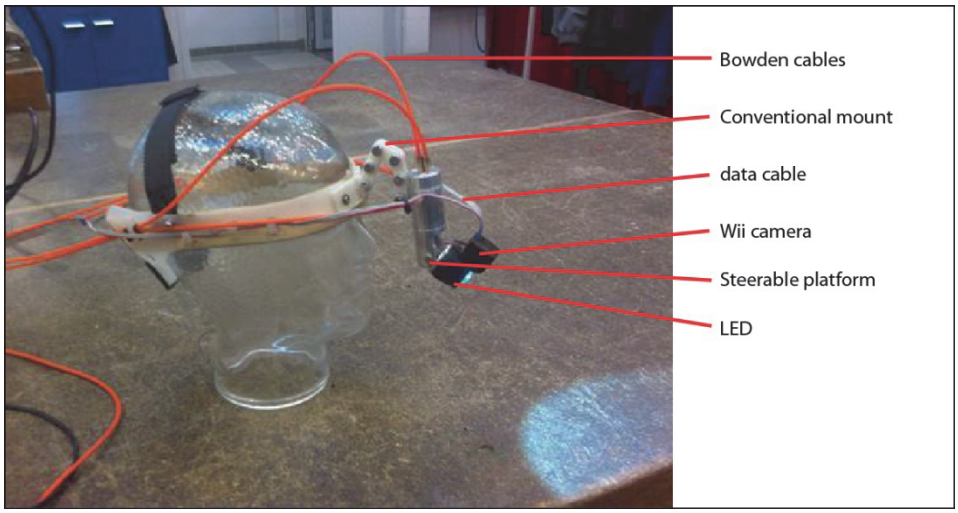

Figure A.1 A picture of the prototype steerable head-mounted light.

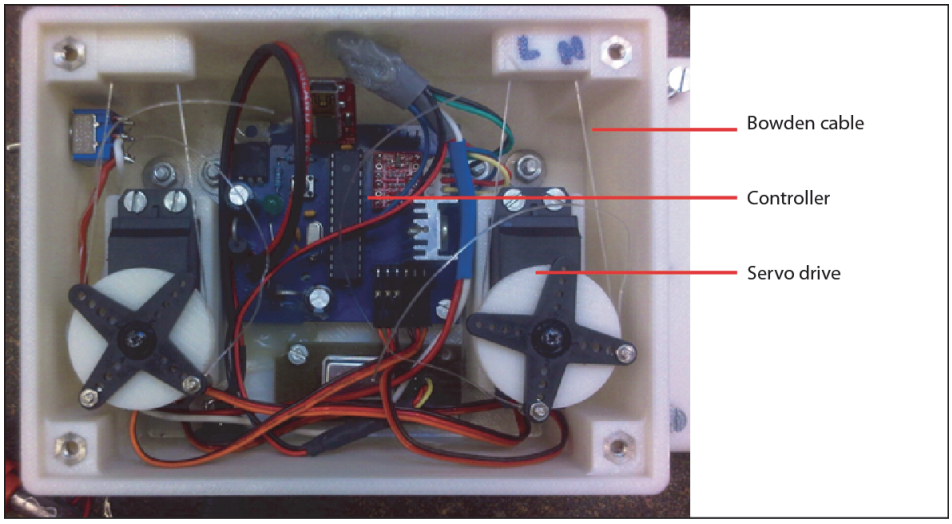

Figure A.2 The casing with two servo drives and the controller.

Figure A.3 Demonstration of the functionality of the steerable head-mounted light, when moving the head to the right of the wound (left picture) and to the left of the wound (right picture).

A.3 Evaluation

The prototype was tested on functionality. One of the IR LEDs was placed at the centre of a red circle, while a subject was wearing the light. When the subject moved his body or head the steerable light corrected the angles of the light beam to stay aimed at the red circle (Fig. A.3).

Although the control was not perfect yet, the principle of the steerable light had proven its functionality. Once the design and controller are optimized the steerable head-light needs to be evaluated during use by surgeons on realistic and relevant tasks.

Dankwoord

Geen boek, artikel, project, onderzoek, product of resultaat zonder hulp; onmisbare hulp waarvoor veel dank verschuldigd is. Aan dit geheel gaven talloze mensen hulp op allerlei manieren; van inhoudelijke bijdragen tot motiverend woorden. In dit dankwoord probeer ik iedereen die een bijdrage gegeven heeft te danken.

Vanuit de TU is de begeleiding gegeven door Jenny Dankelman en Kees Grimbergen onder de paraplu van het LIFE-OR project. Dank voor jullie wijsheid, inbreng, reviews en sturing. Jenny, in het bijzonder dank voor je enorme inbreng in de laatste fase, het was anders niet gelukt! Ik hoop op nog vele jaren van contact en samenwerking in de komende jaren en wens je alle goeds.

Ik ben ook veel dank verschuldigd aan een flink aantal studenten die voor een (afstudeer-)project een flinke bijdrage geleverd hebben aan dit werk en wat vaak tot publicatie heeft geleidt. Ik noem Rik, Jeroen, Jan Jouke, Ana Laura, Eda, Jesse, Marco en Elly. Dank voor jullie inzet, voor het vele werk wat jullie verzet en opgeleverd hebben!

Uit verschillende hoeken van de medische wereld, academische wereld en bedrijfsleven is een bijdrage geleverd aan dit project. Observaties zijn gedaan in het Reinier de Graafgasthuis en Leids Universitair Medisch Centrum, voornamelijk via Laurents en Frank Willem. Dank voor de toegang die jullie gaven! Metingen aan operatielampen konder verricht worden in het Academisch Medisch Centrum van Amsterdam. Dank Coen, voor de begeleiding en de mogelijkheid om aan te sluiten bij jullie orientatie op OK lampen. Dank Daniel en Wouter voor de support die vanuit het NMi gegeven is voor deze metingen. Fokko, bedankt voor je input en het linken van Jean-Pierre. Jean-Pierre, thank you for your input and hospitality at Maquet, and your invitation to present my findings within the IEC workgroup on Safety standards for Surgical Lights. Thanks to Ondal Medical Systems for hosting us, for sharing information on pendant systems, and supplying a pendant system for our experiments. Ook dank aan de commissieleden die tijd geinvesteerd hebben in het lezen, reviewen en de ceremonie.

Veel dank ook aan vrienden. Arjo, Carola, Klaas, Winfred, Ida, Gert: bedankt voor de Delftse brainstorm sessies, het reviewen, het adviseren, het omslagontwerp, de foto's, de (koffie-/reis-/feestjes-/congres-)gezelligheid, de (berg-)tochten, het koken, de frituur, het bier en de vriendschap! *(doorstrepen indien niet van toepassing).*

Ik wil ook mijn familie danken voor al hun zorg en steun, met name mijn ouders die me grootgebracht en altijd ondersteund hebben. Ik hoop jullie op mijn beurt te kunnen steunen in de avond van jullie leven.

Corine, je bent de liefde van mijn leven! Dank dat je mijn vrouw en vriendin bent. Dank dat je de lieve zorgzame moeder bent voor Mirthe en Naomi. Dank voor al je gepush om dit toch eens af te ronden ondanks dat ik het niet nodig vond :-) Dank voor je

vertrouwen. Dank voor je liefde, zorg en steun. Samen en met God kunnen we de toekomst aan, waar die ons ook leidt :-)

Dank aan God van wie ik geloof dat Hij mijn/ons leventje leidt. Dank voor wijsheid en kracht die U geeft. Dank voor Uw leiding in ons leven, ook in de toekomst.

About the author

Arjan Knulst was born on November 21st, 1981 in Bergen op Zoom. He followed VWO education from 1994 until 2000. After that, he went to Delft University of Technology to study Mechanical Engineering from September 2000 until November 2007, specializing in Medical Technology. During his studies he employed several side activities. His PhD research mainly was performed December 2007 until February 2012. After that, he went to work for Lely Industries as Product Engineer of Lely Astronaut milking robots. Meanwhile, he worked on finishing his PhD thesis. Besides his professional activities, he is married to Corine, and has two daughters. He is involved in volunteering work within the PKN church of Delft. He likes tennis and sailing. He also likes walking and hiking, especially in the mountains.

List of publications

1. Threshold Amplitude and Frequency for Ocular Tissue Release from a Vibrating Instrument: an Experimental Study. *Invest. Ophthalmol. Vis. Sci. April 2008. (Contributing author).*
2. Micro-Scale Thermal Tissue Gripper. *Minimally Invasisve Therapy & Allied Technologies. 2009. (Primary author).*
3. Standards and Performance Indicators for Surgical Luminaires. *LEUKOS, July 2009. (Primary author).*
4. Choosing Surgical Lighting in the LED Era. Surgical Innovation. December 2009. (Primary author)
5. Indicating Shortcomings in Surgical Lighting Systems. *Minimally Invasive Therapy & Allied Technologies. September 2011. (Primary author).*
6. Evaluation of a New Surgical Light Source for difficult Visibility Procedures. *Surgical Innovation. September 2011. (Primary author).*
7. The effect of shadows on stereo visual pointing tasks: is shadow-free surgery ideal? *LEUKOS. October 2011. (Primary author).*
8. Single-sided and small-scaled grasping of delicate tissues: Effectiveness of indirect heat-induced attachment and detachment. *Minimally Invasive Therapy & Allied Technologies. December 2011. (Contributing author).*
9. A simulation model that predicts handling forces required to reposition surgical lights. *Journal of Medical Engineering & Technology. March 2012. (Primary author).*